Biochemical and structural analysis on the molecular interaction between FK-506 binding protein (FKBP) 38 and anti-apoptotic protein BCL-2

Kang, Congbao

2006

Kang, C. B. (2006). Biochemical and structural analysis on the molecular interaction between FK-506 binding protein (FKBP) 38 and anti-apoptotic protein BCL-2. Doctoral thesis, Nanyang Technological University, Singapore.

https://hdl.handle.net/10356/6582

https://doi.org/10.32657/10356/6582

BIOCHEMICAL AND STRUCTURAL ANALYSIS ON THE MOLECULAR INTERACTION BETWEEN FK-506 BINDING PROTEIN (FKBP) 38 AND ANTI-APOPTOTIC PROTEIN BCL-2

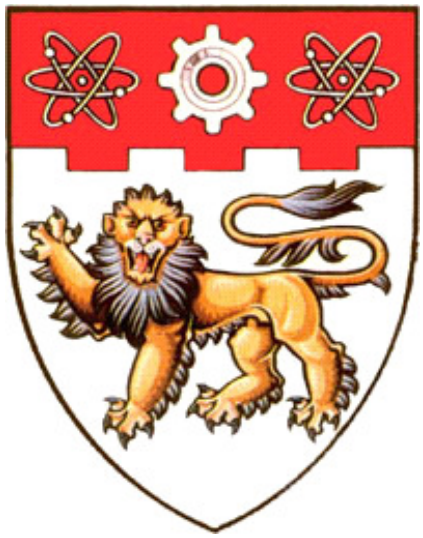

KANG CONGBAO

SCHOOL OF BIOLOGICAL SCIENCES

NANYANG TECHNOLOGICAL UNIVERSITY

2006

Biochemical and structural analysis on the molecular interaction between FK-506 binding protein (FKBP) 38 and anti-apoptotic protein Bcl-2

Kang Congbao

School of Biological Sciences

A thesis submitted to the Nanyang Technological University

in fulfilment of the requirement for the

degree of Doctor of Philosophy

2006

Acknowledgement

The work presented in this thesis was performed under the supervision of Prof. Yoon Ho Sup to whom I would like to express my deepest gratitude for his kind guidance in work and life. Without him this work would have not been possible at all.

I woluld like to express my sincere appreciation for the helps of Dr. Michael Sattler and Dr. Bernd Simon in European Molecular Biology Laboratory (EMBL) who kindly provided opponrtunities for me to get familiar with several NMR software such as NMRPipe, NMRview and Aria and provided us with valuable scripts and pulse programs. Also, I would like to thank Prof. Lescar, Julien for his helps with x-ray crystallography and many others.

I thank Prof. Alex Law very much for his concerning about my work and life. I would like to thank Profs. James Tam, Lars Nordenskiold, Li Jinming, Surajit Bhattacharyya, Rupert Wilmouth, Thanabalu Thirumaran, Jaumes Torres, Liu Chuanfa, Liu Dingxiang, and Mu Yuguang for their kind advices and helps during the period of my graduate study.

A special thank to Dr. Helena Kovacs from Bruker for her friendship and training on NMR. Thanks to Ms Wong Siew Ying and Angela Lim for teaching me how to manage NMR machine.

Thanks to all the members in our group; thanks for their wish in sharing knowledges to Feng Lin, Ye Wenhui, Xu Huibin, Liang Yu with whom I worked for the last years; I would like to thank Joel and Jeff for their helpfulness; thanks to Dr. Ye Hong for working hard together; thanks to Dr. Vivek, Dr. Bohwa, Ravi and professor Prof. Kim Kyong-Tai. Thanks to all the staffs and graduate students in our school.

I would like to express a special thank to Singapore Millennium Foundation (SMF) for their generous financial support.

I would like to present this thesis to my parents and my wife, Dr. Li Qingxin.

Content

List of Figures

Table list

Summary

FK506 binding protein (FKBP) 38, which is a tripartite TPR domain-containing member in the FKBP family, can help Bcl-2 localize at the mitochondrial membrane and modulate apoptosis. The regulation of Bcl-2 function by forming heterodimeric complexes with its pro-apoptotic partners is well studied. Bcl-2 is also regulated at the posttranslational level through phosphorylation of specific residues within the flexible loop. Bcl-2 contains an unusually long loop between the first and the second helices. This loop has been shown to be highly flexible based on NMR and X-ray crystallographic analyses of this region. Currently, the molecular basis of alternative regulatory mechanism of Bcl-2 remains poorly understood. Towards this end, in this study, we first investigated the molecular interaction between FKBP38 and Bcl-2, and demonstrated that Bcl-2 interacts with FKBP38 through the unstructured loop, and the molecular interaction appears to regulate the phosphorylation reactions in the flexible loop of Bcl-2. We also showed that the flexible loop of Bcl-2 displays differential phosphorylation and dephosphorylation profiles by protein kinases and phosphatases. Our results show that, S87, of the four known phosphorylation sites in the loop of Bcl-2, appears to be the preferred phosphorylation site for extra-cellular signal ERK2 while PP2B prefers T56 and PP1 and PP2A prefer T74 as substrates in phosphatase reactions *in vitro*. We presented here by CD and NMR that the peptides derived from the flexible loop of Bcl-2 undergoes a conformational change upon phosphorylation. Also we demonstrated that only the phosphorylated peptide showed the interaction with Pin1, suggesting that the interaction requires a phosphorylation-dependent conformation change at pT/pS-Pro motif in the flexible loop of Bcl-2.

To further understand the biological function of FKBP38, here, we studied its molecular characteristics and a potential regulatory role on the anti-apoptotic protein

Bcl-2. Our results suggested that FKBP38 appears to show chaperone activities in the citrate synthase aggregation assays during thermal denaturation and affect solubility of Bcl-2 when they are co-expressed. The FKBP family proteins bind the immunosuppressive drug FK-506 through the FK-506 binding domain and consequently inhibit the activity of calcineurin. In this study, from our NMR studies and calcineurin assays *in vitro*, we demonstrated that the N-terminal fragment of FKBP38 containing the FK-506 binding domain does not bind FK-506 at molecular level.

To gain insights into the function of FKBP38 and its structural and molecular mechanism, NMR structures of the N-terminal isomerase domain of human FKBP38 has been determined. The NMR structure revealed that the overall structural fold is similar to that of the typical FKBP domain, but lacks the full complement of residues that would enable it to behave as a canonical FKBP. NMR data showed that a number of long-range inter-residue NOEs were observed in the N-terminal tail of FKBP38, suggesting that the-N-terminal tail is not free but might interact with its own FK-506 binding domain. The binding of Ca^{2+}/CaM to the putative CaM-binding domain at the C-terminus of FKBP38 is important for the molecular interaction with Bcl-2. Here, we demonstrated that the calmodulin-binding domain is also involved in the molecular interaction with its own the FK-506 binding domain. This unique structural feature and cross-talk observed between the N-terminal and the C-terminal domains might provide insights into its molecular mechanism of FKBP38 in modulating interacting partners, such as Bcl-2 in apoptosis.

Abbreviations

3-AT……. 3-amino-1,2,4-triazole
Amp…… Ampicillin
Apaf1……..…… Apoptotic protease-activating factor 1
ARIA ……Ambiguous Restraints for Iterative Assignment
Bad …….... Bcl-xL/Bcl2 associated death promoter
Bcl-2……... B-cell lymphoma/leukaemia 2
BH…… Bcl-2 Homology
Bim…… Bcl-2 interacting mediator
BSA…… Bovine serum albumin
Cam……...Calmodulin
CaN A…….. Calcineurin subunit A
CaN B……... Calcineurin subunit B
CARD…… Caspase recruitment domain
CASPASE……. Cysteine Aspartate Specific Protease
CBD……..Calmodulin binding domain
CD……. Circular dichroism
COSY……. Correlation Spectroscopy
CS…….. Citrate synthase
CsA…….. Cyclosporin A
CYANA…… Combined assignment and dynamics algorithm for NMR applications
Cyp40……...Cyclophilin 40
Cyt c……. Cytochrome c.
DISC……The Death Inducing Signaling Complex
DIABLO…… ……Direct IAP(inhibition of apoptosis)-binding protein with low pI
DLC……Dynein light chain
DED……. Death effector domain
DMSO……...Dimethyl sulfoxide
DQF-COSY…… Double-Quantum Filtered COSY
DTT……... Dithiothreitol
EB..... Ethidium bromide
EGTA……Ethylene glycol-bis-(β-aminoethyl ether)- N,N,N´,N´-tetraacetic acid
EndoG ……...Endonuclease G
ERK2……. Extracellular signal-Regulated Kinase 2 or p42 MAP Kinase
FADD…… Fas Receptor Death Domain
FKBP38…… FK-506 binding protein 38
FPLC……Fast Performance Liquid Chromatography
GST…… Glutathione-S-transferase
HMQC……. Heteronuclear Multipe Quantum Correlation
HPLC…….High performance liquid chromatography
HSP……...Heat shock protein
HSQC……..Heteronuclear single quantum correlation spectroscopy

HtrA2 ……..……High temperature requirement protein A2
ICE…….... Interleukin-1 beta-converting enzyme
IGF-1…….. Insulin like grwth factor
IPTG…… Isoporpyl-Thio-B-D-galactopyranoside
JNK……...C-Jun-N-terminal Kinase 1α1
Kan…… Kanamycin
LB.....Luria-Bertani
MAPK…….. The mitogen-activated protein kinase
MEK4, MAPKK4…….Mitogen-activated protein kinase kinase 4
MKK4……...Mitogen-activated protein kinase kinase 4
NF-AT……Nuclear factor of activated T cells
MOMP…….. Mitochondrial outer membrane permeabilization
NIMA…… Never-in-mitosis A
NMR……...Nuclear magnetic resonance
NMT……Myristoyl-CoA: protein N-myristoyltransferase
NOESY……. Nuclear Overhauser Effect Spectroscopy
ONPG…….O-nitrophenyl b-D-galactopyranoside
P-Bcl-2…… Phosphorylated Bcl-2
PCR…… Polymerase Chain Reaction
Pin1……..PPiase NIMA-interacting 1
PMSF…….Phenylmethylsulfonyl fluoride
PP…… protein phosphatase
PP2B……. Calcineurin
PPIase……...…Peptidyl prolyl *cis-trans* isomerase
PVDF……..…….Polyvinylidene difluoride
PS1……...Presenilins 1
RNAi……... RNA interference
RNFR……Tumor necrosis factor
ROESY……...Rotating-frame Overhauser Effect Spectroscopy
RT-PCR……..Reverse transcription-polymerase chain reaction
SD……. Synthetic Dropout
SDS-PAGE……Sodium dodecyl sulfate-polyacrylamide gel electrophoresis
SiRNA…… Small interfering RNA
TAE……... Tris-acetate-EDTA
TB.....Terrific broth
TBS…….Tris-buffered saline
TCR…… T cell receptor
TM…….Trans membrane
TNF…….Tumor necrosis factor
TOCSY…….. Total Correlation Spectroscopy
TPR…….Tetratricopeptide repeats
TRAIL…….. TNF related apoptosis-inducing ligand
YPD……Yeast Extract/Peptone/Dextrose

1 Introduction

1.1 Apoptosis

Multicellular organisms have a requirement to adjust their cell number in different tissues under different developmental stage to maintain their proper function and morphology (Vaux *et al.*, 1996, Vander Heiden *et al.*, 1999). Mitosis is the mechanism to increase the cell number, while cell death is the process to decrease the cell number. Cell death can occur by two distinct pathways, necrosis and apoptosis. Necrosis, that is an accidental cell death, is the pathological process which occurs when cells are exposed to a serious physical or chemical insult (Fanti *et al.*, 2004). Apoptosis, also called as programmed cell death, is the physiological process by which unwanted or useless cells are eliminated during development and other normal biological processes.

Apoptosis is used by multicellular organisms to maintain homeostasis within mature tissues during development (Vander heiden *et al.*, 1999, Satchell *et al.*, 2003). Apoptosis occurs during the course of several physiological processes and if it is not regulated correctly, it can contribute to several diseases (Cuconati *et al.*, 2002). Diseases caused by suppression of apoptosis include cancer, autoimmune disorders (systemic lupus erythematosus) and viral infections; diseases which are caused by increased apoptosis include Acquired Immune Deficiency Syndromes (AIDS), neurodegenerative disorders, toxin-induced liver disease and some autoimmune disorders (Zha *et al.*, 1996, Sattler *et al.*, 1997, Zonrig *et al.*, 2001). In cancer treatment, apoptosis always is the target (Kasibhatla *et al*., 2003).

1.2 Apoptotic pathways

In mammalian cells, the apoptotic response is mediated by two apoptosis activation pathways. One is an intrinsic pathway (mitochondrial pathway) where

cytochrome *c* is released from the mitochondria and activates upstream caspase-9. The other is extrinsic (death receptor mediated pathway) (Fesik, 2000, Palmer *et al.*, 2000, Riedl *et al.*, 2004, Ferri *et al.*, 2001) where TNF family of death receptors activate upstream caspase 8. The immediate objectives of these apoptotic signalings are to activate procaspases and disable the mitochondrial function. Caspases, a subclass of cysteine protease that cleaves substrates after aspartic acid residues, are central to the execution of apoptosis (Crow *et al.*, 2004). Human caspases are subdivided into upstream (apical, signaling) caspases (caspases 2, 8, 9, 10 and 12) and downstream (effector, executioner) caspases (caspase 3, 6, 7). Upstream procaspases are activated by dimerization, while downstream procaspases, which exist as inactive precursors, are activated by proteolytic cleavage usually performed by already activated upstream caspases (Crow *et al.*, 2004). Both of the two pathways will activate a major downstream caspase 3 (Fig.1.1) (Schimmer *et al.*, 2001).

1.2.1 Receptor-mediated pathway

The receptor-mediated pathway is one of the most well characterized routes in which cells are induced to undergo caspase activation and apoptosis. Caspase-8 is the principal initiator molecule in receptor-mediated apoptosis. The receptor-mediated pathway begins with the TNF family of cytokine receptors that includes Fas (CD95) and tumor necrosis factor receptor (TNFR) I. These receptors differ in their ligand specificity, activating binding partners and downstream effectors. After binding with some ligands, activated TNFR and Fas receptors recruit the Death Inducing Signaling Complex (DISC) with the adaptor protein Fas Receptor Death Domain (FADD). The FADD recruits and activates pro-caspase-8, which initiates a cascade of effector caspases that catalyze the biochemical reaction leading to apoptosis (Zornig *et al.*, 2001). The function of the DISC in the activation of caspase-8 is thought to be same

as that of the apoptosome in the activation of caspase-9, although the detailed molecular mechanism remains unknown. The receptor mediated pathway can crosstalk with the mitochondria pathway through the caspase-8-mediated cleavage of BID (a BH3-only member of the Bcl-2 Family proteins), which then triggers the release of mitochondrial proteins. Figure 1.1 gives the overview of the apoptotic activation pathways (Riedl et *al.*, 2004, MacFarlane *et al.*, 2004).

1.2.2 Mitochondria pathway

Mitochondria play important roles in transmitting and amplifying death signals and function as the interface between upstream apoptotic pathways and the caspases and other downstream death machinery. The mitochondria mediated pathway is initiated by mitochondrial damage in response to extracellular stimuli including deficiencies in survival/trophic factors/nutrients, radiation, and other chemicals such as drug and physical stresses and intracellular stimuli including oxidative stress, DNA damage and protein misfolding. In response to a variety of pro-apoptotic stimuli, the mitochondrial outer membrane permeabilization (MOMP) is changed, which causes the release of apoptogenic proteins into cytosol. These proteins include cytochrome *c*, Smac (second mitochondria-derived activator of caspase)/DIABLO (direct IAP (inhibition of apoptosis)-binding protein with low pI), HtrA2 (high temperature requirement protein A2) and EndoG (Endonuclease G). The release of these proteins activates apoptotic events in the cytosol and nucleus.

The mechanisms that mediate the release of the apoptogenic mitochondrial proteins are poorly understood. Cytochrome *c* has been studied and several models have been proposed for its release. One of the earliest postulated that cytochrome c release is linked to the mitochondrial permeability transition (MPT) which is triggered by changes in the permeability of the inner mitochondrial membrane. But this model

can not explain the release of cytochrome *c* before or without mitochondrial swelling or collapse of the inner mitochondrial membrane. Other models have focused primarily on more selective permeabilization of the outer mitochondrial membrane. Bax and Bak play central roles in these models by inducing other proteins to form channels for cytochrome *c* release, either forming channels themselves, or inducing lipid channel formation. The hint that the Bcl-2 protein might be capable of pore formation was proved by the three dimensional structure of Bcl-xL, which resembles diphtheria toxin and colicins. In fact, Bax, Bcl-2 and Bcl-xL are able to form ion channels in artificial membranes and under some conditions, Bax channels can be inhibited by Bcl-2.

Once cytochrome *c* is released from the inter-membrane space of mitochondria into the cytoplasm, it binds to the C-terminus of the adaptor protein Apaf-1 (apoptotic protease activating factor-1) and activates it in the cytoplasm by inducing a conformational change that allows the nucleotide binding domain of Apaf1 to bind to ATP/dATP which are already present in the cytoplasm. These events are thought to stimulate a conformational change in Apaf-1 that results in its homo-oligomerization which is mediated through the nucleotide binding domain. The association of procaspase-9 with the caspase recruitment domain (CARD) in Apaf-1 can form a more than 1 MDa complex called apoptosome (Crow *et al*., 2004). The dimerization of procaspase-9 in the apoptosome leads to its activation. Once activated, caspase-9 cleaves and activates downstream procaspase-3, which is also recruited into the apoptosome and in turn, futher activate caspase-9 in a feed-back mode.

Another mitochondrial protein that promotes cell death when released into cytoplasm is apoptosis-inducing factor (AIF), a flavoprotein with oxidoreductase activity. AIF translocates from mitochondria to the nucleus in a manner dependent on

PARP (poly (ADP-ribose) polymerase) activation which is activated by genotoxic and oxidative stresses. In the nucleus, AIF triggers the degradation of DNA to 50 kb fragments, which subsequently undergo internucleosomal cleavage by endonucleases. AIF has no endonuclease activity, but can trigger mitochondria to release cytochrome c. Although AIF released from mitochondria is caspase-dependent in some models, its action after release is independent of caspase activation. Thus the AIF pathway is distinct from but intricately involved with caspase-mediated cell death.

The net result of apoptotic signaling is mitochondrial dysfunction and caspase activation. The activation of down stream caspases leads to the cleavage of numerous structural and regulatory cellular poteins.

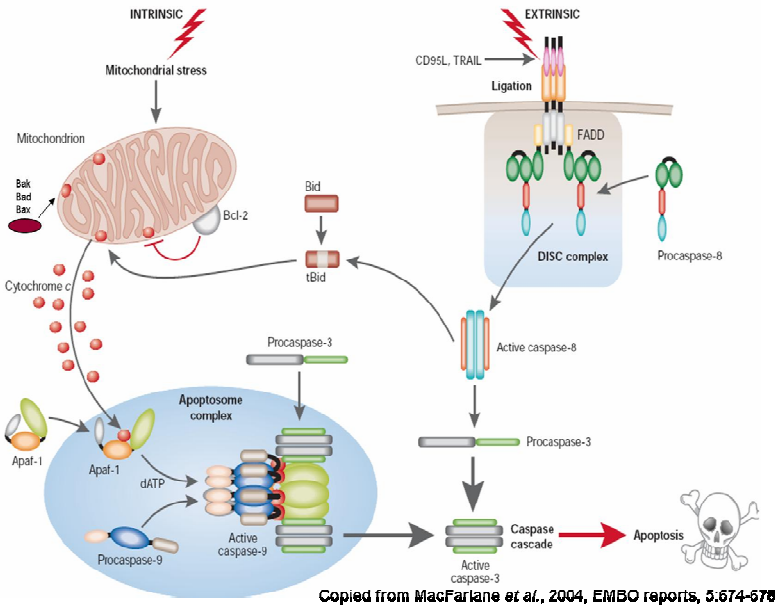

Fig.1.1 The apoptosis activation pathways

Two major apoptotic pathways, one is activated through death receptor activation and the other by stress-inducing stimuli. In the intrinsic pathway, stress induced apoptosis results in perturbation of mitochondria and relase of protein, such as cytochrome *c*. The extrinsic pathway is that extrinsic signal triggers cell suface death receptors of the TNF receptor recruitment to a trimerized receptor-ligand complex (DISC) through the adaptor molecular FADD. These two pathways will active caspase 3 and induce apoptosis. (MacFarlane *et al.*, 2004)

1.3 The endoplasmic reticulum (ER) pathway

The mitochondria are appropriately viewed as the central organelle in the apoptotic pathway. In some circumstances, the ER (or sarcoplasmic reticulum in muscle cells) plays an important role in the mitochondrial apoptotic pathway. The mechanism by which the ER brings about cell death are poorly understood, increases in intracellular Ca^{2+} appear to be necessary. ER Ca^{2+} stores are thought to be increased by Bax and Bak, which are localized on both ER and mitochondria. Bcl-2, which also resides at the ER membrane to decrease the Ca^{2+} stores.

Increasing cytoplasmic Ca^{2+} may activate several apoptotic mechanisms. The mitochondrial Ca^{2+} overload can trigger MOMP opening and cytochrome c release, which can be amplified by positive feedback in which cytochrome c binds the inositol 1,4,5-triphosphate (IP3) receptor-one of the Ca^{2+} release channel to release Ca^{2+}. Also, Ca^{2+} can also activate calpain, which can activate Bid by cleaving it. Calpain can also cleave procaspase 12 and the cleaved caspase 12 translocates to the cytoplasm and activates caspase-9 independently of apoptosome formation. These events provide a mitochondria-independent mechanism for ER-mediated apoptosis.

1.4 Bcl-2 family proteins play important roles in regulating apoptosis

There are at least 20 Bcl-2 relatives which share at least one Bcl-2 homology domain in mammalian cells. The Bcl-2 family members can be divided into three major groups, the anti-apoptotic proteins (Bcl-2, Bcl-xL, Bcl-w and Mcl1), the pro-apoptotic proteins which are also divided into Bax subfamily (Bax, Bak) and the BH3-only members(Bid, Bim) (Boise *et al.*, 1993, Cory *et al.*, 2002). The protein members of Bax subfamily have sequences similarity to the anti-apoptotic family, especially in the BH1, BH2 and BH3 domains (Cory *et al.*, 2002). The BH3-only family proteins contain a BH3 motif, which are unrelated to any known protein, and only Bik and Blk have some similarity (Adams *et al.*, 1998). The two kinds of the pro-

apoptotic proteins are all required for the induction of apoptosis: the BH3-only proteins seem to be a kind of damage sensor and the Bax-like proteins will act the further downstream (Cory *et al.*, 2002). These proteins regulate apoptosis in part by affecting the mitochondrial compartmentalization of cytochrome *c*. Expression of Bcl-2 and Bcl-xL prevents the redistribution of cytochrome *c* in response to multiple death-inducing stimuli. In mixing experiments using cell-free systems, Bcl-2 could prevent cytochrome *c* releasing only from the mitochondria on which it resided (Vander heiden *et al.*, 1999, Komatsu *et al.*, 2000).

All members of the Bcl-2 family (except Bad and Bid) contain a hydrophobic C-terminus (trans-membrane (TM) domain), which serves to anchor these proteins to membranes. Accordingly Bcl-2 family proteins are often localized to the mitochondria or to other intracellular compartments. Bad lacks this sequence and is located throughout the cytoplasm (Hengartner, 2000). But the TM domain is not essential for the protective effect of Bcl-2 or Bcl-xL, because the deletion of the domain from Bcl-2 does not alter its anti-apoptotic activity (Borner *et al.*, 1994). Fig.1.2 shows the domains of different Bcl-2 family proteins and the structure information based upon the 3D structures of Bcl-2 and Bcl-xL, which were previously solved by NMR and X-ray crystallography (Muchmore *et al.*, 1995, Petros *et al*., 2001).

Bcl-2 family proteins contain shared Bcl-2 homology (BH) domains, BH1, BH2, BH3 and BH4. The BH1 and BH2 domains are present in all of the anti-apoptotic proteins as well as the pro-apoptotic proteins Bax, Bak and Bod (Mtd). These domains are likely involved in the channel formation as their 3D structures resemble the pore-forming regions of the diphtheria toxin (Liang *et al.*, 1997; Muchmore *et al.*, 1996; Suzuki *et al.*, 2000). There are some different charged amino acids between pro- and anti-apoptotic proteins in the BH1 and BH2 domains, which may account for the

differences in function between these molecules.

The BH3 domain is a death-promoting region present in all of the Bcl-2 family members. The BH3 domain contains a core sequence of 8 amino acids and there are leucine at position 1 and an aspartic acid at position 6 that are important for the heterodimerization. In the anti-apoptotic members, the BH3, BH2 and BH1 domains can form a pocket, which can bury the BH3 domain so that it can not exert its pro-apoptotic activity and be a docking site for BH3 domains of the pro-apoptotic proteins. Heterodimerization with pro-apoptotic proteins inhibits the function of these proteins.

BH4 domain is found primarily in the anti-apoptotic proteins and seems to be important to be involved in protein-protein interactions. Some proteins (such as calcineurin) are shown to interact with Bcl-2 through this domain (Adams *et al.*, 1998).

1.4.1 Bcl-2 pro-survival family

The anti-apoptotic (pro-survival) proteins can inhibit the apoptosis by interacting with some pro-apoptotic proteins. The 3D structures of the anti-apoptotic proteins are solved by NMR or X-ray crystallography.

1.4.1.1 Bcl-2

Bcl-2 (B-cell lymphoma/leukaemia 2) was originally cloned from pre-B-cell leukaemia cells (Tsujimoto *et al.*, 1986). The Bcl-2 protein has all 4 BH domains, a loop domain and a TM domain in its carboxyl-terminal end. The TM domain makes Bcl-2 localize to mitochondrial membrane but also to endoplasmic reticulum and nuclear membrane. The loop domain can be a target of many kinases and phosphatases which can add or remove phosphate from the loop domain (Ojala *et al.*, 2000). The loop domain can be phosphorylated by JNK or ERK2 at different sites (T56, S70, T74 and S87), which may change its function (Huang *et al.*, 2002). The

mechanism of the phosphorylation of Bcl-2 in the loop domain is still unknown (Wang [b] *et al.*, 1999). Bcl-2 and its homologues (Bcl-xL and Bcl-w) potently inhibit apoptosis in response to many cytotoxic insults. Bcl-2 is an integral membrane protein in both healthy and cancer cells (Cory *et al.*, 2000). Bcl-w and Bcl-xL only become tightly associated with the membrane after the cytotoxic signal, which is indicative of an induced conformational change (Cory *et al.*, 2000). The core structure is well conserved in Bcl-xL, Bcl-2 and Bcl-w. The residues from BH1, BH2 and BH3 form a hydrophobic groove that can bind with BH3 helix of an interacting BH3-only protein. In Bcl-2, the groove can be occupied by its carboxyl-terminal tail, so the BH3 ligand sometimes needs to displace the tail.

Now it is evident that every nucleated cell requires protection by at least one Bcl-2 homologue and regulates tissue homeostasis. Bcl-2 itself is required for the survival of kidney and melanocyte stem cells mature lymphocytes. Apart from its anti-apoptotic function, Bcl-2 seems to play an important role in differentiation and maturation. Bcl-2 can also induce differentiation of neural cell line (Zhang *et al.*, 1996). Bcl-xL is important for the survival of the neuronal and erythroid cells (Gonzalez-Garcia *et al.*, 1995, Reed, 1997).

1.4.1.2 Bcl-xL

Bcl-xL has similar 3D structure to that of Bcl-2 according to the NMR structure study. It belongs to Bcl-x which was cloned by a low stringency hybridisation using Bcl-2 as a probe. Bcl-x was found to be alternatively spliced into two proteins, Bcl-xL (long protein), Bcl-xs (short protein) (Biose *et al.*, 1993) and Bcl-xβ (Gonzalez *et al.*, 1994). Bcl-xL contains all the BH domains and Bcl-xs lacks the BH1 and BH2 domains while Bcl-xβ lacks the carboxyl-terminal TM domain. Bcl-xL has similar function as that of Bcl-2 and can protect cells from cell death after various apoptotic

stimuli, whereas Bcl-xs exhibits a pro-apoptotic function by inhibiting the activity of pro-apoptotic protein Bcl-2 (Boise *et al*., 1993, Gonzalez *et al.*, 1995). Bcl-xβ appears to have different function under different systems (Shiraiwa *et al.*, 1996). Bcl-xL, not Bcl-xs can protect cells from death by inhibiting the availability of cytochrome *c* in the cytosol (Kharbanda *et al.*, 1997). Bcl-xL also contains a long loop between BH3 and BH4 domain and some study shows that removal of the loop domain improves the anti-apoptotic activity of Bcl-xL in hybridoma cells grown in stationary batch culture (Charbonnear *et al.*, 2001). The serine 62 is an important site for taxol- or 2-methoxyestradiol-induced phosphorylation of Bcl-xL in prostate cancer cells. JNK is responsible for the phosphoryation of Bcl-xL and the phosphorylation of Bcl-xL by stress response kinase signaling may oppose the anti-apoptotic function of Bcl-xL to permit prostate cancer cells to trigger apoptosis (Basu *et al.*, 2003, Bachelor *et al.*, 2004). It is also reported that JNK can interact with Bcl-xL and phosphorylate other two sites on Bcl-xL such as threonine 47 and threonine 115 (Kharbanda *et al.*, 2000).

1.4.1.3 Bcl-w

Bcl-w is a Bcl-2 family member with anti-apoptotic activity (Sorenson, 2004, Kaufmann *et al.*, 2004). Bcl-w was cloned using polymerase chain reaction based upon its homology with Bcl-2. Bcl-w can protect haematopoietic cells from cell death induced by growth factor withdrawal, glucocorticoid treatment and γ-irradiation (Gibson *et al.*, 1996). Similar to its closest relatives Bcl-2, Bcl-w localizes to the intracellular membranes of the nuclear envelope, mitochondrial and endoplasmic reticulum (Oreilly *et al.*, 2001). Bcl-w is expressed in the brain, spinal cord, and haematopoietic tissues, but no expression was observed in liver, muscle or salivary gland (Sorenson, 2004). Bcl-w was also detected in mature B and T cells in lymph modes, granulocytes, monocytes and erythroid cells from bone marrow. Despite the

wide spread expression of Bcl-w, development proceeds normally in its absence and only with one exception in which Bcl-w is essential for spermatogenesis (Sorenson, 2004, Print *et al*., 1998).

The structure of the Bcl-w has been recently determined by two groups using NMR spectroscopy (Hinds *et al.*, Denisov *et al.*, 2003). Its overall structure is similar to that of Bcl-2, Bcl-xL and Bax. Bcl-w contains a hydrophobic groove on its surface. The difference between Bcl-2 and Bcl-xL is that Bcl-w contains a shorter loop.

1.4.2 The BH3 proteins

All the somatic cells in *Caenorhabditis elegans* (*C.elegans*) require the single BH3-only protein EFL-1 when they undergo apoptosis. Most of the BH3-only proteins in mammalian cells are widely expressed. They are thought to be active by binding and neutralizing the anti-apoptotic proteins and they must function in upstream of Bax and Bak in the same pathway because without Bax or Bak, the BH3-only proteins have no function (Cory *et al.*, 2002).

The BH3-only proteins are regulated by many mechanisms. Bim and Bmf are sequestered by binding to dynein light chains which are associated with the microtubules (Bim) and actin cytoskeleton (Bmf) (Mollinedo *et al.*, 2003). Bad can bind with 14-3-3 scaffold proteins by phosphorylation with kinase (Rosenquist, 2003). Bid can get higher activity after proteolytic cleavage. Some of the knockout studies show that the BH3-only proteins have specialized physiological roles in the tissue. Bid can facilitate the death of hepatocyte that is provoked by anti-Fas antibody. Bim is a main regulator of hematopoietic homeostasis because leukocyte number rises and plasma-cell accumulation provokes the onset of an autoimmune disease without it, which is equivalent to elicit by the over-expression of Bcl-2. Bim also participates in neuronal death. Bid seems to be important to promote cell death by activating Bax

and Bak and might also inactivate pro-survival relatives. Bid may act by inducing Bax and Bak to oligomerize and form pores in the membrane, but the oligomers do not contain Bid. It is likely to form homo-trimers in the membrane.

1.4.2.1 Bad

Bad (Bcl-xL/bcl2 associated death promoter) is a pro-apoptotic Bcl-2 family member containing BH3-only, that was cloned as an interacting partner for Bcl-2 and with Bcl-xL. It was shown that Bad can selectively dimerize with Bcl-xL and Bcl-2, but not with Bax, Bcl-xs, Mcl-1 or itself. Bad binds more strongly to Bcl-xL than Bcl-2 in mammalian cells, and it reverses the death repressor activity of Bcl-xL, but not Bcl-2. When Bad was dimerized with Bcl-xL, Bax was displaced and apoptosis was restored (Yang *et al*., 1995). Bad can be phosphorylated on at least three different serine residues resulting in the disruption of the binding of Bad to Bcl-xL at the mitochondria, which sequesters Bad to cytosol by the protein 14-3-3 (Zha *et al*., 1996) and produce more free Bcl-xL that can bind to Bax. This results in reduction of the amount of free Bax. The disruption of the balance between pro- and anti-apoptotic Bcl-2 family members inhibits the release of cytochrome *c* and the activation of the apoptotic pathway. Bad can also be dephosphorylated in response to apoptotic stimuli. Glutamate was shown to induce dephosphorylation of Bad through activation of phosphatase-calcineurin, which induces the interaction between Bad and Bcl-xL and results in the activation of apoptosis (Wang *et al*., 1999). Insulin like growth factor (IGF-1) can induce the phosphorylation of Bad via phosphatidylinositol 3-kinase (PI3-K) and protein kinase B (PKB/Akt) in cerebellar granule cells, thereby promote the survival of these neurons (Kelekar *et al*., 1998).

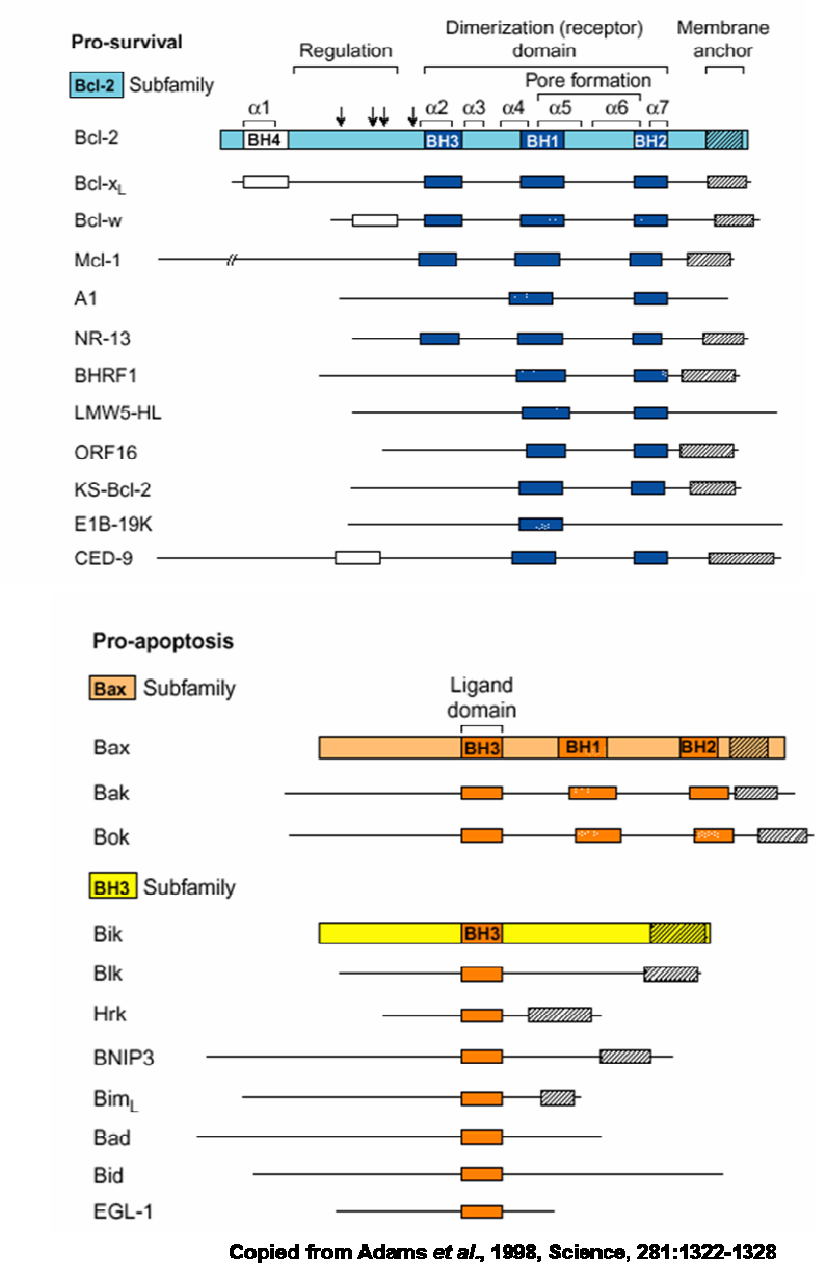

Copied from Adams *et al.*, 1998, Science, 281:1322-1328

Fig.1.2 The structure of the Bcl-2 family proteins

The Bcl-2 cohort promotes cell survival, whereas the Bax and BH3 cohorts facilitate apoptosis. The Bax subfamily resembles the Bcl-2 subfamily but lacks a functional BH4 domain. Except for the BH3 domain, the BH3 subfamily is unrelated to Bcl-2. α1 to α7 indicate helices identified in Bcl-xL, in which a core of two hydrophobic helices (α5 and α6) is flanked by five amphipathic helices, and a flexible (nonconserved) loop connects α1 with α2. Arrows indicate Ser and Thr residues phosphorylated in Bcl-2. All proteins compared are from mammalian (usually human), except for NR-13 (chicken), CED-9, and EGL-1 (*C. elegans*), and the viral proteins BHRF1, LMW5-HL, ORF16, KS-Bcl-2, and E1B-19K (Adams *et al.*, 1998).

1.4.2.2 Bid

Bid is a member of pro-apoptotic BH3-only family that can heterodimerise to either Bcl-2 or Bax. Bid protein possesses only the BH3 domain and lacks the carboxyl-terminal signal-anchor segment. It is found in both cytosolic and membrane locations. Bid counters the protective effect of Bcl-2. Moreover, expression of Bid, without another death stimulus, can induce interleukin-1 beta-converting enzyme (ICE)-like proteases and apoptosis. Mutagenesis analysis revealed that an intact BH3 domain of Bid was required to bind the BH1 domain of either Bcl-2 or Bax (Wang *et al*., 1996).

Bid is an important link in cell death induced by tumor necrosis factor (TNF) or Fas since these stimuli induce the cleavage of Bid by Caspase-8 (Li *et al*., 1998). The cleavage product, C-terminus truncated fragment (tBid), remains associated with the amino terminal fragment (nBid) after cleavage. By a mechanism that is currently not well characterized, tBid becomes dissociated from nBid and translocates from the cytoplasm to mitochondria to induce oligomerization of Bax/Bak and release of cytochrome *c* (Fig.1.1, Fig.1.3, Liu *et al.*, 2005). Bid can translocate to mitochondria after cleavage and has a stronger death-inducing activity than that of full length Bid by either modulating other Bcl-2 family members or by itself acting as an ion channel (Schendel *et al*., 1999).

1.4.3 Bax subfamily

1.4.3.1 Bax

Bax was identified by coimmunoprecipitation with Bcl-2. It is a 21 kDa protein that can form heterodimers with Bcl-2 and Bcl-xL. Bax can promote cell death and inhibit Bcl-2's protective function in a concentration-dependent manner. Bax is alternatively spliced into Bax α containing the BH1, BH2 and BH3 domains as well as

a putative carboxyterminal transmembrane domain. Bax β is a protein which lacks the transmembrane domain. Bax γ lacks extro 2 and is truncated due to frameshift. Bax δ lacks the BH3 domain (Oltvai *et al*., 1993). Bax can induce cell death without additional death stimuli (Vekrellis *et al*., 1997). In the adult, Bax is expressed widely particularly in kidney, liver and pancreas which contain little or no Bcl-2 (Sorenson *et al*., 2004, Vekrellis *et al.*, 1997). Bax-induced caspase activation is dependent on mitochondria and involves release of cytochrome *c* from mitochondria. Also, Bax can induce caspase independent cell death in certain systems (Lindenboim *et al.*, 2000).

The putative TM domain of Bax does not seem to function for inserting Bax into membranes in healthy cells and most Bax resides in the cytoplasm and it can localize at mitochondria upon apoptosis stimuli (Wolter *et al*., 1997, Montessuit *et al.*, 1999). A conformation change of Bax can be induced after many apoptotic stimuli, which facilitates Bax insert into the membrane and translocate Bax from cytosol to the mitochondria. This kind of conformational change can be induced by many apoptotic stimuli such as staurosporin, growth factor withdrawal and Fas ligation (khaled *et al*., 1999, Murphy *et al*., 1999). It was shown that the BH3-only protein Bid can bind with Bax and induce the conformational change, which may also result in Bax oligomer formation that is required for the channel activity, inducing cytochrome *c* release (Desagher *et al*., 1999, Antonsson *et al*., 2000).

1.4.3.2 Bak

Bak is a pro-apoptotic family member that is closely related to Bax containing BH3, BH1 and BH2 and a transmembrane domain. Bak is expressed in most organs in the adult (Krajewski *et al*., 1996). The $Bak^{-/-}$ mice did not develop any age-related abnormalities and the isolated cells behaved normally when induced to apoptosis (Lindsten *et al.*, 2000). In this family, Bax and Bak are widely distributed and the

little-studied protein Bak is more prevalent in reproductive tissues. Some studies show that inactivation of Bax affected apoptosis only slightly and disruption of Bak had no clear effect on apoptosis. When the two genes were both inactivated, the apoptosis in many tissues were dramatically impaired, which means that either Bax or Bak is essential for apoptosis in many cells.

Bax and Bak are thought to function mainly at the mitochondria, but some studies show that they play some important roles in ER. Bax and Bak oligomers are widely believed to provoke or contribute to the permeabilization of the outer mitochondria which allows efflux of apoptogenic proteins. One model that is based on the structural resemblance of Bcl-2 family members and diphtheria toxin is that Bax and Bak can form channels. The Bax oligomers can form pores in the membrane and the cytochrome *c* can be released (Fig.1.3).

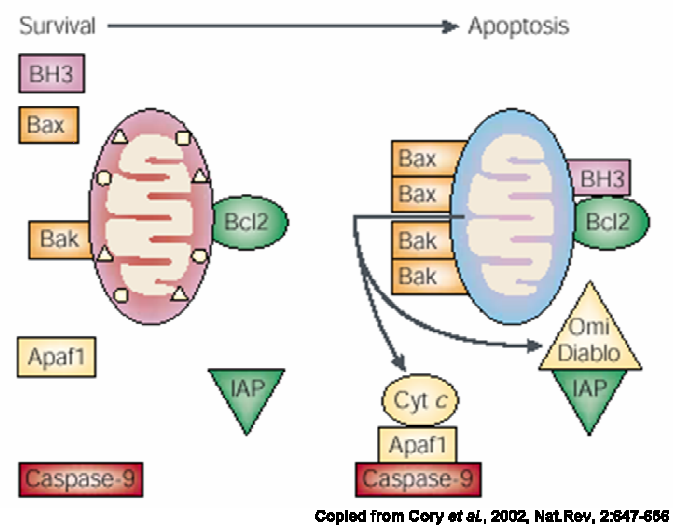

Fig.1.3 The model for Bcl-2 survival activity

Protection of mitochondrial integrity. Bcl-2 and its anti-apoptotic homologues guard mitochondrial membrane integrity until neutralized by a BH3-only protein. Bax and Bak then form homo-oligomers within the mitochondrial membrane, resulting in the release of the cytochrome *c*, which activates Apaf1, allowing it bind to and activate caspase-9. Other pro-apoptotic molecules that exit from the mitochondria include Omi and Diable, which antagonize inhibitor of apoptosis proteins (IAPs). Protein complexes are shown as juxtaposed boxes or triangles (Cory *et al.*, 2002).

1.5 Regulation of Bcl-2 by kinases and protein-protein interaction

Bcl-2 is an important member of a protein family that functions to suppress apoptosis in a variety of cell systems. Several mechanisms have been proposed to explain the antiapoptotic function of Bcl-2. Bcl-2 might act as a regulator of Ca^{2+} homeostasis or as an antioxidant. Bcl-2 forming heterodimers with the pro-apoptotic protein Bax might thereby neutralize its death effectors properties (Breitschopf *et al.*, 2000, Gotow *et al.*, 2000). It was also reported that Bcl-2 can also regulate some gene expression such as down-regulating expression of the endogenous αβ-crystalline gene through modulating the transcriptional activity of lens epithelium-derived growth factor (Feng *et al.*, 2004).

Although recent studies have established that Bcl-2 function is primarily modulated by heterodimerization with pro-apoptotic members of the Bcl-2 family. There are other regulatory mechanisms such as phosphorylation. Phosphorylation of Bcl-2 was first demonstrated in Sf9 cells which ectopically express Bcl-2 with a baculovirus expression system. Since then, there are several reports dealing with Bcl-2 phosphorylation, but its functional significance remains controversial (Yokote *et al.*, 2000). Some reports indicated that anticancer drug-induced apoptosis was accompanied by Bcl-2 phosphorylation, suggesting that phosphorylation inactivates the function of Bcl-2. By contrast, other groups demonstrated that Bcl-2 phosphorylation is essential for anti-apoptotic activity (Furukawa *et al.*, 2000). In any case, studying on the phosphorylation of Bcl-2 could provide some information regarding to the regulation of Bcl-2.

1.5.1 Bcl-2 can be phosphorylated by multiple kinases

Bcl-2 contains several consensus phosphorylating sites by various protein kinases, more interest is focus on the loop domain. It contains protein kinase Cα (PKC) or

cyclic AMP (cAMP)-dependent protein kinase (PKA) site (RXS/T), an evolutionarily conserved serine site (Ser70), and several mitogen-activated protein (MAP) kinase sites for extra cellular signal-regulated kinases 1 and 2 (ERK2) (PXXS/TP) at position 56, 74 and 87 (Breitschopf *et al.*, 2000). Bcl-2 undergoes several types of phosphorylation. One of these occurs during mitosis in stressed cycling cells and involves only a proportion of Bcl-2 molecules, apparently phosphorylation at a single site, identified in one study is Thr 56. Two kinases, CDK1/cyclin B and JNK have been implicated in this type of Bcl-2 phosphorylation. Also, it was demonstrated that the mitotic Bcl-2 phosphorylation is CDK-dependent (Du *et al.*, 2005). A second prominent form of phosphorylation occurs in response to treatment of cells with drugs, such as paclitaxel and vinca alkaoids result in the phosphorylation on its loop domain of Bcl-2. Several different kinases or kinase pathways have been implicated in this drug-induced phosphorylation, including Raf-1, JNK, PKA, CDK1 and mTOR (Du *et al.*, 2005, Asnaghi *et al.*, 2004, Mai *et al.*, 2003).

1.5.2 Bcl-2 can interact with phosphatase

It was shown that Bcl-2 interacts with phosphatases such as calcineurin (PP2B), PP1 and PP2A. Its phosphorylation status can be controlled by these phosphatases. Bcl-2 can form tight complex with PP2B through its BH4 domain (Shibasaki *et al.*, 1997). Our experiment also showed that PP2B can use phosphorylated Bcl-2 as substrate. PP2A is also a serine/threonine-specific protein phosphatase which can also interact with Bcl-2, and the phosphorylation status of Bcl-2 can be regulated by PP2A on the mitochondria (Tamura *et al.*, 2004, Simizu *et al.*, 2004). The phosphatase PP1 was also reported that it could interact with Bcl-2 and JNK in mitochondria (Brichese *et al.*, 2004). Bcl-2 phosphorylation appears to be coordinated in a complex, dynamic network, and multiple molecules are participating in this process. Accumulating

evidence shows that the phosphorylation of Bcl-2 may affect its function (Ruvolo *et al.*, 2001). Phosphorylation of Bcl-2 might trigger Bcl-2 to be degraded by proteasome pathway (Basu *et al.*, 2002) or its dephosphorylation might target Bcl-2 for the substrate of ubiquitin-dependent degradation (Dimmeler *et al.*, 1999).

1.5.3 Pin1 can interact with P-Bcl-2

Ser/Thr-Pro motifs are phosphorylated by a large family of important Pro-directed protein kinases. They exist in *cis* and *trans* isomers, the conversion of which can be catalyzed by the PPIase (Lu, 2004). Peptidyl-prolyl isomerization of some proteins provides a mechanism for switching a protein to different conformation and influencing protein activity. Human Pin1 and its homologs (Pin1-type PPIases) are the only known enzymes that efficiently isomerized pSer/Thr-Pro bonds. Recent studies have confirmed the original function of Pin1 in the cell cycles and uncovered many important novel functions of this enzyme in many cellular processes including regulation of cell cycle, cell signaling, transcription and RNA processing, DNA damage response, the development of germ cells and the human disease, notably in cancer, Alzheimer's disease and cancer pathogenesis. Previous studies showed that over-expression of Pin1 in cancer cells in correlated with poor clinical prognosis, suggesting that Pin1 may act as a new diagnostic and therapeutic target (Lu, 2004)

Pin1 is a protein that can bind with phosphorylated protein and selectively catalyzes peptidyl-prolyl cis/trans isomerization of phosphorylated Ser/Thr-Pro of proteins after they have been targeted by Ser/Thr-Pro directed kinases (Bayer *et al.*, 2003). Pin1 consists of two domains; the N-terminal domain called WW domain mediates protein-protein interaction and targets Pin1 to the nucleus. The residue Ser^{16} is involved in ther regulation. On the other hand, the C-terminal part domain of Pin1 is PPIase domain which is homologous to the FKBP domain in FKBP family proteins.

This domain catalyzes the peptidyl-prolyl isomerization of pSer/pThr-Pro moieties of the substrate. It was shown that in assay with phosphorylated Ser/Thr-Pro peptides, the WW domain of Pin1 is completely inactive, whereas the separated PPIase domain is 90% as active as the full-length protein. The WW domain has no PPIase activity, but it binds to the phosphorylated peptides with higher affinity than the PPIase domain does. There is no much binding affinity difference between full length Pin1 and WW domain of Pin1 toward peptide substrates, but the PPIase domain show moderate affinity or no affinity toward them. In binding studies with cellular substrates of Pin1, the WW domain was shown to be responsible for interaction and Pin1 PPIase domain does not bind any of the protein substrates. NMR solution structure shows that there is weak interaction between the WW domain and the PPIase domain in the full length Pin1, but the further study shows that the interaction between the two domains is regulated by different peptides. Pin1 can either behave as two independent domains connected by a flexible loop between the two domains or as a single intact domain with some amount of hinge bending motion depending on the sequence of the bound peptide (Jacobs *et al.*, 2003). It was shown that Pin1 interacts with phosphorylated Bcl-2, so the interaction between Pin1 and phosphorylated peptides from the loop region of Bcl-2 will be characterized (Basu et al., 2002).

1.5.4 FKBP38 could help Bcl-2/xL localize in mitochondria

In the mitochondria pathway Bcl-2 family proteins can activate or inhibit apoptosis (Kluck *et al.*, 1997, Basu *et al.*, 2002). During this pathway, some death stimuli can make some proteins such as Bik localized in the ER which can inhibit anti-apoptotic protein such as Bcl-2, and facilitates pro-apoptotic protein Bax to form channel, and Ca^{2+} release from ER (Bassic *et al.*, 2004). The Ca^{2+} and other factors can induce some other proteins or enzymes, which make Bak form channel in

mitochondria and cytochrome *c* can be released from mitochondria, then the down stream apoptotic pathway could be induced. Bcl-2 and Bcl-xL can block apoptosis by inhibiting cytochrome *c* releasing from mitochondria (Fig.1.4) (Adams, 1998, Yang *et al.*, 1997).

It was demonstrated that FKBP38 could help Bcl-2/xL localize at the mitochondria and inhibit apoptosis (Shirane *et al.*, 2003). FKBP38 could inhibit the Bcl-2 dependent apoptotic pathway. The endogenous FKBP38 could act as a docking molecule by attracting Bcl-2 and Bcl-xL to the mitochondria and the suppression of its function appear to result in the promotion of apoptosis through the mislocalization of these proteins (Shirane *et al.*, 2003).

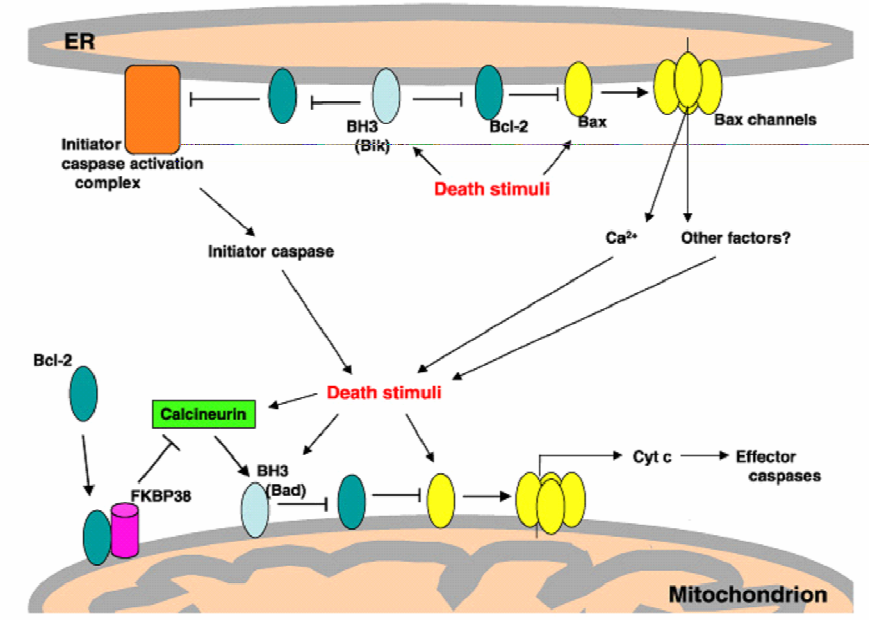

Copied from Germain *et al.*, 2003, Sci STKE., 173:10

Fig.1.4 The apoptotic pathway from ER to mitochondria

All three groups of the Bcl-2 family: anti-apoptotic proteins, pro-apoptotic proteins and BH3-only proteins have the potential to target mitochondria and ER. Death stimuli that are propagated and regulated by the Bcl-2 family and ERK might subsequently require amplification via mitochondria apoptotic pathways, which themselves can also respond directly to death stimuli. FKBP38 may play an important role in regulating Bcl-2 by affecting their localization on mitochondrion (Germain *et al.*, 2003).

1.5.5 FKBP38 promotes apoptosis by interaction with presenilins

Presenilins 1 and 2 (PS1.2) are multi-pass trans-membrane proteins localized predominantly in the endoplasmic reticulum (ER) and Golgi apparatus. Alzheimer's disease (AD), the most common cause of dementia in the elderly, is neuro-pathologically characterized by the prominent neuronal loss with astrogliosis and by the appearance of extracellular amyloid plaques and intracellular neurofibrillary tangels in the cerebral cortex (Wang *et al.*, 2005). The PS1/2 are highly homologous and consist of eight transmembrane domains and a large hydrophilic loop between transmembrane domain 1 and 7. Mutations in PS1/2 are responsible for the majority of autosomal dominant forms of familial Alzheimer's disease (FAD). Independent of the original cloning of PS1/2 as genes causing FAD, functional screening identified PS1/2 as an apoptosis-linked molecule. Meanwhile, PS1/2 are cleaved by activated caspase-3 family proteases during apoptosis in cultured cells. Similar to the ALG-3 polypeptide, over-expression of polypeptides corresponding to the C-terminal PS1/2 fragments generated by caspase cleavage inhibits apoptosis. These findings strongly suggest that PS1/2 are involved in the regulation of apoptosis under physiological and pathological conditions. Previous reports have shown an interaction between PS1 and Bcl-2 as well as between FKBP38 and Bcl-2 (Alberici *et al.*, 1999). It was observed that these membrane proteins are incorporated into macromolecular complexes. It was found that Bcl-2 coimmunoprecipitated with FKBP38 even in the absence of PS1/2, but a very small amount of Bcl-2 co-precipitated with PS1 or PS2 in FKBP38-depleted cell lysates. This result suggests that PS1/2 are associated with Bcl-2 mainly by binding with FKBP38. PS1/2 down-regulate the accumulation level of Bcl-2 and sequester Bcl-2 in the ER/Golgi compartments in an expression level-dependent manner. As a result, the amount of mitochondrial Bcl-2 increases in the absence of PS1/2 and decreases when over-expressing PS1/2 (Wang *et al.*, 2005).

PS1/2 shift Bcl-2 from the mitochondria to the ER/Golgi in an expression level-dependent manner. The pro-apoptotic activity of PS1/2 correlates well with the reduction in mitochondrial Bcl-2, and this can be antagonized by over-expression of FKBP38. Thus, PS1/2 competes with FKBP38 for regulation of the amount of mitochondrial Bcl-2, and this competition probably depends on the relative levels of FKBP38 and PS1/2. The more potent effect of PS2 (relative to PS1) may be due to its higher affinity for FKBP38 (Wang *et al*., 2005).

The pro-apoptotic activity of PS1/2 mainly depends on their binding with FKBP38 and a reduction of mitochondrial Bcl-2 for the following reasons. Firstly, over-expression of FKBP38 could neutralize the pro-apoptotic activity of PS1/2 by redistributing Bcl-2 from the ER/Golgi to the mitochondria. Secondly, in FKBP38-deleted cells, PS1/2 did not have the pro-apoptotic activity and effect on localization of Bcl-2. Finally, C-terminally truncated PS2 that lacks the binding site for FKBP38 had no effect on apoptosis susceptibility and Bcl-2 localization. So the accumulating result clearly showed the importance of FKBP38 in the PS1/2 involved Bcl-2 localization to ER (Wang *et al*., 2005).

1.6 FKBP38 protein belongs to FK-506 binding protein family

FKBP family members are the immunosuppressive drug FK-506 binding proteins. The FKBP family members have the following characteristics: FK-506 binding activity, PPIase activity and chaperone activity. Recently, an increasing number of FKBP family proteins have been identified and showed different functions in different tissues and cells. Most FKBP proteins are functional in the presence of their ligand (Fong *et al.*, 2003).

In 1989 two research groups found the intracellular target for the potent immunosuppressive drug FK-506 before introduced for experimental clinical use in

transplantation of organs (Harding *et al*., 1989, Siekerka *et al*., 1989). The principal intracellular target for the FK-506 is a soluble and abundant FK-506 binding protein with 12 kDa molecular weight (FKBP12). Using FK-506 gels, many isoforms of FK-506 binding proteins have been isolated from various mammalian organs such as FKBP 13, FKBP 25 and FKBP 52. Sequencing of the cDNA libraries of various mammalian sources have so far revealed 14 unique gene products containing FK-506-like binding domain. Plants and inverterbrates contain less diverse FKBPs and fungi and prokaryotic organisms express up to four different FKBPs (Adina *et al.*, 2002, Balat, 2000). FKBPs are ubiquitous with wide phylogenetic distribution and unique cellular localization. In FKBP family possessing PPIase activity or different FK-506 binding affinity is dependent on the structural features of the ligands and the conservation of the binding cleft (Galat, 2000). The FK-506, Rapamycin and cyclosporin A can act as a kind of immunosuppressive agents in the presence of their partners and they have the same mechanism which will be introduced in the following part (Clardy, 1995).

1.6.1 FKBP family proteins have chaperone activity

Chaperones are proteins that can recognize non-native proteins, preventing unwanted inter- and intra-molecular interaction and influence the partitioning between productive and unproductive folding steps. The chaperones do not form part of the final structure of the folded protein. There are many examples of FKBPs functioning as chaperons, the mammalian FKBP52, the wheat FKBP73 and Archaea bacteria FKBP (Breiman *et al*., 2002). Recently, some studies also shows that the FK-506 binding protein from malaria parasite has chaperone activity (Kumar *et al*., 2005, Monaghan *et al.*, 2005).

It was found that FKBP52 had chaperone activity *in vitro* by suppressing the aggregation of the chemically and heat denatured citrate synthase (CS). The chaperone activity was not inhibited by FK-506 or rapamycin suggesting that this activity is independent of the PPIase activity. FKBP52 also affects the reactivation of CS after thermally unfolding increasing the amount of reactivatable intermediates of CS (Boise *et al*., 1996). Wheat FKBP73 possesses chaperone activity being able to inhibit aggregation of CS. Recently the chaperone activity was shown for bacterial FKBPs and all cases reported, the chaperone activity was independent of PPIase activity (Breiman *et al*., 2002). So the FKBP family protein can regulate the function of other proteins by using the chaperone activities.

1.6.2 FKBP family proteins possess PPIase activity

The FK-506-binding proteins (FKBPs) belong to the large super-family of peptidyl prolyl *cis/trans* isomerase (PPIase), (EC 5.2.1.8) (Yu *et al.*, 2002, Reimer *et al.*, 1997, Galat, 2000). *Cis-trans* isomerization of peptidyl prolyl bonds is one of the rate-limiting steps in protein folding, and the PPIase, which includes cyclophilins, FKBPs and parvulins, are involved in the slow phases of protein folding and conserved in all organisms from Archebacterial to primate (Andrain *et al.*, 2002, Suzuki *et al.*, 2003, Ou, 2004). The PPIase was originally discovered as a helper enzyme for accelerating the restructuring of the polypeptide backbone, and it has a proline-directed binding capability proposed to be of exclusive biological importance (Fischer *et al*., 2000, 1998). Catalysis of the prolyl bond isomerization was discussed as a side effect attributable to the hydrophobic nature of the substrate binding site of the PPIase (Fischer *et al*., 1998, Stein, 1993). The FKBP domain has the PPIase activity, the PPIase activity may also be important for the chaperone activity of FKBP family proteins because it can change the *cis-trans* conformation of proteins.

1.6.3 Mechanism of FKBP family to be immunosuppressive agent

FK-506 is an immunosuppressive agent and used in preventing organ transplant rejection. It is effective only in the presence of its binding ligand FKBP members such as FKBP12. Its mechanism to induce immunosuppressive reaction is same as that of cyclosporine A (Yin *et al.*, 2003). One of the T cell activation pathways is the T cell receptor (TCR)-mediated signal transduction pathway (Constanzo, 2001). Antigen recognition by the TCR causes an increase in intracellular Ca^{2+}, which activates calmodulin and calcineurin B to bind to Ca^{2+}. The binding of activated calmodulin to calcineurin leads to a conformational change which allows the autoinhititory domain of calcineurin A to move away from the catalytic active site of calcineurin (Sugiura *et al.*, 2001). Nuclear factor of activated T cells (NF-AT) protein is phosphorylated and make it retain in the cytoplasm. Calcineurin dephosphorylates the NF-AT. The dephosphorylated NF-AT is translocated into the nucleus to activate transcriptions such as interleukin (IL)-2 (Abraham *et al.*, 1996). Immunosuppressant CsA is bound to cyclophilin, while FK-506 is bound to FKBP. In the presence of the FKBP-FK-506 or CsA-cyclophilin complex (Siekerka *et al.*, 1989, Vekrellis *et al.*, 1992), it will inhibit calcineurin, thereby preventing the dephosphorylation of NF-AT that is required for IL-2 gene expression and T cell activation (Fruman *et al.*, 1994), Cyclosporin A or FK-506 can make calcineurin inactive by forming complex with cyclophilin or FKBP respectively (Fig.1.5). During this step, FKBP family member does not bind with calcineurin directly. They are using the drug FK-506 as a kind of bridge, which can ligate the FKBP family members with calcineurin, which can not make the substrate interact with the active site of calcineurin so that the activity of calcineurin can be inhibited.

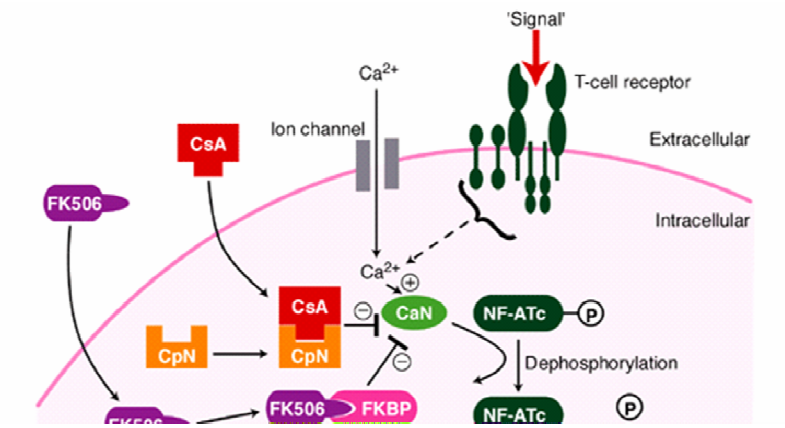
'Signal'
Ca^{2+}
T-cell receptor
Ion channel
Extracellular
CsA
FK506
Intracellular
Ca^{2+}
CsA
CaN
NF-ATc
P
CpN
CpN
Dephosphorylation
FK506
FKBP
NF-ATc
P

and Cyclophilin 40. The Homology to FKBP12 and 52 are about 35, 32%, respectively (Lam *et al.*, 1995). FKBP38 has some differences from many of the other FKBPs. It lacks the well-conserved Trp^{59} of FKBP12, having instead a Leu at the corresponding position (residue 98). The Trp (or Phe in FKBP12.6) is important for the interaction with FK-506 and forms the base of the hydrophobic drug-binding cavity. FKBP38 also lacks the highly conserved Phe corresponding to aa 36 of FKBP12, having instead a Val (aa 79) at that position. The FKBPs are PPIases that catalyzes the *cis-trans* isomerization about the peptidyl-prolyl bonds in peptides and proteins. In FKBP12 replacement of the Phe^{36} by a Tyr residue results in significantly lower PPIase activity. A predicted α-helical region in FKBP38 is characterized by the presence of a Leu residue at every seventh position and is confirmed that a consensus leucine zipper spans three amino acids. The Leu residues may form a hydrophobic surface that becomes the region of contact between paired helices.

Alignment of FKBP38 with FKBP52 shows significant identity between the two proteins. FKBP52 is a heat shock protein (Hsp59) and found to be associated with non-transformed steroid receptor heat shock protein 90 (Hsp 90) and its 3 D structure has been solved by X-ray crystallography. It contains two FKBP12-like domains. One FKBP12-like domain of the FKBP38 is similar to the N-terminal FKBP12-like domain of FKBP52 (Davies *et al.*, 2005). The 40 kDa cyclophilin 40 (CyP40) has been found to be associated with non-transformed steroid receptors. CyP40 and FKBP52 have a three-unit tetratricopeptide repeat (TPR) and a putative camodulin-binding site. The TPR motif is a 34-amino acids block of variable sequence which has defined a family of proteins involved in cell cycles regulation, RNA synthesis, neurogenesis, protein transport, Ser-Thr dephosphorylation and heat-shock response. The C-terminal half of FKBP38 shares homology with the C-terminal halves of both

CyP40 and FKBP52. FKBP38 also have 3 TPR which are not fully conserved 34-aa TPR motifs. All the TPR domains in FKBP38 contain many of the basic elements used to define the TPR consensus sequence. These features include the presence of a small, unchanged aa at position 5, 17 and 24, a hydrophobic aa at position 1, 4, 7, 14, 18 and 25, the presence of an aromatic aa at position 21 and the presence of a Pro at position 29. The second and the third TPR domains of FKBP38 are in better agreement with the TPR consensus sequence that is the corresponding domains in FKBP51 and FKPB52 (Sinars *et al.*, 2003). Like leucine zippers, TPR elements are thought to form coiled-coil structures. The presence of these regions suggests that FKBP38 might form homomultimers with itself or interact with other proteins (Lam *et al.*, 1995).

Studies showed that FKBP38 could be chaperone protein for Bcl-2 and Bcl-xL and help them localized to the mitochondria. It neither has PPIase activity nor FK-506 binding activity. Recently, it was demonstrated that the FKBP38 is an endogeneous inhibitor of calcineurin. It was also shown that Ca^{2+}/calmodulin interacts with FKBP38 and activate the PPIase activity of FKBP38 (Eddicle *et al.*, 2005). Surprisingly, PS1/2, which is thought to be associated with the onset of FAD, forms complex with FKBP38 and Bcl-2 (Wang *et al.*, 2005). In view of this, the biological function of FKBP38 appears to be diverse and multi-purpose. The protein-protein study was performed using co-expression and NMR titration methods, which provides the possibility of a role of FKBP38 in regulation of apoptosis through its interaction with Bcl-2 and other proteins.

1.7 Objective of my thesis

FKBP38 is a unique protein among its family and may be a representative of a new class and appears to be an important regulator of anti-apoptotic protein Bcl-2.

The biochemical characteristics of FKBP38 are still unknown and there is no direct evidence to explain why this protein does not interact with FK506 except the information from the amino acids sequence alignment. The molecular characteristics and nature of the interaction between FKBP38 and Bcl-2 currently remain to be defined. Phosphorylation of Bcl-2 may cause its conformational change so as to interact with Pin1, but detail evidence needs to be provided. To answer these questions, the structural and biochemical study on FKBP38, Bcl-2 and their interaction can provide information to understand the mechanism of Bcl-2 regulation and characteristics of FKBP38, which can provide more information regarding the regulation of Bcl-2.

In summary, our project is as follows: First, cloning, expression and purification of proteins such as FKBP38, FKBP12, Pin1, Bcl-2, Bcl-xL and kinases. Second, characterization of interaction between FKBP38 and Bcl-2. Third, phosphorylaiton and de-phosphorylation study on the loop region of Bcl-2. Forth, structure study on the peptides from the loop region of Bcl-2. Fifth, characterization study on FKBP38, structure study on the N-terminal domain (NTD) of FKBP38 by NMR and its insights for the regulation by calmodulin/Ca^{2+} complex.

The bacterially-produced recombinant FKBP38 was stable, and CD, NMR studies indicated that the protein was folded. A biochemical function of FKBP38 emerged from *in vitro* studies that employed the citrate synthase aggregation assays during thermal denaturation, suggesting that chaperone activities of FKBP38 and this chaperone activities were further supported by showing an effect of FKBP38 on the solubility of Bcl-2 when they are co-expressed. From the NMR results and calcineurin assays *in vitro*, we found that the N-terminal fragment of FKBP38 which contains the FK-506 binding domain does not bind FK-506 at molecular level nor inhibits the

phosphatase activity of calcineurin.

Bcl-2 contains a long and disordered loop between BH4 and BH3 regions. It is expected that the disordered loop of proteins is associated with those interacting proteins and undergoes conformational change or protects it from cellular proteases (Ciechanover, 1994). In our studies, to characterize the molecular interaction and further define the binding sites, we studied several truncation mutants of Bcl-2 in the flexible loop region of Bcl-2. It demonstrated that the flexible loop of Bcl-2 is responsible for the molecular interaction with FKBP38. Bcl-2 is phosphorylated in response to a variety of stimuli, and it was shown that the phosphorylation is restricted to the flexible loop (Huang, *et al.*, 2002). The biological functions of cellular proteins are modulated by the posttranslational modification such as phosphorylation. Our studies showed that the phosphorylation and dephosphorylation of Bcl-2 is dynamic and modulated by selective protein kinases and phosphatases. The phosphorylation of Bcl-2 showed the reduced affinity to FKBP38, suggesting a potential role of relevant kinases and phosphatases in the molecular interaction between FKBP38 and the flexible loop of Bcl-2.

To define the molecular and structural basis of FKBP38 and insight of its molecular recognition with Bcl-2 and other associating proteins, we determined the NMR three-dimensional structure of the N-terminal fragment of FKBP38 (FKBP38NTD). The structural information revealed that the overall topology of FKBP38NTD is similar to that of the typical FKBP domain, but some differences were observed in the FK-506 binding pocket. Another interesting finding was that FKBP38NTD appears to interact with the putative calmodulin binding site of FKBP38, which provides the insight for the regulation of FKBP38 by Ca^{2+}/calmodulin.

2 Materials and Methods

2.1 Materials

2.1.1 Chemicals

Antibodies against Bcl-2 (N-19), 6 his tag, GST and Bcl-xL were purchased from Santa Cruz Biotech (Santa Cruz, CA, USA). Antibody against human FKBP38 was a kind gift from Prof. Keiichi I. Nakayama. Ni^{2+}-NTA resin, RNeasy Mini Kit, plasmid purification kit, PCR purification kit, gel extraction kit *Escherichia coli* BL21 (DE3), Dulbecco's Modified Eagle Medium (DMEM) and carbenicillin were from Qiagen (Hilden, Germany) and Invitrogen (Carlsbad, CA, USA). The dNTP (dTTP, dATP, dGTP and dCTP) mixtures were purchased from invitrogen or Finnzymes (Espoo Finland). Immun-Star Chemiluminescent protein detection system and protein molecular weight marker were from Bio-Rad Laboratories (Hercules, CA, USA). C-Jun-N-terminal Kinase 1α1 (JNK) was from Upstate (Lake Placid, NY, USA). γ-^{33}P-ATP and ^{32}P-ATP (3000 Ci/mmol), HiPrep 16/60, 26/60 Sephacryl S-200, 26/60 sephacryl S-100 and Bulk and RediPack GST Purifcation Module were from Amersham Biosciences (Buckinghamshire, UK). Phenylmethylsulfonyl fluoride (PMSF), Reverse transcription-polymerase chain reaction (RT-PCR) kit, restriction enzymes, T4 ligase, 1, 4-Dithiothreitol (DTT), Protease inhibitors complete-mini protease tablets and expand long PCR system were from Roche (Indianapolis, IN, USA). Ethylene glycol-bis-(β-aminoethyl ether) - N, N, N´, N´-tetraacetic acid (EGTA), lysozyme were purchased from Sigma-Aldrich (St. Louis, Mo, USA). The DNA polymerase pfu and site directed mutation kit were purchased from Novagen (Madison, WI, USA). Synthetic Dropout (SD) medium was from Clontech (Palo Alto, CA, USA). Isoporpyl-Thio-B-D-galactopyranoside (IPTG) was from Promega

(Madison, WI, USA). All the other chemicals were of high purity and purchased either from Sigma, Merk or BioRad. FK-506 (Tacrolimus) was purchased from LC Laboratories (MA, USA). Ampicillin and kanamycin Sulfate were purchased from US Biological (Massachusetts, USA) or Invitrogen. The X-gal (1-Bromo-4-Chloro-3-indolyl-β-D-galactopyranoside) was from Bioline (Luckenwalde Germany). Econo Column was from Bio-RAD. Bacterial Alkaline Phosphatase was from Fermentas. The chemicals for NMR experiment such as D_2O, ^{13}C labeled glucose, ^{15}N labeled NH_4Cl were from Chambrige isotope. Cell lines were from American Type Culture Collection (Manassas, VA). MitoTracker® Deep Red 633 and Prolong Antifade reagent, Alexa Fluor® 546 goat anti-rabbit IgG were from Molecular Probes (Eugene, OR, USA).

2.1.2 Bacterial strain, yeast strain and mammalian cell lines

Different bacterial strains were used in the study. DH5α was used for the plasmid purification and protein expression if the pGEX plamid is used. XL1-blue was purchased for the site directed mutation experiment. *E.coli* (Escherichia coli) BL21 (DE3), BL21 (DE3) PlysS and Codon Plus RLP were used for the protein expression. The yeast strain *Saccharomyces cerevisiae* PJ69-4A (*MATa his 3 leu 2 ura 3 trp 1 gal4Δ gal 8Δ met 2::GAL7-lacZ GAL2-Ade 2 LYS2::GAL1-his 3*) was used for the yeast two-hybrid system for the analysis for protein-protein interaction. Cancer cells Hela and MCF-7 were used for the analysis of protein expression and mRNA purification.

2.1.3 Vectors

Different plasmids were used for the expression of protein in *E.coli*. For pET series of vectors which contain *T7* promoter were used for expression in BL21 (DE 3) cells and the pGEX and other vectors which contain *Tac* promoter were used for the

expression in DH5 α. The following table (Table 2.1) gives the name of commercial plasmids and their application. The resulting plasmids containing different genes will be listed later.

Table 2.1 Plasmids used in the study

Vector Name	Resistance	Expression Host	Remarks
pET29b	Kan	BL21 DE 3	Protein expression. Generate C-his tag fusion proteins
pET16b	Amp	BL21 DE 3	Protein expression. Generate N-his tag fusion proteins
pACYC184	Chloramphenicol	BL21 DE 3	For the protein co-expression system
pGEX-4T-m1	Amp	DH5 α	Protein expression to generate GST fusion protein
pcDNA3.1	Amp	Mammalian cell	Protein expression
pACT2	Amp	Yeast	Yeast two-hybrid system
pAS2-1	Amp	Yeast	Yeast two-hybrid system
pCL1	Amp	Yeast	Yeast two-hybrid system
pACDUT	Amp	BL21 DE3	Co-expression system
pETDUT	Amp	BL21 DE3	Co-expression system

2.1.4 Primers used for PCR reaction

The oligodeoxyribonucleotides were used for PCR amplification, site directed mutagenesis, sequencing, deletion mutagenesis shown in Appendix. Restriction sites introduced by the PCR primers are labeled.

2.1.5 DNA molecular size markers

The DNA molecular ladders were purchased from Bio-Rad, New England Biolad and other companies.

2.1.6 Protein molecular weight markers

The protein standard was purchased from BioRad. And the pre-stained molecular weight was used for western blot analysis, it can be used as a indicator not only to check the molecular weight, but also to show if the proteins are transferred to the

membrane. The protein standard for the SDS-PAGE contains the following fractions: myosin 200 kDa, galactosidase 116.25 kDa, phosphorylase b 97.4 kDa, Serum albumin 66 kDa, Ovalbumin 45.0 kDa, Carbonincanhydrase 31.0 kDa, Trypsin inhibitor 21.5 kDa, Lysome 14.4 kDa, Aprotinin 6.5 kDa. The Prestained SDS-PAGE standard containing Phosphorylase B 113 kDa, Bovine serum albumin 92.0 kDa, Ovalbumin 52.3 kDa, Carbonic anhydrase 35.3 kDa, Soybean trypisn inhibitor 28.7 kDa, Lysozyme 21.3 kDa.

2.1.7 Medium (Sambrook *et al*)

2.1.7.1 Antibiotics stocks

Ampicillin (100 mg/ml in dd H_2O, 100 µg /ml working solution), kanamycin (30 mg/ml in *dd* H_2O, 30 ug/ml working solution), Chloramphenicol (15 mg/ml stock in ethanol, 15 ug/ml working solution).

2.1.7.2 Luria-Bertani(LB) medium

10 g bacto-tryptone, 5 g bacto-yeast extract, 5 g NaCl, in 1000 ml dd H_2O, autoclave.

2.1.7.3 LB agar plates

In the LB medium, 2% agar was added and autoclaved. Plates were poured when the LB agar temperature reaches about 50-60 ℃.

2.1.7.4 SOC medium

2% Bactotryptone, 0.5% yeast extract, 10 mM NaCl, 2.5 mM KCl, 10 mM $MgCl_2$, 10 mM $MgSO_4$, 20 mM Glucose, add H_2O to 1000 ml and autoclave.

2.1.7.5 M9 medium (mineral medium)

The M9 medium was made according to the following ways. After autoclave all the component first, the components were mixed before use. To make 1 L of M9 medium, the following components were added into an autoclaved bottle: 52.7 ml 1 M Na_2HPO_4, 26.5 ml 1 M KH_2PO_4, 2 ml 5 M NaCl, 1.2 ml 1 M $MgSO_4$, 1.2 ml 100

mM $CaCl_2$, 1.2 ml 0.5%(w/v) thiamine HCl, 22.7 ml 20% glucose, 1 ml antibiotic (1000× stock), 22 ml 1M NH_4Cl, added autoclaved water to 1 L.

2.1.7.6 YPD medium

20 g/L Difco peptone, 10 g/L Yeast extract, 20 g/L Agar (for plates only). For adenine-supplemented YPD (YPDA), add 15 ml of a 0.2% adenine hemisulfate solution per liter of medium (final concentration is 0.003%, in addition to the trace amount of Ade that is naturally present in YPD). Adenine hemisulfate tolerates autoclaving. Add H_2O to 950 ml. Adjust the pH to 6.5 if necessary, then autoclave. Allow medium to cool to ~ 55 ˚C and then add dextrose (glucose) to 2% (50 ml of a sterile 40% stock solution). Adjust the final volume to 1 L if necessary.

2.1.7.7 SD medium

It contains 6.7 g Yeast nitrogen base without amino acids, 20 g Agar (for plates only), 850 ml H_2O, different DO Supplement. Adjust the pH to 5.8 if necessary and autoclave. Allow medium to cool to ~ 55 ˚C before adding 3-AT to 2 mM and glucose stock to 2%.

2.1.7.8 3-AT stock solution

Prepare 1 M 3-AT (3-amino-1,2,4-triazole; Sigma #A-8056) in dd H_2O and filter sterilize. Store at 4ºC. Store plates containing 3-AT sleeved at 4˚C for up to 2 months.

2.1.8 Buffers and solutions

2.1.8.1 Solution and buffer for agarose gel

TAE (Tris-acetate-EDTA, 50×)

Prepare a 50× stock solution in 1 liter of H_2O: 242 g of Tris base, 57.1 ml of glacial acetic acid, 100 ml of 0.5 M EDTA, pH 8.0.

Agarose gel

1% (w/v) agarose in 1× TAE and heated in microwave for several minutes.

6×DNA loading buffer

0.25% (w/v) bromophenol blue, 0.25% (w/v) xylene cyanol FF, 40% (w/v) sucrose in H_2O, Stored at 4°C.

Ethidium bromide (EB)

10 mg/ml stock in H_2O.

2.1.8.2 Buffers for Ni^{2+}-NTA purification

Resuspension buffer

20 mM phosphate buffer (pH 7.8), 0.5 M NaCl, 5 mM 2-mercaptoethanol.

Washing buffer

20 mM phosphate buffer (pH 7.2), 1 M NaCl, 20 mM imidazole, 5 mM 2-mercaptoethanol.

Elution buffer

20 mM phosphate buffer (pH 6.0), 0.5 M NaCl, 0.5 M imidazole, 5 mM 2-mercaptoethanol.

2.1.8.3 Buffers for FPLC purification

Gel filtration buffer

50 mM Tris-HCl, pH 8.0, 150 mM NaCl, 1 mM DTT, 0.01% NaN_3.

50 mM Tris-HCl, pH 7.5, 150 mM NaCl, 1 mM DTT, 0.01% NaN_3.

50 mM Na-PO_4, pH 7.0, 150 mM NaCl, 1 mM DTT, 0.01% NaN_3.

Ion exchange buffer

Buffer A: 50 mM Tris-HCl, pH 8.0, 1 mM DTT, 0.01% NaN_3.

Buffer B: 50 mM Tris-HCl, pH 8.0, 1M NaCl, 1 mM DTT, 0.01% NaN_3.

2.1.8.4 SDS-PAGE buffers

5×Tris-glycine electrophoresis buffer

5×25mM Tris (15.1g/L), 5×250 mM glycine (94g/L) pH 8.3, 5×0.1% SDS (50 ml

10% SDS stock/L)

SDS-PAGE gel-loading buffer (2×)

100 mM Tris-Cl (pH 6.8), 200 mM dithiothreitol, 4% SDS, 0.2% Bromophenol blue, 20% (v/v) glycerol, Stored at -20°C.

30% arylamide mix

Dissolve 29g acrylamide and 1g N,N'-methylene-bioacrylamide in about 70 ml water, then adjust to 100ml. the pH should be or less than 7.0. Store at 4°C.

10% ammonium persulfate

Dissolve 1g ammonium persulfate in 10 ml water. Store at 4°C.

Destain solution

Mixing the following parts; Methanol: H_2O: glacial acetic acid= 450:450:100

Stain solution

Dissolve 0.25% Brillant Blue R-250, 0.25g in 100ml of destaining solution.

Gel storage buffer

5% methanol, 7.5% glacial acetic acid.

2.1.8.5 Western-blot buffers

Membrane transfer buffer

3.03g Tris, 14.4 g glycine, add water to 1L. Do not adjust pH!

Tris-buffered saline (1× TBS)

(20 mM Tris, 500 mM NaCl, pH 7.5) If using Bio-Rad liquid concentrate 10× TBS, add 110 ml of 10×TBS to 990 ml of water.

Wash solution (TTBS)

(20 mM Tris, 500 mM NaCl, 0.1% Tween-20, pH 7.5) Add 0.8 ml of Tween-20 to 800 ml of 1× TBS.

Blocking solution

(0.2% non-fat dry milk in TBS) Add 0.2 g of non-fat dry milk to 100 ml of 1×TBS.

Antibody buffer

(0.2% non-fat dry milk in TTBS) Add 0.4 g of non-fat dry milk to 200 ml TTBS. Stir until dissolved.

2.1.8.6 Other stock buffers

1 M Tris buffer pH 8.0

Weigh 121.12 g Tris to 800 ml dd H_2O and using HCl (~50 ml) adjust pH to 8.0, and then adjust to 1000 ml.

1M Tris buffer pH 7.5

Weigh 121.12 g Tris to 800 ml dd H_2O and using HCl (~66 ml) adjust pH to7.5, and then adjust to 1000 ml.

5 M NaCl

Weigh 292 g NaCl into 1000 ml, filter through 0.2 mm membrane.

Phosphate Buffer (Deutscher, 1990)

A: 0.2 M NaH_2PO_4, weigh 27.8 g in 1000 ml dd H_2O.

B: 0.2 M Na_2HPO_4, weigh 28.4 g in 1000 ml dd H_2O.

Mix A and B in the following table to get the different pH stock buffers.

Table 2.2 The table for making different pHs phosphate buffers

A(ml)	B(ml)	pH	A(ml)	B(ml)	pH
93.5	6.5	5.7	45.0	55.0	6.9
92.0	8.0	5.8	39.0	61.0	7.0
90.0	10.0	5.9	33.0	67.0	7.1
87.7	12.3	6.0	28.0	72.0	7.2
85.0	15.0	6.1	23.0	77.0	7.3
81.5	18.5	6.2	19.0	81.0	7.4
77.5	22.5	6.3	16.0	84.0	7.5
73.5	26.5	6.4	13.0	87.0	7.6
68.5	31.5	6.5	10.5	90.5	7.7
62.5	37.5	6.6	8.5	91.5	7.8
56.5	43.5	6.7	7.0	93.0	7.9
51.0	49.0	6.8	5.3	94.7	8.0

2.1.8.7 Solutions used for Ni^{2+}-NTA regeneration

6M guanidinium chloride/0.2M acetic acid

Weigh appropriate guanidinium chloride to dd H_2O and add some acetic acid (17.4M) to get final solution.

2 %(w/v) SDS

Weigh 2 g SDS in 100 ml H_2O and dissolve it. Do not put it on ice.

2.1.8.8 Solutions used for regeneration of Glutathione Sepharose 4B

Washing buffer 1: 0.1 M Tris-HCl, 0.5 M NaCl, pH 8.5.

Washing buffer 2: 0.1 M sodium acetate, 0.5 M NaCl, pH 4.5.

PBS: 140 mM NaCl, 2.7 mM KCl, 10.1 mM Na_2PO_4, 1.8 mM KH_2PO_4, pH 7.3.

2.1.8.9 Crystallization buffer

The plates (24-well polysterene trays for hanging drop method), grease, siliconised cover slides and the crystallization screen kits were all purchased from Hampton Research.

2.1.8.10 Buffers for yeast two-hybrid

Z buffer

The following components were used: Na_2HPO_4• $7H_2O$ 16.1 g/L, NaH_2PO_4• H_2O 5.50 g/L, KCl 0.75 g/L, $MgSO_4$ • $7H_2O$ 0.246 g/L. Adjust to pH 7.0 and autoclave. The solution can be stored at room temperature for up to 1 year.

10× Stop Solution

1 M Na_2CO3 in deionized H_2O (Sigma #S7795).

ONPG (o-nitrophenyl b**-D-galactopyranoside;** Sigma #N-1127**)**

4 mg/ml in Z buffer. Adjust to pH 7.0 and mix well. It requires 1-2 hr to dissolve ONPG.

1× NaOAc

0.5 M sodium acetate, pH 4.5 (Sigma #S7545).

10× TE buffer

0.1 M Tris-HCl, 10 mM EDTA, pH 7.5, autoclave.

50% PEG 3350

(Polyethylene glycol, average molecular weight=3,350, Sinama, #P-3640) prepared with sterile deionized H_2O.

100% DMSO (Dimethyl sulfoxide from Singma, #D-8779)

10× LiAC

1 M lithium acetate, adjust pH 7.5 with dilute acetic acid and autoclave.

2.2 Methods

2.2.1 Growth of strains

Bacteria were grown on plate or liquid medium at 37 ℃, for the induction case, the temperature is different. Yeast cells were incubated in YPD or SD medium at 30 ℃.

2.2.2 Making competent cells by $CaCl_2$

A colony was picked up from LB plate and inoculated into a 2ml LB medium and cultured at 37°C overnight. 2 ml of a fresh LB overnight culture was inoculated into 50 ml of fresh LB medium and incubated in shaking incubator at 37°C to A_{600} of 0.4 - 0.5, not more than 0.8. The culture was transferred to sterile centrifuge bottles and immediately put on ice. The cells were spun down at 2600 g (5500rpm) at 4 °C for 10 minutes. The cells were resuspended in 25 ml of **ice cold** sterile 100 mM $MgCl_2$.

The cells were spun down at 2600 g (5500rpm) for 10 minutes at 4°C. The supernatant was decanted and the cells were resuspended in 5 ml of **ice cold** sterile 100 mM $CaCl_2$ for 2 hours to become transformation competent ones. Or the cells can be put at 4°C overnight. 2 ml sterile ice cold 50% glycerol was added into the cells and mixed briefly. **Make sure cells remain cold at all times.** 200 µl aliquot of the cell suspension was put into every ice cold tube and stored at -80°C. Note: Keep

$CaCl_2$ and $MgCl_2$ on ice at all times.

2.2.3 Transformation DNA to *E.coli*

20 µl of competent cells was added into the tube (ice cold). 1 µl plasmid DNA (or dilution) was added into the tube and incubated on ice for 30 min. The tube was heated for 45 second at 42 °C and quickly put on ice for 1-2 min to cool to R.T. 1ml SOC medium was added into the tube and incubated in 150rpm shaker at 37 °C for 1 hr. 200 µl of the culture was plated on LB/antibiotic and incubated O/N at 37°C.

2.2.4 Isolation of plasmid DNA

The bacteria were incubated in 2 ml LB with antibiotic overnight and the plasmid was purified according to the manual provided by the plasmid purification kit.

2.2.5 DNA electrophoresis

1% agarose gel was made and EB was added to final concentration of 0.1-0.5 ug/ml. Samples were loaded into the gel soaked in 1× TAE buffer and run the gel at 100 V for 20-30 min. Stop running when the dyes come to the half of the gel. Put the gel under UV to visualize the bands.

2.2.6 Extract DNA from the agarose gel

Samples were loaded into the 0.8% agarose gel and run it for separation. The DNA band should be cut off from the gel and the DNA fragment in the gel can be purified according to the manual provided with the gel extraction kit.

2.2.7 Extraction of mRNA from Hela and MCF-7 cell line

Human cervical cancer Hela cells and breast cancer MCF-7 cells were cultured in DMEM medium supplemented with 10 % fetal calf serum and cultured at 37 ºC with 5% CO_2. The cells were harvested and centrifuged by centrifuging at 500× g for 10 min to collect the pellet, after washing with PBS and the total RNA or mRNA purification was performed according to the manual provided with the RNA

purification kit.

2.2.8 Polymerase Chain Reaction (PCR) amplification

The DNA polymerase Tag polymerase or *pfu* Turbo polymerase were used for the PCR amplification to get DNA fragment for cloning. The Tag polymerase was used for the colony PCR, which is used for checking the ligation product. The PCR reaction was performed as follows (50 µl reaction volume): 5 µl 10× reaction buffer, 0.5 µl 10 mM dNTP mixture, template plasmid, 1 µl 10 uM forward primer, 1 µl 10 uM reverse primer, 1 U of polymerase or different amount according to the manual provided by the company, add pure water to 50 ul. The mixture was added into the thin-wall 0.2 ml PCR tube and put into GneeAmp® PCR system 9700 from Applied Biosystems for the reaction. Reaction was performed using the following procedure: 95 ºC 3 min, 95 ºC 30 sec, 50-60 ºC, 45 sec, 72 ºC for tag polymerase or 68 ºC for *pfu* polymerase for some time (1kb/min), which is dependent on the size of the PCR product. Generally 25 cycles were used for the reaction.

For site-directed mutation PCR reaction, the special primers were mixed with the template, all the components were same as the general PCR, only difference is that the annealing temperature is 55ºC and *pfu* tubo was used for the reaction. Also, the PCR cycle is 18 instead of 25.

2.2.9 RT-PCR

RT-PCR was used to amplify the cDNAs. The reverse transcription reaction was performed by using reverse transcription kit purchased from Invitrogen. Total mRNA was purified from MCF-7 cell line with mRNA purification kit from Qiagen. The RT-PCR reactions were performed according to the protocol from company. The RT-PCR kit was purchased from Roche. The RT-PCR was performed according to the following way (the PCR tube contains the following components).

10 × amplification buffer	2 ul
20 mM solution of dNTPs	1 ul
Reverse primer	1 ul
20U/RNase inhibitor	1 ul
100 mM DTT	2 ul
Reverse transcriptase	1 ul
Template	2 ul
H_2O	To 20 ul

Put the tube at 65 °C for 10 min and put on ice, after adding reverse transcriptase the tube will be at 42 °C for 1 h. The R.T. product can be used as template for the PCR reaction.

2.2.10 Cloning the PCR product into plasmid

The plasmid was purified with the plasmid purification kit. The plasmid was digested with different restriction enzymes according to the manual provided by the company. After put the digestion mixture at 37 ℃ for 2-3 hours, the digestion product was loaded into the agarose gel and the band was cut from the gel. The purified band was used for the ligation with PCR product. The PCR amplified product was purified with PCR purification kit and the purified product was digested with restriction enzymes which were same as that used for the digestion of plasmid. After purification with PCR purification kit, the PCR digestion product was ligated with digested plasmid. Generally 20 μl volume of ligation system was used and the ratio between plasmid and the PCR product is 1:3. The T4 ligase was used and ligation condition was at room temperature for 3 hours or 4 ℃ overnight. The ligation product was transformed into DH5α and colony PCR can be performed to get the positive colony.

2.2.11 Quotation of DNA

The concentration of DNA or RNA can be measured using the following way: Purify the DNA by suitable ways; Dilute the sample with TE buffer, the dilution time should be decided according to the concentration of the DNA. Measure the OD_{260} with the spectrophotometer. The DNA concentration can be calculated by the

following equation: DNA concentration (ug/ul) = OD_{260}×(dilution factor)×A/1000; A has different values according to the samples: A=50 ug/ml for double stranded DNA or plasmid; A=33 ug/ml for single stranded DNA ; A=40 ug/ml for single stranded RNA.

The ratio of OD_{260}/OD_{280} should be determined in order to assess the purity of the sample. If the ratio is 1.8-2.0, the absorption should be due to nucleic acids. A ratio less than 1.8 indicates that there may be proteins or/and other UV absorbers in the sample, in which case it is advisable to re-precipitate the DNA. A ratio higher than 2.0 indicates the sample may be contaminated with chloroform or phenol and should be re-precipitated with ethanol.

2.2.12 Site-directed and deletion mutagenesis

The site-directed mutagenesis and deletion mutations were performed by using the site-directed mutation kit. Generally the following steps were used for the reaction. First the PCR using *pfu* tubo was performed and the PCR product was purified with the PCR purification kit. One µl of *Dpn I* restriction enzyme was added into the PCR product to remove the template DNA, the resulting product can be directly transformed into XL1-blue competent cells and cultured on the LB plate containing both *Tel* and other antibiotic. The colony PCR was performed to check the positive colony.

2.2.13 Colony PCR screening

In order to know if the PCR product is inserted into the vector, the colony screen by PCR was performed using the liquid culture as template. The PCR screen was performed as follows: the ligation product was transformed into competent cells and spred onto LB/ with antibiotic selection plates. The colonies were inoculated into the LB liquid with antibiotic individually and cultured at 37 ºC, 250 rpm for some time,

when the OD_{600} of the culture get to about 0.8, 2 µl of the culture was used as template for the PCR reaction. *Taq* polymerase was used as the amplification enzyme and the primers for amplifying the insert were used as primers. Only the bacteria containing the ligation product can be amplified by PCR. After confirmed the positive colony, its liquid culture will be used for the plasmid purification and for further sequencing.

2.2.14 Small scale protein induction

The plasmid containing different target gene was transformed into BL21 DE 3 (for *T7* promoter plasmid) or DH5α (containing *Tac* promoter) and cultured on the LB plate with antibiotic. A single colony was inoculated into LB/antibiotic and cultured at 37 ºC, 250 rpm, when the OD_{600} get to 0.6-1.0, IPTG was added to 1 mM final concentration, then the cells were cultured for another 2 hours. The cells were mixed with SDS-loading dye and heat at 100 ºC for 10 min and loaded into SDS-PAGE for analysis.

2.2.15 Large scale protein induction

A single colony was inoculated into 25 ml LB with antibiotic in 125 ml flask and cultured at 37 ºC, 250 rpm overnight, 5 ml of the overnight culture was transferred into 500 ml LB medium with antibiotic in a 2 L flask and cultured at 37 ºC, 250 rpm. IPTG was added to 1 mM final concentration when the OD_{600} get to 0.6-1.0, and the induction was performed at 30 ºC, 250 rpm for 2-3 h. The cells were harvested by centrifuging at 8000× g for 5 min for protein purification. The cell pellet can be stored at -80ºC for the purification later.

2.2.16 Cell lysis

Cell pellets were broken by sonication. Cells were first completely resuspended in Resuspension buffer (1g pellet adding with10 ml respension buffer) and 0.1 mg/ml

lysozyme was added to ease cell breakage. The cells solution was incubated on ice for 30 min, cell were sonicated for 20 min at 20% power. In order to confirm if the cells were broken completely, protein concentration was measured in the supernatant, if there is no increase in protein concentration when the sonication time is extended, the sonication should be finished.

2.2.17 Purification of protein by Ni^{2+}-NTA affinity column

The sonicated cell lysate was cleared by centrifuging at 20, 000× g for 30 min; the supernatant was used for further purification. The Ni^{2+}-NTA resin was loaded into the disposable column from BioRad, 1 ml resin was used for the purification. About 10 ml of resuspension buffer was used to equilibrate the resin to remove the resin storage buffer. The supernatant obtained from the lysate was loaded to the column and then followed by 30-40 ml washing with washing buffer to remove the unspecific binding proteins. To elute the His tag fusion protein, 5 ml of elution buffer was used. The elusion fractions were loaded into SDS-PAGE for analysis. During this purification step, DTT or EDTA can not be used in any of the buffers.

2.2.18 Regeneration of NTA-Ni^{2+} agarose

NTA-Ni^{2+} agarose can be reused almost indefinitely if it is washed well and regenerated. If the resin has been oxidized or depleted (loss of light blue color or appearance of yellow/brown color), it is better to be washed with 0.2 M acetic acid in 30% glycerol. The following steps should be used for the regeneration of the resin: First wash the column successively with 2 volumes of 6M guanidinium chloride/0.2M acetic acid (or other stripping reagent); add 5 volumes of H_2O; then 2 volumes of 2% SDS; wash it with 1 volume of 25%, 50% and 75% ethanol; 5 volumes of 100% ethanol; wash it with 1 volume of 75%, 50% and 25% ethanol; 1 volume of H_2O; 5 volumes of 100 mM EDTA; 1 volume of H_2O; regenerate the column with <2

volumes of 0.1 M $NiSO_4$, wash it with H_2O, and equilibrate with the appropriate chromatographic buffer. The column should be white after the EDTA wash (or after elution of protein with EDTA) and should return to a pale blue color after regeneration.

2.2.19 GST affinity chromatography

The glutathione-S-transferase affinity (GST) resin was used to purify the GST fusion protein. 1 ml of Glutathione sepharose 4B was loaded to the disposable column and washed with 10 ml PBS to remove the ethanol in the buffer. Gently load the supernatant to the resin or mix the supernatant with resin and incubate them at 4 ℃ for about 2-4 hours. About 20 ml of PBS was used to wash the column to remove the unspecific binding protein. To remove the protein, add 1 ml of the elution buffer containing 10 mM reduced glutathione, 50 mM Tris-HCl (pH 8.0), incubated at room temperature for 5 min to elute the protein. Repeat the step for several times to make sure the protein can be eluted completely.

2.2.20 Regeneration of Glutathione Sepharose 4B

Wash the gel with two-bed volume of washing buffer 1, followed by 2-bed volume of washing buffer 2, repeat the steps for 4-5 times, if necessary, washing the gel with 2-bed volume of 6 M guanidine hydrochloride to remove precipitated or denatured substances or wash the matrix with 3-or 4-bed volume of 70% ethanol (or non-ionic detergent with 0.1% concentration) to remove hydrophobic bound substances, then followed by re-equilibration with 3-to 5-bed volume of PBS.

2.2.21 purification of protein by fast performance liquid chromatography (FPLC)

After the protein was purified by affinity column, the sample can be further purified with FPLC. For the gel filtration, 1 ml/ min flow rate was used. The UV_{280}

was detected and the corresponding fractions were analyzed by SDS-PAGE. For the ion-exchange chromatography, the flow rate was also 1 ml/min. Generally the buffer B concentration was increased from 0 to 100% in 40 min when the Mono Q column was used.

2.2.22 SDS-PAGE electrophoresis

The SDS-PAGE was used to check the purity of protein purified. Generally 12% separation gel was used for analysis which depends on the size of the protein sample, so separation gel concentration can be varied. The sample first was mixed with 2× loading buffer and heated at 90-100°C for about 2-3 min. Then the samples were loaded into the SDS-PAGE gel (generally 10 µl for each well, which depends on the concentration of the samples). For the running of the SDS-PAGE gel, the constant current was used, normally 30 mA for one piece of gel was used. When the tracing dye reaches to the end of the gel, the gel can put into staining buffer on Belly Dancer that was from STOVALL life science, Greensboro NC USA for 15 min, the gel can be destained in the destain solution. Then the protein bands can be visualized by putting the gel on the light box. After storage in the storage buffer for some time, the gel can be dried by the gel drier machine.

2.2.23 Western Blot analysis

Western Blot was used to specificly detect protein using its antibody. The following steps were used for the analysis. The PVDF membrane was pre-wet in 100% methanol for about 10 min. SDS-PAGE was run according to SDS-PAGE protocol. Soak all the filter papers and transfer membrane in transfer buffer for about 30 min and make sure that there is no bubble trapped in the filter papers. After electrophoresis, equilibrate the SDS-PGE gel in transfer buffer for 15-30 min. Assemble the transfer cassette (the Trans-Blot® SD Semi-Dry transfer cell was from

and incubated at 30°C for 3 hr with shaking (230 rpm). At this point, the OD_{600} should be 0.4-0.6. The cells were put into a 50-ml tube and centrifuged at 1,000× g for 5 min at room temperature (20-21°C). The cell pellets were thoroughly resuspended in sterile TE or distilled H_2O. The final volume is 25-50 ml.

The tube was centrifuged at 1,000× g for 5 min at room temperature. The cell pellet was resuspended in 1.5 ml of freshly prepared, sterile 1×TE/1×LiAc. 0.1 mg of plasmid DNA and 0.1 mg of herring testes carrier DNA were added into a fresh 1.5-ml tube and mixed. 0.1 ml of yeast competent cells was added into each tube and mixed well by vortex. 0.6 ml of sterile PEG/LiAc solution was added into each tube and vortexed at high speed for 10 sec to mix.

All the tubes were incubated at 30°C for 30 min with shaking at 200 rpm. 70 µl of DMSO was added into every tube and mixed well by gentle inversion. **Do not vortex**. The tube was heated for 15 min in a 42°C water bath. The cells were chilled on ice for 1-2 min. The cells were centrifuged for 5 sec at 14,000 rpm at room temperature and resuspended in 0.5 ml of sterile 1× TE buffer. 100 ml of the cells was plated on each SD agar plate for selecting the desirable transformants. All the plates were incubated, up-side-down, at 30°C until colonies appeared (generally, 2-4 days).

2.2.25 Checking the protein-protein interaction on the SD/-His, Leu, Trp plate

FKBP38 was cloned into pAS2-1 using *Bam HI* and *Xho I* restriction enzymes to generate GAL4 activation domain fusion protein. Bcl-2 and Bcl-2 loop deletion mutants were cloned into pACT2 using *Nde I* and *Sal I* restriction enzymes to generate GAL4 DNA binding domain fusion proteins. *Saccharomyces cerevisiae strain* PJ69-4A (*MATa his 3 leu 2 ura 3 trp 1 gal4Δ gal 8Δ met 2::GAL7-lacZ GAL2-Ade 2 LYS2::GAL1-his 3*) was grown in YPD medium containing 1% yeast extract, 2% polypetone, and 2% glucose. Cells were grown on the minimal synthetic dropout

(SD) medium lacking Leu, Trp or SD medium lacking Leu, Trp, His to check protein-protein interaction.

2.2.26 Liquid Culture Assay and β-Galactosidase Using ONPG as Substrate

5-ml overnight culture was prepared in liquid SD selection medium appropriate for the system and plasmids. On the day of the experiment, ONPG was dissolved at 4 mg/ml in Z buffer with shaking for 1-2 hr. The tube containing the overnight culture was vortexed for 0.5-1 min to disperse cell lumps and 2 ml of the culture was immediately transferred to 8 ml of YPD.

The fresh culture was incubated at 30˚C for 3-5 hr with shaking (230-250 rpm) until the cells were in mid-log phase (OD_{600} of 1 ml = 0.5-0.8). 1.5 ml of culture was placed into each of three 1.5-ml tubes and centrifuged at 14,000rpm (10,000× g) for 30 sec. The supernatants were carefully removed. 1.5 ml of Z buffer was added into each tube and vortexed until cells were resuspended. The cells were centrifuged again. Each pellet was resuspended in 300µl of Z buffer.

0.1 ml of the cell suspension was transferred to a fresh tube. The tubes were placed into liquid nitrogen for 0.5-1 min until the cells were frozen. The frozen tubes were placed in a 37˚C water bath for 0.5-1 min to thaw. The freeze/thaw cycle was repeated two more times to ensure that the cells had been broken.

A blank tube was set up with 100 µl of Z buffer. 0.7 ml of Z buffer + β-mercaptoethanol was added into the reaction and blank tubes. Then, 160 µl of ONPG was immediately added into all the tubes and incubated at 30˚C. After the yellow color was developed, 0.4 ml of 1 M Na_2CO_3 was added into the reaction and blank tubes. The reaction tubes were centrifuged for 10 min at 14,000 rpm to pellet cell debris. The supernatants were carefully transferred to clean cuvettes.

The spectrophotometer was calibrated against the blank at A_{420} and the OD_{420} of

the samples were measured relative to the blank. The ODs should be 0.02-1.0 within the linear range of the assay, every assay will be repeated 3 times. β-galactosidase units were calculated as follows: 1 unit of β-galactosidase was defined as the amount which hydrolyzes 1 μmol of ONPG to o-nitrophenol and D-galactose per min per cell. β-galactosidase units = $1{,}000 \times OD_{420} /(t \times V \times OD_{600})$.

2.2.27 Phosphorylation of Bcl-2

The Purified 6 μM Bcl-2 was incubated with 0.5 μM JNK for 2 h at 30 °C in a buffer containing 10 mM Tris-HCl pH 7.5, 25 mM $MgCl_2$, 1 mM EGTA, 1 mM ATP, 1 μCi γ-^{32}P-ATP, and 250 μM PMSF. For the phosphorylation of Bcl-2 by ERK2, the different buffer was used. ERK2 was incubated with purified Bcl-2 in the buffer containing 50 mM Tris-HCl, 10 mM $MgCl_2$, 2 mM dithiothreitol, 1 mM EGTA, 0.01 % Brij 35, pH 7.5. The samples were separated in 12.5 % SDS-PAGE and followed by autoradiography for visualization.

2.2.28 Checking the phosphorylation of Bcl-2 by gel shift assay

After phosphorylation, the SDS-PAGE pattern of P-Bcl-2 will be changed. The phosphorylated Bcl-2 moves lower than the unphosphorylated one. 15% SDS-PAGE gel was used for checking the phosphorylation of Bcl-2. After phosphorylation, the samples were loaded into the 15% SDS-PAGE for separation, and the western blot using anti-Bcl-2 antibody was performed. The band shift will be seen if the protein is phosphorylated (Tamura *et al.*, 2005).

2.2.29 Phosphorylation of peptides

200 μM peptides were mixed with 10 μM JNK or ERK2 in the reaction buffer described in phosphorylation of Bcl-2. The reaction was performed at 30 °C for 1 h, the reaction mixture was put at 90°C to kill the activity of the kinases. We performed the experiments in triplicates. The samples were loaded to the Ni^{2+}-NTA column to

remove the His-tag fused kinases, and the flow-through samples were loaded to the C-18 column for HPLC analysis. 20 µl of the samples were injected into the C-18 column with a flow rate of 1 ml/min. The peptide was eluted with a linear gradient of acetonitrile from 0 to 30%, and the peptide peaks were detected at 225 nm. The followings are the peptide sequence:

Table 2.3 Peptide sequences synthesized

Peptide	Sequence
T56	QPGH**T**PHPAA
pT56	QPGHp**T**PHPAA
S70	PVART**S**PLQT
pS70	PVARTp**S**PLQT
T74	PLQ**T**PAAPGA
pT74	PLQp**T**PAAPGA
S87	GPAL**S**PVPPV
pS87	GPALp**S**PVPPV

Phosphorylated residues are in bold and numbered according to their positions in the Bcl-2 sequence. The p means that the residue is phosphorylated.

2.2.30 Calcineurin assay

The calcineurin assay using commercial substrate RII (Asp-Leu-Asp-Val-Pro-Ile-Pro-Gly-Arg-Phe-Asp-Arg-Val-pSer-Val-Ala-Ala-Glu (MW. 2192.0)) was performed according to the protocol provided by the company (CalBiochem, USA). The reaction buffer for the calcineurin is 50 mM Tris, pH 7.5, 100 mM NaCl, 6 mM $MgCl_2$, 500 uM $CaCl_2$, 0.5 mM DTT, 0.025% NP-40, 250 nM calmodulin.

Calcineurin (human Recombinant) activity was measured in the presence of calmodulin (Bovine Brain, 25 uM in H_2O). Dilute calmodulin to 250 nM in the reaction mixture. The stock of RII peptide is 0.75 mM. Prepare the serial dilutions of the phosphate standard plus a distilled H_2O to get different concentration of $(PO_4)^{3-}$. Add 25 µl of phosphate dilutions and 25 µl of 2× assay buffer with calmodulin to 50 µl of final volume. Add 100 µl of malachite Green reagent, allow the color develop for about the 20-30 min, read the OD_{620} and plot the standard curve between OD_{620}

and the concentration of $(PO_4)^{3-}$. For the test sample or inhibitor assay, add 25 µl of 2× reaction buffer with calmodulin to the well and 5 µl of diluted calcineurin to wells, final amount should be about 2 U per well, RII peptide was added with calcineurin, add 10 µl H_2O and 10 µl inhibitor and 10 µl RII peptide to start reaction and incubate at 30 ℃ for 30 min. Add 100 µl Malachite Green reagent to stop the reaction and check the OD_{620}. The experiments were performed in triplicates. Using the OD_{620} to calculate the $(PO_4)^{3-}$ released (Mondragon *et al.*, 1997).

2.2.31 Deposphorylation of phosphorylated proteins

After kinase reaction, the phosphorylated proteins were passed through P_6 BioSpin Column (Bio-Rad), and the purified proteins were mixed 20 µg PP2B for 2 h at 30℃ in a buffer (50 mM Tris, pH 7.5, 100 mM NaCl, 6 mM $MgCl_2$, 500 uM $CaCl_2$, 0.5 mM DTT, 0.025% NP-40, 250 nM calmodulin), then SDS sample buffer was added to the reaction mixtures, separated on 12.5% SDS-PAGE, and followed by western blot analysis using anti-Bcl-2 antibody.

2.2.32 Dephosphorylation of Peptides

The synthesized phosphorylated peptides were mixed with PP2B, PP1 or PP2A (2 U of each enzyme was added. The definition of the enzyme activity was based upon the description from the company) in the following buffers: the reaction buffer for PP1 is 50 mM HEPES, 5 mM dithiothreitol, 0.025 % Tween-20, 0.1 mM Na_2EDTA, pH 7.0 ; the reaction buffer for the calcineurin is 50 mM Tris, pH 7.5, 100 mM NaCl, 6 mM $MgCl_2$, 500 uM $CaCl_2$, 0.5 mM DTT, 0.025% NP-40, 250 nM calmodulin; the buffer for PP2A is 20 mM MOPS, pH 7.4, 100 mM NaCl, 60 mM 2-mercaptoethanol, 1 mM $MgCl_2$, 1 mM EGTA, 0.1 mM $MnCl_2$, 1 mM DTT, 10% glycerol, 0.1 mg/ml serum albumin. The reaction (50 µl) was performed at 30 ℃ for 1 hour. All the experiments should be performed in triplicates. After 1 hour, 100 µl of Malachite

green was added and the absorbance at 620 nm was measured and the release of phosphate was calculated according to the standard curve.

2.2.33 GST pull-down assay

GST fusion FKBP38 was purified by the Glutathione-Sepharose 4B resin provided in the Bulk RediPack GST Purification Module and Superdex 75 gel filtration column chromatography. 3 µg of GST fustion FKBP38ΔTM was incubated with 3 µg of Bcl-2 and phosphorylated Bcl-2 on ice for 4 h, individually. Then protein samples were mixed with 40 µl of Glutathione-Sepharose 4B resin on ice for 2 h and washed with PBS with 1 mg/ml BSA. The resin was eluted with reduced glutathione. The eluted samples were loaded onto SDS-PAGE and for western analysis.

2.2.34 Co-expression and purification of FKBP38 and Bcl-2 complexes

In order to check the interaction between FKBP38 and Bcl-2, FKBP38 was cloned into pACYC184 with T7 promoter to generate His tag fusion protein and Bcl-2 was cloned into pET29 b to generate Bcl-2 without any tag. These two plasmids were co-transformed into BL21DE3 and induction was performed. After large scale induction and purification by Ni^{2+}-NTA, the complex of FKBP38 and Bcl-2 was obtained.

2.2.35 Protein concentration assay

The dye from Bio-Rad was used for the assay. The protein concentration was checked by the following way: Prepare dye reagent by diluting 1 volume of Dye Reagent Concentrate with 4 volumes of distilled, deionized water; Filter through Whatman #1 filter (or equivalent) to remove particulates; This diluted reagent may be used for approximately 2 weeks when kept at room temperature; Prepare three to five dilutions of a protein standard, which is representative of the protein solution to be tested; The linear range of the assay for BSA is 0.2 to 0.9 mg/ml, whereas with IgG the linear range is 0.2 to 1.5 mg/ml; Pipet 100 µl of each standard and sample solution

into a clean, dry test tube. Protein solutions are normally assayed in duplicate or triplicate; Add 5.0 ml of diluted dye reagent to each tube and vortex; Incubate at room temperature for at least 5 minutes; Absorbance will increase over time; Samples should incubate at room temperature for no more than 1 hour; Measure absorbance at 595 nm; Plot the standard curve based upon the known protein concentration; Get the relationship between the protein concentration and the OD_{595}; Using the OD_{595} of protein sample to calculate the protein concentration (Fig. 2.1 A).

Also the purified protein concentration can be detected by checking OD_{280}. Diluting sample and measuring the OD_{280}, and using the analysis data from Vector NTI, the concentration of the protein sample can be obtained.

2.2.36 Protein molecular weight determination by gel filtration

The gel filtration (sizing column) is also one of ways to check the molecular weight of proteins. The unknown protein molecular weight can be calculated according to the standard curve. The molecular weight standard from BioRad was used for the calculation of protein molecular weight. The standard contains the following proteins: Thyroglobulin (bovine), 670 kDa; R-globulin (bovine), 158 kDa; Ovalbumin (Chicken), 44 kDa; Myoglobin (horse), 17 kDa; Vitamin B12, 1.350 kDa. After run the standard in the S-200 column, the V_0 and Vt of the column can be obtained. Based upon the V_e of each standard, the relationship between Kav (Kav=(Ve-Vo)/(Vt-Vo)) and log (molecular weight) should be linar. Based upon the liner relationship, the molecular weight of the known protein sample can be calculated according to its Ve (Fig.2.1 B, C).

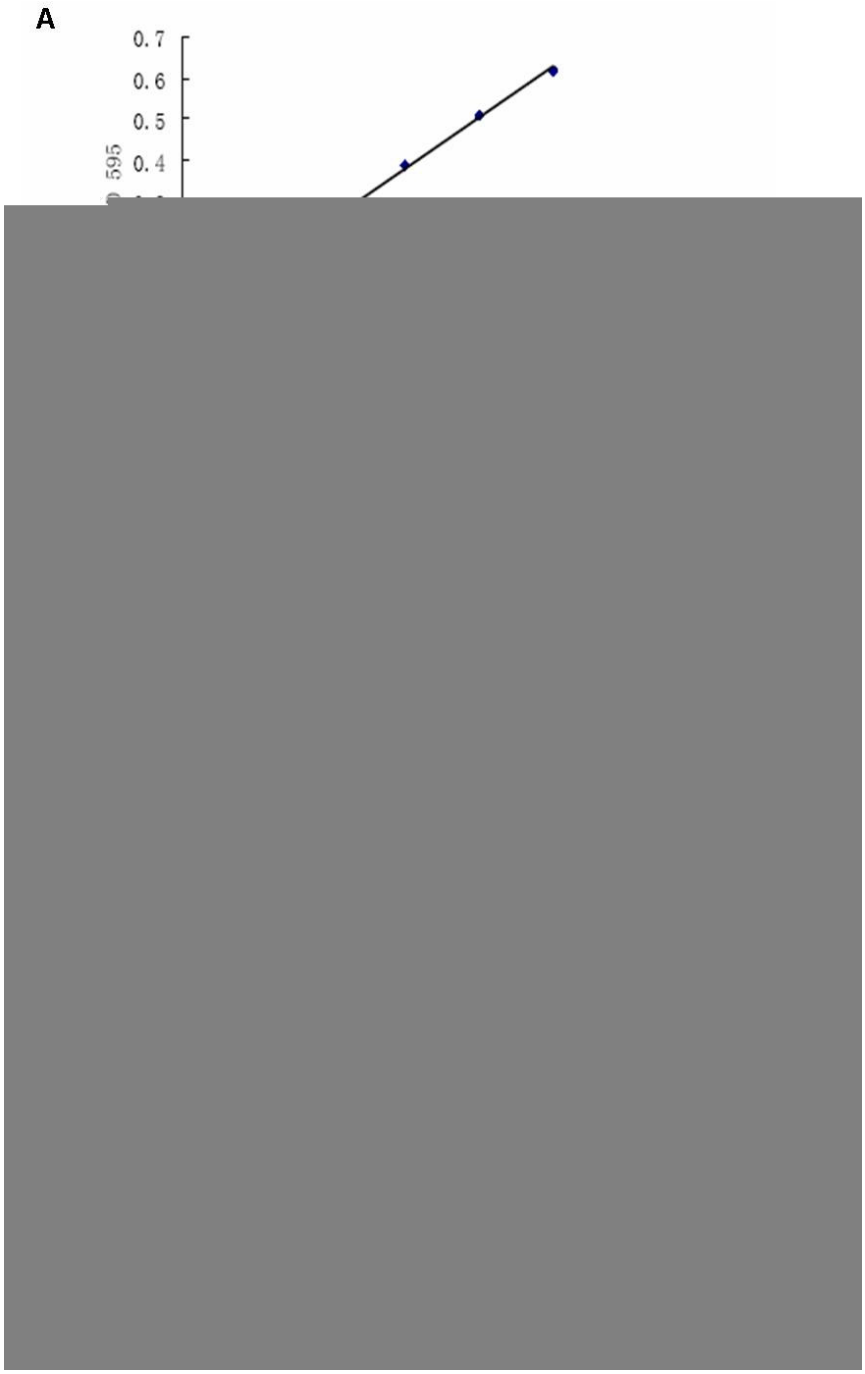

Fig. 2.1 Protein concentration assay standard curve and protein molecular weight estimation standard

A) Protein concentration assay standard curve. The standards with different concentration were mixed with dye and OD was measured, the unknown protein sample concentration can be obtained by fitting the OD into the equation. B) The standard curve of proteins in the S-200 sizing column. The buffer containing 20 mM Tris-HCl, pH 8.0, 150 mM NaCl, 1.0 mM DTT, 0.01% NaN_3. The buffer flow rate is 0.5 ml/min. C. The relationship between molecular weight and K_{av} is shown. The unknown protein molecular weight can be obtained by fitting the K_{av} value into the equation.

2.2.37 PPIase assay

The substrate for PPIase assay N-succinyl-Ala-Ala-Pro-Phe-p-nitroanilide (Sigma-Aldrich Chemie Gmbh, Siteinheim Germany) was dissolved in methanol (2.1mM), and α-chymotrypsin (2mg/ml) in 100 mM Tris-HCl pH 8.0 was added to the following preincubation of PPIase with the test peptide at 0 ºC (on ice). The reaction mixture (1ml) containing the test peptide (63uM), chymotrypsin 0.06mg/ml, and varying amounts of protein were placed into a spectrophotometer cell at 12 ºC, first reading was taken at 5 sec to account for the dead time in the mixing of the sample, and reading were taken at 10-sec interval (Kofron *et al.*, 1991, Garcia-Echeverria *et al.*, 1993, Janowski *et al.*, 1997, Ou *et al.*, 2001).

2.2.38 Determination of protein molecular weight by SDS-PAGE

After the SDS-PAGE gel, the Rf has linear relationship with the log of molecular weight of the protein, where Rf is equal to *Dp*/*Dd* (*Dp* is distance of migrated by protein; *Dd* is distance migrated by dye). After drawing a standard curve between the log of molecular weight and the Rf of the standards, the linear relationship between Rf and log (M.W) can be obtained, using the standard curve the molecular of the unknown protein can obtained. The following standard curve was obtained from 12% SDS-PAGE gel. If the more accurate result can be obtained, draw the standard curve of the molecular weight during every experiment (Fig. 2.2).

2.2.39 Circular dichroism (CD)

The protein in phosphate buffer was concentrated to 1 mg/ml and the CD was measured by using a Chirascan Spectropolarimeter (Applied Photophysics Limited, Surrey, UK). First using the PBS or phosphate buffer run as baseline, then the sample was loaded into the cuvette and the wavelength from 180 to 280 nm was measured. The experiments were repeated for 4 times and the average data was used for analysis.

2.2.40 Citrate synthase aggregation assay

To measure the chaperone activity, the thermal denaturation of citrate synthase was performed as previously described (Kumar *et al*, 2005, Monaghan *et al*, 2005). Briefly, prior to use the citrate synthase in the assay, the citrate synthase was changed from the buffer (2.2 M $(NH_4)_2SO_4$) into TE buffer (50 mM Tris-HCl, pH 8.0, 2 mM EDTA), concentrated to 1 mg/ml. The citrate synthase or citrate synthase mixed with 1mg/ml FKBP38 or other proteins were incubated at 42 ℃ for 20 min, and the level of aggregation during denaturation was measured by monitoring the increase in absorbance at 360 nm.

2.2.41 Protein crystallization screen

The crystallization screen was performed using the screen kit from Hampton Research. A concentrated solution of the protein (10-15 mg/ml) was centrifuged in an Eppendorf tabletop centrifuge at 4 ℃ for 2 min to remove precipitates or dust. Hanging drop method was used for the screen. Mix 1 µl of buffer with 1 µl of protein sample on the siliconised cover slide and seal the plate well with grease. The plates were stored at 19 ℃, the plates were examined under microscope every day.

2.2.42 Co-immunoprecipitation analysis of protein-protein interactions

Cells were cultured in medium in 75 cm^2 flask and after 48 hours, harvest cells and wash with PBS. Transfer cells into appendorf tube and lyse each tube of cells with 1ml of buffer containing 20 mM Tris, pH 7.5, 100 mM NaCl, 0.5% NP-40, 0.5 mM EDTA, 0.5 mM PMSF, 0.5% protease inhibitor cocktail (Sigma), pipet cells up and down extensively and then sit on ice. Spin down the cell extracts at max speed for 10 minutes at 4°C. Pool the extracts into a 15 ml tube and add 10 ml polyclonal serum. Incubate ng for 2 hours at 4°C. Wash 50 µl of Protein A/G Sepharose (Sigma) with 1 ml of lysis buffer for about 3 times and then remove last of excess buffer carefully.

After the 2-hour incubation of the lysate, add the washed Protein A/G Sepharose to the immunoprecipiates and mix for 1 hour at 4°C. Wash immunoprecipitates 3 times with 1 ml of lysis buffer and remove last of buffer carefully. Add 50 µl of 2× SDS-PAGE sample buffer and boil it for 5 min. Load onto SDS-PAGE gel and perform western blot using different antibody.

2.2.43 Secondary structure analysis by Fourier-Transformed infrared spectroscopy (FTIR)

FTIR spectra were recorded on a Nexus 470 spectromerter purged with N_2 and equipped with a MCT/A detector cooled with liquid nitrogen. 3mg/ml sample was dissolved in D_2O. Spectra were collected at room temperature and without a polarizer.

2.2.44 Sample preparation for NMR experiment

2.2.44.1 Sample for ^{1}H experiment

For the 1D ^{1}H experiment, the protein sample was prepared with the same way as that of the general protein. The buffer for the protein sample is 20 mM Na-PO_4, 100 mM NaCl, 1 mM DTT, 0.01% NaN_3, pH 6.8, 10% D_2O. For the 1D proton experiment, the water suppression was used and before collecting the data, the 90 degree P1 pulse was calculated.

2.2.44.2 Preparation of sample uniformly labeled with the ^{15}N

The M9 medium was used and the $^{15}NH_4Cl$ was used to take the place of the general NH_4Cl with a concentration of 1g/L, after induction, the protein was purified and concentrated to about 0.5 mM concentration in the same buffer as that in the ^{1}H experiment. The sample can be stored at -80 ℃ if it is stable after frozen. The HSQC data was collected using the program provided by the Bruker.

2.2.44.3 Preparation of samples uniformly labeled with the ^{13}C and the ^{15}N

Freshly transferred cells on the M9 plate which contains ^{13}C labeled glucose (1g/L)

and the ^{15}N labeled NH_4Cl (1g/L) were inoculated into the same M9 liquid medium and cultured at 37 ºC overnight. The culture was transferred into the same medium and the large scale induction was performed. After purification, the sample was concentrated to 0.5-1 mM in appropriate buffer.

2.2.44.4 Preparation of Sample labeled with ^{13}C and the ^{15}N in D_2O

If the sample was dissolved into 100% D_2O, the following steps can be used. The buffer can be changed by using the concentrator or using the PD10 column especially for the buffer exchange. But this can not completely remove the H_2O in the same. The lyophilisation was used. First freeze the sample in the liquid nitrogen and do lyophilisation, then the D_2O was added and do lyophilisations for the second time, then add D_2O again. It is better to add same amount of D_2O as that of the H_2O lyophilisated so that the salt concentration can not be changed. The sample can also be kept at -80 ºC for further application.

2.2.45 NMR titration to study protein-peptide interaction

NMR experiments were performed on a Bruker 700 MHz with a cryoprobe. ^{15}N uniformly labeled protein with concentration of 0.1mM was prepared in a buffer containing 20 mM Na-PO4, pH 7.0, 10 mM NaCl, 0.01% NaN3, 1 mM DTT. The HSQC was performed at 300 K. For the NMR dissociation constant calculation experiment, lyophilized peptides aliquots were mixed with 15N labeled protein with different molar ratio and the HSQC was recorded. The one to one binding of protein, P, and peptide, L to form a protein-peptide complex, PL can be expressed as [P]+[L]↔[PL]. The equilibrium dissociation constant, KD is expressed as [P]*[L]/[PL]. Based upon the protein sample concentration, $[protein]_0$ and ligand total concentration, $[L]_0$, which is explained as $[Protein]_0=[P]+[PL]$, and $[L]_0=[L]+[PL]$, the relationship between chemical shift perturbations $\Delta\delta=(\Delta H^2+(0.154*\Delta N)^2)^{0.5}$ and

K_D can be obtained from the equations which is shown as follows $\Delta\delta(ppm)=0.5*\Delta\delta max\{1+X+K_D/[Protein]_0-[(1+X+K_D/[Protein]_0)^2-4X]^{0.5}\}$, where X is the molar ratio of ligand on protein. $\Delta\delta max$ is set at the $\Delta\delta$ value at the protein saturation level (Smet et al., 2005, Bayer et al., 2003, Kim et al., 2001). The K_D can be obtained by fitting the $\Delta\delta$ and X into equation.

2.2.46 The NMR experiment for protein structure determination

For the protein structure determination, the following experiments were performed for data collection. After the data were collected, they were processed with NMRpipe (Delaglio *et al*., 1995), the spectrum can be read by NMRView (Johnson, 2004).

2.2.46.1 1D ^{1}H NMR experiment

The 1D ^{1}H experiment was recorded using water suppression with watergate W5 pulse sequences with gradients. The pulse program is 'zggpw5', TD (size of fid) is 12K, the DS is 4 and a sweep width of is 16 ppm. The recording temperature is 303 K and the o1p is 4.7 ppm which is decided with the gs mode. The receiver gain was obtained by the command rga. The number of scan was decided by the concentration of sample. For the protein sample with a concentration of 0.2-0.5 mM, the 8-16 scans was used for the data collection. The D19 delay for water suppression was set to 90-100 us for the water suppression (for 700 MHz, D19=100 us; for 600 MHz, D19=125 us.). Other parameters are set according to the program from Bruker.

2.2.46.2 2D ^{1}H,^{15}N-HSQC

The 2D ^{1}H, ^{15}N-HSQC was collected using the pulse program hsqcf3gpph19 with water suppression. The acquisition mode in the ^{1}H dimension was DQD and States-TPPI in the ^{15}N dimension. Or we used the other program hsqcetf3gpsi2 with the acquisition mode of Echo-Antiecho in the ^{15}N dimension. The TD in the F1 is 256 and F2 is 4048. The CNST4 is set to 90 which is the J (NH). D1 is 1 sec, and other

parameters were set by the program. The number of scans was set depending on the concentration of sample, usually used 2 scans for most of the experiment. The spectral width for ^{15}N is 40 ppm and 1H is 16 ppm. The option for zg -DLABLE_CN was used when the ^{15}N and ^{13}C labeled sample was used. The receiver gain was set by the 'rga' command.

2.2.46.3 HNCACB

The water suppression with watergate HNCACB experiment was used for the data collection. The pulse program for the experiment is hncacbgpwg3d. Acquisition mode for the data collection is DQD for 1H, States-TPPI for both ^{13}C and ^{15}N. The spectral width is 16 ppm for 1H, 34 ppm for 15N and 80 ppm for 13C. The o1p is 4.7 ppm, o2p is 39 ppm and o3p is 119 ppm. The TDs for the 3 dimensions were as follows: ^{1}H, 2048, ^{13}C, 128 and ^{15}N, 96. The receiver gate was set by rga or in the gs mode. Also the shaped power (sp1) for water suppression was optimized in the gs mode. Other parameters were obtained by using command 'getprosol'. Also, if the 90 degree pulse for proton is different from the prosol, the command 'getprosol' was used to change it accordingly. The ^{15}N, ^{13}C hard pulse were adjusted according to the standard pulse programs, the water flip pulse and the shape pulse for decoupling were also obtained from the programs provided by Dr. Sattler and Dr. Simon in EMBL.

2.2.46.4 CBCACONH

The CBCACONH was recorded using the same way of that of HNCACB. The pulse program cbcaconhgpwg3d was used and with the acquisition mode similar to that of HNCACB. Other parameters were same as that of HNCACB. The scan number is 16. The shaped power sp1 for water suppression was set in the prosol or re-set in the gs mode.

2.2.46.5 HNCA and HNCOCA

The HNCA and HNCOCA experiments were performed using the pulse program hncagpwg3d or hncocagpwg3d with the water suppression using watergate. The acquisition mode for ^{1}H, ^{13}C and ^{15}N were DQD, States-TPPI and States-TPPI, individually. The spectral widths for ^{1}H, ^{13}C and ^{15}N were 16 ppm, 32 ppm and 34 ppm. The frequency offset for ^{1}H, ^{13}C and ^{15}N were 4.7 ppm, 54 ppm and 119 ppm. The number of scans was 32. The acquisition option -DLABEL_CN was used. The receiver gain was set by command rga. Other parameters were obtained by getprosol or set by the pulse program.

2.2.46.6 HNCO

The HNCO experiment was performed using the pulse program hncogpwg3d with the water suppression using watergate. The acquisition mode for ^{1}H, ^{13}C and ^{15}N were DQD, States-TPPI and States-TPPI, individually. The spectral widths for ^{1}H, ^{13}C and ^{15}N were 16 ppm, 24 ppm and 34 ppm. The frequency offset for ^{1}H, ^{13}C and ^{15}N were 4.7 ppm, 54 ppm and 119 ppm. The number of scans was 32. The TD in the ^{1}H, ^{13}C and ^{15}N are 2048, 96, 96. The receiver gain was set by command rga. Other parameters were obtained by getprosol or set by the pulse program.

2.2.46.7 HNHA

The HNHA experiment was performed using the pulse program hnhagp3d. The acquisition mode for ^{1}H, ^{1}H and ^{15}N were DQD, States-TPPI and States-TPPI, individually. The spectral widths for ^{1}H, ^{1}H and ^{15}N were 14 ppm, 14 ppm and 35 ppm. The frequency offset for ^{1}H, ^{13}C and ^{15}N were 4.7 ppm, 54 ppm and 119 ppm. The number of scans was 32. The TD in the ^{1}H, ^{1}H and ^{15}N are 2048, 128, 96. The receiver gain was set by command rga. Other parameters were obtained by getprosol or set by the pulse program.

2.2.46.8 HCCCONH and _CCCONH

HCCCONH and _CCCONH experiments were performed using the hccconhgpwg3d2 and hccconhgpwg3d3 individually. The same acquisition mode was used for the data collection. The spectral widths for ^{1}H, ^{13}C and ^{15}N were 14 ppm, 80 ppm and 35 ppm. The frequency offset for ^{1}H, ^{13}C and ^{15}N were 4.7 ppm, 39 ppm and 119 ppm. The number of scans was 32. The TD was same as that of other experiments. The receiver gain was set by command rga. Other parameters were obtained by getprosol or set by the pulse program.

2.2.46.9 ^{15}N-HSQC-NOESY and ^{13}C-HSQC-NOESY

^{15}N-HSQC-NOESY and ^{13}C-HSQC-NOESY experiments were performed using the bruker standard pulse program, with the noesyhsqcetgp3d (^{13}C) and noesyhsqcetf 3gp3d (^{15}N). The parameters were same as other experiments. For the ^{13}C-HSQC-NOESY the GPZ2 with 20.1 was used. For the ^{15}N-HSQC-NOESY the GPZ2 8.1% gradient was used. We also used the pulse program from EMBL (Provided by Dr. M.Sattler and Dr. B.Simon). We used 4 scans for the double labeled sample. The TD and sw of the program were same as those of other experiments. The mixing time was 100ms. The rga command was used for the rg determination. Also, for the ^{13}C-HSQC-NOESY data collection, double (^{13}C and ^{15}N) labeled sample was used and dissolved in 100% D_2O.

2.2.46.10 2D NOE experiment

The data of 2D NOE experiment were collected using the bruker standard program noesyesgpph. The acquisition mode was DQD and States-TPPI, individually. The spectral widths were both 14 ppm. The frequency offset for ^{1}H was 4.7 ppm or set by the gs mode. The number of scans was 64. The TDs in the 1H, 1H were 2048, 512. The receiver gain was set by command rga. Other parameters were obtained by

getprosol or set by the pulse program. The normal sample either in D_2O or H_2O was used for data collection.

2.2.46.11 2D TOCSY experiment

The data of 2D TOCSY experiment were collected using the bruker standard program mlevesgpph. The acquisition mode for was DQD and States-TPPI, individually. The spectral widths were both 10 ppm. The frequency offset for ^1H was 4.7 ppm or set by the gs mode. The number of scans was 16. The TDs in the ^1H, ^1H were 2048, 256. The receiver gain was set by commond rga. Other parameters were obtained by getprosol or set by the pulse program. The 4-5 mM peptide in buffer was used for data collection with 80 ms mixing time.

2.2.46.12 2D ROESY experiment

The data of 2D ROESY experiment were collected using the bruker standard program roesygpph19 with water suppression. The acquisition mode was DQD, and States-TPPI, individually. The spectral widths were both 11 ppm. The frequency offset for ^1H was 4.7 ppm or set by the gs mode. The number of scans was 64. The TDs in the ^1H, ^1H were both 2048, 512. The receiver gain was set by command rga. The pL11 (f1 channel power level for roesy spin lock) was set to 30 dB. Other parameters were obtained by getprosol or set by the pulse program. The 4-5 mM peptide in buffer was used for data collection with a mixing time 300 ms.

2.2.46.13 RDC experiment

The RDC experiment was performed using Filamentous phage Pf1 as alignment medium. The phage was mixed with ^{15}N labeled protein in the same buffer as that motioned before. The spectra with or without phage were recorded. The RDC values were obtained by comparing the split peak values in the two spectra. The data was collected in EMBL and processed by nmrPipe and analyzed by NMRview using

scripts provided by Dr. Sattler and Dr. Simon.

2.2.47 Structure determination using ARIA

ARIA 1.2 (Ambiguous Restraints for Iterative Assignment) was used for the structure calculation. The ^{15}N-HSQC-NOESY peaklist, ^{13}C-HMQC-NOESY and 2D NOESY peaklists from NMRview were used for calculation. The TALOS (Cornilescu *et al.*, 1999) processed phi, psi angles and hydrobond restrains were also used in the calculation. The CNS (Brunger *et al.*, 1998) was used for the refinement. Total 180 pdb files were generated, and 20 refined structure structures were generated. In each round of structure calculation, the new NMR structures were used to re-assign ambiguous NOE cross-peaks and correct erroneous assignments. The structures were fined with water using CNS in the ARIA and analyzed with Procheck in ARIA.

2.2.48 Structure visualization

The ARIA and CYANA generated PDB files were visualized in Molmol (Karodi *et al.*, 1996) and the protein-protein interaction binding sites were mapped by using Insight II (Accelrys) or PyMol (DeLano, 2002).

2.3 Acknowledgement

Thanks to Prof. Julien Lescar for providing us with crystallization screen kits. Thanks to Prof. Keiichi I. Nakayama for providing us with anti-FKBP38 antibodies. Thanks to Prof. Thanabalu Thirumaran for providing us with the plasmids. Thanks to Prof. Valerie Lin for providing us with pCDNA plasmid. Thanks to Prof. Peter Droge for providing us with the pRED plasmid. Thanks to Prof. Peter Preiser for raising anti-FKBP38 and Bcl-2 antibodies and the cDNA library from malaria. Thanks to Prof. Torres Jaume for helping us in the FTIR analysis and peptide synthesis. Thanks to Prof. Liu J.O for providing us with the calcineurin expression system. Thanks to Prof. Cobb M.H for providing us with the kinases (JNK and ERK2) expression systems.

3 Results of expression and purification of proteins involved in this thesis

The current study involves the biochemical and functional analysis for the molecular interaction between FKBP38 and Bcl-2, requiring several proteins in apoptotic cell death pathways. This chapter gives the introduction about the gene cloning strategy, gene mutation, protein expression and purification procedures for Bcl-2, Bcl-xL, Bax, FKBP12, Pin1, calmodulin, calcineurin, ERK2 and JNK kinases.

3.1 cDNA cloning and purification of Bcl-2, Bcl-xL and Bax

3.1.1 Isolation of cDNA clones of human Bcl-2 and Bcl-xL

The cDNAs of human Bcl-2 and Bcl-xL lacking TM were amplified by RT-PCR using the RNA purified from MCF-7 cell line as template. The cDNAs products were purified and inserted into pET16b with *Nde I* and *Xho I* to generate pET16-Bcl-2 ΔTM which can be used for the expression of N-terminal His fusion Bcl-2 without TM domain in *E.coli* (Fig.3.1). To generate Bcl-2 without any tag, Bcl-2 cDNA was cloned into pET29b and the expression of the protein was checked in *E.coli*. The same strategy and protocol were applied to isolate cDNA of Bcl-xL (Table 3.1).

Table 3.1 Different constructs made for Bcl-2 and Bcl-xL.

Plasmid Name	Restriction enzymes	Fusion tag	Purpose of the clone
pET16-Bcl-2 ΔTM	*Nde I* and *Xho I*	N-his tag fusion protein	Protein purification
pET29-Bcl-2 ΔTM	*Nde I* and *Xho I*	No tag	Protein interaction
pGEXT-Bcl-2 ΔTM	*Nde I* and *Xho I*	GST fusion protein	Protein purification
pET29-Bcl-xLΔTM	*Nde I* and *Xho I*	C-his tag fusion protein	Protein purification
pGEX-Bcl-xLΔTM	*Nde I* and *Xho I*	GST fusion protein	Protein purification

The constructs for expression of Bcl-2, Bcl-xL in different vectors with *Nde I* and *Xho I* restriction enzyme sites. All constructs were used for expression of N-His, C-His and GST fusion proteins.

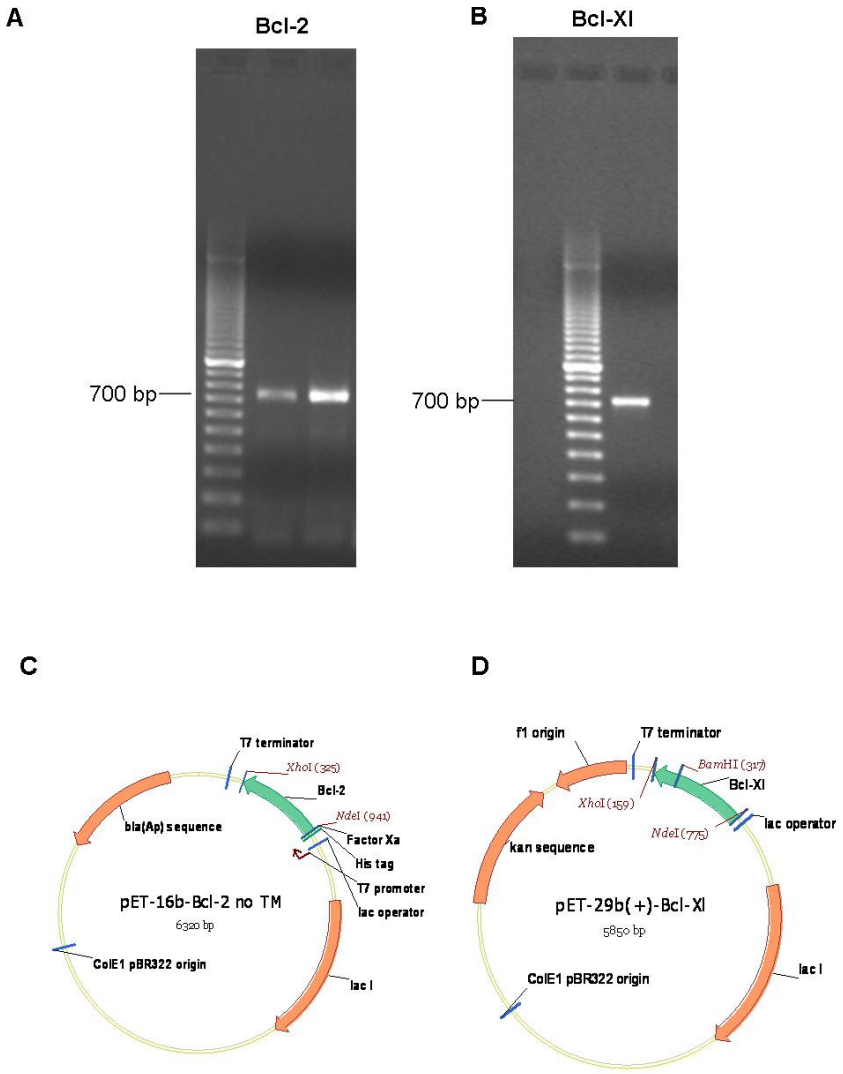

Fig.3.1 Constructions of Bcl-2 and Bcl-xL in different vectors

A and B are RT-PCR results of Bcl-2 and Bcl-xL. The RT-PCR was performed using mRNA from MCF-7 cell line as template. The products were loaded into 1% agarose gel and run at 100 V for 20-30 min and visualized under UV. C and D are the plasmid maps for Bcl-2 (BC027258) and Bcl-xL (Z23115) in pET29 system. The cDNA of Bcl-2 or Bcl-xL was purified by the PCR purification kit and after digested with *Nde I* and *Xho I,* the digested product was ligated with pET 29 digested with *Nde I* and *Xho I.*

3.1.2 Purification of Bcl-2 by Ni^{2+}-NTA column

N-terminal $(His)_{10}$-tagged Bcl-2 was expressed in *E.coli* BL21 (DE3) cells with the T7 RNA polymerase system. The *E.coli* lysate was loaded onto Ni^{2+}-NTA column.

Then weakly bound proteins were removed by extensive washing of the column by a buffer containing low concentration of imidazole. The enriched Bcl-2 was isolated upon elusion with elusion buffer (Fig.3.2 A).

Subsequently, the enriched fractions from Ni^{2+}-NTA column were concentrated to 3-4 mg/ml and loaded onto Sephacryl S-200 for a further purification. The fractions from the sizing column were collected and analyzed on SDS-PAGE. The purified Bcl-2 was homogenous adjudged on a SDS-PAGE gel. The purification procedure was quick and effective and allowed us to obtain 8-10 mg of Bcl-2 protein from 1 liter culture (Fig.3.2). The purified Bcl-2 was concentrated to about 3 mg/ml using concentrator and frozen in liquid nitrogen and stored at -80 ºC for further applications.

3.1.3 Constructions of Bcl-2 loop deletion mutants

The deletion mutatants of Bcl-2, which are shown in Fig.3.3, were inserted into pET16 plasmid with *Nde I* and *Xho I* sites and the resulting plasmids were used for the expression and purification of the N-terminal $(His)_{10}$-tagged fusion proteins. The truncated constructs in pET29 were used for expression of proteins without any tag, which can be used in the co-expression study between FKBP38 and Bcl-2.

The purification steps of Bcl-2 loop-deletion mutants were same as that of Bcl-2. The purified deletion mutants were analyzed on a SDS-PAGE gel and stored at 4 °C for a short term and frozen in liquid nitrogen and stored at -80 °C for a long-term storage. CD analysis was performed to check the folding of the loop-deletion mutants. Fig.3.3 D shows the CD spectrum of Bcl-2ΔTM, indicating mainly α-helical secondary structure. Other constructs showed similar CD patterns and all purified proteins were stable under the short-term storage conditions.

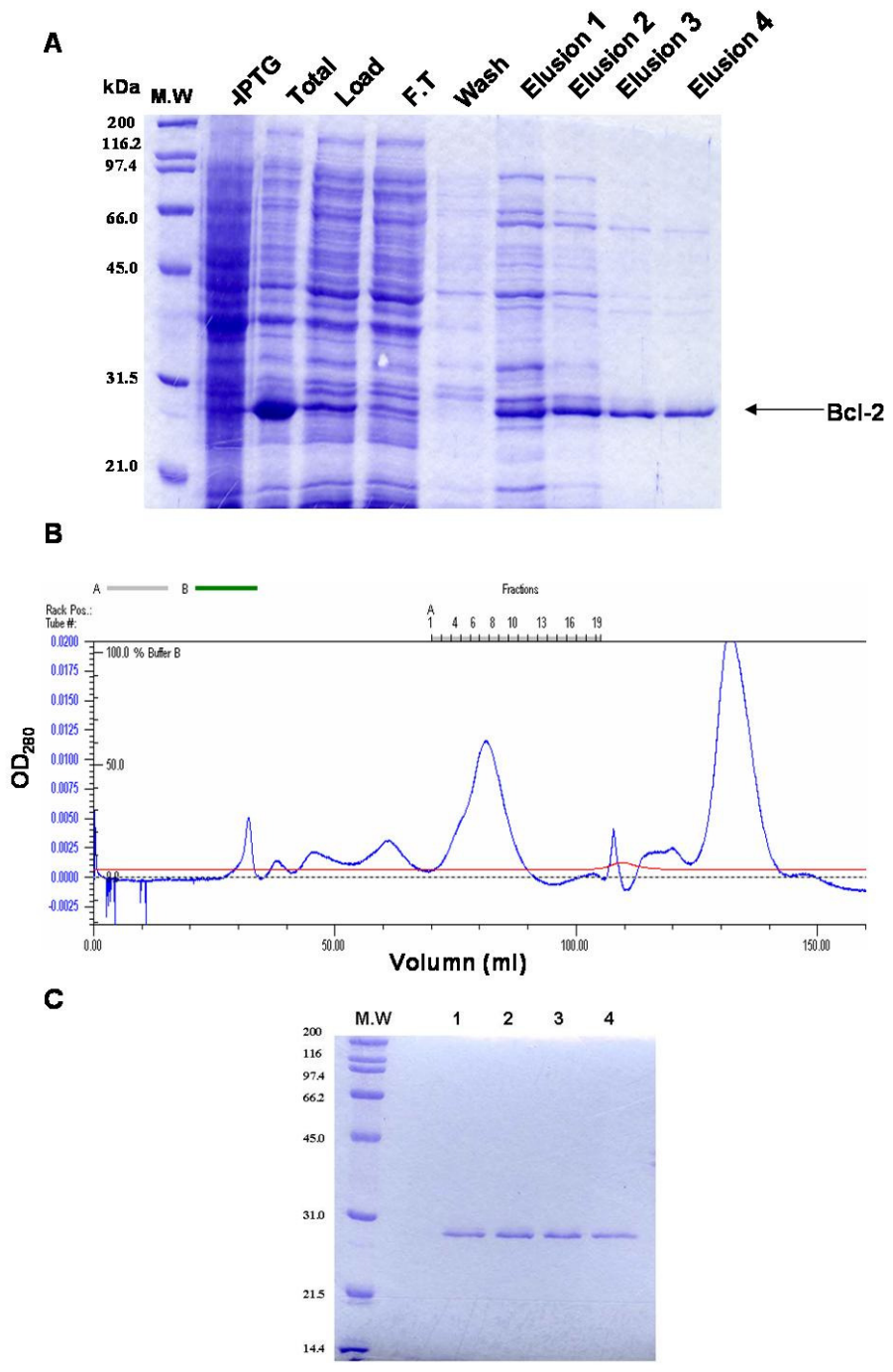

Fig.3.2 Purification of Bcl-2 by Ni^{2+}-NTA column and FPLC

A) Purification of Bcl-2 by affinity purification. The Bcl-2 was induced in *E.coli* and cell lysate was purified by Ni^{2+}-NTA affinity column. The fractions were collected and analyzed by SDS-PAGE. B) FPLC purification of Bcl-2. The Ni^{2+}-NTA purified Bcl-2 was loaded onto sizing column S-200. The fractions with high UV absorbance were collected. Flow rate was 0.5 ml/ml. C) SDS-PAGE analysis of the purified Bcl-2 from sizing column. The purified fractions from the gel filtration column were loaded onto SDS-PAGE to analyse the purity.

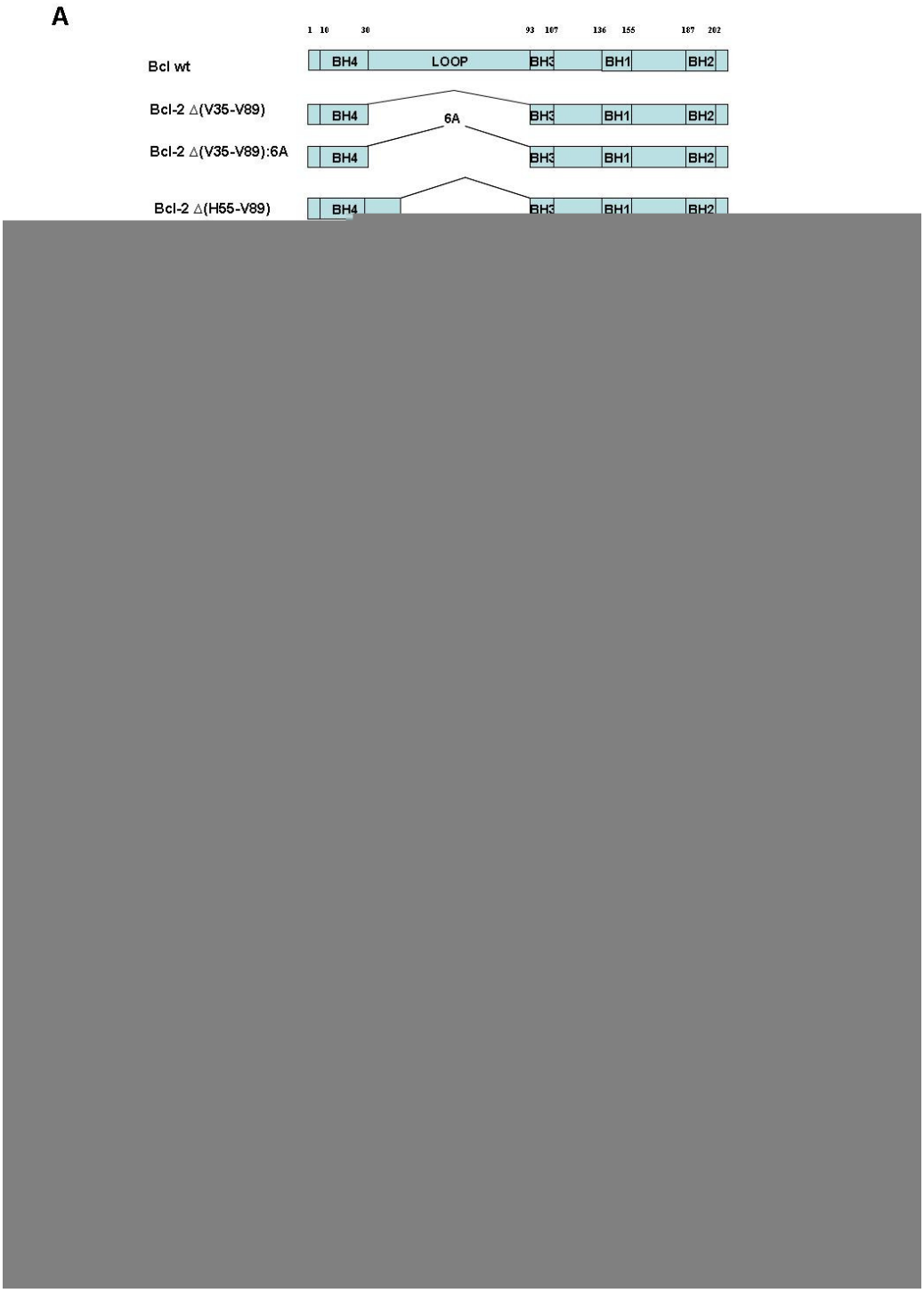

Fig.3.3 Purification of Bcl-2 loop deletion mutants

A) The diagram of Bcl-2 deletion mutants. A series of Bcl-2 loop deletion constructs were constructed. B) Induction of Bcl-2 deletion mutants in *E.coli*. C) Purified Bcl-2 loop deletion mutants by affinity and sizing column. D) CD analysis of purified Bcl-2 protein.

3.1.4 Purification of GST fusion Bcl-2

GST pull-down is a good way to study the protein-protein interaction. To obtain GST-Bcl-2 fusion protein, the cDNA of Bcl-2 was inserted into pGEX4T-1-m1 to generate pGEX4T-Bcl-2ΔTM. The resulting plasmid was transformed into DH5α and induced with IPTG to produce GST-Bcl-2. The GST-Bcl-2 was isolated on a glutathione-sepharose 4B followed by Sephacryl S-200 column (Fig.3.4). When the protein was used in the phosphorylation reaction, the buffer was changed into the following buffer containing 20 mM Tris-HCl, pH 7.2, 150 mM NaCl, 1 mM DTT.

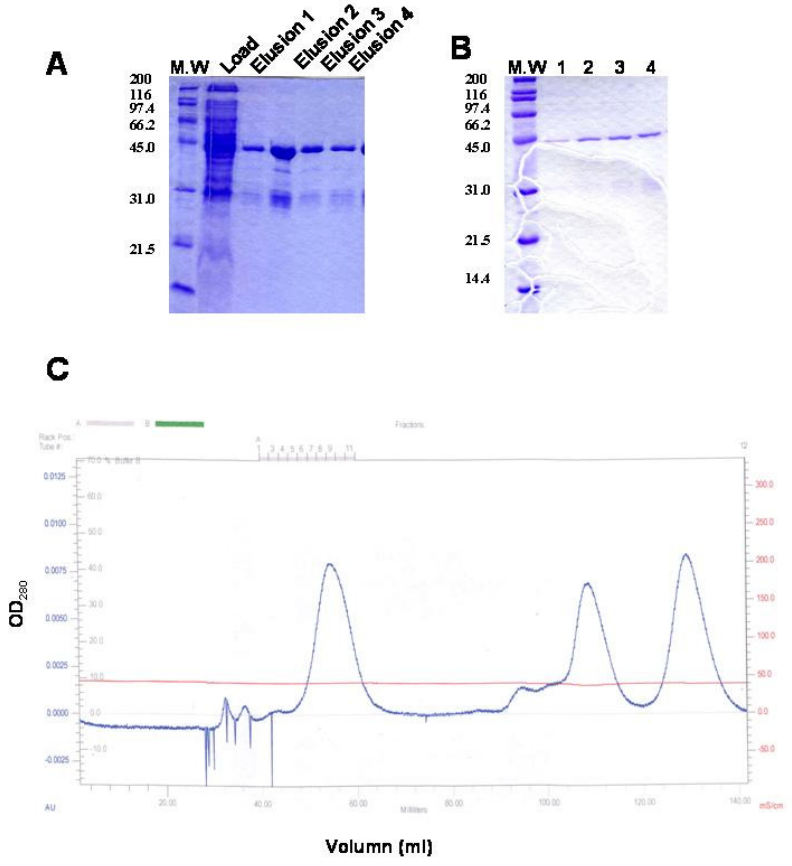

Fig.3.4 Purification of GST-Bcl-2

A) GST purification column to purify GST-Bcl-2. The GST-Bcl-2 was induced and purified by the GST purification kit and analyzed by SDS-PAGE. B, C) The sizing column purification of GST-Bcl-2. The purified protein was loaded onto a Sephacryl S-200 and purified fractions were analyzed by SDS-PAGE.

3.1.5 Purification of Bcl-xL

The cDNA of Bcl-xL lacking TM (Fig.3.1 B) was inserted into pET29 to produce C-terminal $(His)_6$-tagged Bcl-xLΔTM (Fig.3.1 D). The C-terminal His-tag fusion Bcl-xLΔTM was purified by the same purification procedure used for Bcl-2. It was reported the Ser 62 in the loop domain of Bcl-xL was important for the phosphorylation of Bcl-xL by some kinase such as JNK.

In order to perform some kinase studies, the deletion in the loop region lacking M45-A84 was made according to the same procedure as that of the Bcl-2. Also, this construct has been confirmed to be stable and its NMR structure has been solved (Muchmore *et al.*, 1996).

The Bcl-xL Δ(M45-A84)ΔTM was purified by the same way as that of the Bcl-xLΔTM. The purifed proteins were homogenous on SDS-PAGE gel (Fig.3.5). The purified proteins were concentrated to 8-10 mg/ml and stored at -80 ℃ for long-term storage.

To check if the proteins purified were correctly folded, NMR spectroscopy was used for analysis. The purified protein was concentrated to 5 mg/ml in the buffer containing 20 mM Na-PO_4, 20 mM NaCl, 1 mM DTT, 0.01% NaN_3 and the 1 D ^1H spectrum was recorded on 700 MHz NMR machine equipped with cryoprobe.

The water suppression program was used to suppress the water peak and spectrum was recorded at 303 K. The result showed very good dispersion of the peaks (Fig.3.6), which means the protein was correctly folded. The Bcl-xLΔTM and Bcl-xLΔ(M45-A84)ΔTM have the similar 1D spectra.

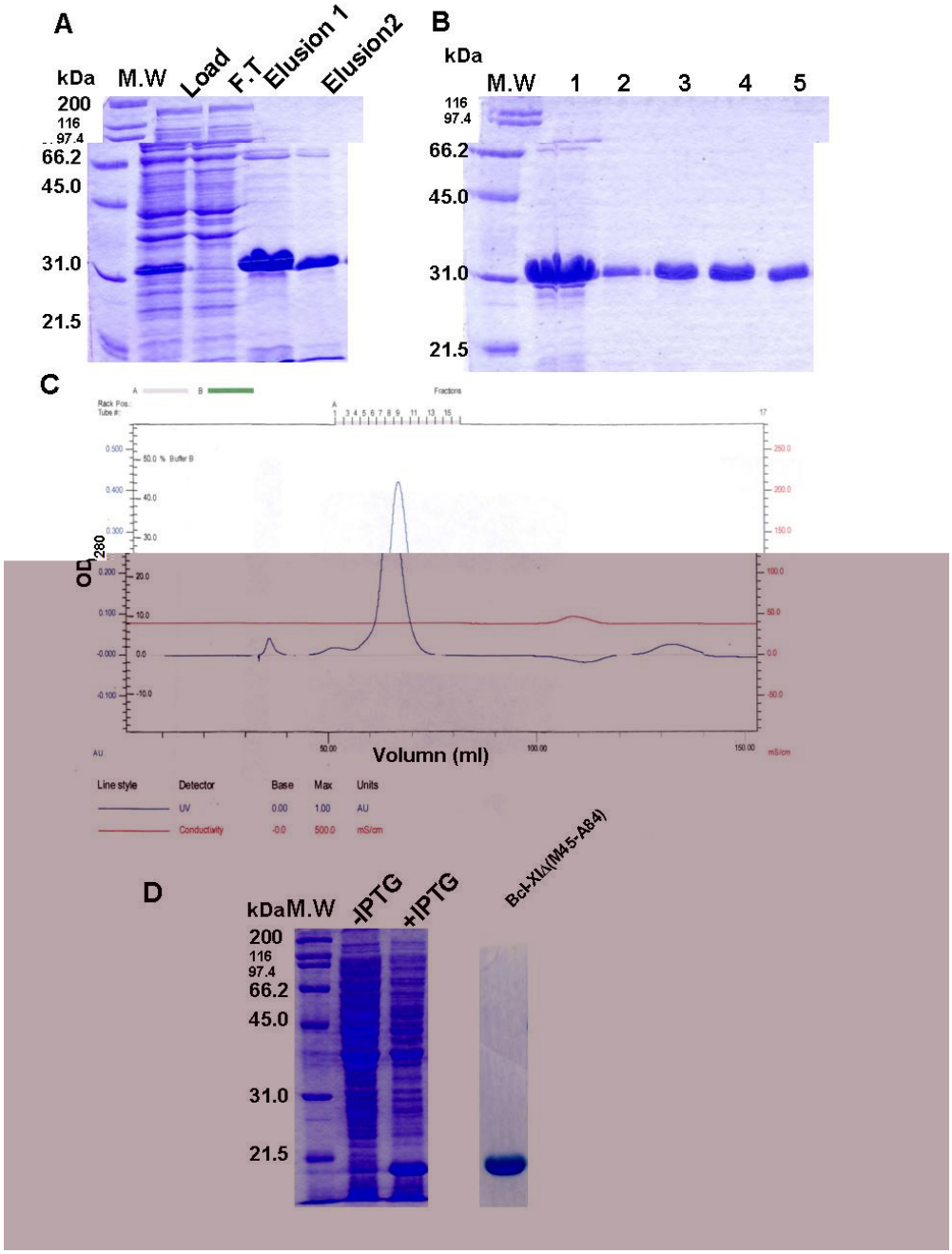

Fig.3.5 Purification of Bcl-xL and Bcl-xLΔ(M45-A84)

A) Purification of Bcl-xL ΔTM with affinity resin. The fractions during protein purification were collected and analyzed by SDS-PAGE. B) SDS-PAGE analysis of the purified Bcl-xL from sizing column. The purified Bcl-xL by Ni^{2+}-NTA column was further purified by sizing column and the fractions were collected and analyzed by SDS-PAGE. C) The sizing column purification of Bcl-xL. The buffer used is 50 mM Na-PO_4, pH 7.2, 150 mM NaCl, 1 mM DTT, 0.01% NaN_3. D) Purification of Bcl-xLΔ(M45-A84). Bcl-xLΔ(M45-A84) was purified under the same condition as the Bcl-xL and the purified protein was analyzed by SDS-PAGE.

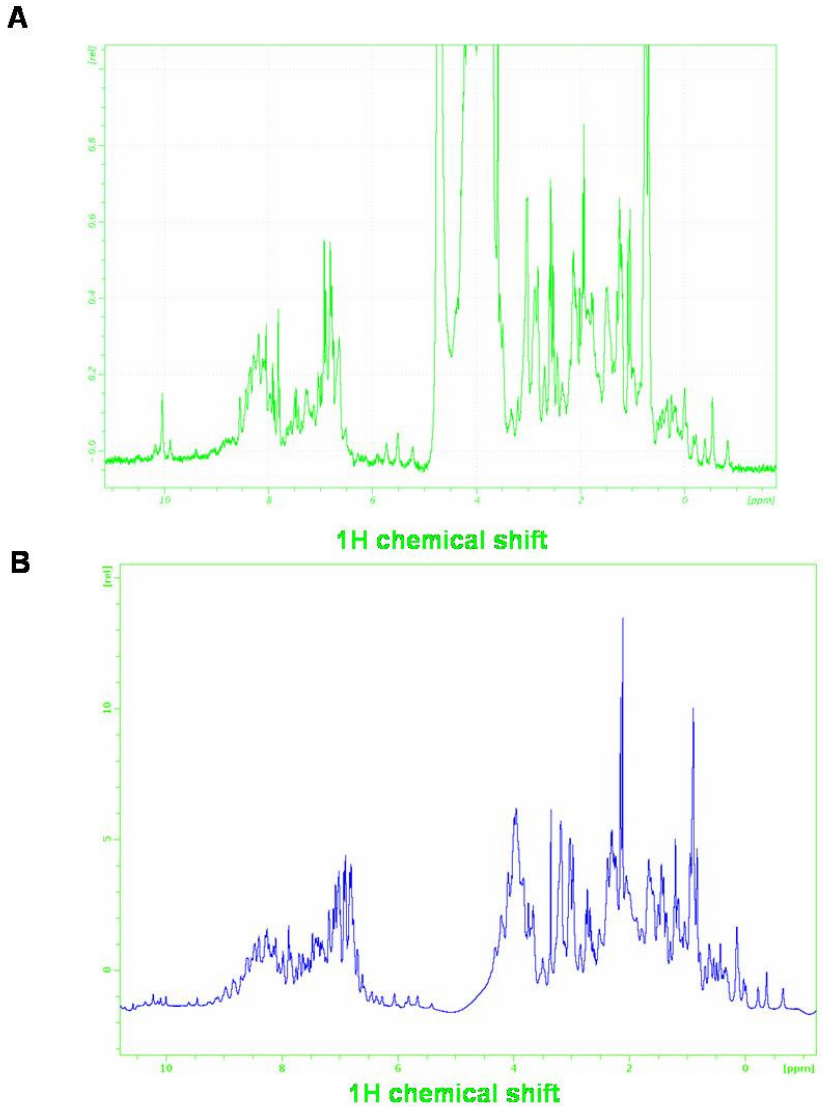

Fig.3.6 The 1D ^{1}H NMR spectra of purified Bcl-xL and Bcl-xL Δ(M45-A84)

The Bcl-xL (A) and Bcl-xL Δ(M45-A84) (B) were purified and concentrated with the concentrator. The 1D ^{1}H spectrum was recorded in the 700 MHz NMR with cryoprobe. The temperature is 303K.

3.1.6 The cDNA cloning and purification of BAK

BAK is a pro-apoptotic protein in the Bcl-2 family. It was shown that this protein could interact with Bcl-2 and the interaction could influence the function of Bcl-2. Bcl-2 is phosphorylated by several kinases in response to stresses. Phosphorylation modulates the function of Bcl-2. In order to study the binding between the Bcl-2 or phosphorylated Bcl-2 and BAK, the BAK (CR457419) was amplified by RT-PCR and inserted into pGEX-4T-m1 with *Nde I* and *Xho I* to generate GST fusion protein. The

gene cloning and ligation were performed as same as other constructs such as FKBP38. GST-BAK was first purified by GST purification kit and further purified by sizing column and used for the binding with Bcl-2. The purification of GST-BAK was shown in Fig.3.7.

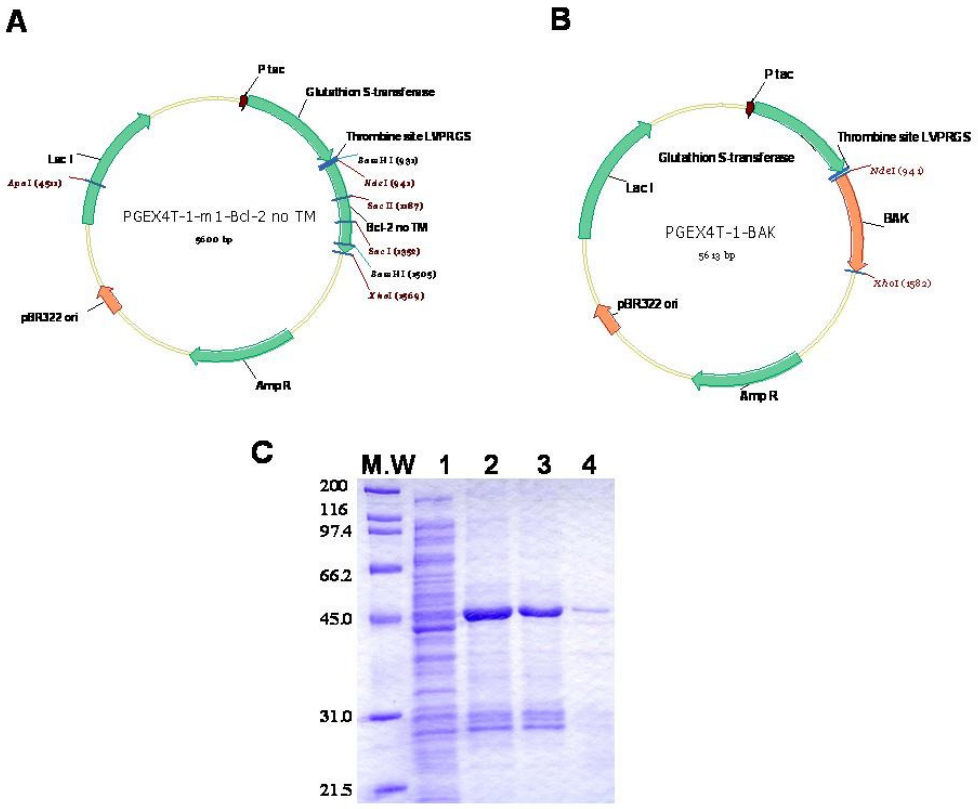

Fig.3.7 Purification of GST-BAK

A) The plasmid map of GST-Bcl-2. The cDNA of Bcl-2 was inserted into pGEX-4T-m1 to generate pGEX4T-m1-Bcl-2 ΔTM and used for protein expression. B) The cDNA of BAK from RT-PCR was inserted into pGEX4T-m1 to generate pGEX4T-1-BAK. C) Purification of GST-BAK. The GST-BAK was purified by GST purification kit and analyzed by SDS-PAGE. 1, load; 2, 3,4, elusion fractions.

3.2 Purification of FKBP12

FKBP12 is a widely spread protein in many tissue of human being. It was the first protein to interact with ryanodine receptor (Lam *et al.*, 1995). FKBP12 can interact with the immunosuppressive drug FK-506 and its complex can inhibit the activity of calcineurin (Park *et al.*, 1992). FKBP12 has the PPIase activity. So, FKBP12 was as a

positive control for both FK-506 bind assay and the calcineurin inhibition assay.

3.2.1 cDNA cloning of FKBP12

The cDNA of FKBP12 was obtained by RT-PCR using the RNA purified from MCF-7 cells. After *Nde I* and *Xho I* digestion, the PCR product was inserted into pET29 or the pACYC184 to generate the constructed plasmids, pET29-FKBP12 and pACYC184-FKBP12 (Fig.3.8) to produce C-terminal $(His)_6$-tagged protein.

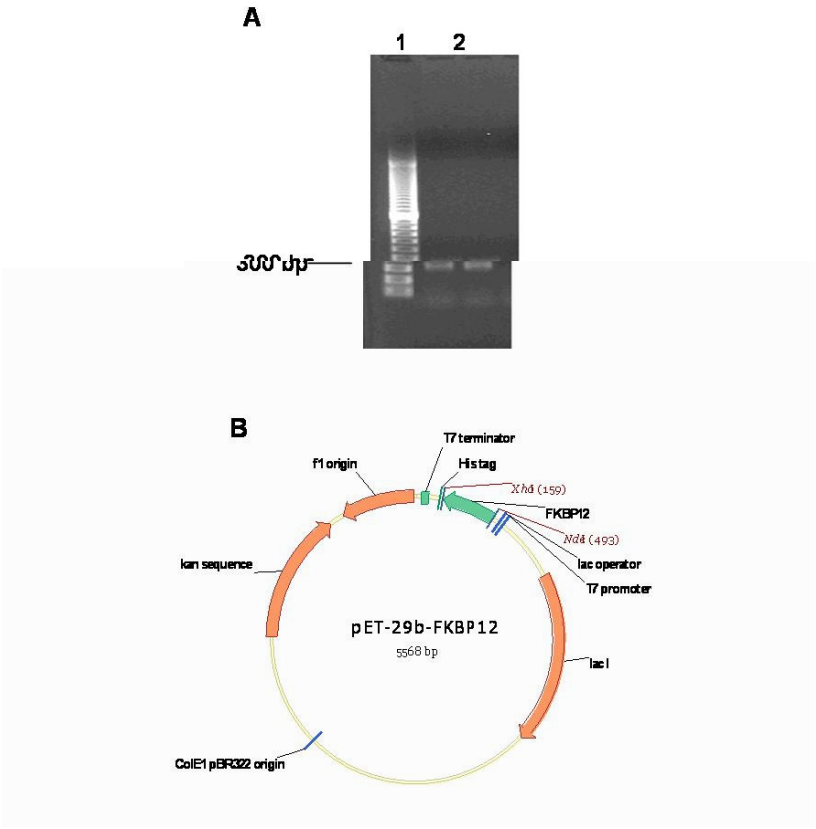

Fig.3.8 The RT-PCR result of FKBP12

A) The RT-PCR result of amplifying cDNA of FKBP12. It contains 327 bp (NM_000801, M93060, M80706). The RT-PCR was performed using RNA purified from MCF-7 cell line. 1, DNA molecular weight ladder; 2, the RT-PCR product. B) The plasmid map of pET29b-FKBP12. The cDNA of FKBP12 was digested with *Nde I* and *Xho I* and inserted into pET29b, the resulting plasmid was used for the expression of C-terminal His tag fusion protein.

3.2.2 Purification of FKBP12

Human FKBP12 is a 12 kDa protein, comparing 107 residues in length. It is the major cytosolic immunophilin (immunosuppressant-binding protein) in mammalian cells and inhibits T-cell proliferation when bound to FK-506 or rapamycin (Main *et al.*, 1999). The structure of FKBP12 is characterized by a large, amphiphilic, antiparallel five-stranded β-sheet. The β-sheet has a right handed twist and wraps around the helix to form a well-ordered hydrophobic core. The immune-suppressant-binding site, which contains many aromatic side-chains, forms a large, shallow hydrophobic pocket between the α-helix and β-sheet (Main *et al.*, 1999).

Based upon the solution conformation of FKBP, it was defined a possible binding region as an extensive aromatic cluster composed of Tyr^{26}, Phe^{46}, Phe^{48}, Trp^{59}, Tyr^{82}, and Phe^{99}, these residues pack together to form a hydrophobic pocket in which FK-506 or rapamycin bind (Van Duyne *et al.*, 1991).

In our study, FKBP12 was purified as a control for FK-506 binding assay or chaperone activity assay. FKBP12 was purified using the same procedure as that of Bcl-2. The purified FKBP12 was homogenous as adjudged by SDS-PAGE gel (Fig.3.9). The 1D ^{1}H NMR of the purified FKBP12 showed the characteristics of properly folded proteins, featuring good dispersion of resonance lines in the regions of methyl protons, α-protons and amide protons (Fig.3.10 A). Also, the FKBP12 was uniformly labeled with ^{15}N by growing the *E.coli* cells in M9 containing $^{15}NH_4Cl$. The ^{15}N uniformly labeled FKBP12 was analyzed by the NMR.

The 2D ^{1}H-^{15}N HSQC NMR data showed a good dispersion of the cross-peaks between ^{15}N and ^{1}H of backbone amide (Fig.3.10 B), which is another evidence of its suitability for further study. All the purified protein was kept at -80°C for a long-term storage.

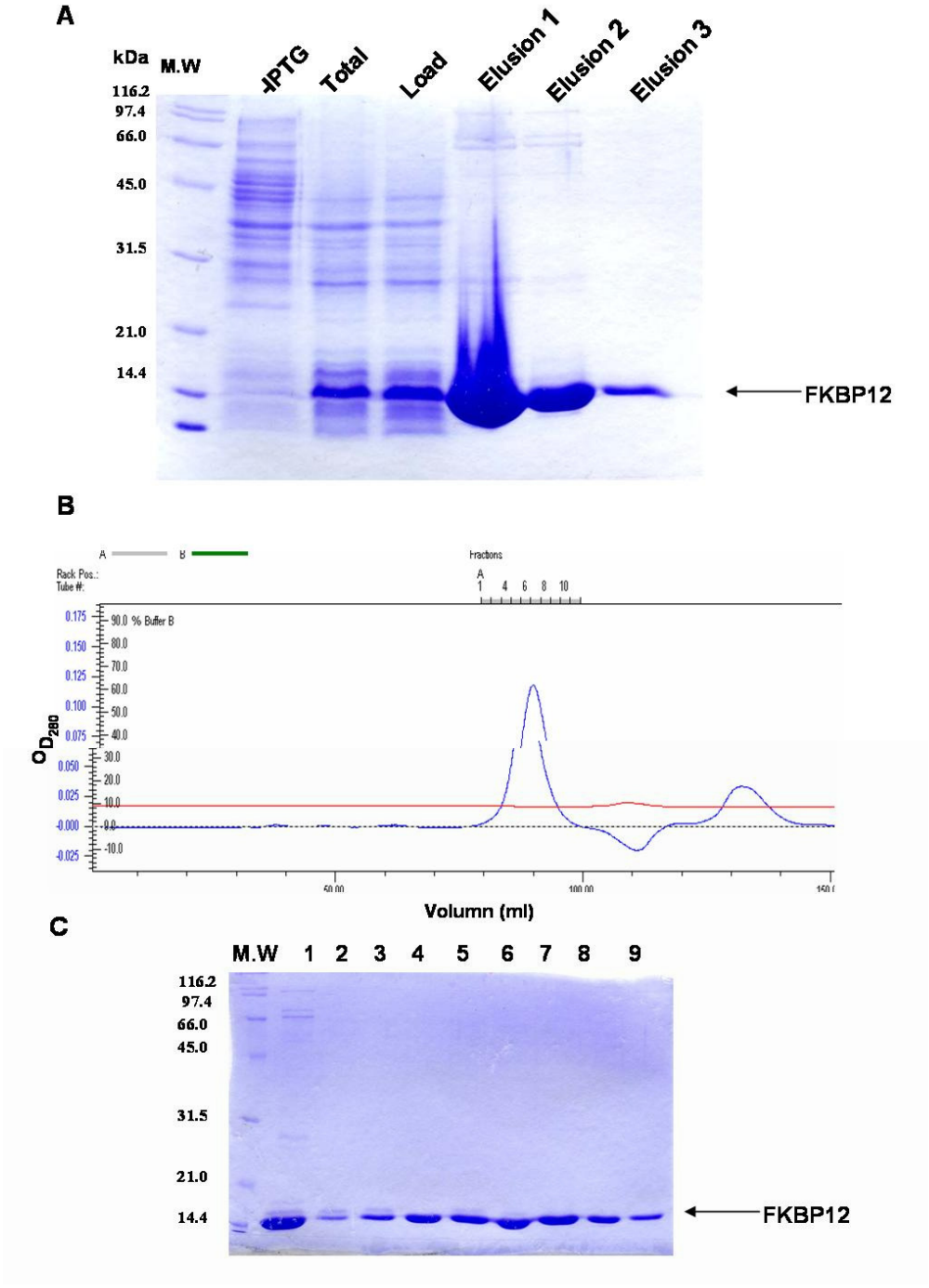

Fig.3.9 Purification of FKBP12

A) Purification of FKBP12 by Ni^{2+}-NTA. SDS-PAGE was used to analyze the purified proteins. B) The sizing column result is shown. The purified fractions from Ni-NTA affinity column were further analyzed on a sizing column and purified. C) SDS-PAGE analysis of the fractions from sizing column.1, sample loaded onto the sizing column; 2-9, fractions from FPLC purification.

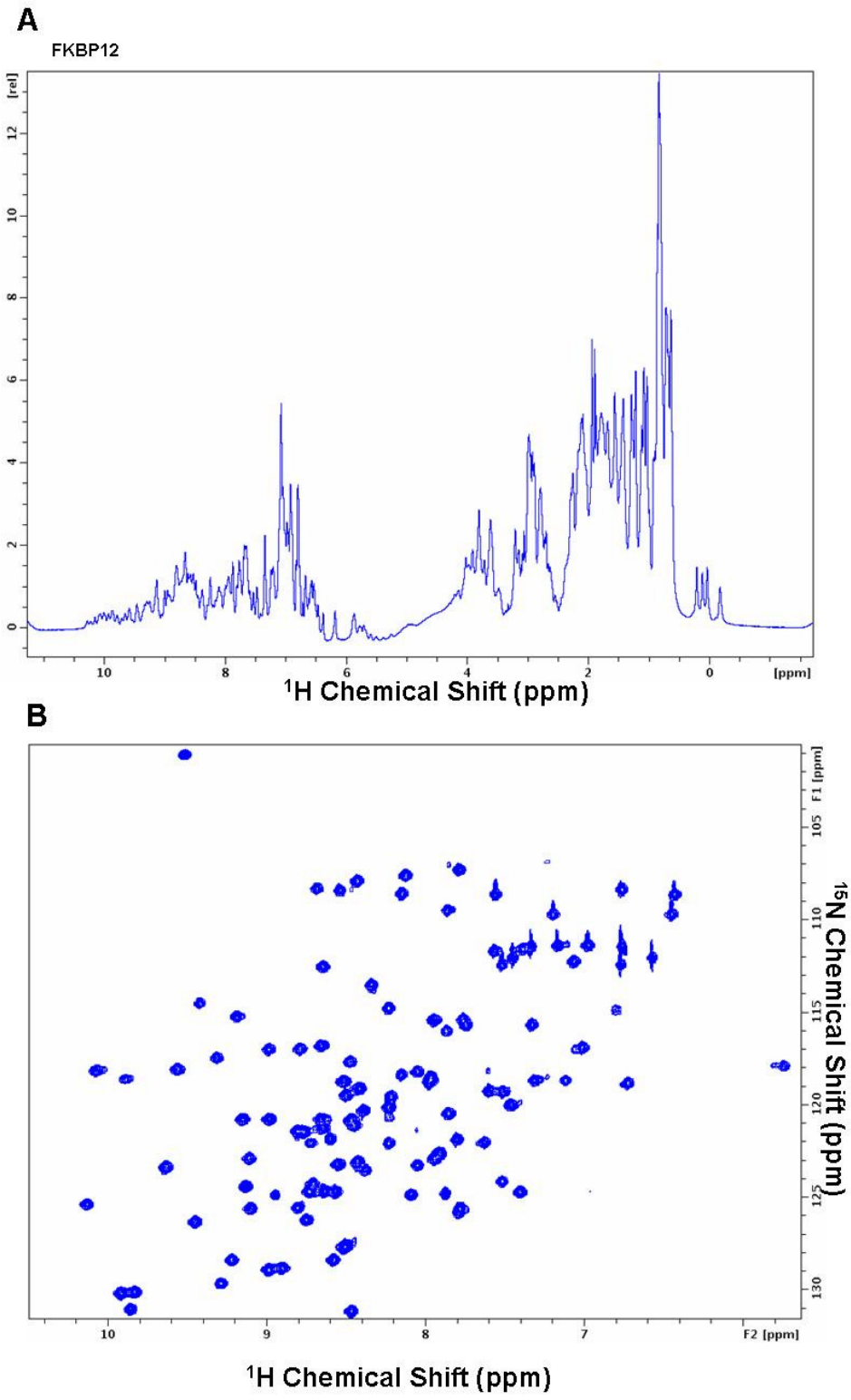

Fig.3.10 NMR analysis of the purified FKPB12

A) 1D ^{1}H spectrum of FKBP12. Purified FKBP12 was analyzed by NMR with water suppression. B) HSQC spectrum of FKBP12. FKBP12 was uniformly labeled with ^{15}N and purified by Ni^{2+}-NTA and sizing column through FPLC. The spectrum was recorded in 700 MHz NMR machine with 2 scans.

3.3 The cDNA cloning and purification of Pin1

Human Pin1 (protein (peptidyl-prolyl cis/trans isomerase) toxicity of mitotic kinase never-in-mitosis A (NIMA) -interacting 1) is a key protein in post-phosphorylation regulatory mechanisms. It was originally identified in a two-hybrid screen as a protein interacting with and suppressing the NIMA (Bayer *et al.*, 2003).

In order to study the interaction between p-Bcl-2 and Pin1, the cDNA of Pin1 was obtained by RT-PCR using mRNA from MCF7 cell line as template and the RT-PCR was performed. The RT-PCR product was inserted into pET29 or pET16 with *Nde I* and *XhoI* to generate the plasmid pET29-Pin1 or pET16-Pin1 which can produce C-terminal his tag fusion protein or N-His fusion protein (Fig.3.11 A, B). The pET16-Pin1 finally was used for protein expression and purification.

The recombinant Pin1 was purified using affinity purification with Ni^{2+}-NTA column and sizing column. After the purification, the homogenous protein was obtained (Fig.3.11 C).

1D ^{1}H and 2D ^{1}H, ^{15}N-HSQC showed that the purified protein was correctly folded. As Pin1 can interact with the phosphorylated Bcl-2, the interaction between phosphorylated peptides from the loop domain of Bcl-2 and Pin1 was studied by NMR titration experiment.

The protein used for the NMR analysis was in the buffer containing 20 mM Na-PO_4, pH 6.8, 10 mM NaCl, 0.01% NaN_3, 1 mM DTT, 10% D_2O with a protein concentration of 3.3 mg/ml. All of the spectra were recorded in the 600 and 700 MHz spectrometers equipped with a cryoprobe at 303K (Fig.3.12).

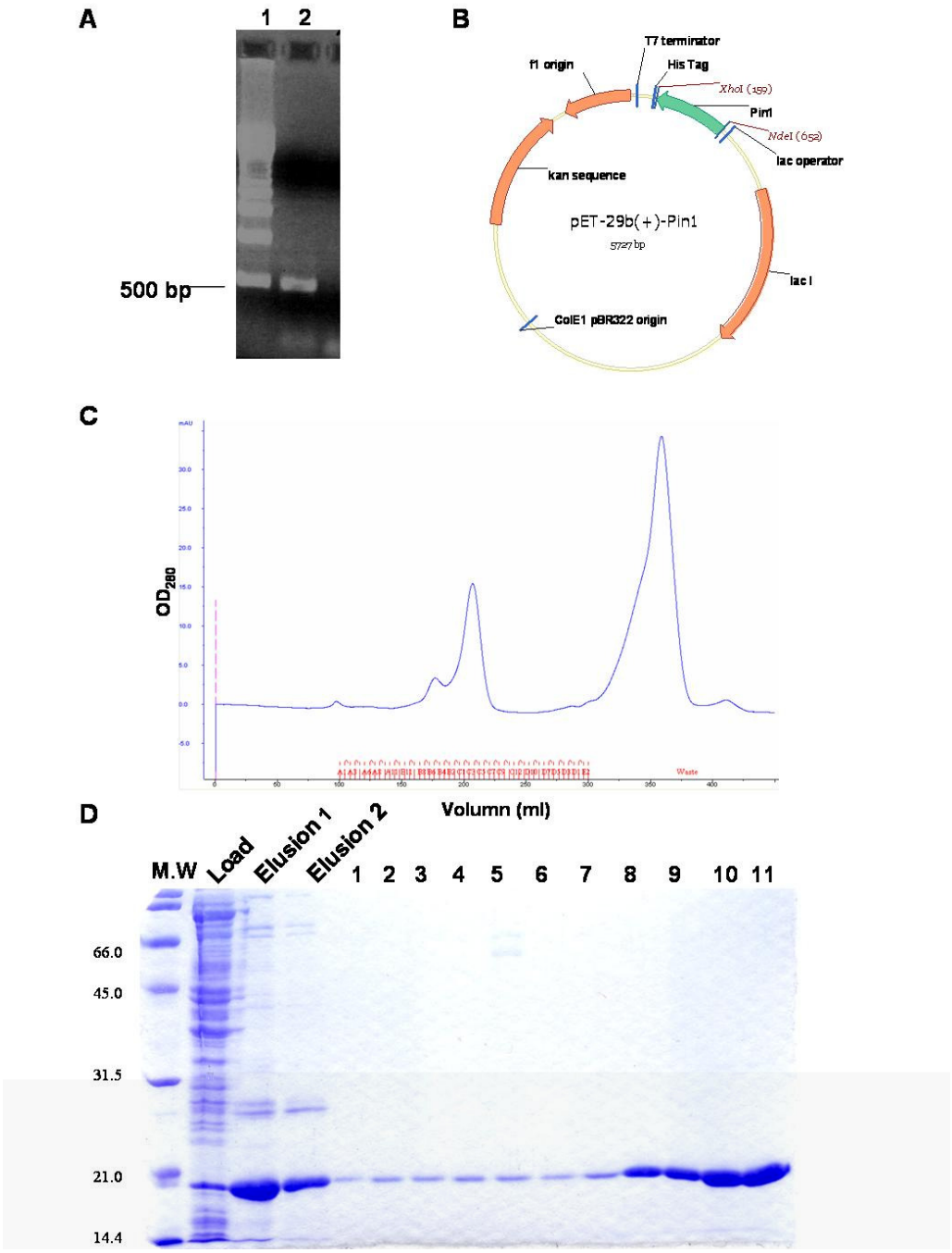

Fig.3.11 Purification of Pin1 from *E.coli*

A) The RT-PCR was performed using the RNA from MCF-7 as template. 1, DNA ladder; 2, RT-PCR product. B) The cDNA of Pin 1 (NM_006221) was inserted into pET29 b to generate pET29-Pin1. C) Sizing column spectrum of Pin1 purificaiton. D) Purification of Pin1 by affinity and sizing column. Elusion is from Ni^{2+} -NTA column purification. 1-7 are the fractions purified from sizing column. 8-11 are concentrated pin 1 after the sizing column purification.

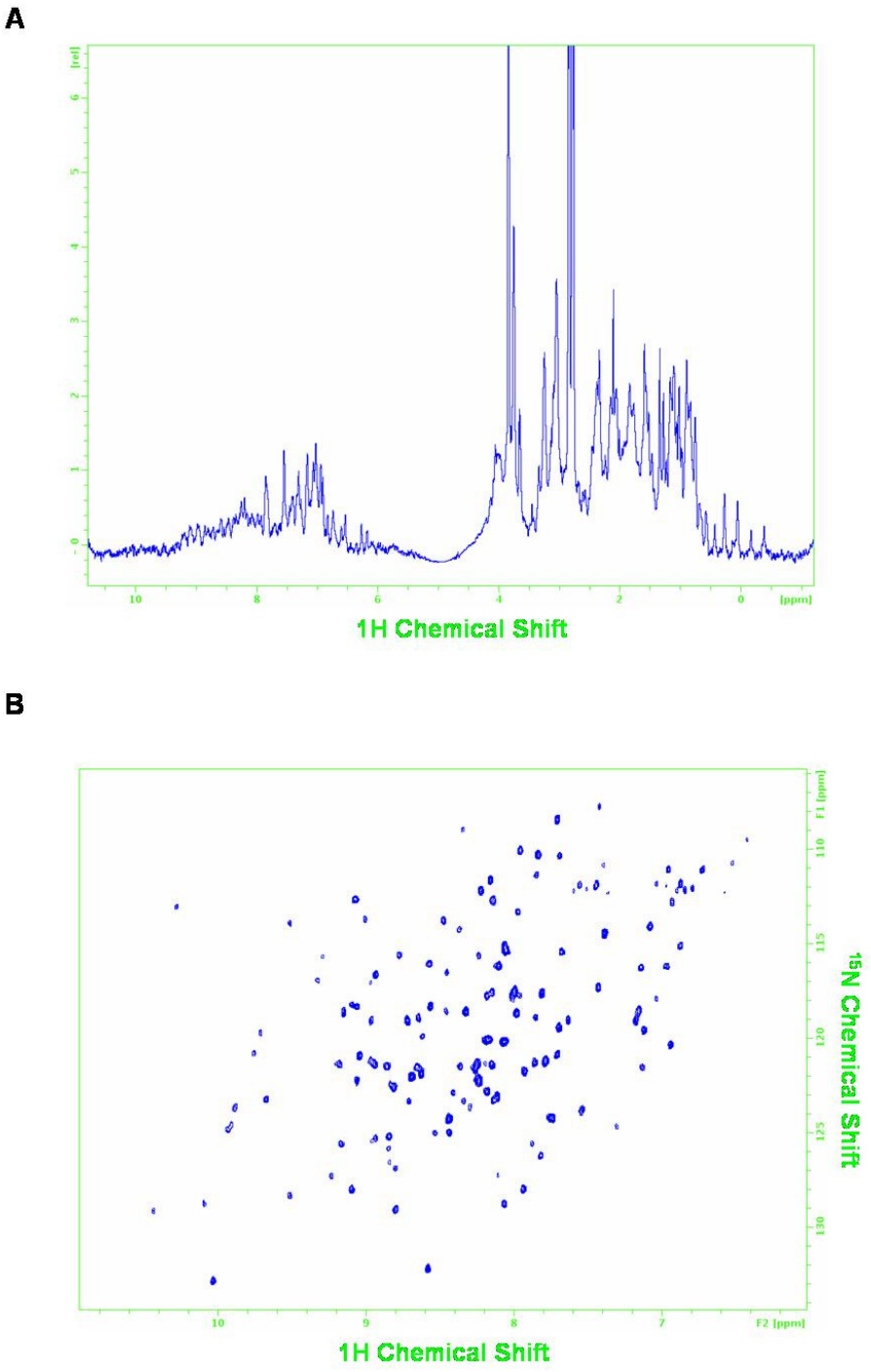

Fig.3.12 NMR analysis of purified Pin1

A) 1D ^{1}H spectrum of Pin 1. Pin1 was concentrated with concentrator and analyzed on 600 MHz NMR machine. B) HSQC spectrum of ^{15}N uniformly labeled Pin1. Pin1 was labeled with ^{15}N by growing and inducing in M9 medium containing ^{15}N labeled NH_4Cl and purified for analysis.

3.4 The cDNA cloning of NMT and calmodulin for the expression of active calcineurin

Calcineurin or protein phosphatase-2B (PP2B) is a phosphatase that can remove phosphate from the phosphorylated serine or threonine. Calcineurin plays important roles in several intracellular signal transduction pathways. It is also the common molecular target for two clinically important immunosuppressive drugs, cyclosporine A and FK-506. Calcineurin has two subunits, the catalyitic A subunit (CaNA) and the regulatory subunit B (CaNB). The activity of calcineurin can be modulated by calcium and calmodulin and the calmodulin can enhance the activity. So the cDNA of calmodulin was amplified by RT-PCR using the mRNA from MCF-7 cell line. The cDNA of calmoldulin was inserted into pET29 to generate His fusion protein (Fig.3.14 A).

Also, it was found that the yeast myristoyl-CoA (protein N-myristoyltransferase) could myristoylate calcineurin B subunit at its N-terminal glycine, which makes calcineurin more stable. The myristoyl-CoA:protein N-myristoyltransferase (yNMT) has been extensively characterized (Ames *et al.*, 1997). So the cDNA of yNMT was amplified by PCR using the genomic DNA purified from *Saccharomyces cerevisiae* (Fig.3.13 A). The PCR product was ligated with pACDuet with *Nco I* and *Hind III* sites. The resulting plasmid pACDuet-NMT was used for the expression of yNMT without any fusion tag and used for the co-expression with pETCNα that was used for expression of calcineurin.

Fig.3.13 shows the PCR amplification of NMT using yeast genomic DNA as template. The plasmids' maps for both calmodulin and NMT were shown in Fig.3.13 and Fig.3.14.

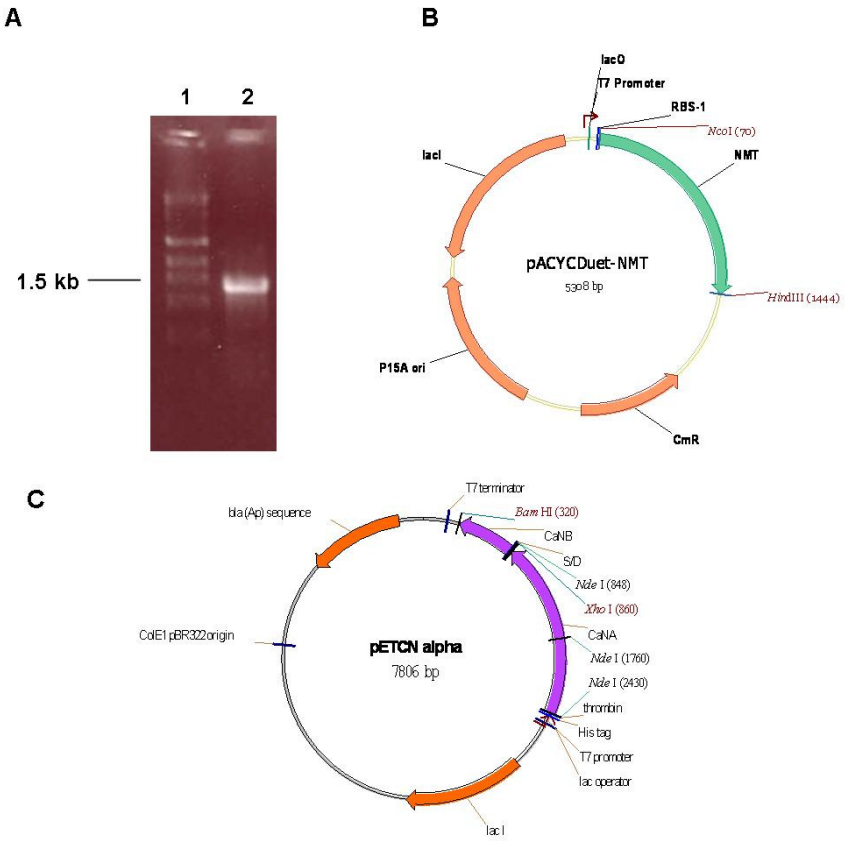

Fig.3.13 Construction NMT for purification of active calcineurin

A) PCR using yeast genomic as template to amplify NMT. 1, DNA ladder; 2, NMT PCR product using yeast genomic as template. B) NMT (M23726) was inserted with pAYCDuet plasmid with *Nco I* and *Hind III* restriction sites to generate pACYCDuet-NMT for co-expression with pETCNα. C) The plamid map for pETCNα. It is a tandem expression system for co-expression of CaNA and CanB.

3.5 Purfication of calmodulin from *E.coli*

Calmodulin is a calcium binding protein and important for the regulation of calcineurin. The cDNA of calmodulin was RT-PCR amplified and inserted into pET29. The C-His tag fusion protein was also purified according to the same protocol as that of other proteins (Fig.3.14 B, C). The NMR data confirmed the conformational change in the presence of Ca^{2+} (Fig.3.15) which is consistant as descriped before (Zhang et al., 1995, Kuboniwa et al., 1995, Osawa et al., 1996).

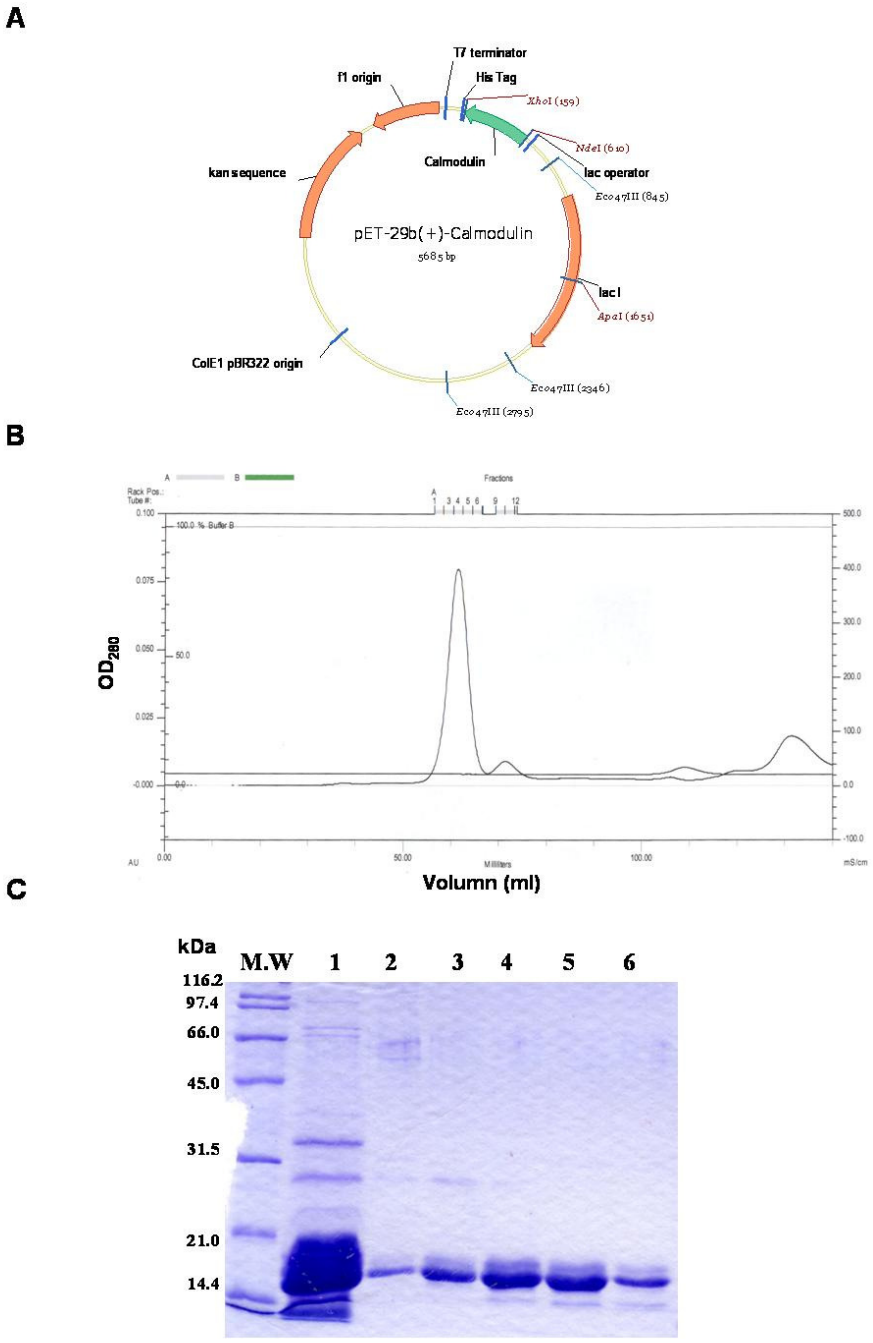

Fig.3.14 The plasmid map of pET29 b-calmodulin

A) The plasmid map for pET-calmodulin. The cDNA of calmodulin (J04046) was RT-PCR amplified and digested with *Nde I* and *XhoI,* the digested DNA was inserted into pET29 to generate plasmid pET29b-Calmodulin plasmid. B) The sizing column purification of calmodulin. C) SDS-PAGE analysis of sizing column purification of calmodulin. The Ni-NTA purified protein was loaded to sizing column for further purification and checked by SDS-PAGE. 1, Ni^{2+}-NTA affinity purified protein fractions; 2-6 are fraction from sizing column.

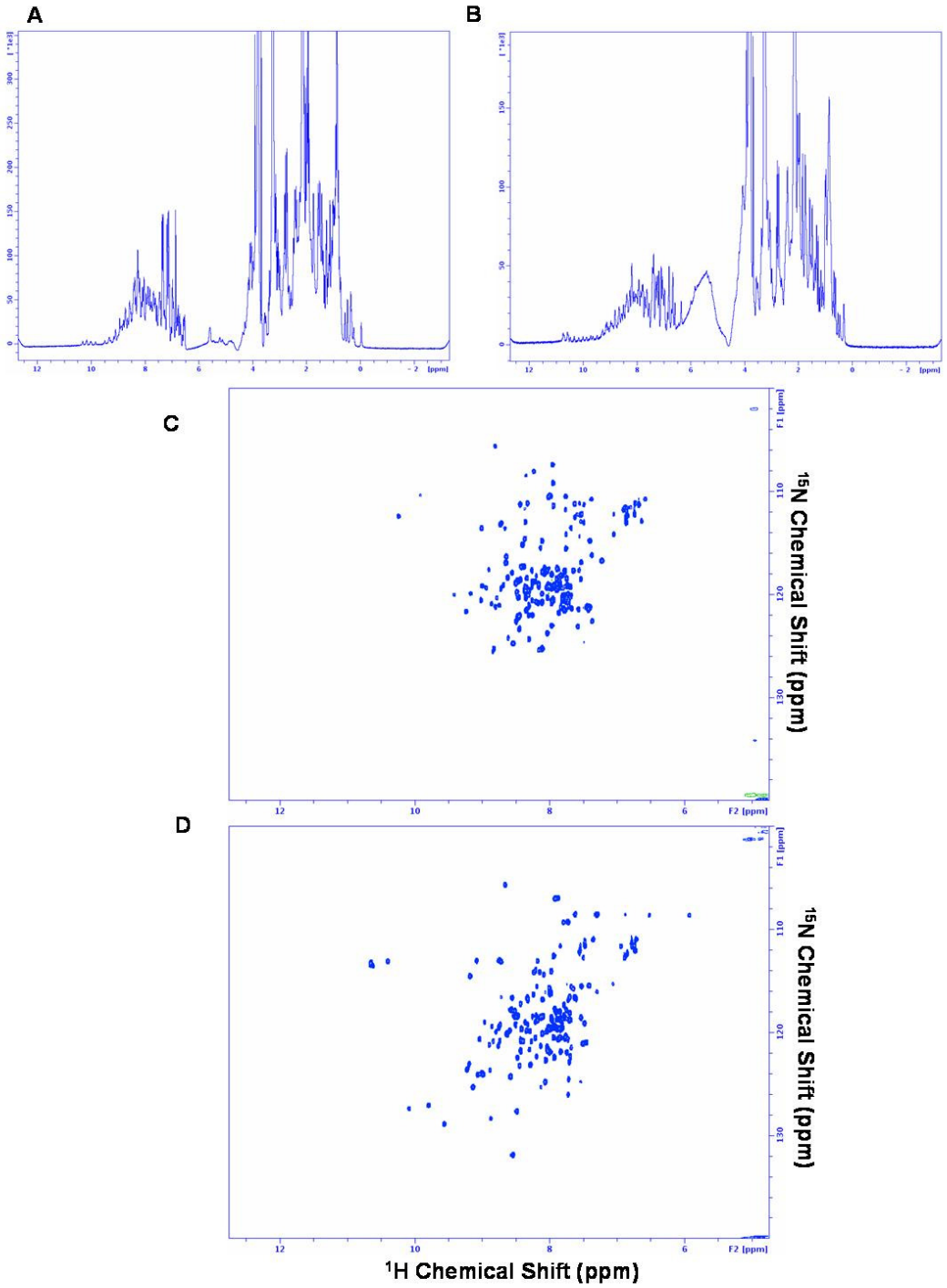

Fig.3.15 NMR analysis of purified calmodulin

The ^{15}N uniformly labeled calmodulin was purified as described previously. The sample was in 20 mM bis-Tris buffer, pH 6.8, 20 mM NaCl, and 1 mM DTT. The 1D proton spectrum was recorded and is shown in A. The ^{15}N HSQC was also recorded and the result in C. The 1D and 2D spectra were also recorded in the presence of 2 mM Ca^{2+}, and the change in the chemical shifts confirmed the conformational change in the presence of Ca^{2+}.

3.6 Expression and purification of calcineurin by affinity and FPLC

To purify active calcineurin, the construct pETCNα derived from pET15 was used for expression. Both CNAα and CNB were cloned into the pET15 to generate pETCNα which is shown in Fig.3.13 C (Mondrageon *et al.*, 1997). There are two S/D (Shin/Dalgarno) sequences in the front of each gene of CAN (NM_000945) and CNB (NM_000944) to express two proteins at the same time under the same promoter.

The figure (Fig.3.16 A) shows the induction of the calcineurin and purification by Ni^{2+}-NTA column (Fig.3.16 B). It was shown that CNB is myristoylated at its N-terminal glycine and the myristoylation of calcineurin B can make calcineurin more stable and soluble. The plasmid pETCNα was co-transformed with pACDuet-NMT into BL21 (DE3) and selected on an LB plate containing both ampicillin and chloramphenical. When the Abs_{600} of the culture in LB containing both ampicillin and chloramphenical reached about 0.6, both IPTG and myristic acid (0.2 M stock in methanol) were added to a final concentration of 0.6 mM and 0.2 mM, respectively. The culture was shaken at 30 ºC for additional 3 h. The cells were harvested by centrifuge and broken as described in the material and methods. CNAα contains N-terminal His tag and it can form complex with CNB, so the Ni^{2+}-NTA purification can be used for the purification of the protein complex. After Ni^{2+}-NTA column purification, the elution fractions were loaded onto Sephacryl S-200 sizing column and the eluted fractions were further purified by MONO Q ion-exchange chromatography. The relatively homogenous protein was obtained after these purification steps. The SDS-PAGE gel clearly shows the difference between the myristoyled and unmyristoyled CANB because myristoylated form migrated faster (Fig.3.16 D). The purified protein also can be stored at -80 ºC in a concentrated form or in the presence of 20% glycerol.

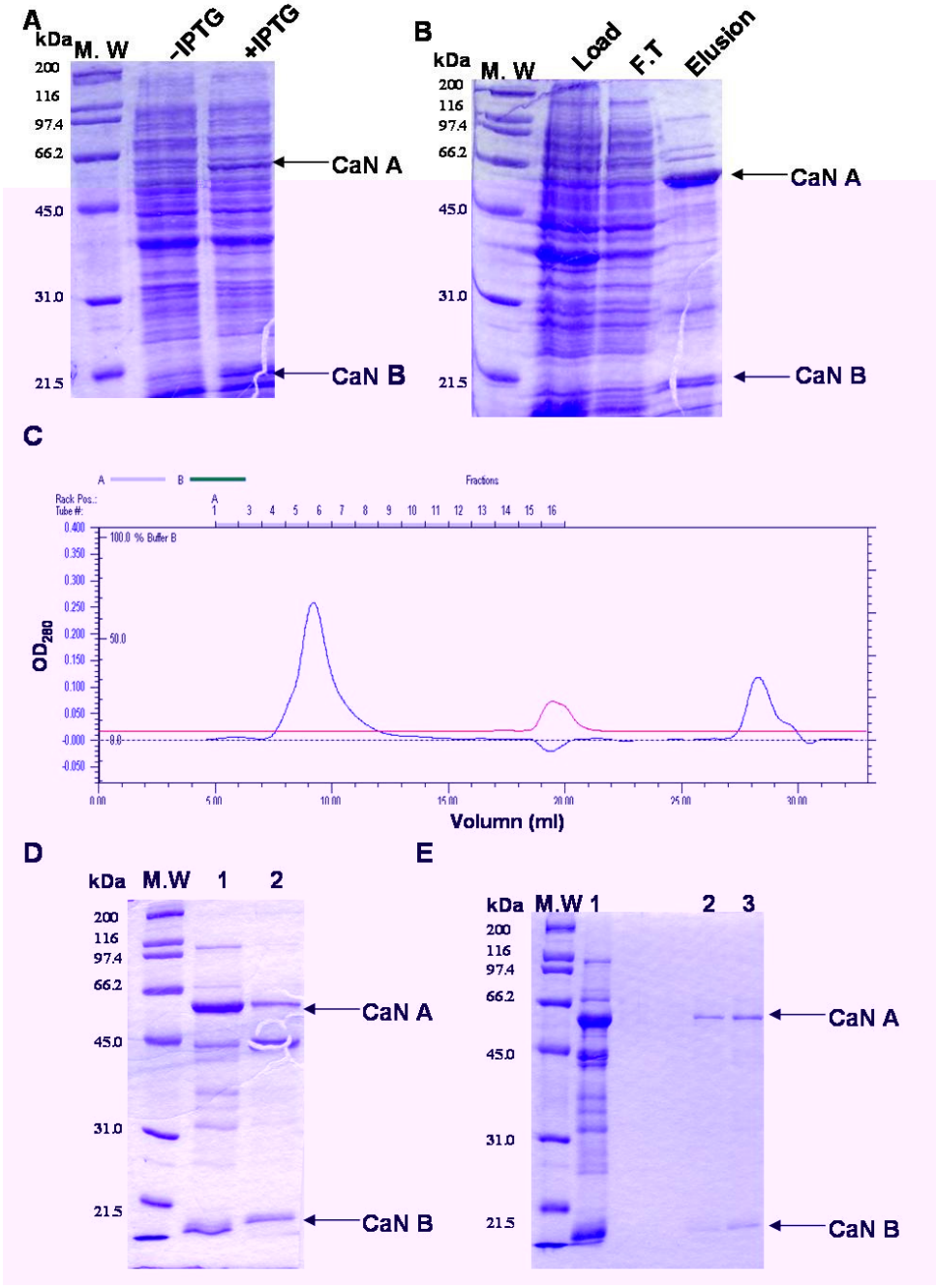

Fig.3.16 Purification of Calcineurin

Induction (A) and purification (B) of CaN-A and CaN-B complex by Ni^{2+} -NTA affinity column are shown. C) The purified CaN-A and B complex by sizing column. D) The purification result of calcineurin by sizing column. 1, un-myrostoylated calcineurin; 2 is myrostoylated calcineurin. E is the purified protein after iron exchange column. 1, load sample after sizing column purification; 2, 3, elusion fractions.

3.7 Purification of kinases

The c-Jun N-terminal protein kinase (JNK, also known as stress-activated protein kinase, SAPK, L26318) is a member of the mitogen-activated protein kinase (MAPK) super family and has been demonstrated to play a critical role in many cellular activities. JNK can be activated by sequential protein phosphorylation through a MAP kinase module (Fig.3.17 A) and can phosphorylate many Bcl-2 family proteins (Yu *et al.*, 2004, Deng *et al.*, 2001). ERK1 and ERK2 (M84489) are well-characterized MAPKs activated in response to growth stimuli with a molecular weight of 43 and 41 kDa, respectively (Chen *et al.*, 2001, Boulton *et al.*, 1991). ERKs are activated by the phosphorylation of a threonine^{183} and a tyrosine^{185} residue by the dual-specificity MAPK kinase MEK1 (L11284) and MEK2 (Pearson *et al.*, 2001). MEKs also require two phosphorylations, both on serine or threonine, for high activity, thus, to get higher active ERK2 in *E.coli* (Kloklatchev *et al.*, 1997, Canagarajah *et al.*, 1997). Constitutively active mutants of MEK1 and MEK2 have been described that have several hundred-fold elevated activities toward ERKs. With some mutations, the constitutively active MEK can be obtained (Mansour *et al.*, 1994) and still can active ERK2 *in vitro*. The MEK1 mutants, MEK ΔN3 S218D (referred as MEK1-R4F) can still be active when it was expressed in *E.coli*. So the *E.coli* co-expression system was set up for the expression of active kinases long time ago (Kloklatchev *et al.*, 1997). The following is the scheme for the activation of kinase (Cobb *et al.*, 1995, Wada *et al.*, 2004). For expression of active ERK2, the MEK1 R4F which is consistently active in *E.coli* was co-expressed with it, after induction, the MEK 1R4F can activate ERK2, so the active ERK2 can be obtained. For the expression of JNK, the MEKK catalytic domain was co-expressed with it and MEK4. After induction, MEKK can activate MEK4 which can activate JNK (Fig.3.17 A).

3.7.1 Purification of ERK2

The purification of ERK2 was performed according to the previously published protocol (Kloklatchev *et al.*, 1997). MEK1R4F and ERK2-pET His_6 were transformed into *E.coli* BL21 (DE3). Cells were grown at 37ºC with shaking to Abs_{600} of 0.2-0.4. The kinases were expressed by the addition of isopropyl-β-D-thiogalactophyranoside (IPTG) to a final concentration of 0.3 mM for overnight with shaking at 30 ºC. Then the cells were harvested and the kinase was purified according to the same procedure as that of other proteins. The purification of ERK2 by affinity and FPLC was shown in Fig.3.18. The purified kinase was concentrated to high concentration and stored at -80ºC for a long-term storage.

GST-ERK2 kinase was also purified in this study. MEKR4F was cloned into pACYC184 and pGEX-4T-m1 to generate pACYC184-MEK-R4F and pGEX-ERK2, respectively. Both plasmids were co-transformed into *E.coli* BL21 (DE3) cells and the expression was performed the same as before. The GST-ERK2 was purified by affinity and sizing column.

3.7.2 Purification of JNK

JNK was purified by co-transforming the plasmids of pBB131/MEKK-C and NpT7-5/α-MAPK+MEK4 into BL21 DE 3 and selected on the LB plate containing both Amp and Kan. The induction and purification were performed by the same way as that of ERK2. The purified JNK (Fig.3.18) was used for the activity assay. The assay results showed that all the kinases purifed were active (Fig.3.19 F). For the ERK2, the His tag fusion proteins were used in all the assay experiments.

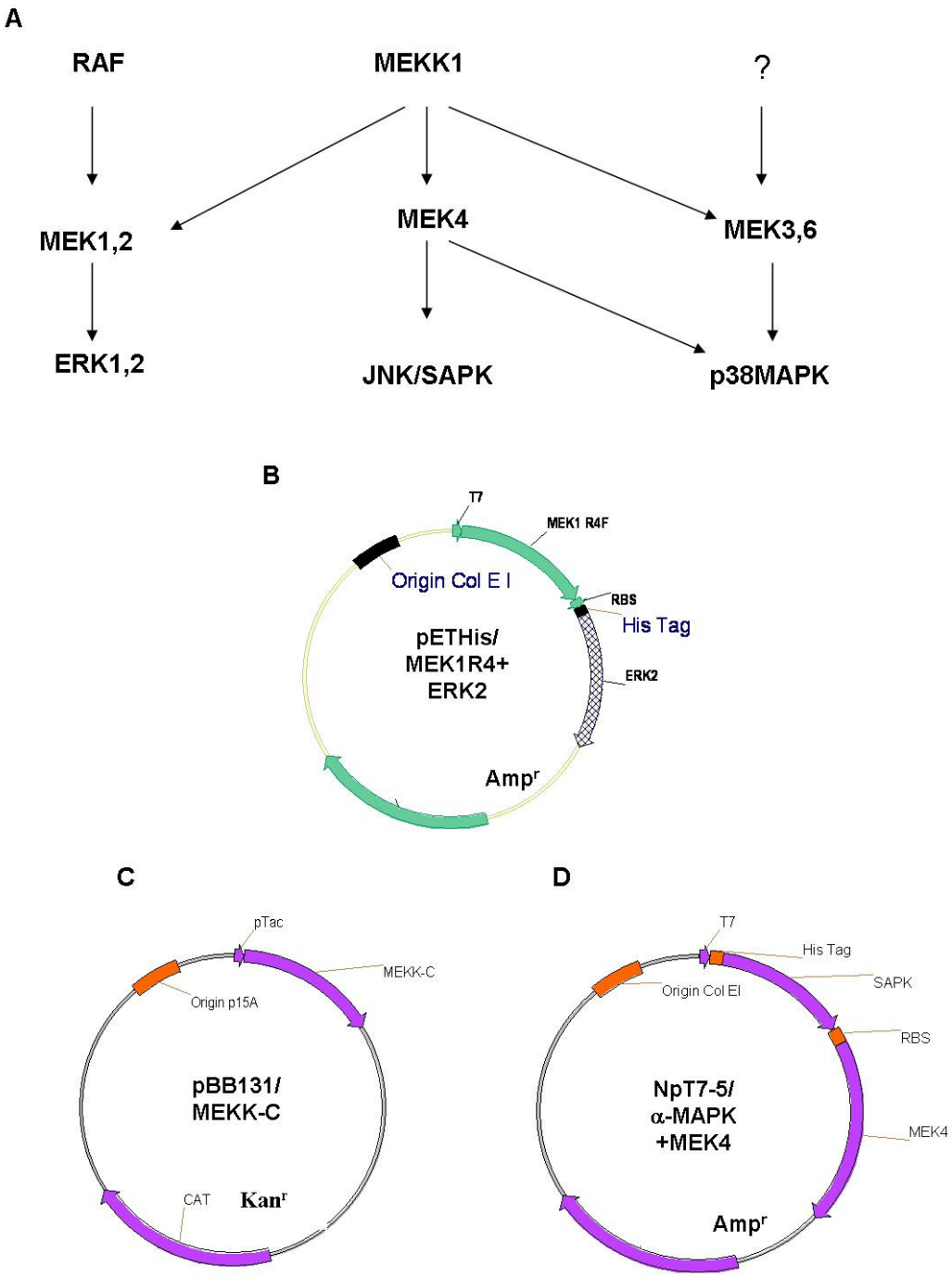

Fig.3.17 The plasmid maps for the active kinase expression in *E.coli*

A) The kinases' activation cascade. B) The plasmid map for the expression of active ERK2. The MEK1R4F is an active kinase and can active ERK2. C) The plamid map of pBB131-MEKK-C that can be used for expression of active JNK. The MEKK-C can active MEK4 and make JNK active. D) The plasmid NpT7-5/α-MAPK+MEK4 for co-expression of pBB131/MEKK-C to get active JNK (Kloklatchev *et al.*, 1997, Cobb *et al.*, 1995).

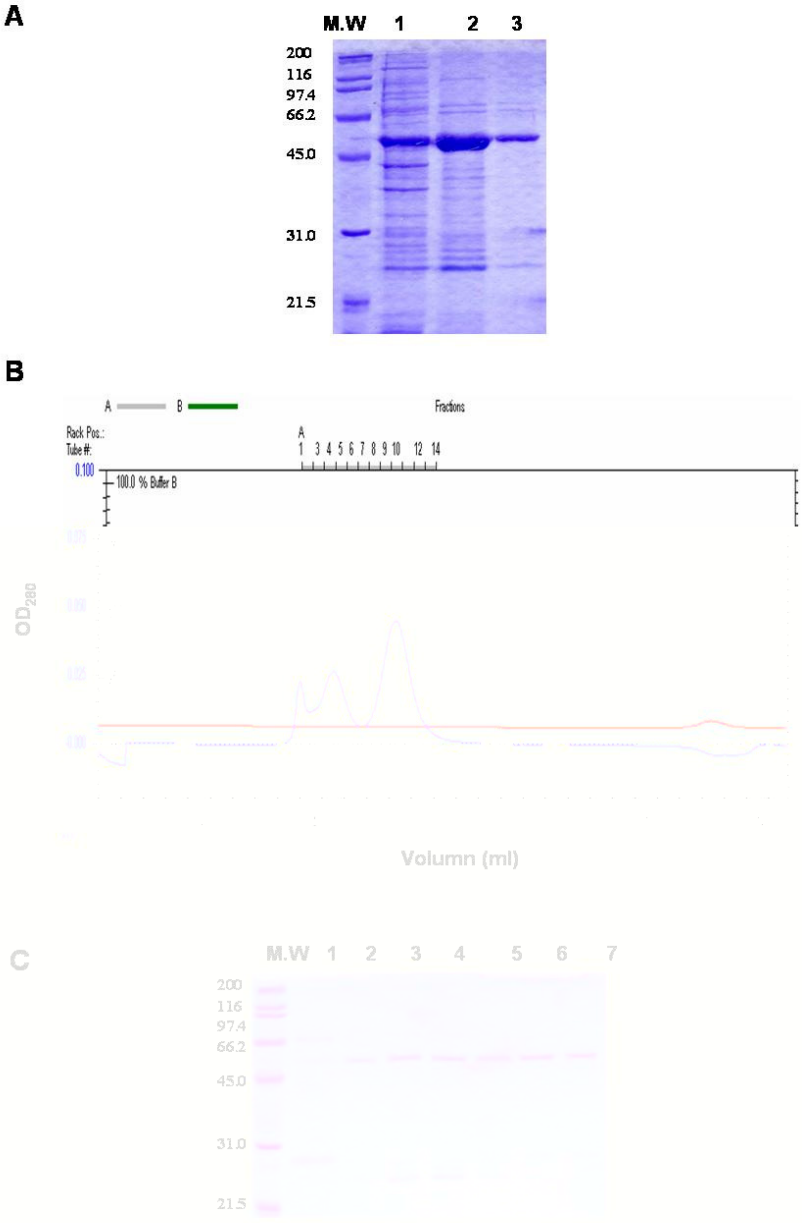

Fig.3.18 Purification active JNK from *E.coli*

A) Affinity purification of JNK from *E.coli*. The JNK was induced and purified by Ni^{2+}-NTA column purification. B) Purification of JNK by sizing column. The fraction from affinity purification was loaded onto the sizing column (Sephacryl S-200) and purified. The buffer used is 50 mM Tris-HCl, pH 8.0, 150 mM NaCl, 1 mM DTT, 0.01% NaN_3. Flow rate for the column is 0.5 ml/min. The fractions with high UV absorbance were collected and analyzed by SDS-PAGE. The pure fraction was stored. C) The fractions collected from sizing column.

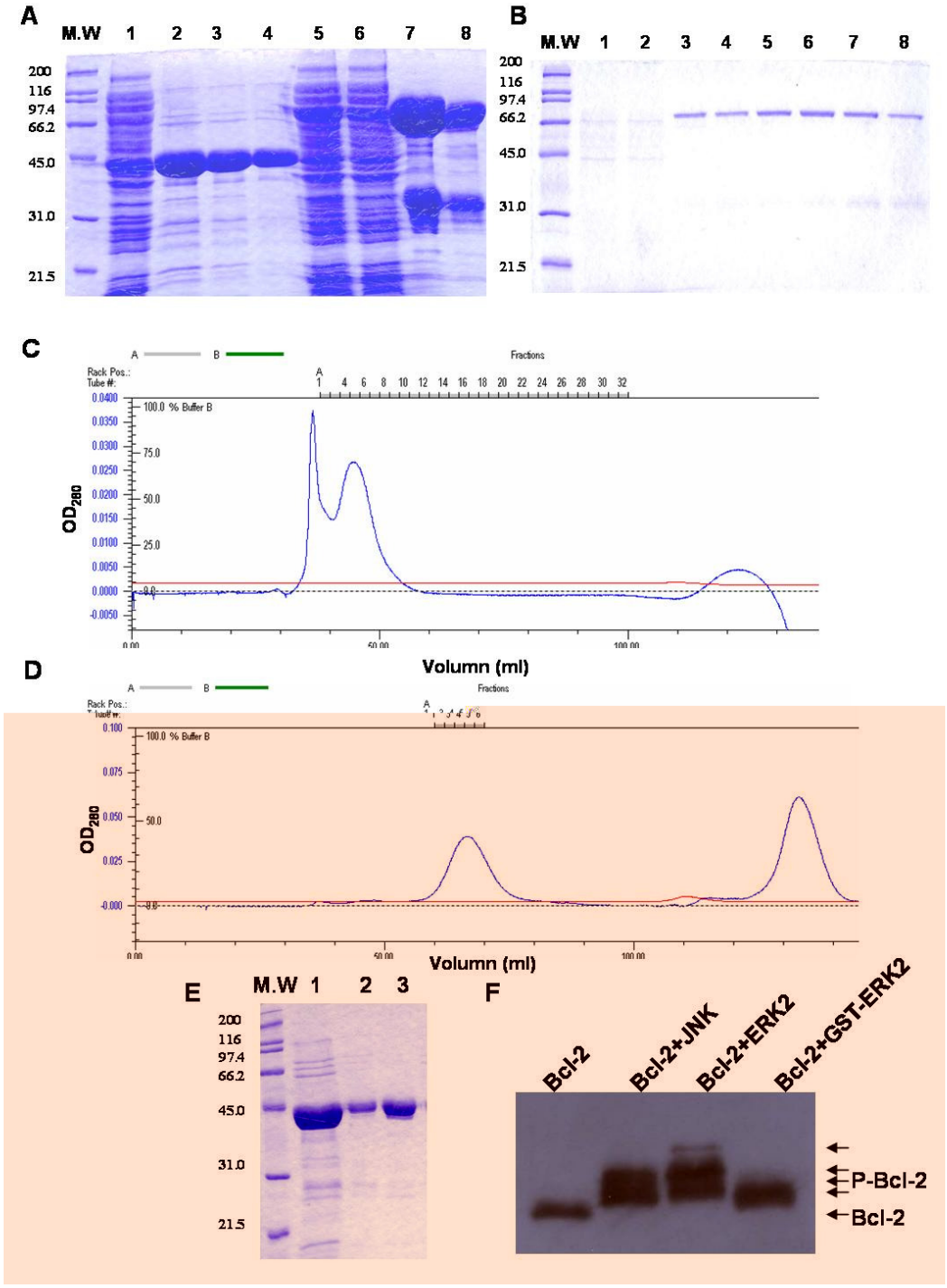

Fig.3.19 Purification ERK2 from *E.coli*

A) Purification of GST-ERK2 and His-ERK2. 1-4 are the purification of ERK2 and 5-8 are the purified fractions of the GST-ERK2. B is the sizing column purification of GST-ERK2. C and D are the spectra for GST-ERK2 and His ERK2 from sizing column. E) Purification His ERK2 from sizing column. 2, 3 are purified protein. F) The kinase reaction using purified JNK, His ERK2, and GST ERK2. After mixing Bcl-2 with different kinases, the western blot using anti-Bcl-2 antibody was performed and the band shift shows the phosphorylation of Bcl-2.

3.8 Purification of P-Bcl-2 in *E.coli*

The active ERK2 could be expressed in *E.coli*. It was also confirmed that Bcl-2 can be the substrate of ERK2. The phosphorylation of Bcl-2 may change some characteristics of Bcl-2's. The co-expression of kinase and Bcl-2 was performed to obtain P-Bcl-2 in *E.coli*. The pACDuet two-promoter system was used for the expression of active ERK2 without any tag. The MEK1R4F was cloned into pACDuet with *Nco I* and *Hind III* to remove the N-his tag. Then ERK2 was inserted into the same plasmid with *Nde I* and *Xho I* to generate the plasmid pAC-MEK-ERK. The plasmid was co-transformed into *E.coli* with pET16-Bcl-2ΔTM. The expression of the proteins was same as that of kinases, and the only difference was that after the induction, cells were harvested and broken by sonication and the supernatant was obtained by centrifuge. 10 uM of ATP was added to the supernatant and let the reaction last on ice for 1-2 hours to get Bcl-2 phosphorylated, then the P-Bcl-2 was purified by affinity purification. The results showed that the purified Bcl-2 migrated slower than the wild-type Bcl-2, indicating that Bcl-2 was phosphorylated (Fig.3.20).

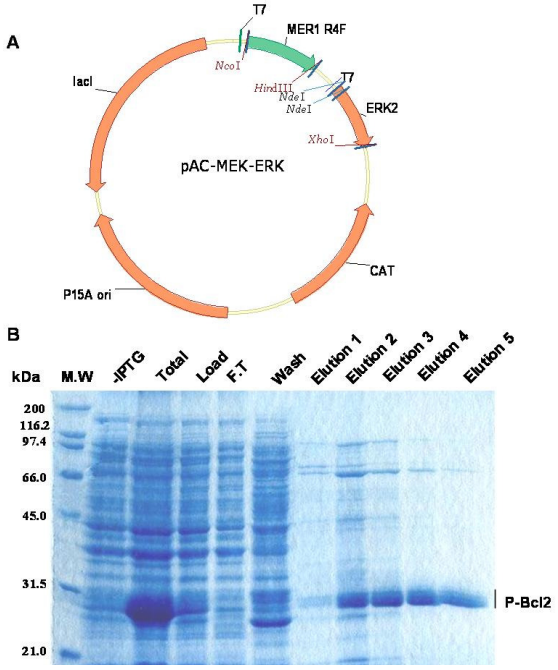

Fig.3.20 Purification of P-Bcl-2 from E.coli

A) The plasmid map for expression of active ERK2 in pACDuet. B) The purification result of P-Bcl-2 by co-expression.

4 Cloning, purification and characterization of FKBP38

FKBP38 has been shown to be unique among FKBP family proteins and localized at mitochondria (Edlich *et al.*, 2005, Kang *et al.*, 2005). Recently, it has been also shown that function of FKBP38 was pro-apoptotic in neuronal cells, and calmodulin binding can make FKBP38 active in the presence of calcium (Edlich *et al.*, 2005). Accumulating reports on potential function of FKBP38 suggest that FKBP38 appears to be multi-functional protein in many regulatory processes. To better understand the function of FKBP38, the biochemical characteristics studies of FKBP38 including chaperone activity, FK-506 binding activity and the effect on the phosphatase activity of calcineurin were performed *in vitro*.

4.1 Isolation of cDNA coding for human FKBP38

FKBP38 is a unique protein among the FKBP family. Sequence alignment of the FKBP domain with other FKBP family proteins demonstrated the lack of conservation of residues involved in FK-506 binding and PPIase activity (Fig.4.1). To study these characteristics of FKBP38, the cDNA coding for FKBP38 was cloned, and FKBP38 was expressed and purified for biochemical and structural studies.

The cDNA coding for human FKBP38 was amplified by RT-PCR using total RNA purified from MCF-7 cell line and inserted into pET29b to generate pET29-FKBP38 full (full length). This plasmid was used as a template for sub-cloning of FKBP38 fragments into different vectors. The pET system such as pET29 and pET16 were used for expression of proteins in *E. coli*.

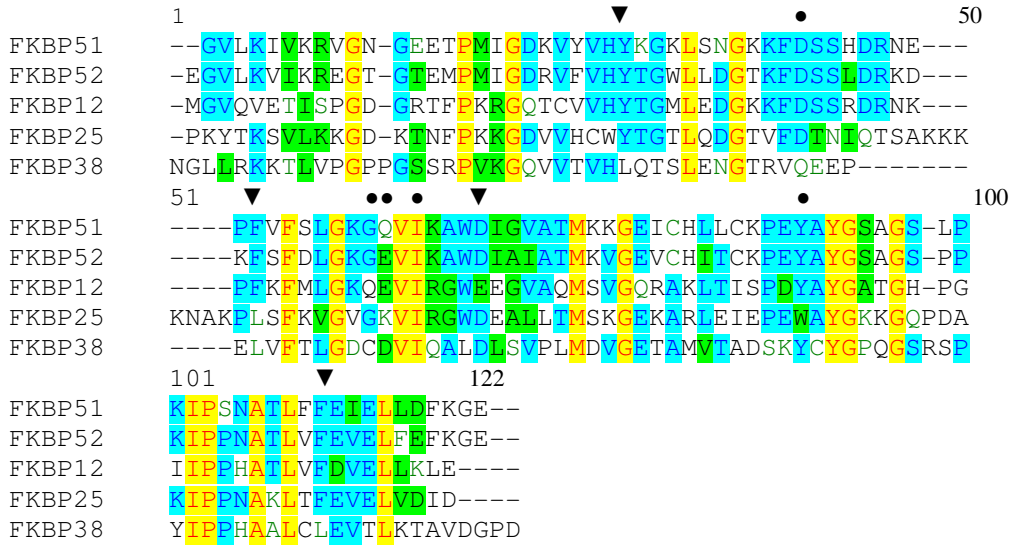

Fig.4.1 Multiple sequence alignment of FKBP family proteins

FKBP51 (JC5422), FKBP52 (A46437), FKBP12 (A35780), FKBP25 (JQ1522), and FKBP38 (AAB00102). The multiple protein alignment was generated by Vector NTI Align X (Informax). The residues in the active pocket for binding FK-506 are indicated by reverse triangles (▼), and those which are involved in interaction with FK-506 through hydrogen bonding are indicated by filled circles (●). NCBI protein data base accession number is indicated in parenthesis corresponding to the FKBP family proteins.

FKBP38 contains a hydrophobic region at the C- terminus, which is the trans-membrane domain (TM) of FKBP38, and this part was shown to be important for the localization of FKBP38 to the mitochondria (Shirane *et al.*, 2003). In the presence of the TM, it was difficult for the protein to be expressed in *E. coli*. So, the construct of FKBP38 ΔTM was made by PCR using the pET29-FKBP38 as template and inserted into pET29, pET16, pGEX-4T-m1 to generate pET29-FKBP38ΔTM, pET16-FKBP38ΔTM and pGEX-4T-FKBP38ΔTM (Fig.4.2), respectively. The resulting plasmids were used for the expression of FKPB38 with C-terminal His tag, N-terminal His tag and GST fusion protein, respectively.

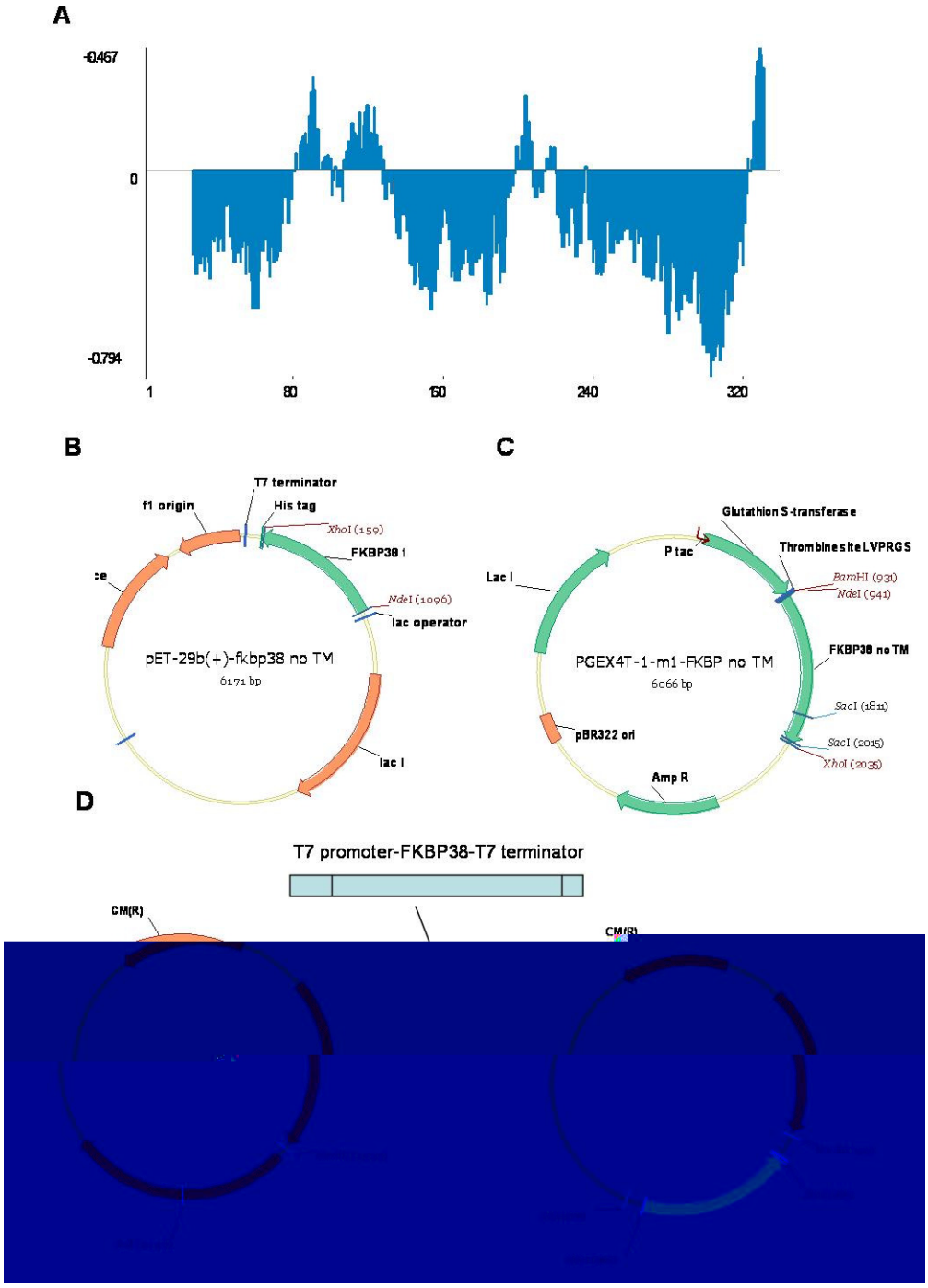

Fig.4.2 FKBP38 ΔTM in different vectors

A) Hydrophobic analysis about FKBP38. This is the hydrophobic analysis about this protein using Vector NTI software. The value that is higher than 0 means that the region is hydrophobic. The amino acid sequence of FKBP38 is from NCBI website (NM_012181). The TM depletion was made based upon the hydrophobic analysis. B, C) The plasmid maps of FKBP38ΔTM in different vectors. D) The plasmid map of pACYC184-FKBP38ΔTM. The PCR was performed to amplify FKBP38 ΔTM containing T7 promoter and terminator and the resulting PCR product was inserted into pACYC184.

Bcl-2 and Bcl-xL were shown to interact with FKBP38 (Shire *et al.*, 2003). To study the interaction between Bcl-2 and FKBP38, co-expression system in *E.coli* was used. The cDNA of FKBP38ΔTM was inserted into pACYC184 to generate pACYC184-FKBP38 ΔTM (Fig.4.2 D). The resulting plasmid pACYC184-FKBP38ΔTM was under *T7* promoter control. As pACYC184 has different replication origin from that of pET system, it can be co-expressed with pET29 system in *E.coli*.

The plasmid pACYC184-FKBP38ΔTM can produce a fusion protein containing C-terminal His-tag, while the pET29-Bcl-2 or pET29-Bcl-2 loop deletion mutants can produce recombinant protein without any tags. When these plasmids are co-transformed into *E.coli*, the induction can be performed by adding IPTG in BL21 (DE3) because both protein inductions were controlled under T7 promoter.

4.2 Purification of recombinant human FKBP38 ΔTM

The small-scale inductions were performed and the induction results could be seen from the SDS-PAGE. From the induction result, it was very clear that the FKBP38 without TM domain could be induced easily (Fig.4.3 A, B). The following purification experiment shows that the protein can be easily purified by Ni^{2+}-NTA purification (Fig.4.3 C, D). The affinity purified sample was further purified by FPLC chromatography and the purification result was shown in Fig.4.3 (C, D, E).

4.3 Characterization of *E.coli* expressed FKBP38 ΔTM

FKBP38 was a unique member in FKBP family. The purified recombinant FKBP38 was characterized physically and immunologically.

4.3.1 Physical and immunological characterization of FKBP38

The purified protein was confirmed by western blotting using anti-FKBP38 antisera (Fig.4.9 F). From the figure, we could detect only one band which is FKBP38

band. The identification of the purified FKBP38 was further characterized by Mass Spectrometry (MS) analysis. The Tandem Mass Spectrometry (MS-MS) and the Blast search showed that the purified protein was FKBP38 (Fig.4.4). Taken together, the data suggest that the purified protein is human FKBP38.

The native molecular size of FKBP38ΔTM was 76 kDa, as determined by gel filtration through a sephacryl S-200, indicating that FKBP38ΔTM may exist as dimmer in solution. The denatured FKBP38ΔTM exhibits an apparent molecular weight of 38 kDa relative to calculated size of 35 kDa.

The folding of the purified protein was examined. The CD data predicted a mixture of α-helix and β-sheet secondary structure in the purified protein. The 1D ^{1}H NMR spectrum showed characteristic of a well folded protein featuring good resonance dispersions in the regions of the methyl protons, α-protons and amide protons. Taken together, our results indicated that the purified protein was correctly folded and ready for biochemical and structure studies (Fig.4.5).

4.3.2 Functional characterization of FKBP38ΔTM

4.3.2.1 Analysis of the molecular interaction between FKBP38 and Bcl-2

It was demonstrated that FKBP38 could interact with Bcl-2/xL and help them localized at the mitochondria (Shirane *et al.*, 2003). In order to study the FKBP38-Bcl-2/Xl complexes, the co-expression system in *E.coli* was performed. The co-expression and purification of FKBP38 and Bcl-2/Xl were performed according to the methods described before (Kang *et al.*, 2005). By Ni^{2+}-NTA affinity purification, both Bcl-2 and FKBP38 could be purified. Because Bcl-2/xL has no His fusion, the only way to purify them with Ni^{2+}-NTA is through their interaction with FKBP38 which is a His-tag fusion protein. Western blot confirm that there were Bcl-2/xL and FKBP38

in the purified fraction (Fig.4.6 A), indicating that these two proteins interacted with each other.

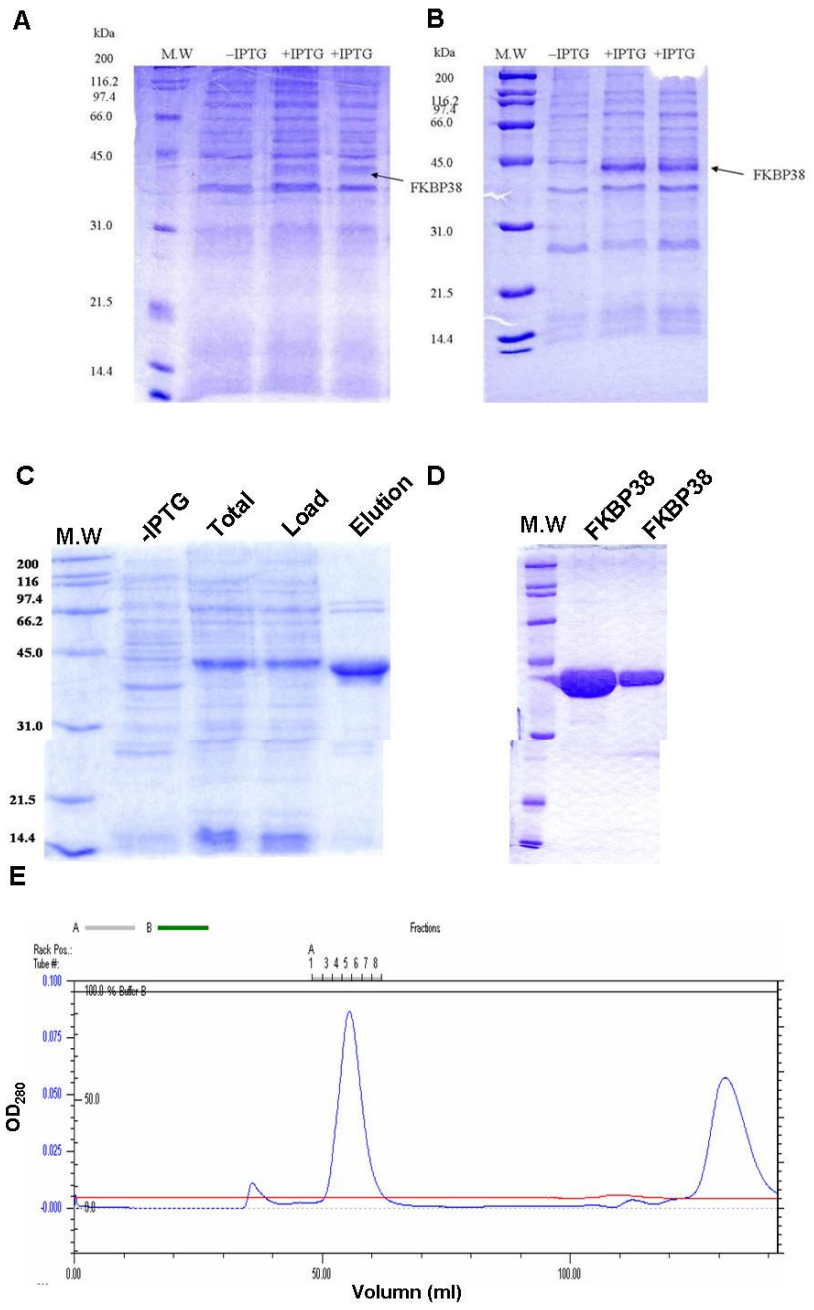

Fig.4.3 Expression and purification of FKBP38 ΔTM from *E.coli*

A) The expression of FKBP38ΔTM in pET29 system. The plasmid pET29-FKBP38ΔTM was transformed into BL21 (DE3) and induction was performed and checked by SDS-PAGE. B. The expression of FKBP38ΔTM in pACYC184 system. C, D) Purification of FKBP38 by affinity and sizing column. C) 1-7 are purified fractions from sizing column. E) The Chromatogram of gel filtration. The S-200 (16/60) column was used for purification with a flow rate of 0.5 ml/min. For the S-200 (26/60) column, the flow rate was 1 ml/min.

A

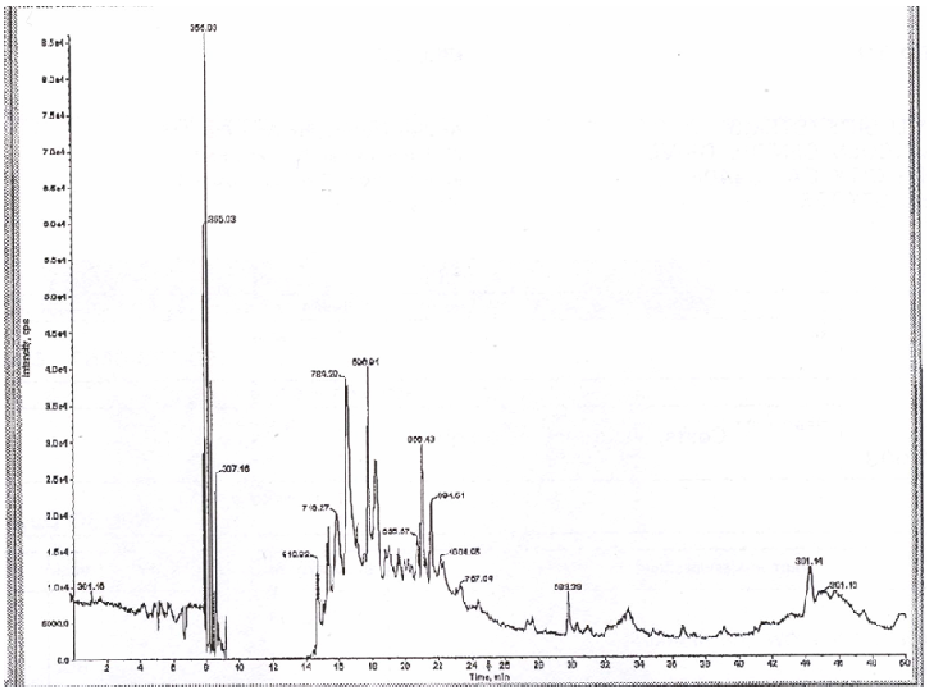

B

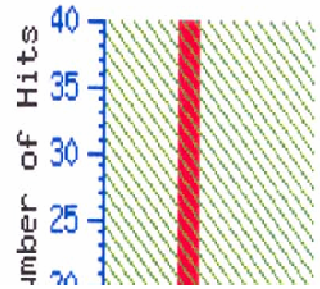

C MS/MS Fragmentation of **GQPPAEEAEQPGALAR**
Found in **AAH09966**, BC009966 NID: - Homo sapiens

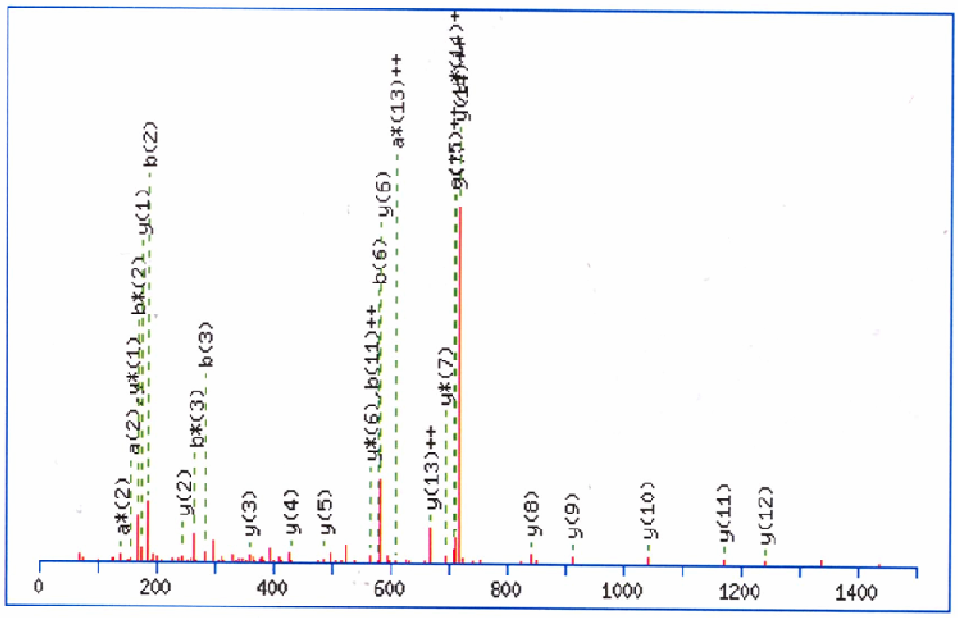

D MS/MS Fragmentation of **VLAQQGEYSEAIPILR**
Found in **AAH09966**, BC009966 NID: - Homo sapiens

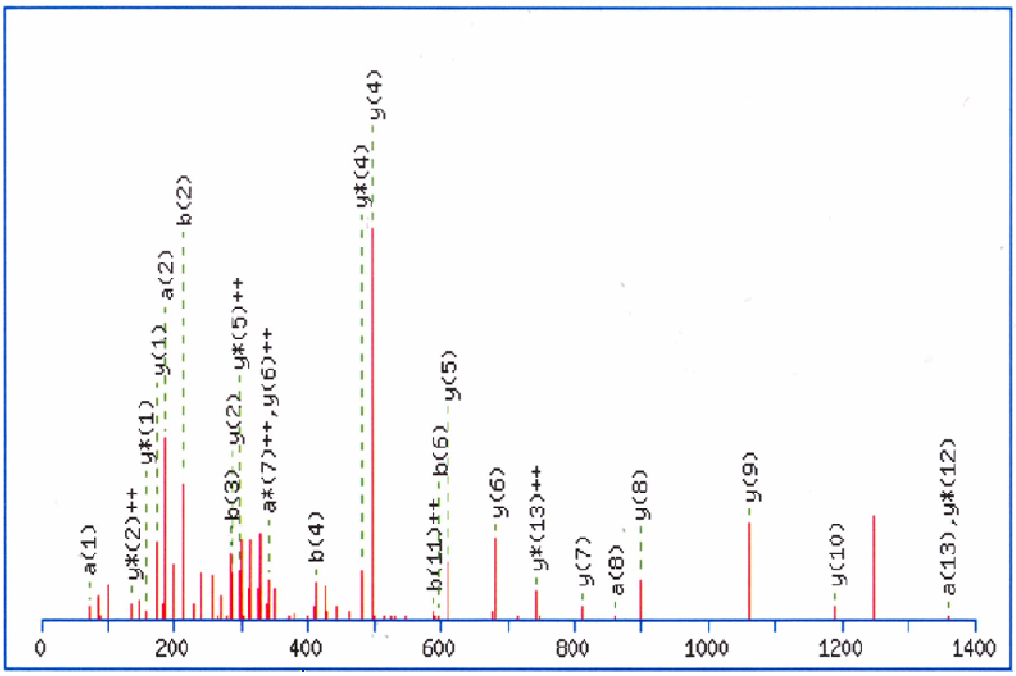

E

MS/MS Fragmentation of **TAVDGPDLEMLTGQER**
Found in **AAH09966**, BC009966 NID: - Homo sapiens

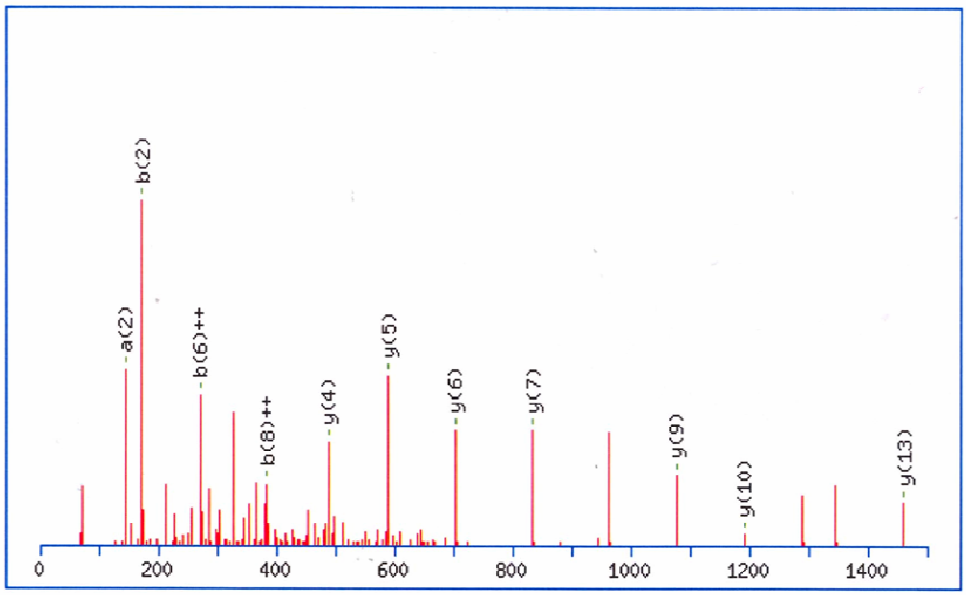

F

Matched peptides shown in **Bold Red**

```
   1 MGQPPAEEAE QPGALAREFL AAMEPEPAPA PAPEEWLDIL GNGLLRKKTL
  51 VPGPPGSSRP VKGQVVTVHL QTSLENGTRV QEEPELVFTL GDCDVIQALD
 101 LSVPLMDVGE TAMVTADSKY CYGPQGRSPY IPPHAALCLE VTLKTAVDGP
 151 DLEMLTGQER VALANRKREC GNAHYQRADF VLAANSYDLA IKAITSSAKV
 201 DMTFEEEAQL LQLKVKCLNN LAASQLKLDH YRAALRSCSL VLEHQPDNIK
 251 ALFRKGKVLA QQGEYSEAIP ILRAALKLEP SNKTIHAELS KLVKKHAAQR
 301 STETALYRKM LGNPSRLPAK CPGKGAWSIP WKWLFGATAV ALGGVALSVV
```

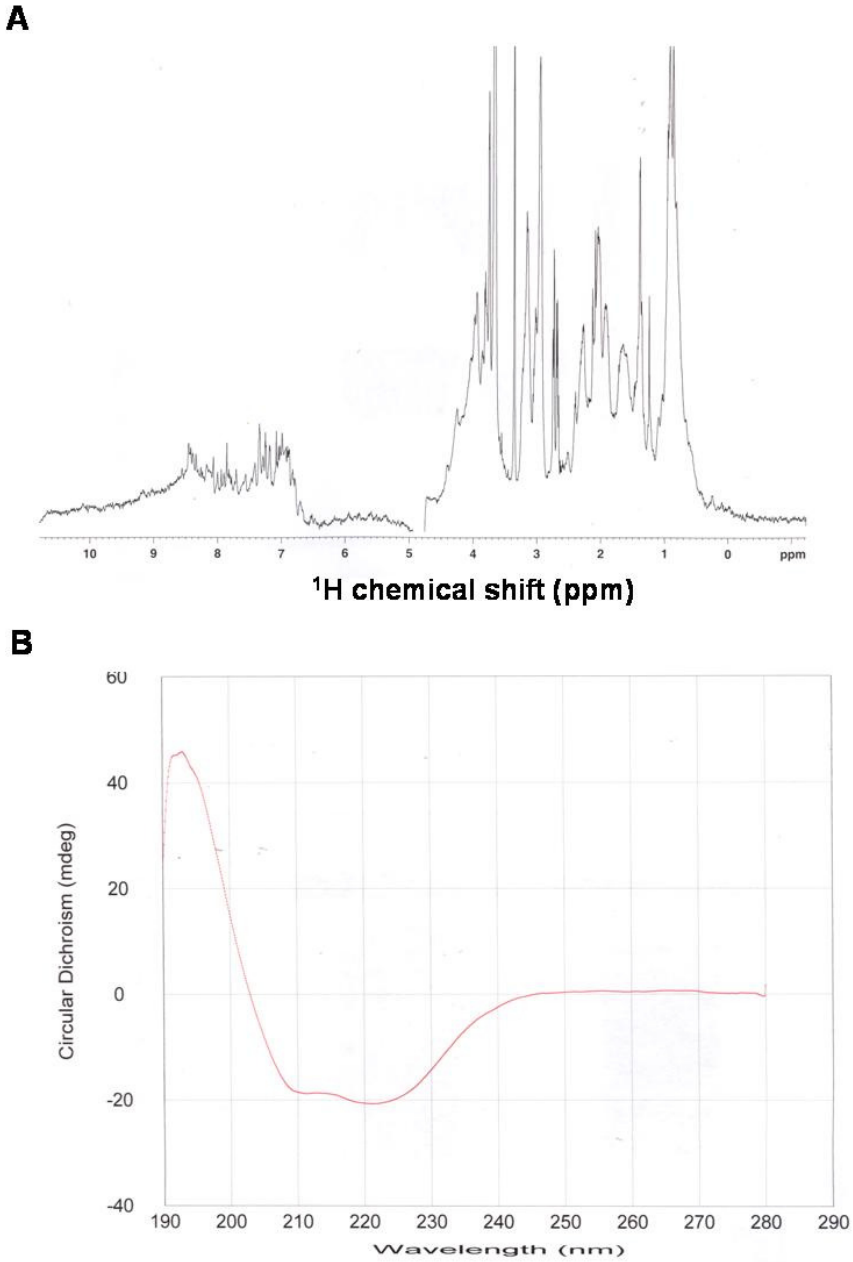

Fig.4.5 NMR and CD analysis of purified FKBP38 ΔTM

A)1D ^{1}H NMR analysis on the purified FKBP38. FKBP38 was purified and concentrated to 8 mg/ml and analysis in the Bruker 700 MHz machine with TXI probe. B) CD analysis on the purified FKBP38. The FKBP38 was purified and in the 20 mM Na-PO_4 buffer, pH 7.2, 100mM NaCl, 2 mg/ml. the CD was measured at described in material and methods. The sample was also concentrated to the same buffer containing 10% D_2O for the NMR analysis.

4.3.2.2 Chaperone activity of FKBP38

It has been shown that FKBP family proteins assist protein folding along with other biological function in cells (Galat, 2003). Recently, it has been reported that FKBP38 exhibited PPIase activity after the formation of the complex with Ca^{2+} and calmodulin (Edlich *et al.*, 2005). This observation led us to further characterize and test potential chaperone activities from FKBP38.

Here, we employed citrate synthase as a model substrate for the chaperone activity assay. It has been shown that the thermal denaturation and subsequent refolding of citrate synthase is a good system to monitor the effect of potential chaperone activity, since it is characterized by low recovery of active enzyme and high degree of forming aggregates during the assay procedure (Kumar *et al.*, 2005, Monaghan *et al.*, 2005).

Also, the chaperone protein can help protein folding or enhance the protein solubility when they are co-expressed together (Fruman *et al.*, 1994, Yasukawa *et al.*, 1995). It was found that when Bcl-2 was induced at 37 ºC, most of the protein was not soluble, but when FKBP38 and Bcl-2 was co-expressed under the same condition, the solubility of Bcl-2 could be enhanced (Fig.4.7), which means that FKBP38 is a chaperone for Bcl-2. Most proteins in FKBP family have chaperone activity to help protein folding or prevent protein from aggregation.

Some data show that FKBP family has the PPIase activity and help protein or enzymes folded correctly (Furutani *et al.*, 2000, Ideno *et al.*, 2004, 2001, Yasukawa *et al.*, 1995). After we checked the effect of FKBP38 on the solubility of Bcl-2, we used the citrate synthase model for further evaluation of the potential chaperone activity.

Our data showed that FKBP38 significantly reduce the level of aggregates of citrate synthase, while FKBP12, which belongs to the FKBP family, and bovine serum

albumin (BSA) had no effect on the aggregate formation of citrate synthase, which is the evidence that FKBP38 is a chaperone protein. It's interaction with Bcl-2 may help Bcl-2 fold correctly.

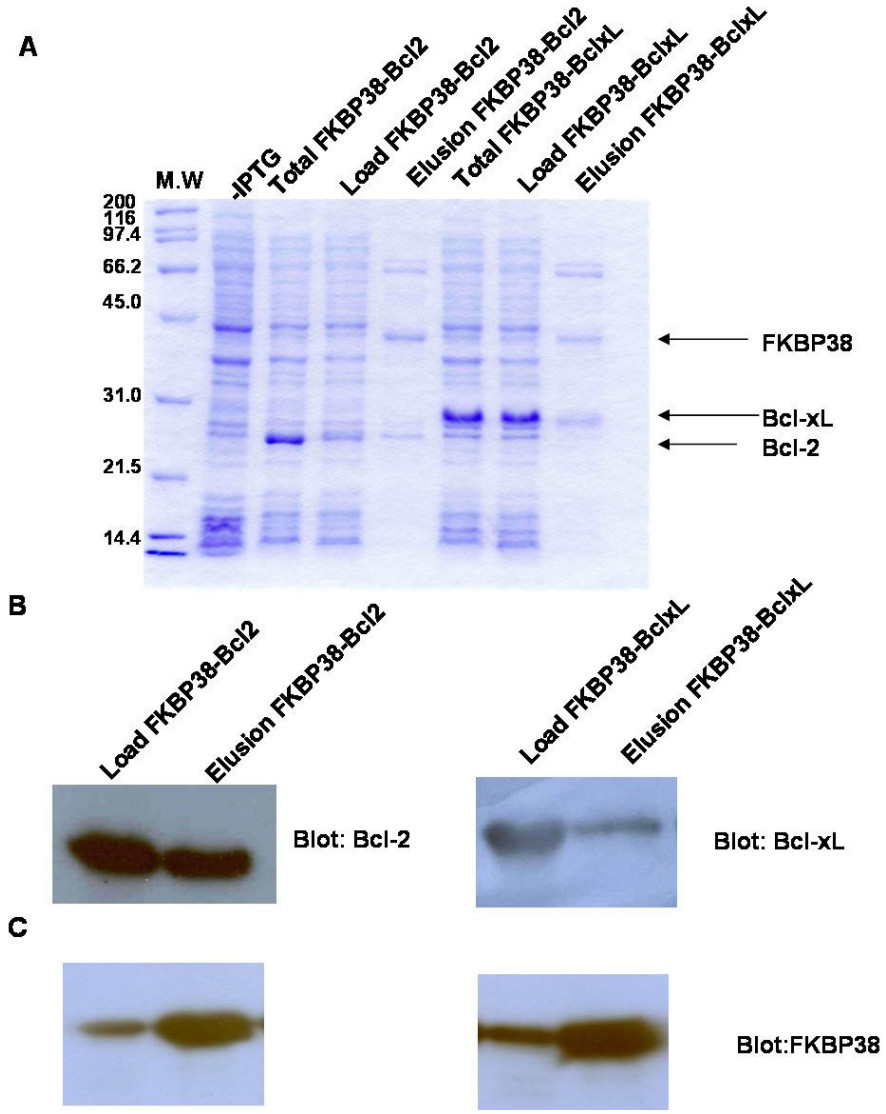

Fig.4.6 Purification of FKBP38-Bcl-2/xL complex

A) Purification of FKBP38 and Bcl-/xL complex from *E.coli*. The plasmid pACYC184-FKBP38 ΔTM can produce a fusion protein containing C-terminal His tag, while the pET29-Bcl-2 and pET29-Bcl-xL produce recombinant protein without any tags. These proteins were co-transformed into *E.coli* and purified by Ni^{2+}-NTA affinity column and analyzed by SDS-PAGE. B) Western blot analysis of the co-expression and purification fractions. C) Western blot using anti-FKBP38 antibody to check the presence of FKBP38.

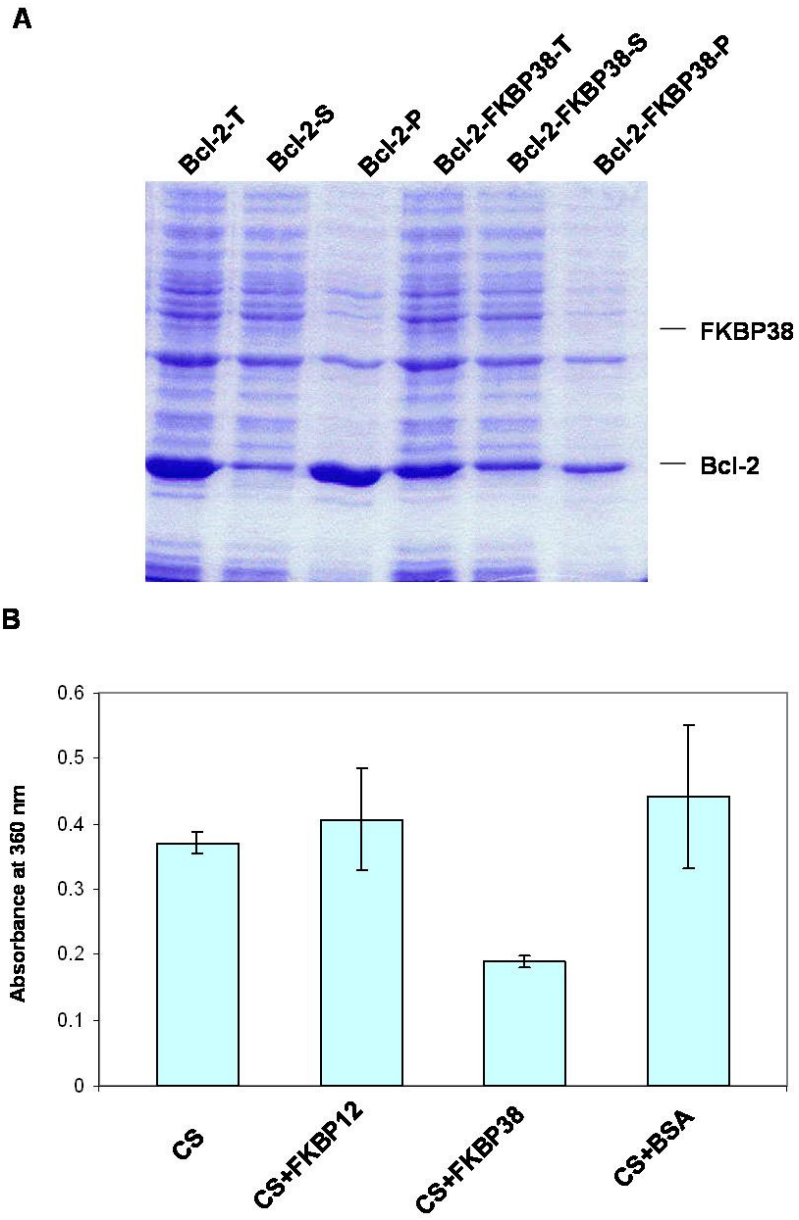

Fig.4.7 Chaperone assay of FKBP38

A) Co-expression of FKBP38 with Bcl-2. The cDNA of FKBP38 lacking trans-membrane was cloned into pACYC184 to generate His fusion protein and Bcl-2/xL was cloned into pET29 to generate proteins without any tag. These two plasmids were co-transformed into BL21 (DE3). The co-expression and purification of FKBP38 and Bcl-2/xL were performed according to the method described. B) Effect of FKBP38 on preventing aggregation of citrate synthase (CS). The protein was mixed with FKBP38 and put at 43 ˚C for 20 min. Then the OD_{360} was measured.

4.3.3 Phosphorylation of FKBP38

Phosphorylation on some proteins can affect their functions. As FKBP38 is a relatively new protein, its regulation mechanism is still unknown. We did some *in vitro* experiment to know if it can be phosphorylated by some kinases.

4.3.3.1 FKBP 38 phosphorylated by ERK2

From the analysis of amino acid sequence of mouse muFKBP38, there appears to be phosphorylation sites in muFKBP38 (Pedersen *et al.*, 1999), FKBP38 was similar to muFKBP38 (Fig.4.8 A), suggesting that FKBP38 may be regulated by some kinases. To check potential phosphorylation of FKBP38, in this study, *in vitro* phosphorylation reactions were performed using two kinases, JNK and ERK2. The data showed that FKBP38 was phosphorylated by ERK2 but not by JNK (Fig.4.8 B). Provided the biological function of FKBP38 still unclear and somewhat controversial (Shrime *et al.*, 2003, Edlich *et al.*, 2005), the *in vitro* phosphorylation data on the potential phosphorylation of FKBP38 might provide information about the role of FKBP38 during apoptosis in cells.

4.3.3.2 Effect of FKBP38 on the activity of calcineurin

The phosphatase activity of calcineurin is inhibited by forming a ternary complex with FK-506 and FKBP12 (Griffith *et al.*, 1995). Given that contradictory observations about the inhibitory effect of human FKBP38 on calcineurin have been reported (Shirane *et al.*, 2003, Weiward *et al.*, 2005). We attempted to investigate the effect of FKBP38 on calcineurin. The commercial substrate for calcineurin RII peptide was used in the study. In the calcineurin assay, we could see the inhibitory effect of FKBP12/FK-506 complex on the activity of calcineurin. For the effect of FKBP38, our results showed unlike FKBP12/FK-506, FKBP38 had no inhibitory effect on the activity of calcineurin in the absence or presence of FK-506 (Fig.4.8 D),

which means FKBP38 has no clearly inhibitory effect on calcineurin. Also, the calcineurin could not use phosphorylated FKBP38 as substrate (Fig.4.8 C). Further functional analysis about the effect of FKBP38 on the activity of calcineurin should be performed.

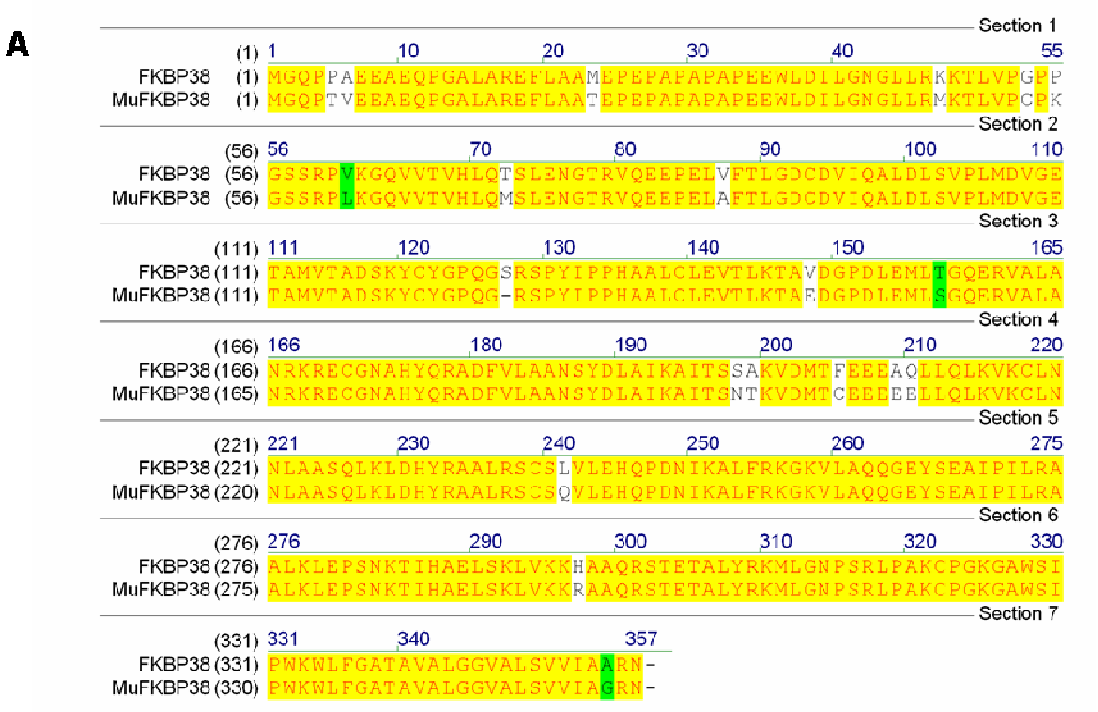

Fig.4.8 The phosphorylation of FKBP38 and its effect on calcineurin activity

A) Sequence alignment between FKBP38 and muFKPB38 using vector NTI.

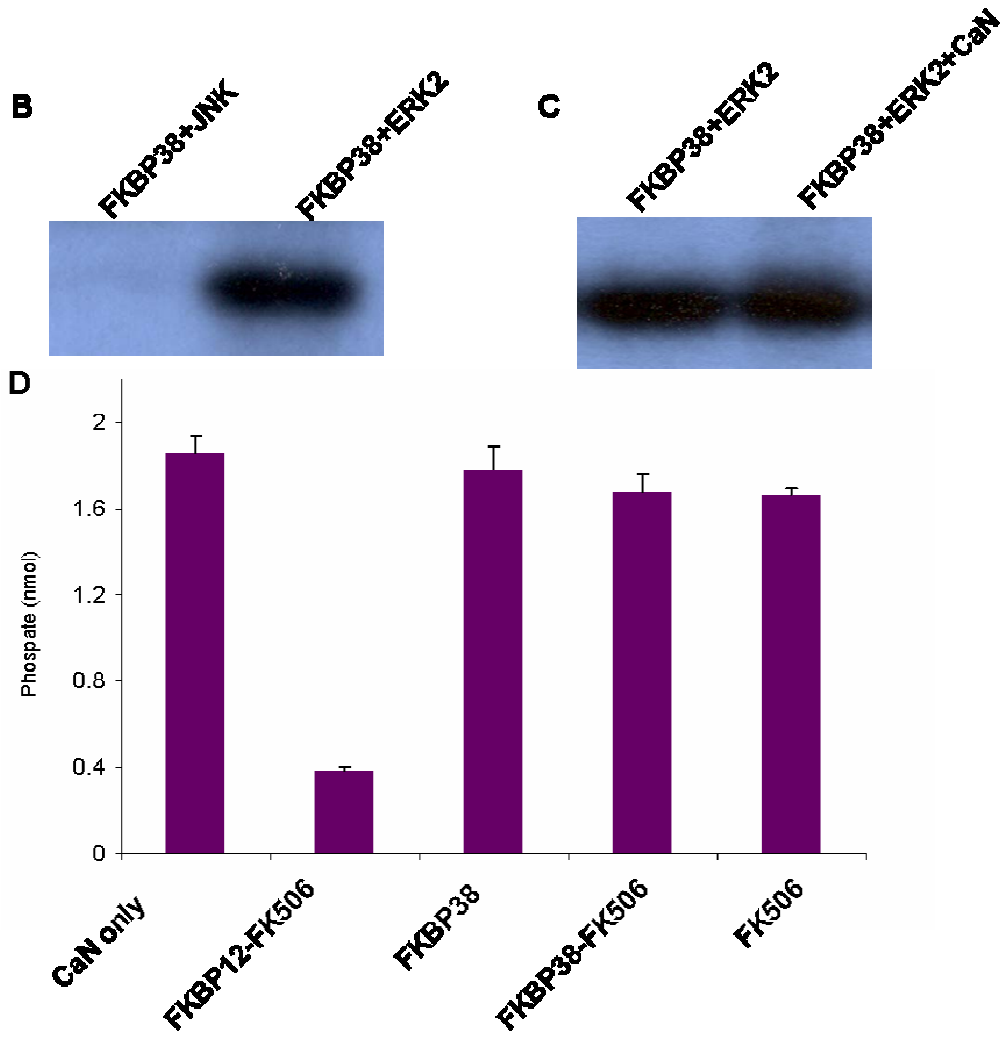

Fig.4.8 The phosphorylation of FKBP38 and its effect on calcineurin activity (Continue)

A) Sequence alignment between FKBP38 and muFKPB38 using vector NTI. B) Phosphrylation of FKBP38 by ERK2 and JNK. C) Effect of calcineurin on the phosphorylated FKBP38. D) Effect of FKBP38 on the activity of calcineurin using RII as substrate.

4.4 Biochemical characterization of the N-terminal domain of FKBP38 (FKBP38NTD)

4.4.1 Construction of FKBP38NTD

It has been confirmed that most FKBP family proteins have PPIase activity and drug binding activity. FKBP38 is different from other proteins, because some amino acids in the FKBP domain were changed. So the structure study on this domain may

explain why this protein behaves differently from other proteins in the FKBP family. Different construction mutations were made by PCR which truncated at different site from the N-terminal part of FKBP38. The PCR product was inserted into pACYC184 with *Nde I* and *Xho I* restriction enzymes sites and the resulting plasmids were transformed into BL21 DE3 for induction. The induction was performed and the fragment from M1 to D149 (FKBP38NTD) was soluble and used for further purification and structural study. The purification step for NTD was same as that of FKBP38. The following part gives the result of NTD induction, purification by Ni^{2+}-NTA column and gel filtration (Fig.4.9). The purified protein was further analyzed by NMR spectrum to see if it was correctly folded. Also, the sample was stored at -80ºC for further application.

4.4.2 Physical characterization of FKBP38NTD

In order to check if NTD is correctly folded, the purified protein was analyzed by CD and NMR. CD data showed that the NTD was mainly β-sheet, which is similar to the predicted structure (Fig.4.10). So the protein was used for further analysis.

The 1D ^{1}H NMR data showed good resonance dispersion in methyl, α-proton and amide regions, which are indicative of a well folded protein. 2D ^{1}H, ^{15}N-HSQC spectrum of the uniformly ^{15}N-labeled FKBP38NTD showed a good resonance dispersion of amide proton (Fig.4.11). Taken together, the purified FKBP38NTD was correctly folded and ready for the further studies.

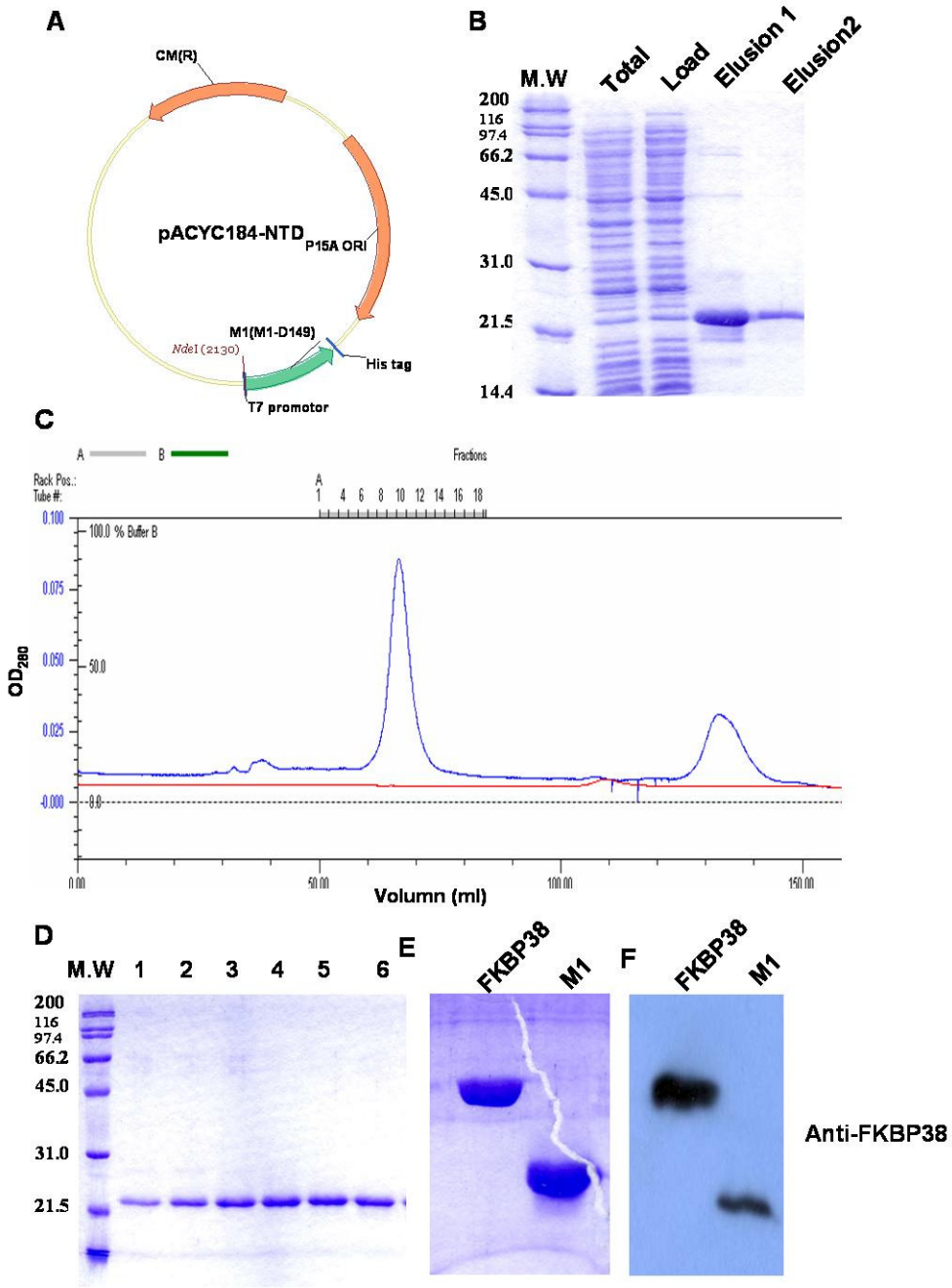

Fig.4.9 Purification of NTD FKBPNTD from *E.coli*

A) The plasmid map to express NTD. The NTD was amplified by PCR using pET29-FKBP38 full as template and inserted into pACYC184 with *Nde I* and *Xho I* restriction sites. The fragment is M1-D149. B, C, D) Purification of NTD by Ni^{2+}-NTA and sizing column. NTD was purified by Ni^{2+}-NTA column and gel filtration. E) NTD and FKBP38 ΔTM were concentrated for crystallization screen. F) Western blot analysis using anti-FKBP38 antibody to confirm the purified proteins.

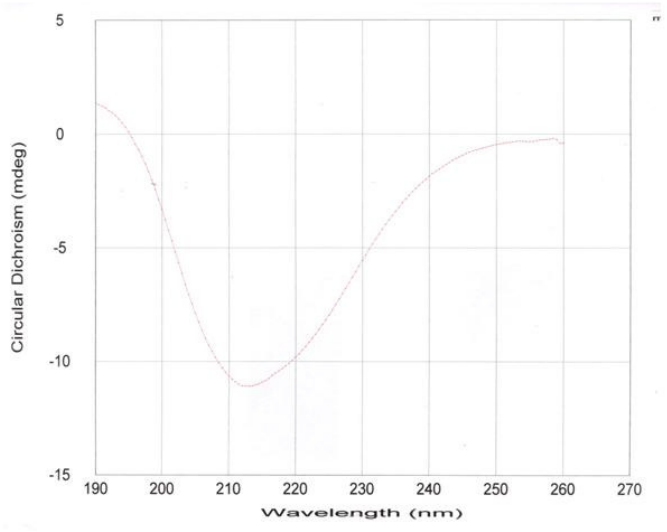

Fig.4.10 CD spectrum analysis of the purified NTD

NTD was purified according to the same way as that of FKBP38. The purified samples were combined together and concentrated to 2 mg/ml in a buffer containing 20 mM Na-PO_4, 100 mM NaCl. The CD spectrum was recorded at room temperature. Using the same buffer without protein as a blank, after doing the subtraction with sample CD spectrum, the protein CD spectrum was obtained.

4.4.3 Functional characterization of FKBP38

FKBP38 contains a unique FK-506 binding domain, which was predicted by a sequence comparison. Currently, the ligand-binding activity of the domain is unclear. Here, we employed a NMR-based binding study using ^{15}N-labled FKBP domain of human FKBP38 to check the interaction with FK-506. As the interaction with FK-506 in the FKBP members, the FKBP domain in FKBP38NTD is the binding site for the interaction. The NMR result clearly showed that upon the addition of FK-506, no apparent spectral changes were detected in ^{15}N-HSQC spectrum (Fig.4.12) while chemical shifts perturbations were observed in the ^{15}N-HSQC spectrum of FKBP12 upon the addition of FK-506 (Fig.4.12). Taken together, the data suggest the FK-506 binding domain of FKBP38 did not bind FK-506.

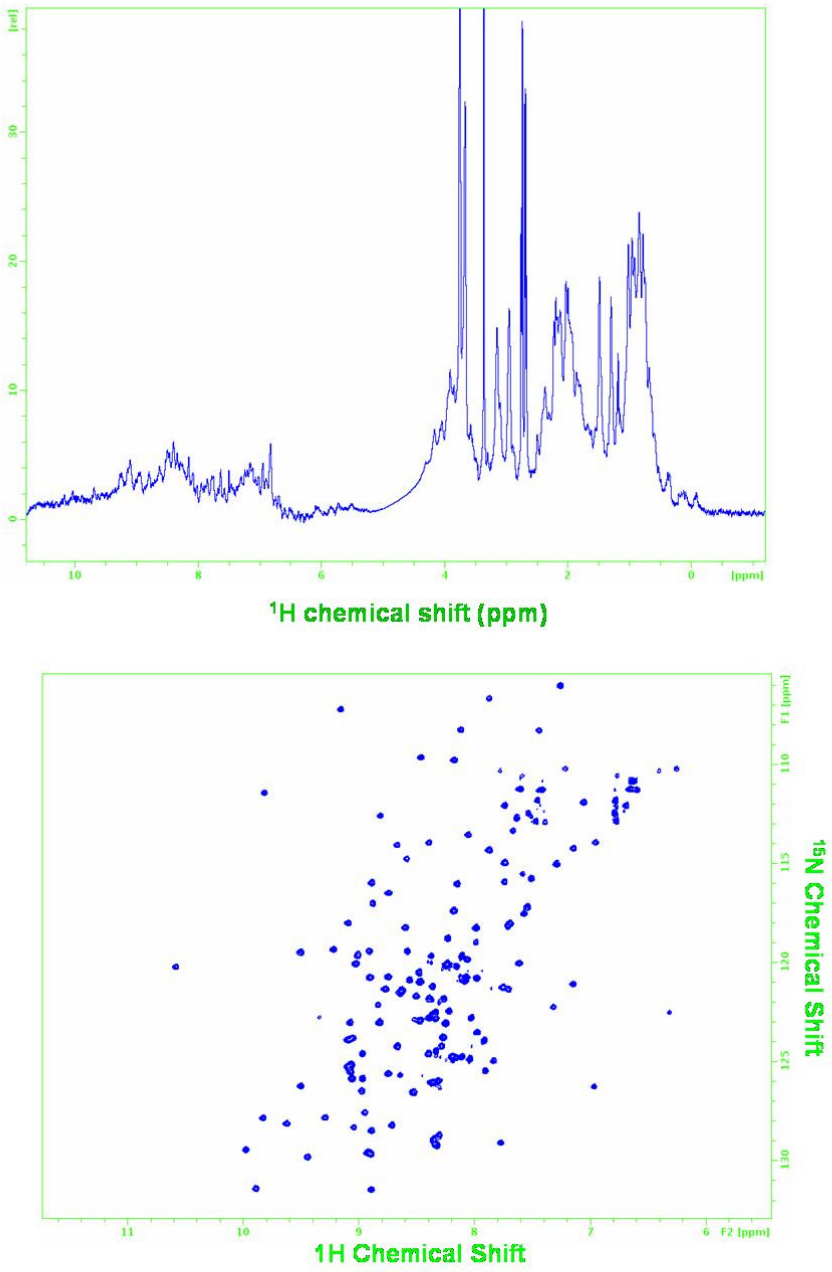

Fig.4.11 NMR analysis of purified NTD

The NTD was purified by affinity and gel filtration. The fractions from sizing column were checked by SDS-PAGE. The pure fractions were combined together and concentrated together. The buffer was changed into the following buffer: 20 mM Na-PO_4, pH 7.0, 10 mM NaCl, 1 mM DTT, 0.01% NaN_3. For the 1D ^{1}H NMR experiment, the normal sample was used for analysis. For the HSQC experiment, the protein was induced in M9 medium supplied with $^{15}NH_4Cl$, the uniformly ^{15}N labeled protein was purified as the same way as that of normal sample. The protein was concentrated and ^{15}N-HSQC spectrum was recorded.

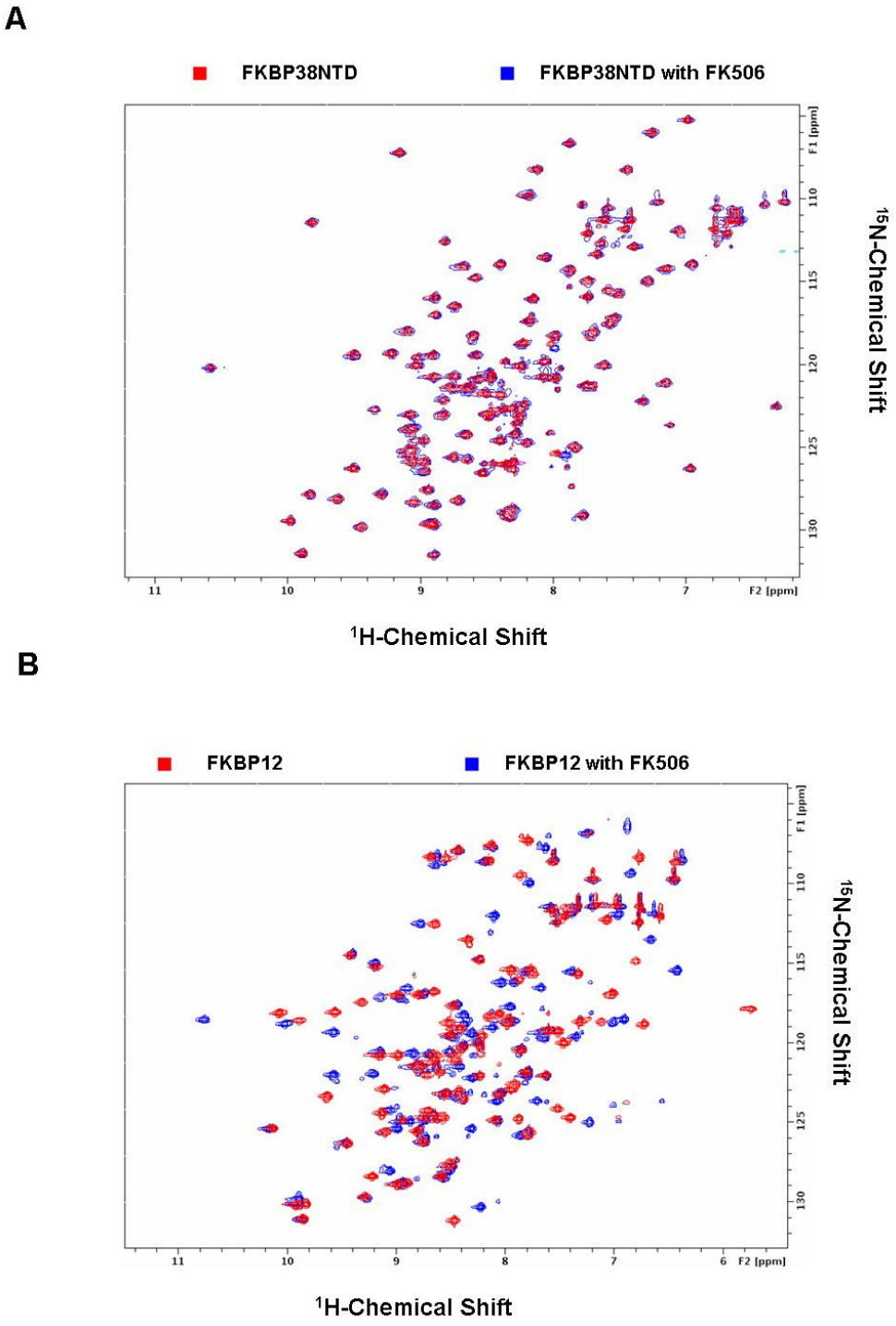

Fig.4.12 Interaction between FK-506 and FKBP12/FKBP38

The FKBP domain of FKBP38 (FKBPNTD) does not bind FK-506 in NMR-based binding assays. Chemical shift perturbations to ^{15}N- labeled FKBP38NTD (A) and FKBP12 (B) were monitored with ^{15}N-heteronuclear single quantum correlation spectroscopy (HSQC) upon addition of FK-506. The HSQC spectra with or without FK-506 were shown in red or blue, respectively.

4.5 Discussion

FKBP38, unlike other FKBP family proteins, has been shown to lack the FK-506 binding activity and inhibitory activity on calcineurin (Shirane *et al.*, 2003). To further understand the biological function of FKBP38, we, in the present study, attempted to investigate the molecular characteristics of human FKBP38 and its regulatory role on the anti-apoptotic protein Bcl-2. Recently, it has been shown that PPIase activity of FKBP38 was activated by complex formation with Ca^{2+}/calmoudulin (Edlich *et al.*, 2005). This led us to further investigate potential chaperone activities of FKBP38. The FKBP38ΔTM was purified in *E.coli* and GST-FKBP38 was also purified for pull-down assay. From our results we demonstrated that FKBP38 exerted molecular chaperone activities by reducing the degree of aggregate in the citrate synthase model system and also increasing solubility of Bcl-2, while FKBP12, which used as a control in this study, did not appear to show similar chaperone activities to those substrates (Fig.4.7), suggesting that FKBP38 appears to work differently in chaperoning other proteins as compared to the typical FKBP family proteins.

To further test whether or not FKBP38 binds FK-506 at molecular level and shows any inhibitory activity on calcineurin, we performed NMR-based binding studies of FKBP38 and phosphatase assays of calcineurin. The data showed that NTD did not show any apparent chemical shift perturbations in the 2D ^{1}H, ^{15}N-HSQC spectrum of NTD upon addition of FK-506 (Fig.4.12 A), suggesting no molecular interaction with FK-506. In contrast, FKBP12 demonstrated significant chemical shift perturbations in the presence of FK-506, indicating apparent binding to FK-506 (Sich *et al.*, 2000).

Sequence comparison study among FKBP family proteins reveals that FKBP38 lacks the well-conserved aromatic residues involved in binding to FK-506 in the active site pocket (Galat, 2000). FKBP38 contains Leu instead at those positions. The

Trp in FKBP12 is important for the interaction with FK-506 and forms the base of the hydrophobic drug-binding cavity. Those sequence variations found in FKBP38 might be one of potential reasons contributing to the difference between FKBP38 and other FKBP family members in recognizing FK-506 as a ligand. On the other hand, FKBP38 contains the extra N-terminal tail, not found in other FKBP family proteins. The significance of this tail of FKBP38 on FK-506 binding remains to be explored.

Three-dimensional structural determination of FKBP38 or NTD would provide important clues for explaining the unique properties of FKBP38. Previously, it was shown that FKBP38 is an endogenous inhibitor of calcineurin (Shirane *et al.*, 2003). Our results demonstrate that FKBP38 did not appear to influence calcineurin activity *in vitro*. Whether the binding of FK-506 is prerequisite for the inhibition on the phosphatase activity of calcineurin remains to be further explored.

Previously potential posttranslational modification sites in the murine FKBP38 were predicted (Pedersen *et al.*, 1999). Since the human FKBP38 has very high homology with the murine FKBP38, to check phosphorylations on the human FKBP38, in this study, we performed *in vitro* phosphorylation reaction using purified protein kinases. The results showed that FKBP38 was phosphorylated by ERK2, but not JNK (Fig.4.8 B), suggesting that FKBP38 potentially could be phosphorylated by a specific kinase such as ERK2. More studies are needed to further characterize the phosphorylation of FKBP38 in cells.

5 Characterization on molecular interaction between FKBP38 and Bcl-2

Apoptosis is an essential and well-orchestrated cellular regulatory mechanism in which pro- and anti-apoptotic proteins are involved in various stages. The proteins of Bcl-2 family are central to the regulation of apoptosis (Adams *et al.*, 2001, Martinou *et al.*, 2001, Kojima *et al.*, 1996, Kelekar *et al.*, 1998). Three dimensional structures of Bcl-xL and Bcl-2 reveal that such proteins contain an elongated hydrophobic cleft through which the anti-apoptotic proteins and their ligands interact to form heterodimers (Muchmore *et al.*, 1996, Petros *et al.*, 2001). Another intriguing feature from the three-dimensional structures is that Bcl-2 and Bcl-xL contain a disordered long loop with about 60 amino acid residues between the first and the second helices. This flexible loop has been shown to have unstructured conformations based on NMR or X-ray crystallographic analyses on this region (Muchmore *et al.*, 1996).

Recently, this flexible loop has been shown to be regulated at the posttranslational levels such as phosphorylation and ubiquitin-dependent degradation, in response to diverse external stimuli (Chang *et al.*, 1997, Breitschopf *et al.*, 2000, Haldar *et al.*, 1998, Bassik *et al.*, 2004). Proteins containing regions of denatured or random coil structure do not normally exhibit long half-lives due to cleavage by cellular protease (Ciechanover *et al.*, 1994). Therefore, it has been suspected that the long disordered loop of Bcl-2 and Bcl-xL is shielded or otherwise protected from rapid degradation by other cellular proteases (Chang *et al.*, 1997). The association of putative chaperones or regulatory molecule including kinases with the unstructured loop is not well understood. Recently, it has been shown that immunosuppressant FK-506 binding protein 38 (FKBP38) is co-localized with Bcl-2 and Bcl-xL at the mitochondria,

suggesting that FKBP38 is a potential docking molecule for the anti-apoptotic proteins (Shrine *et al.*, 2003). However, details and characteristics of the molecular interaction between FKBP38 and the anti-apoptotic proteins remain to be explored. In this study, we have performed the characterization of recombinant human FKBP38 and investigated the nature of molecular interaction between FKBP38 and Bcl-2 to understand a possible, alternative mechanism of apoptotic regulation through a potential chaperone activity of FKBP38 for Bcl-2.

5.1 Interaction between FKBP38 and Bcl-2

We performed co-expression of FKBP38 (his-tag fusion protein) and Bcl-2/xL (without His-tag) in BL21 (DE3) (Fig.5.1). When FKBP38 and Bcl-2/xL were co-expressed in *E.coli*, after purification, there were two bands in the eluted fractions. Western blot confirmed that elution fractions contained FKBP38 and Bcl-2/Bcl-xL factions (Fig.4.6), indicating that FKBP38 can bind Bcl-2/xL. We performed co-immuno-precipatation (IP) using anti-FKBP38 antibody. The Hela cells were first cultured in the medium and the cells were harvest. Then the lysate buffer was added into the cells and anti-FKBP38 antibody was added. The IP product was further detected by anti-Bcl-2 and anti-Bcl-xL antibodies, respectively. The result was consistent with the *E.coli* co-expression experiments. We can get both Bcl-xL and Bcl-2 after IP (Fig.5.1). Both Bcl-2 and Bcl-xL could be pulled down with anti-FKBP38 antibody, but the binding affinity between Bcl-2 and FKBP38 is higher than that of Bcl-xL. So we performed the purification of the FKBP38-Bcl-2 complex by affinity on a Ni^{2+}-NTA. The complex was further purified by sizing column (Fig.5.1). Initially an attempt was make to crystallize the complex, but no sign of crystallization was detected. In this study, major effects were made on the molecular characterization between FKBP38 and Bcl-2 through solution NMR spectroscopy.

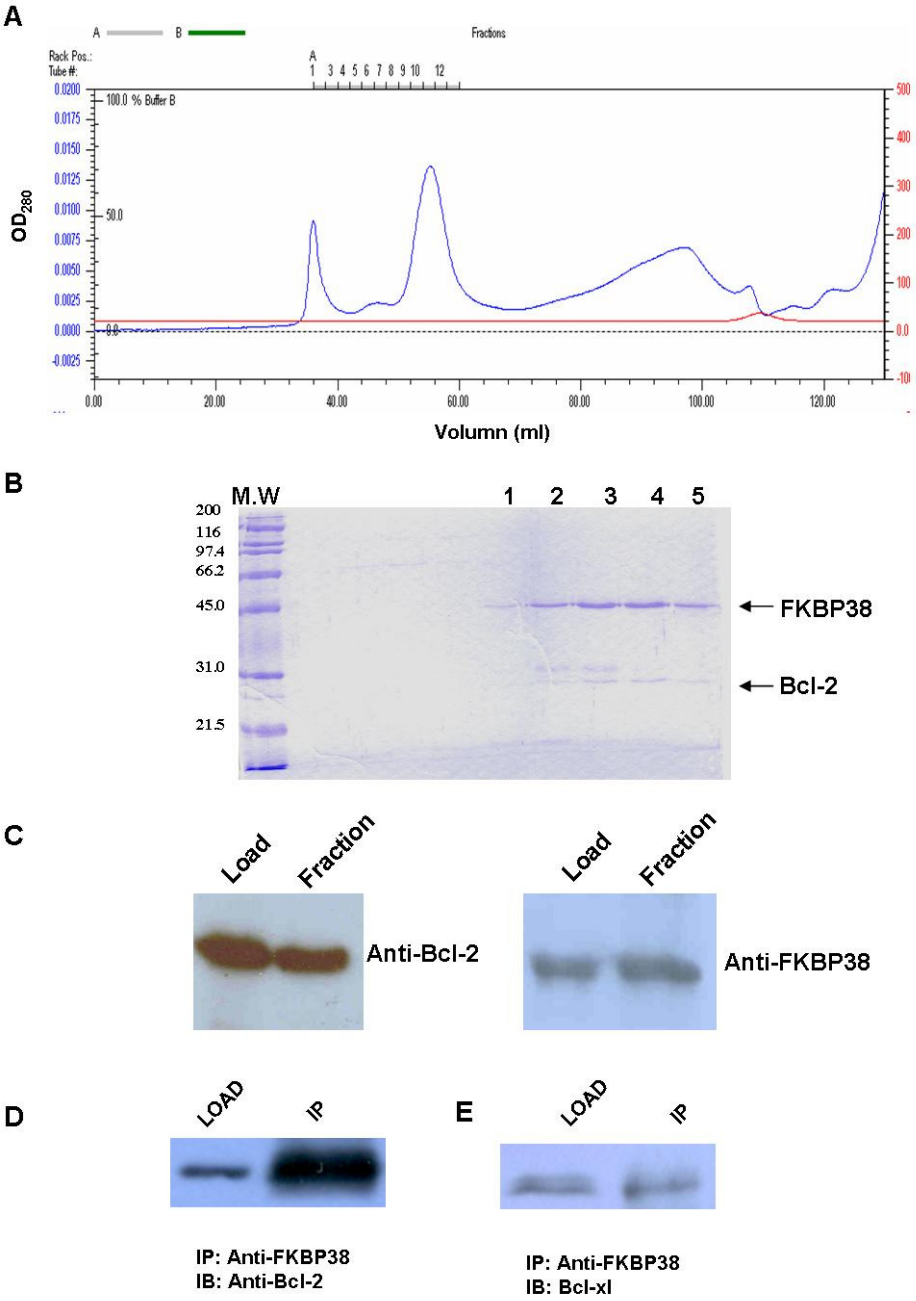

Fig.5.1 Purification of FKBP38-Bcl-2 complex by sizing column

A) Sizing column purification of the FKBP38-Bcl-2 complex. The FKBP38-Bcl-2 complex first purified by Ni^{2+}-NTA column as described in chapter 4. The purified fractions were loaded onto sizing column for further purification. B) SDS-PAGE analysis the purified fractions from sizing column. The fractions of the complex purification from sizing column were analyzed by SDS-PAGE. C) Western blot using anti-FKBP38 and anti-Bcl-2 antibody to make sure that there are two proteins in the fractions. The fractions from sizing column were analyzed by anti-Bcl-2 and FKBP38, respectively. D, E) Co-IP results of FKBP38 and Bcl-2/xL

5.2 Identification of specific interaction of FKBP38 with Bcl-2

To further define and identify a region on Bcl-2 responsible for the molecular interaction with FKBP38, several mutant forms of Bcl-2 were constructed, based on known three-dimensional structural information (Fig.5.2 A). In this study, we have focused on the flexible loop of Bcl-2. The wild type Bcl-2 and mutant forms of Bcl-2 with various deletions in the unstructured loop were expressed and tested their abilities to interact with FKBP38. The results showed that all mutants constructed in this study could be purified in soluble forms as shown in Fig.3.3 C and were stable during the experiment. From the column binding study, the wild type Bcl-2 showed clear binding to FKBP38, whereas the loop deletion mutants, Bcl-2Δ(V35-V89):6A, in which the residues from V35 to V89 were removed and six alanine residues were replaced instead, and Bcl-2Δ(H55-V89), in which the residues from H55 to V89 were removed, failed to bind to FKBP38 (Fig.5.2 B). Bcl-2Δ(V35-V89):6A and Bcl-2Δ (H55-V89) lack three known phosphorylation sites, T56, S70, S87, in the flexible loop of Bcl-2 (Bassik *et al.*, 2004). The deletion mutants Bcl-2Δ(P65-V89), Bcl-2Δ (V35-D64), and Bcl-2Δ(V35-G79) showed binding with FKBP38 to a considerably reduced degree.

To further confirm the interaction of FKBP38 with Bcl-2, yeast two-hybrid experiments were performed (Fig.5.3 A and B). The wild type Bcl-2-containing yeast cells showed growth in the selection media whereas Bcl-2Δloop:6A and Bcl-2Δ(H55-V89) failed to grow in the selection media. The results regarding Bcl-2Δ(V35-V89):6A and Bcl-2Δ(H55-V89) mutants were consistent with the column binding assays shown in Fig.5.2 B. Other loop deletion mutants, Bcl-2Δ(P65-V89), Bcl-2Δ (V35-D64), Bcl-2Δ(V35-G79), unlike the column binding experiments, showed growth under the selection media used in the yeast two-hybrid study, like the same

manner as seen in the wild type Bcl-2. The discrepancy between two approaches regarding Bcl-2Δ(P65-V89), Bcl-2Δ(V35-D64), Bcl-2Δ(V35-G79) could be attributed to the sensitivity difference between two procedures. Also, we performed the β-galactosidase assay (Fig.5.3), which is same as the selection plate assay. Taken together, the results suggest that the molecular interaction of FKBP38 with Bcl-2 would require at least one phosphorylation site or surrounding sequences of the known three sites (T56, S70, T74, S89) in the unstructured loop of Bcl-2.

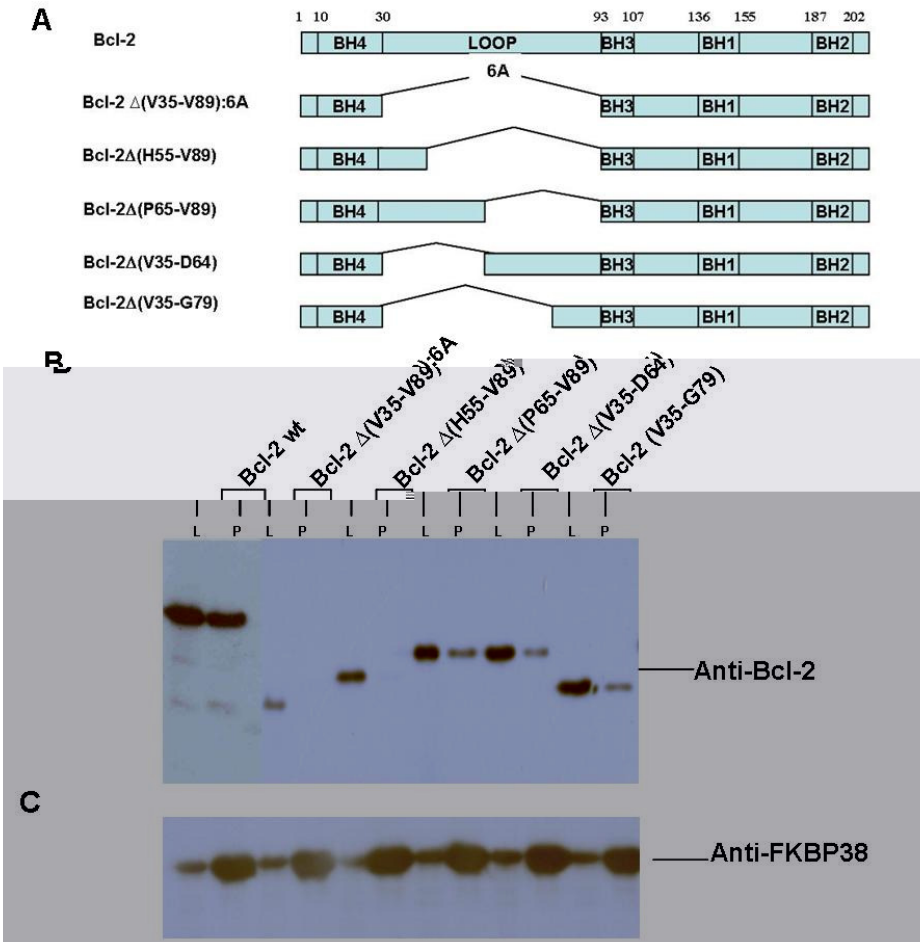

Fig. 5.2 FKBP38 interacts with the unstructured loop of Bcl-2.

A) Loop deletion mutants used in this study are graphically displayed. B) Co-expressed complexes of FKBP with a His-tag and Bcl-2 and the Bcl-2 loop deletion mutants with no-tag were purified by Ni^{2+}-NTA. C) Loading (L lanes) and purified samples from Ni^{2+}-NTA resin (P lanes) were analyzed on 12.5% SDS-PAGE, and subjected to Western blot with anti-Bcl-2 (B) and FKBP38 antisera (C).

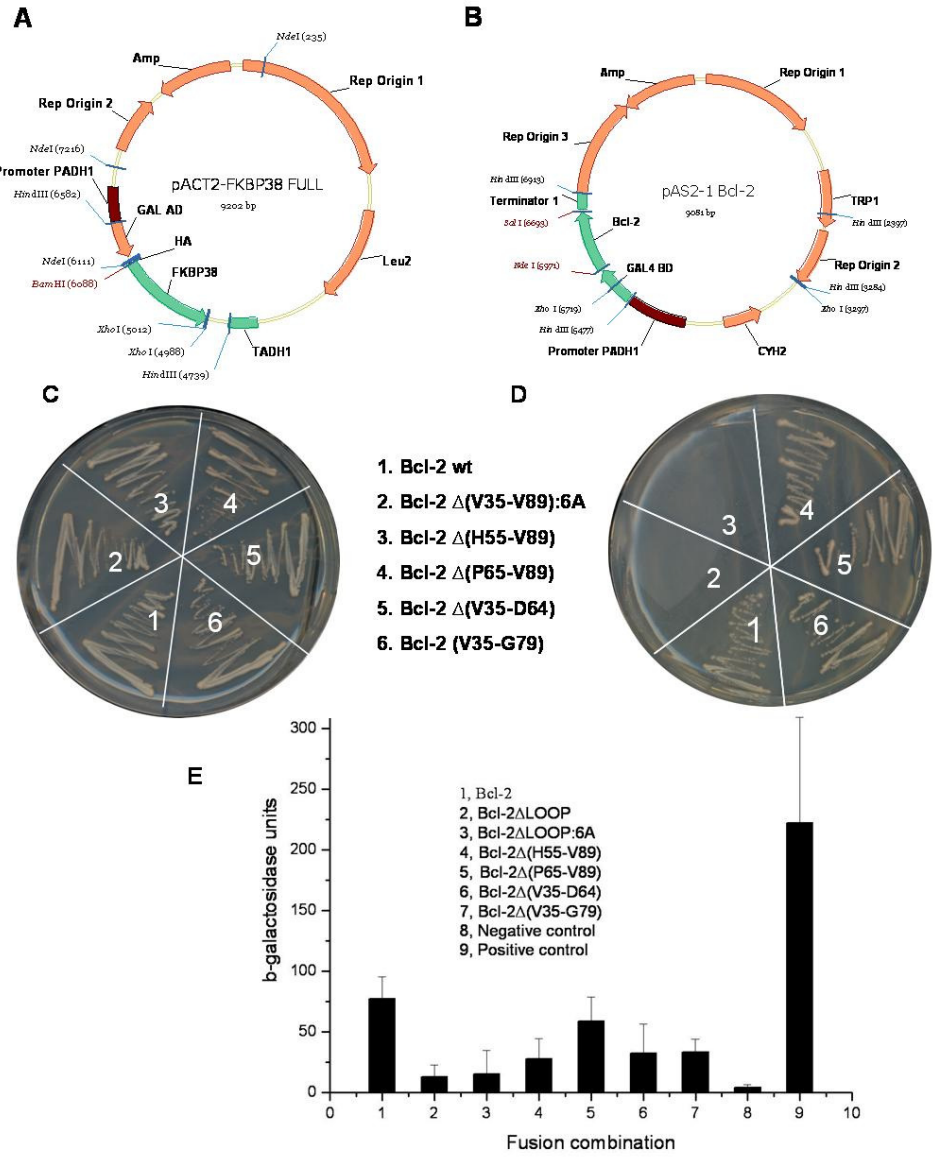

Fig.5.3 Yeast two-hybrid experiments to analyze the interaction

Yeast two-hybrid experiments were carried out to analyze molecular interaction between FKBP38 and Bcl-2 using *Saccharomyces cerevisiae* PJ69-4A with two different selection media: SD/(-)Leu/(-)Trp (C); SD/(-)Leu/(-)Trp/(-)His (D). The wild type and the deletion mutants of Bcl-2 in the flexible loop were tested: 1, wild type Bcl-2; 2, Bcl-2Δloop:6A; 3, Bcl-2Δloop(H55-V89); 4, Bcl-2Δloop(P65-V89); 5, Bcl-2Δloop(V35-D64); 6, Bcl-2Δloop(V35-G79). The AD-FKBP38 plasmid was first transformed into PJ69-4A (A), then the BD-Bcl-2 (B) loop deletion mutants were transformed into the PJ69-4A containing AD-FKBP38. The yeast containing AD and BD fusion protein were cultured on different SD medium and the growth of the yeast was check by visualizing the colonies. E is the β-galactosidase assay using the yeast transformed with BD-Bcl-2 /loop deletion mutants with AD-FKBP38.

5.3 Regulation of Bcl-2 by phosphorylation and dephosphorylation of the loop domain

The interaction study using *E.coli* co-expression and yeast two-hybrid system shows that the loop domain of Bcl-2 is important for the molecular interaction between FKBP38 and Bcl-2. It was found that there were several phosphorylation sites in the loop domain, which can be regulated by some kinases, such as c-jun-N-terminal kinase (JNK). So the phosphorylation experiments were performed to characterize the phosphorylation and dephosphrylation on the loop domain of Bcl-2, which may give some information about regulation of Bcl-2. Bcl-2 could be phosphorylated by several kinases such as stress-activated protein JNK and extra-cellular signal-regulated kinase 2 (ERK2), and the phosphorylated form of Bcl-2 is primarily localized at the endoplasmic reticulum and nuclear (Bassik *et al.*, 2004, Ruvolo *et al.*, 2001, Blagoskonny *et al.*, 2001, Tamura *et al.*, 2004). On the other hand, phosphatases such as PP1, PP2A and PP2B (calcineurin) can also interact with Bcl-2 and modulate the activity of Bcl-2 by changing the phosphorylation status of Bcl-2 (Shibasaki *et al.*, 1997). In addition, some evidence suggests that phosphorylation on the loop of Bcl-2 might be important in drug-induced apoptosis (Rodi *et al.*, 1995). There are many different opinions regarding the phosphorylation and dephosphorylation of Bcl-2 on the loop domain. In view of this, Bcl-2 phosphorylation appears to be coordinated in a complex, dynamic network, and multiple molecules are participating in this process. In this work, to further define and better understand the biological significance and the regulation of Bcl-2 through the phosphorylation of its disordered loop, we studied specificity of relevant kinases and phosphatases which have been shown to be associated with the phosphorylation and dephosphorylation of Bcl-2.

5.3.1 Kinases show specificity on the phosphorylation of Bcl-2

Several kinases have been shown to be involved in the phosphorylation of Bcl-2 (Bassol *et al.*, 2004, Ruvolo *et al.*, 2001). Of those, JNK and ERK2 have been repeatedly shown to be associated with the Bcl-2 phosphorylation (Brichese *et al.*, 2004). To better define the specificity of the relevant kinases on the Bcl-2 phosphorylation, we studied the specificity of JNK and ERK2 on the Bcl-2 phosphorylation. First, we tested the phosphorylation of Bcl-2 and its mutants by JNK and ERK2. The results showed that both JNK and ERK2 phosphorylated the wild-type Bcl-2 (Fig.5.4 A). However, Bcl-2Δ(V35-V89):6A, which lacks the loop domain of Bcl-2, were not phosphorylated by both JNK and ERK2, confirming that the phosphorylation sites for the kinases are mainly localized in the loop domain of Bcl-2. From the results, Bcl-2 appears to be better phosphorylated by ERK2. Previously, Bcl-2 was shown to be phosphorylated at multiples sites (T56, S70, T74, and S87), in response to different stimuli (Bassik *et al.*, 2004). To probe the specificity difference of these two kinases on the aforementioned sites, several Bcl-2 loop-deletion mutants containing different number of phosphorylation sites, and then used them for the kinase reactions (Fig.5.5 A). JNK and ERK2 were able to phosphorylate Bcl-2Δ(P65-V89), which only contains the phosphorylation site at T56, without showing much difference (Fig.5.5 B). On the other hand, Bcl-2Δ(V35-D64), which contains T74, S70, and S87 but lacks T56, was preferentially phosphorylated by ERK2 (Fig.5.6 B, lane 5). To further define which one is the preferred site for ERK2, we tested Bcl-2Δ(V35-D79), which contains only S87. Our data showed that ERK2 preferentially phosphorylated Bcl-2Δ(V35-D79) (Fig.5.5 B, lane 7), even though the degree of phosphorylation is considerably reduced. Our data suggest that of the three sites (S70, T74, and S87), S87 is the primary phosphorylation site for ERK2.

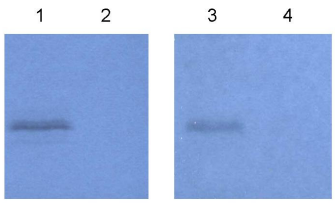

Fig.5.4 Bcl-2 is phosphorylated by ERK2 and JNK

The purified Bcl-2 and Bcl-2Δ(V35-V89):6A were mixed with JNK and ERK2 in the reaction buffer describe in "Materials and methods". After reaction, the proteins were loaded onto 12.5 % SDS-PAGE and followed by autoradiography for visualization. 1, Bcl-2 with ERK2; 2, Bcl-2Δ(V35-V89):6A with ERK2; 3, Bcl-2 with JNK; 4, Bcl-2Δ(V35-V89):6A with JNK.

5.3.2 S87 is preferentially phosphorylated by ERK2

To better and further understand specificity of the kinases, we tested the synthetic peptides which encompass the known phosphorylation sites of Bcl-2 in the flexible loop (Fig.5.5 A). The peptides were treated by JNK and ERK2, and the degree of phosphorylation was determined by analyzing the difference in the elution profiles between the peptides and phosphopeptides on a HPLC column. From the elution profiles, both JNK and ERK2 were able to phosphorylate the T56 peptide without much difference (Fig.5.5 A & B), suggesting that the phosphorylation kinetics of the peptide is similar to that of Bcl-2Δ(P65-V89) (Fig.5.6 C). But the S70 and T74 peptides were poorly phosphorylated by both JNK and ERK2 (Fig.5.5 A & B), while the S87 peptide showed preferred phosphorylation by ERK2, which is consistent with that of the mutant Bcl-2Δ(V35-G79). To confirm the results from the peptide studies, we checked the single mutant forms of Bcl-2: Bcl-2/S56A and Bcl-2/S87A (Fig.5.5 C). The results indicated that both mutants affected the Bcl-2 phosphorylation with more significant reduction with Bcl-2/S87A. Taken together, our data suggest that S70 and T74 sites appear to be poor substrates for both JNK and ERK2; S87 appears to be preferentially phosphorylated by ERK2 and also possibly for JNK, with the help of

the neighboring site encompassing S70 and T74.

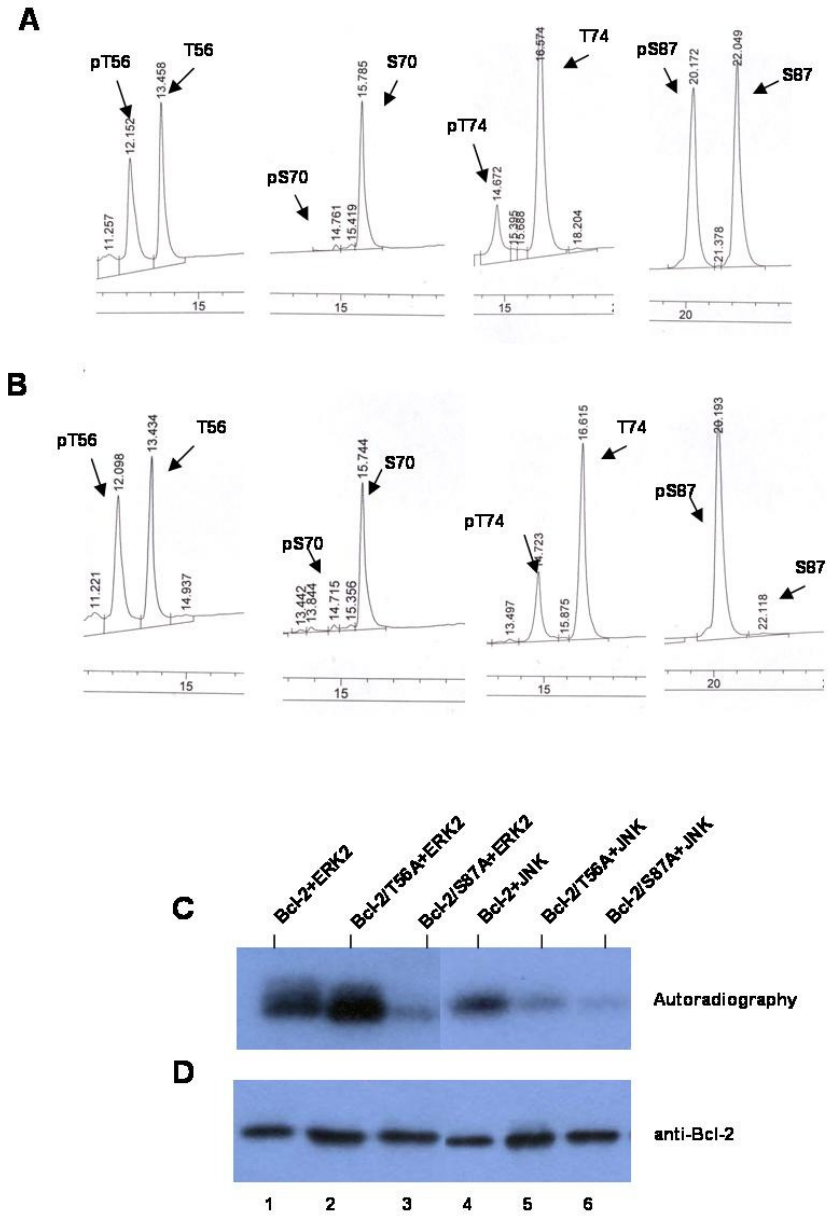

Fig.5.5 Phosphorylation of Bcl-2 in the loop domain of Bcl-2 by ERK2 and JNK

A, B) Different peptides (200 μM) and ERK2 (B) or JNK (A) (10 μM) were added into the reaction mixture. After reaction at 30 °C for 1 h, the samples were heated at 90 °C to inactivate kinase and loaded onto C-18 column for reverse phase-HPLC analysis. C) The point mutations of Bcl-2 (T56A and S87A) were used for the kinase reaction as described in "Materials and methods", and the phosphorylation reactions were analyzed by using γ-^{32}P-ATP and followed by autoradiography. D) Western blot shows the Bcl-2 and its point mutants used in the kinase reactions.

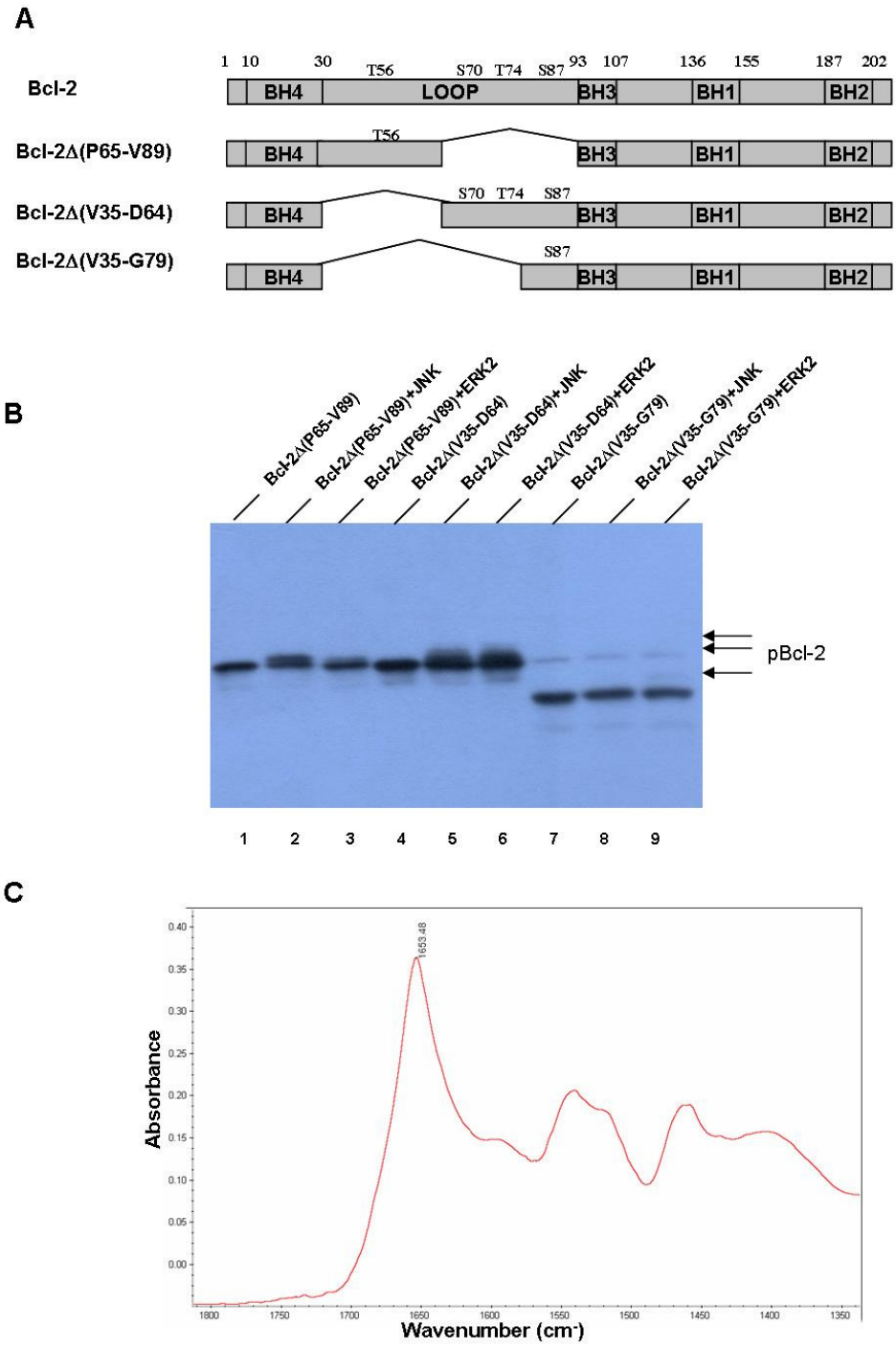

Fig.5.6 Phosphorylation of the Bcl-2 loop-deletion mutants by ERK2 and JNK

A) The Bcl-2 loop-deletion mutants were constructed and used for the kinase assays. The phosphorylation sites in the flexible loop are indicated. B) The purified Bcl-2 loop-deletion mutants were mixed with JNK or ERK2. The reaction samples were analyzed by 12.5% SDS-PAGE and checked by Western blot using anti-Bcl-2 antibody. C) The FTIR spectrum of Bcl-2 loop deletion mutant.

5.3.3 The phosphorylated residues in the loop is differentially dephosphorylated by phosphatases

Previously it was shown that the phosphatase PP2B (calcineurin) could interact with Bcl-2 and form a complex (Shibasaki *et al.*, 1997). We performed GST pull-down assay to check the binding between PP2B and Bcl-2. First GST-Bcl-2 was purified by GST purification kit and followed by sizing column assay. The PP2B was purified as described in chapter 3. The GST pull-down assay was performed as described in the material and methods. The result confirmed the molecular interaction between PP2B and Bcl-2 (Fig.5.8 A, B), which is consistent with the report before (Shibasaki *et al*., 1997). If PP2B can use phosphorylated Bcl-2 as substrate was checked by using ^{32}P labled Bcl-2. The result is shown that PP2B can use p-Bcl-2 substrate.

To define the substrate specificity of PP2B on Bcl-2, the loop deletion mutants in the loop domain were used for analysis. We first prepared the phosphorylated forms of the wild-type and mutant forms of Bcl-2 *in vitro* using kinase. Then the phosphorylated proteins were purified and used as substrate of PP2B. From the results, it was shown that pBcl-2Δ(P65-V89), in which T56 is expected to be phosphorylated, was efficiently dephosphorylated by PP2B (Fig.5.8, lane 3), because the band shift was removed after PP2B was added. The pBcl-2Δ(V35-D64), in which S70, T74, S87 are expected to be phosphorylated, was poorly dephosphorylated by PP2B (Fig.5.8, lane 6, 9), in which only one band shifted was removed when the PP2B was added. To further probe which amino acid in the loop of Bcl-2 is the preferred substrate of PP2B, we used four synthetic peptides (P-T56, P-S70, P-T74, and P-87), in which T56, S70, T74, and S87 derived from the loop of Bcl-2 are phosphorylated. The PP2B assay was performed and the data showed that the P-T56 was preferentially dephosphorylated by

PP2B (Fig.5.9 A). The P-T74 and P-S87 could also be the substrates for PP2B, but their degrees of the phosphorylation were relatively lower compared to that the P-T56. It appeared that PP2B showed no activity with the P-S70. The results from the peptide experiments are consistent with those of Bcl-2 and its mutant proteins, suggesting that T56 appears to be the primary site for PP2B under our experimental condition. To check specificities of different phosphatase, we checked the phosphatase activities of PP1 and PP2A with the four phosphopeptides, since PP1 and PP2A have been shown to be associated with Bcl-2 (Brichese *et al.*, 2004, Deng *et al.*, 2000). Unlike PP2B, our results indicate that the P-T56 and P-T74 are better substrate for PP1 and PP2A compared with the P-S70 and P-S87 (Fig.5.9 B, C). Taken together, it appears that PP1, PP2A, and PP2B exhibit different specificity on the phosphorylated residues in the flexible loop of Bcl-2, which may control the phosphoryaltion status of Bcl-2 by keeping different site of Bcl-2 phosphorylated.

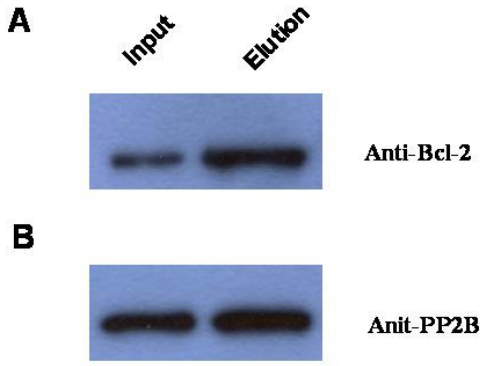

Fig.5.7 GST pull-assay on the interaction between PP2B and Bcl-2

A, B) GST pull-down assay to check the binding between PP2B and Bcl-2. The GST-Bcl-2 and PP2B were purified individually. GST-Bcl-2 was mixed with PP2B and incubated on ice for 1 h, then the mixture was loaded onto the GST purification resin for purification as described in material and methods. The load and elusion were analyzed by SDS-PAGE followed by western blot.

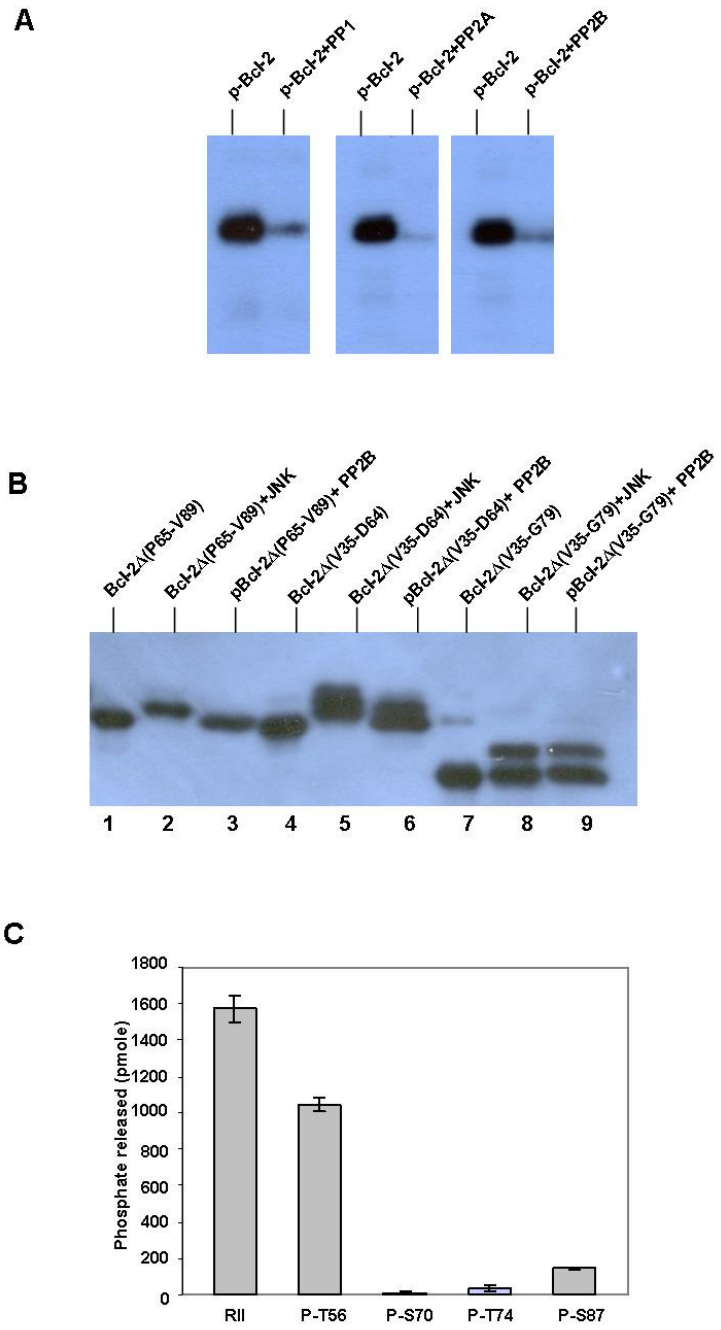

Fig.5.8 Dephosphorylation of Bcl-2 loop-deletion mutants by phosphatases

A) Dephosphorylation of Bcl-2 wt by PP1, PP2A, PP2B. The Bcl-2 (6 μM) was completely phophorylated by JNK (2 μM) in the presence of ^{32}P labled ATP at 30 °C overnight. Then 20 μg PP2B or 2 U of PP1, PP2A were mixed with p-Bcl-2 and incubate at 30 ℃ for 12 h. B) The Bcl-2 loop deletion mutants (6 μM) were phosphorylated by JNK. Then PP2B (20 μg purified from *E.coli*) was added into the sample and incubated at 30 ℃ for 6 h. The samples were analyzed by 12.5 % SDS-PAGE and then subjected to Western blot using anti-Bcl-2 antibody. C) Dephosphorylation of phosphopeptides by PP2B. Different phosphopeptides (200 μM) were incubated with commercial PP2B (2 U of each enzyme) at 30 ℃ for about 1 h, then the release of phosphate was checked by comparing to the standard curve using the Malachite green reagent.

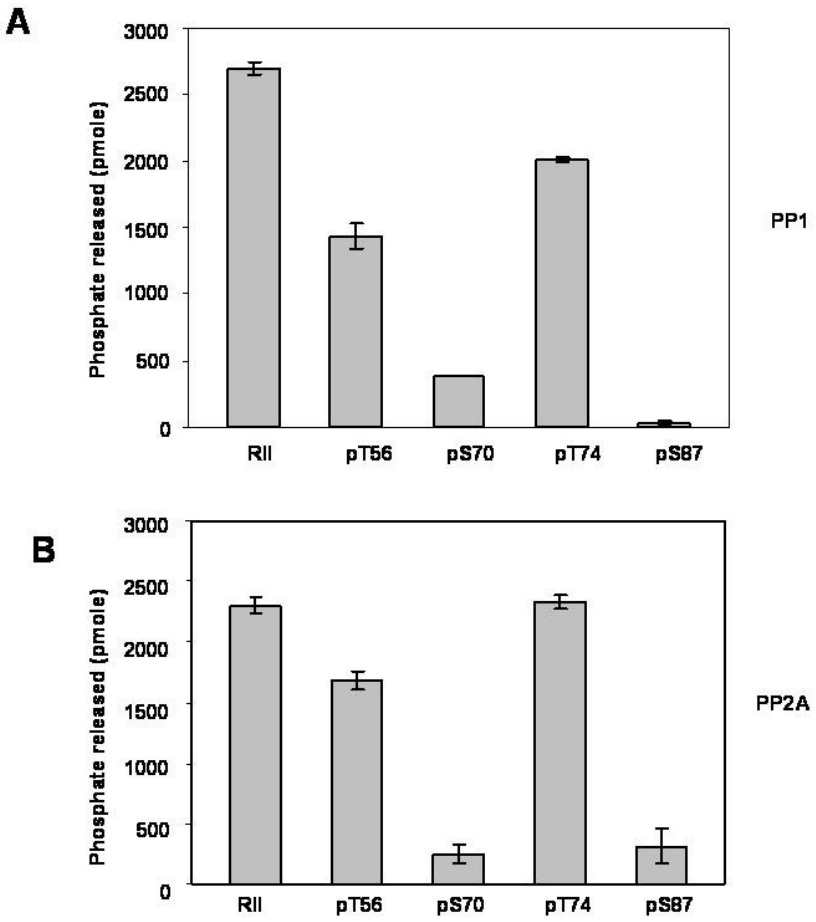

Fig.5.9 Dephosphorylation of the phosphopeptides by PP2A, and PP1

Different phosphopeptides (200 μM) were incubated with commercial PP1, or PP2A (2U of each enzyme) at 30 °C for about 1 h, then the release of phosphate was checked by compare the standard curve using the Malachite green reagent.

5.3.4 Effect of FKBP12-FK-506 complex on the activity of calcinurin

The immunosuppressive agent FKBP12 can inhibit the activity of PP2B in the presence of FK-506 by forming a big complex and the active site of PP2B can not target the substrate. It was already shown that FKBP12-FK-506 complex can inhibit the PP2B activity using the RII peptide as substrate. The effect of FKBP12-FK-506 complex on the activity of PP2B was checked using phophorylated peptide and phosphorylated Bcl-2 as substrates. The phosphorylated peptide (p-T56) and

phosphorylated Bcl-2 were used for the assay. The result indicated that the complex could also inhibit the activity of calcineurin when using phosphorylated Bcl-2 or p-T56 as substrate (Fig.5.10). But FKBP38 could not inhibit the dephosphorylation of p-Bcl-2 or p-T56 by PP2B.

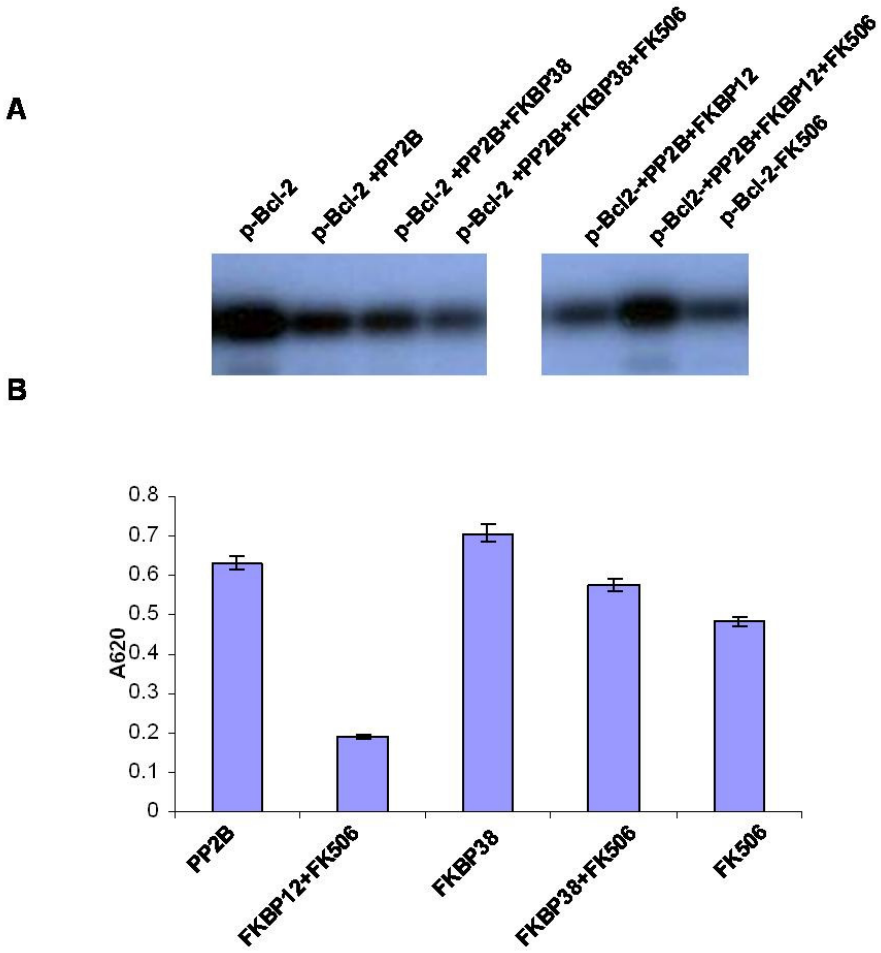

Fig.5.10 Effect of FKBP12-FK-506 on the activity of calcineurin

A) Effect of FKBP12-FK-506 on the activity of PP2B. The purified Bcl-2 was first phosphorylated by JNK with ^{32}P after purification, then PP2B in the presence or absence of FKBP or FK506 was added and the samples were incubated at 30 °C for 2 hours and loaded onto SDS-PAGE for separation and followed by autoradiography. B) The effect of FKBP12-FK-506 on the activity of calcineurin using phsophorylated T56 peptide as substrate. The peptide p-T56 was incubated with PP2B in presence of 20 uM of FKBP12, FKBP12+FK-506, FKBP38, FKBP38+FK-506 or FK-506 alone. The release of phosphate was checked by adding dye and check at 620 nm.

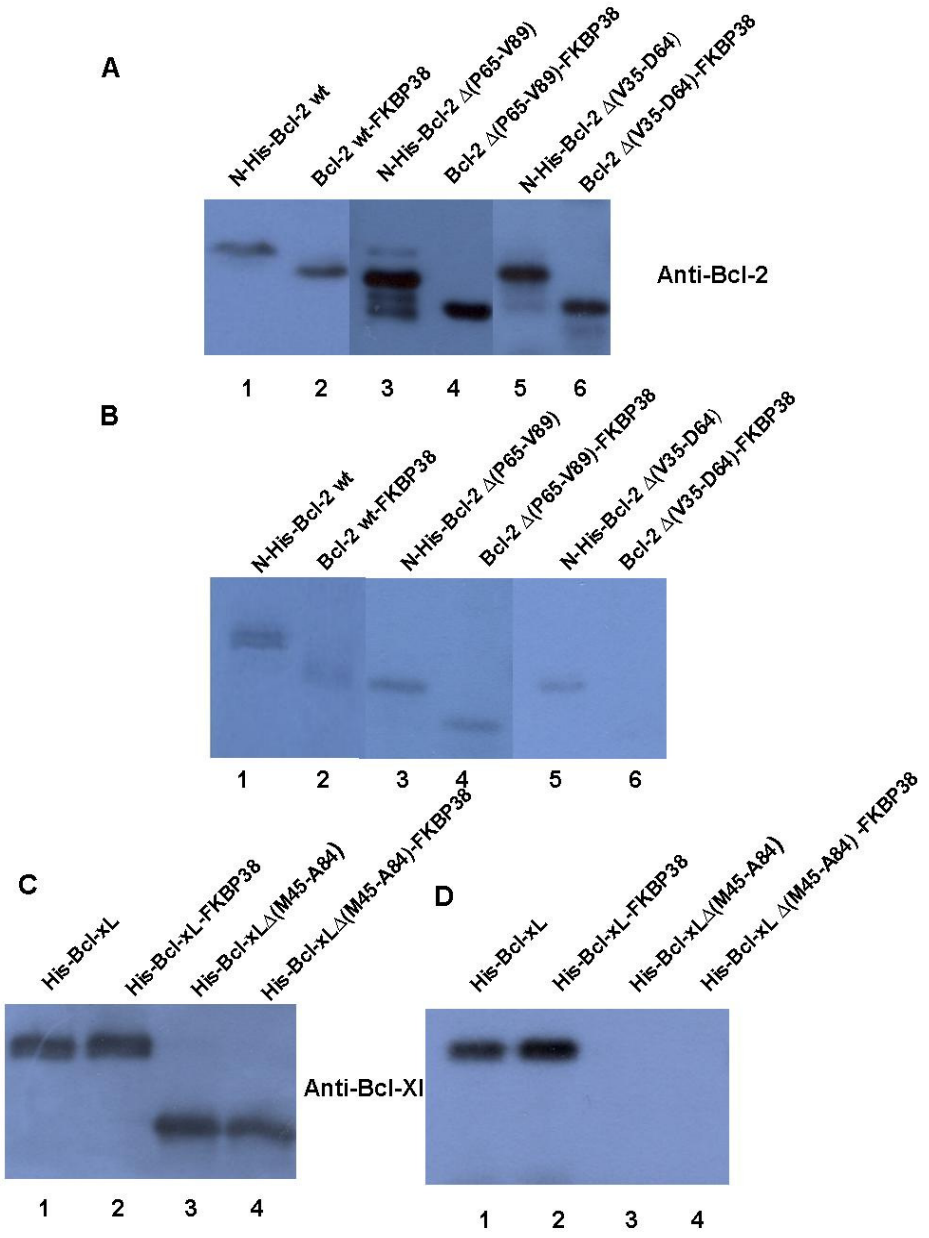

Fig.5.11 FKBP38 affects the phosphorylation of Bcl-2 by JNK

The N-terminal His-tagged wild-type Bcl-2 protein (N-His-Bcl-2-wt), the loop deletion mutant forms of Bcl-2 (N-His-Bcl-2Δ(p65-V89), N-His-Bcl-2Δ(V35-D64), and corresponding Bcl-2-FKBP38 complexes were expressed in *E. coli* BL21 (DE3) cells, and purified by the Ni^{2+}-NTA resin, subjected to Western blot using anti-Bcl-2 antisera (A). The purified Bcl-2-wt and mutants were subjected to phosphorylation by JNK with γ-^{33}P-ATP, and analyzed by autoradiography for visualization (B). His-Bcl-xL and Bcl-xLΔ(M45-A84) were purified, subjected to Western blot using anti-Bcl-xL antisera (C), and JNK-mediated kinase reaction (D), under the same condition described in (A) and (B), respectively.

5.4. FKBP38 affects phosphorylation of the unstructured loop of Bcl-2

The phosphorylation of Bcl-2 was found to be associated with its flexible loop, and JNK has been reported to be one of the kinases responsible for the phosphorylation of T56, T74 and S87 within the unstructured loop of Bcl-2 (Bassik *et al.*, 2004). In this study, to investigate the role of FKBP38 in connection with the posttranslational regulation of the Bcl-2 loop, Bcl-2 phosphorylation experiment was performed using JNK and the purified Bcl-2, its truncation mutants in the flexible loop, and the corresponding FKBP38-Bcl-2 complex as substrates. The purified Bcl-2 mutants were soluble and stable (Fig.5.11 A). The phosphorylation results showed that JNK was able to phosphorylate the purified Bcl-2 in more than one positions, proved by multiple Bcl-2 bands detected (Fig.5.11 B, lane 1). However, the Bcl-2 in FKBP38-Bcl-2 complex showed a considerable decrease in the phosphorylation by JNK (Fig.5.11 B, lane 2). To further analyze the effect of FKBP38 on the Bcl-2 phosphorylation, we next examined the phosphorylation of Bcl-2Δ(V35-D64) and Bcl-2Δ(P65-V89) in the presence or absence of FKBP38. The data demonstrated that Bcl-2Δ(V35-D64) and Bcl-2Δ(P65-V89) showed a difference in the phosphorylation reaction; Bcl-2Δ(V35-D64) showed a marked reduction in phosphorylation compared to Bcl-2Δ(P65-V89) (Fig.5.11 B, lanes 4 and 6). When FKBP38 interacts with Bcl-2Δ (V35-D64), the phosphorylation of Bcl-2Δ(V35-D64) by JNK showed a considerable reduction compared to that of Bcl-2Δ(P65-V89). Bcl-xL, a close homolog of Bcl-2, also has been shown to be phosphorylated in response to external stimuli (Basu *et al.*, 2003, Kharbanda *et al.*, 2000). To further study the effect of FKBP38 on other Bcl-2 family protein, we performed JNK-mediated phosphorylation on Bcl-xL. The Bcl-xLΔTM was purified by affinity and sizing column. The Bcl-xL can also be phosphorylated by JNK (Fig.5.11). The effect of FKBP38 on the phosphorylation of Bcl-xL was also checked according to the same way as Bcl-2, demonstrating that FKBP38 made little effect on the phosphorylation of full-length human Bcl-xLΔTM (Fig.5.11 D, lanes 1 and 2). A mutant form of Bcl-xL, Bcl-xLΔ(M45-A84), was also

purified as described in chapter 3. The effect of FKBP38 on the phosphorylation of Bcl-xLΔ(M45-A84) was also checked, but the result showed no phosphorylation by JNK (Fig.5.11 D, lanes 3 and 4) because the main phosphorylation site on Bcl-xL by JNK is S62 which is localized in the loop domain of Bcl-xL. Taken together, these results suggest that FKBP38 favorably interacts with Bcl-2 and modulates the phosphorylation reactions, in unknown and yet to be identified mechanism, within the unstructured loop, which involves the region containing S70 and S87.

5.5 Phosphorylation in the loop domain of Bcl-2 affects its physical characteristics

It was predicted that the phosphorylation in the loop domain of Bcl-2 may change some of its characteristics. To check any characteristic change of the loop upon phosphorylation, several biophysical experiments were performed.

First, the Bcl-2 and phosphorylated Bcl-2 (p-Bcl-2) were purified, and the sizing column profiles of these two proteins were compared. The elution volume of p-Bcl-2 was smaller than that of Bcl-2 on the sizing column, suggesting physical properties of these two forms are different (Fig.5.12 A). Also the Bcl-2 and p-Bcl-2 were analyzed with CD and followed by CDNN software analysis, the random coil content was reduced greatly in the p-Bcl-2 (Fig.5.12).

There is some conformational change of Bcl-2 after phosphorylation (Rodi *et al.*, 1999) and our CD data confirmed this result. To further examine potential change in the physical characteristics of the peptides derived from the flexible loop of Bcl-2, the six peptides T56, pT56, T74, pT74, S87 and pS87 were analyzed by 1D and 2D NMR. The 2D TOCSY spectra (Fig.5.13, Appendix) were assigned based upon the 2D ROESY spectrum. The assignments of most resonances were shown in Table 5.1, 5.2 and 5.3. The amino protons of each set of peptides (un-phosphorylated and phosphorylated one) were shown in Fig.5.14. It was clear that after phosphorylation, the chemical shifts H^N of the phosphorylated T/S were changed compared with other amino acids, which provides evidence that the chemical environment on the

phosphorylation sites was changed. Also, the 3D structures of the peptides were calculated by using CYANA (Guntert, 2004) (Fig.5.16, 17, 18). The 3D structures of the peptides showed some change after phosphorylation, changing from linear to packed structure in which the pSer/Thr exposed, which is a binding motif for Pin1.

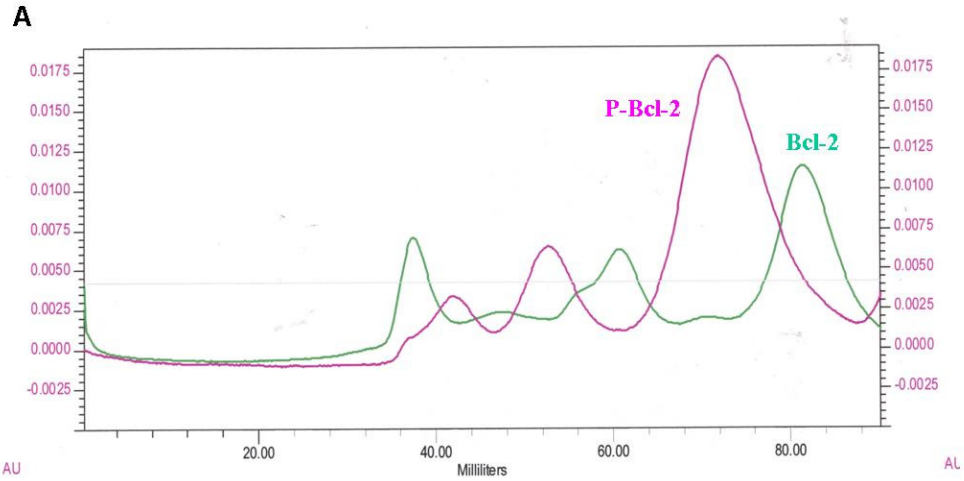

B

	195-260nm	200-260nm	205-260nm	210-260nm
Helix	48.80%	52%	57.00%	54.80%
Antiparallel1	4.70%	4.90%	4.30%	4.30%
Parallel	5.20%	4.90%	4.40%	5.10%
Beta-Trun	14.60%	14.20%	13.50%	13.60%
Rndm.Coil	19.50%	19.90%	19.70%	21.40%

C

	195-260nm	200-260nm	205-260nm	210-260nm
Helix	78.10%	88%	93.00%	92.70%
Antiparallel1	1.00%	1.00%	0.90%	0.70%
Parallel	1.80%	1.10%	0.80%	1.10%
Beta-Trun	10.40%	8.70%	7.80%	7.30%
Rndm.Coil	6.50%	5.40%	4.50%	5.30%

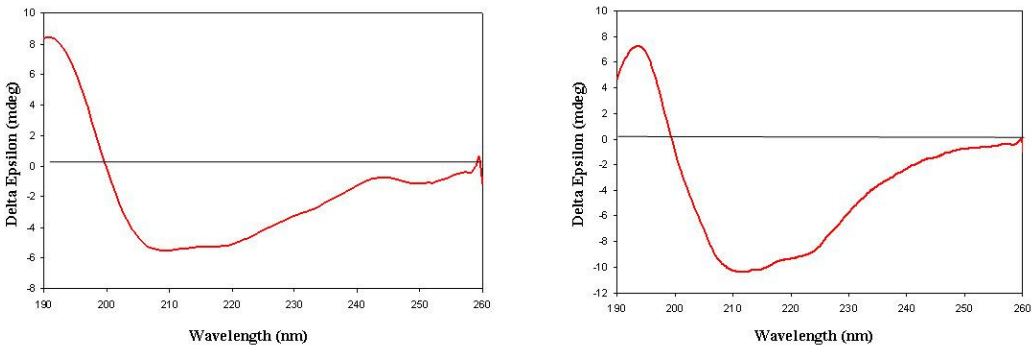

Fig.5.12 Sizing column purification and CD results of Bcl-2 and p-Bcl-2

A) Sizing column patterns of Bcl-2 and p-Bcl-2. The Bcl-2 was purified by Ni^{2+}-NTA column, the purified fraction was loaded onto sizing column for further purification. The purified Bcl-2 was phosphorylated by JNK or ERK2, then the p-Bcl-2 and kinase complex was loaded onto sizing column for further purification. The buffer used for Bcl-2 and p-Bcl-2 purification is 50 mM Tris-HCl, pH 7.5, 150 mM NaCl, 1 mM DTT, 0.01 NaN_3. B) CD spectrum of Bcl-2. The purified Bcl-2 was concentrated to 1 mg/ml and exchanged to the phosphate buffer containing 20 Na-PO_4, pH 7.4, 100 mM NaCl followed with analyzing by CD machine. C) CD spectrum of p-Bcl-2. The purified p-Bcl-2 from sizing column was concentrated to 1 mg/ml in the same buffer as Bcl-2 and analyzed by CD.

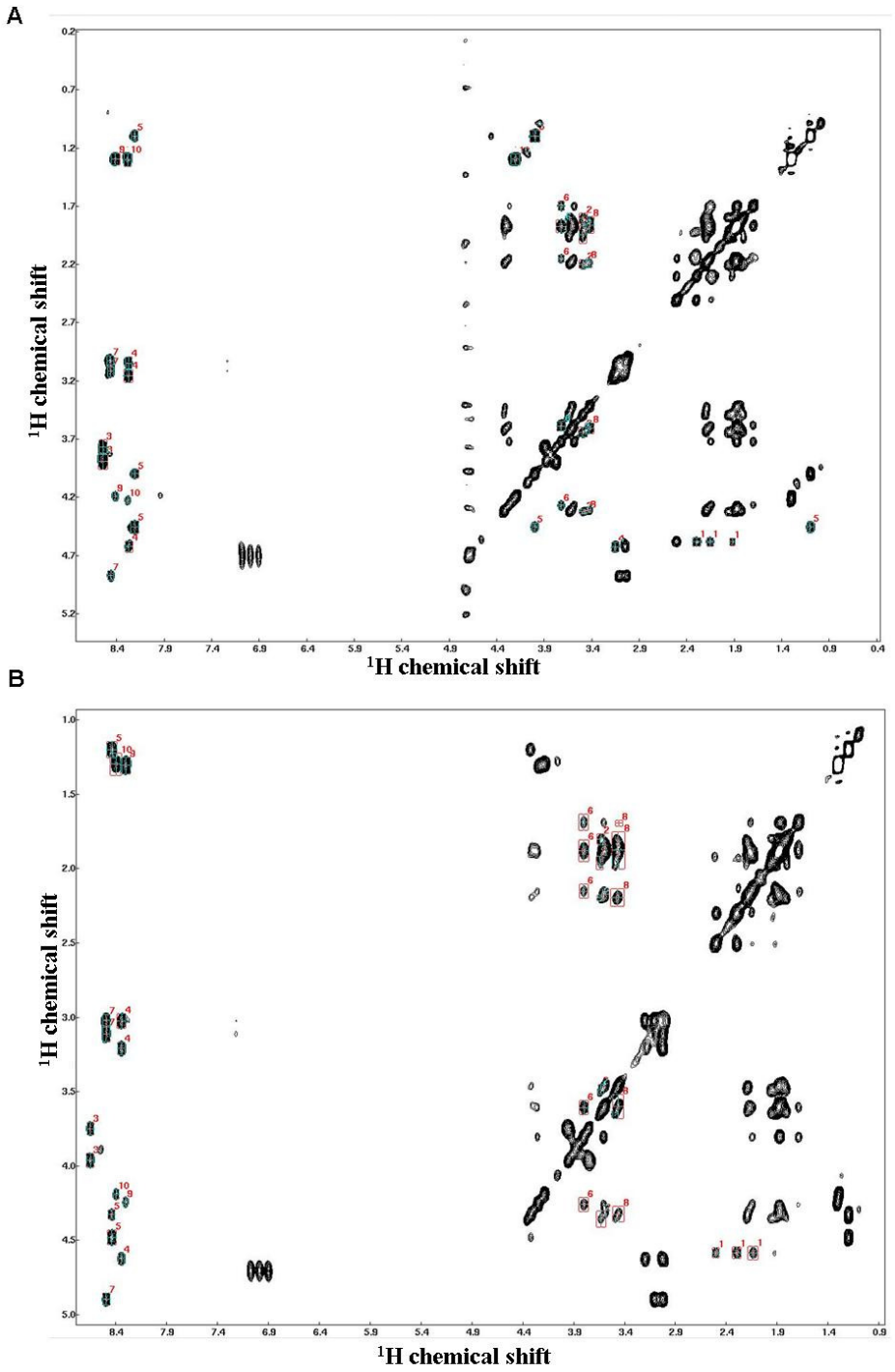

Fig.5.13 The Tocsy spectra of T56 and pT56 peptides

The peptides were dissolved in the Na-PO_4 buffer, pH 6.8. The Tocsy spectrum was recorded as introduced. The TOCSY pattern of each amino acid was analyzed and the assignment of the peptide as done based upon this spectrum and the ROESY spectrum. The red number shows the amino acid number in the peptide sequence. A, B are the spectra of T56 and pT56 peptides individually. The detailed chemical shift value is shown in the following tables. Unphosphorylated peptides are shown in blue and phosphorylated ones in red. The peptides sequences are as follows: T56, QPGHTPHPAA; pT56, QPGHpTPHPAA.

Table 5.1 Assignment of T56 and pT56 peptides

Residue (name)	T56 assignment		pT56 assignment	
Gln	1.HA	4.581	1.HA	4.584
	1.HB2	2.155	1.HB2	2.137
	1.HB1	1.918	1.HB1	1.926
	1.HG2	2.508	1.HG2	2.297
	1.HG1	2.294	1.HG1	2.502
Pro	2.HA	4.322	2.HA	4.355
	2.HB2	2.198	2.HB2	2.197
	2.HG2	1.808	2.HG2	1.802
	2.HG1	1.942	2.HG1	1.961
	2.HD2	3.64	2.HD2	3.633
	2.HD1	3.494	2.HD1	3.484
Gly	3.HN	8.542	3.HN	8.65
	3.HA2	3.89	3.HA2	3.962
	3.HA1	3.772	3.HA1	3.749
His	4.HN	8.274	4.HN	8.345
	4.HA	4.623	4.HA	4.624
	4.HB2	3.156	4.HB2	3.21
	4.HB1	3.048	4.HB1	3.024
Thr	5.HN	8.209	5.HN	8.438
	5.HA	4.455	5.HA	4.479
	5.HB	3.996	5.HB	4.325
	5.HG2	1.09	5.HG2	1.2
Pro	6.HA	4.267	6.HA	4.259
	6.HB2	2.151	6.HB2	2.152
	6.HG2	1.873	6.HG2	1.689
	6.HG1	1.697	6.HG1	1.879
	6.HD2	3.721	6.HD2	3.802
	6.HD1	3.589	6.HD1	3.607
His	7.HN	8.46	7.HN	8.492
	7.HA	4.87	7.HA	4.896
	7.HB2	3.114	7.HB2	3.113
	7.HB1	3.029	7.HB1	3.022
Pro	8.HA	4.311	8.HA	4.324
	8.HB2	2.187	8.HB2	2.195
	8.HG2	1.861	8.HG2	1.694
	8.HG1	1.861	8.HG1	1.876
	8.HD2	3.607	8.HD2	3.454
	8.HD1	3.423	8.HD1	3.601
Ala	9.HN	8.414	9.HN	8.304
	9.HA	4.19	9.HA	4.243
	9.HB1	1.297	9.HB1	1.307
Ala	10.HN	8.283	10.HN	8.397
	10.HA	4.22	10.HA	4.19
	10.HB1	1.3	10.HB1	1.297

Table 5.2 Assignment of T74 and pT74 peptides

Residue (name)	T74 assignment		pT74 assignment	
Pro	1.HA	4.285	1.HA	4.279
	1.HB2	2.35	1.HB1	2.348
	1.HG2	1.937	1.HG1	1.937
	1.HD2	3.295	1.HD2	3.304
	1.HD1	3.296	1.HD1	3.291
Leu	2.HN	8.566	2.HN	8.561
	2.HA	4.248	2.HA	4.25
	2.HB2	1.508	2.HB2	1.508
	2.HB1	1.508	2.HB1	1.508
	2.HG	1.508	2.HG	1.508
	2.HD1	0.803	2.HD11	0.803
Gln	3.HN	8.458	3.HN	8.424
	3.HA	4.295	3.HA	4.269
	3.HB2	1.963	3.HB2	1.941
	3.HB1	1.868	3.HB1	1.889
	3.HG2	2.246	3.HG2	2.248
Thr	4.HN	8.175	4.HN	8.323
	4.HA	4.466	4.HA	4.577
	4.HB	4.026	4.HB	4.508
	4.HG2	1.129	4.HG21	1.225
Pro	5.HA	4.271	5.HA	4.264
	5.HB2	2.194	5.HB2	2.204
	5.HG2	1.786	5.HB1	1.954
	5.HG1	1.909	5.HG1	1.868
	5.HD2	3.735	5.HD2	2.702
	5.HD1	3.593	5.HD1	3.784
Ala	6.HN	8.279	6.HN	8.353
	6.HA	4.149	6.HA	4.175
	6.HB1	1.25	6.HB1	1.247
Ala	7.HN	8.193	7.HN	8.207
	7.HA	4.466	7.HA	4.463
	7.HB1	1.236	7.HB1	1.246
Pro	8.HA	4.31	8.HA	4.296
	8.HB2	2.194	8.HB1	2.189
	8.HG2	1.926	8.HG2	1.945
	8.HG1	1.859	8.HG1	1.84
	8.HD2	3.691	8.HD2	3.704
	8.HD1	3.552	8.HD1	3.551
Gly	9.HN	8.393	9.HN	8.388
	9.HA2	3.814	9.HA2	3.825
Ala	10.HN	7.722	10.HN	7.985
	10.HA	4.043	10.HA	4.232
	10.HB1	1.236	10.HB1	1.302

Table 5.3 Assignment of S87 and pS87 peptides

Residue		S87		pS87
	2.HA	4.318	2.HA	4.312
	2.HB1	2.162	2.HB1	2.157
	2.HG2	1.807	2.HG2	1.784
Pro	2.HG1	1.858	2.HG1	1.865
	2.HD2	3.424	2.HD2	3.424
	2.HD1	3.425	2.HD1	3.422
	3.HN	8.381	3.HN	8.364
Ala	3.HA	4.165	3.HA	4.171
	3.HB1	1.241	3.HB1	1.239
	4.HN	8.213	4.HN	8.179
	4.HA	4.234	4.HA	4.246
Leu	4.HB1	1.412	4.HB1	1.488
	4.HG	1.476	4.HG	1.478
	4.HD11	0.752	4.HD11	0.81
	5.HN	8.211	5.HN	8.322
	5.HA	4.606	5.HA	4.762
Ser	5.HB2	3.658	5.HB2	3.908
	5.HB1	3.73	5.HB1	3.992
	6.HA	4.324	6.HA	4.308
	6.HB2	1.929	6.HB2	2.115
	6.HB1	2.121	6.HB1	1.921
Pro	6.HG2	1.882	6.HG2	1.756
	6.HG1	1.75	6.HG1	1.88
	6.HD2	3.675	6.HD2	3.593
	6.HD1	3.584	6.HD1	3.661
	7.HN	8.169	7.HN	8.167
	7.HA	4.053	7.HA	4.052
Val	7.HB	2.027	7.HB	2.022
	7.HG11	0.829	7.HG11	0.82
	8.HA	4.551	8.HA	4.535
	8.HB2	1.929	8.HB2	1.914
	8.HB1	2.22	8.HB1	2.218
Pro	8.HG2	1.859	8.HG1	1.889
	8.HG1	1.738	8.HD2	2.633
	8.HD2	3.546	8.HD1	3.783
	8.HD1	3.774	9.HA	4.353
	9.HA	4.345	9.HB2	1.907
	9.HB1	2.145	9.HB1	2.14
	9.HG2	1.882	9.HG2	1.866
Pro	9.HG1	1.789	9.HG1	1.784
	9.HD2	3.539	9.HD2	3.517
	9.HD1	3.679	9.HD1	3.684
	10.HN	8.116	10.HN	8.17
	10.HA	4.245	10.HA	4.29
Val	10.HB	1.914	10.HB	1.916
	10.HG11	0.832	10.HG11	0.82

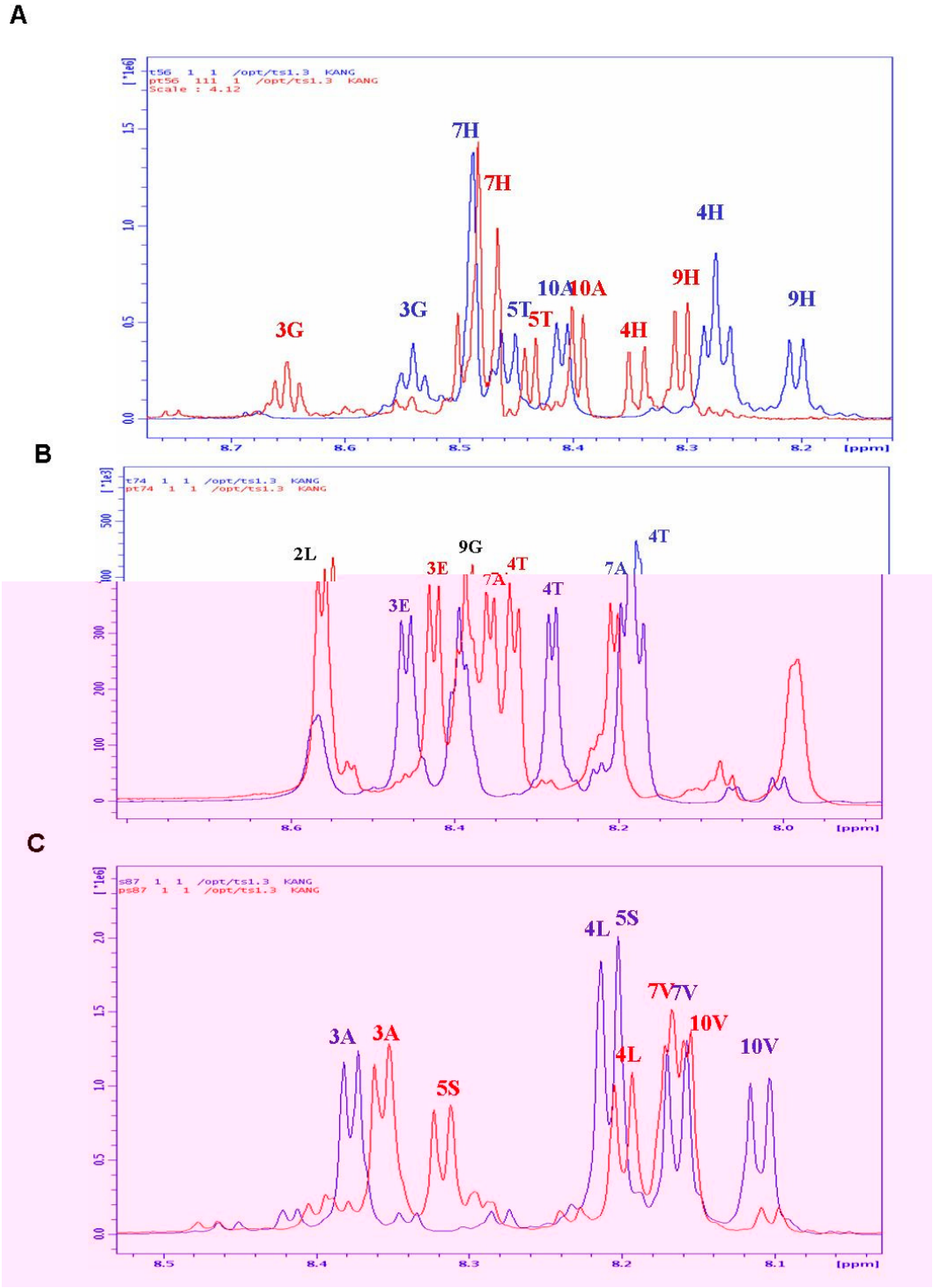

Fig.5.14 1D NMR shows the chemical shift change after phosphorylation

The 1D proton spectra were recorded in 400 MHz equipped with BBO probe and water suppression. T56, T74, S87 peptides and their phosphorylated forms were recorded in 400 MHz NMR machine from Bruker. The temperature is 298 K. Blue, non-phosphorylated peptides; Red, phosphorylated peptides.

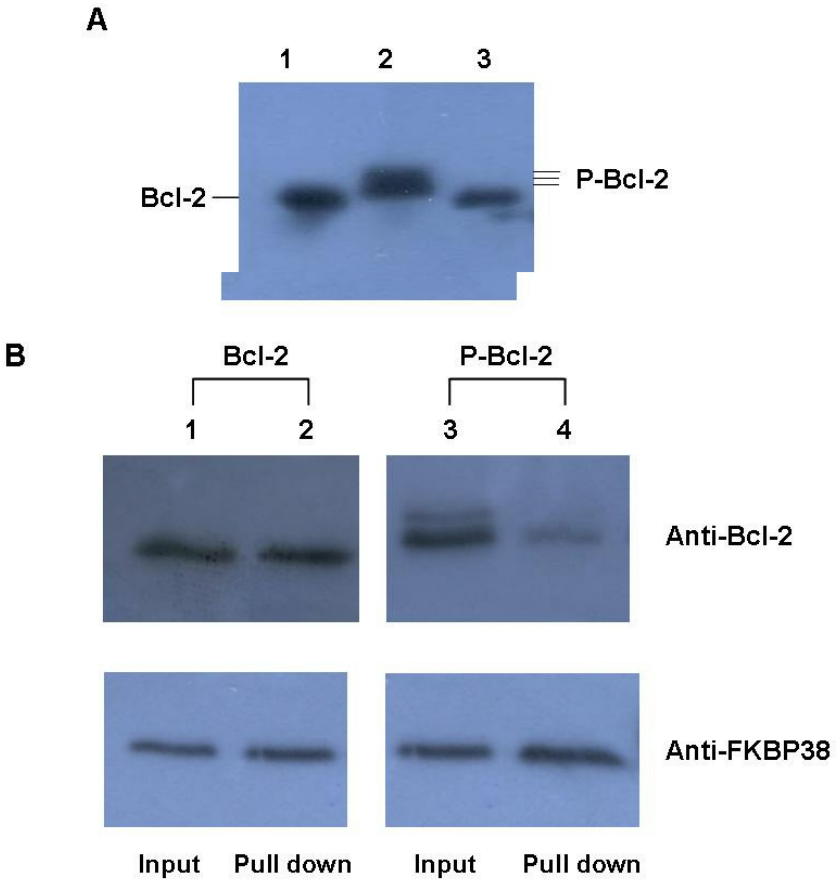

Fig.5.15 Phosphorylation of Bcl-2 influences interactin between FKBP38 and Bcl-2

A) Purified Bcl-2 (lane 1) was phosphorylated by JNK (Lane 2) and the phosphorylated Bcl-2 was purified by superdex 75 gel filtration column. The phosphorylated Bcl-2 was confirmed by the treatment of calcineurin (lane 3). The samples were analyzed by 12.5% SDS-PAGE, and subjected Western blot with anti-Bcl-2 antibody. B) The purified Bcl-2 and P-Bcl-2 were mixed with 10 µg of GST-FKBP38ΔTM, and the bindings between Bcl-2 or P-bcl-2 and FKBP38 were analyzed by in vitro pull-down assay as described. With 3 µg of Bcl-2 or P-Bcl-2 with 10 µg of FKBP38: 1, Bcl-2 before GST pull-down; 2, Bcl-2 after GST pull-down; 3, phosphorylated Bcl-2 before GST pull-down; 4, Phosphorylated Bcl-2 after GST pull-down.

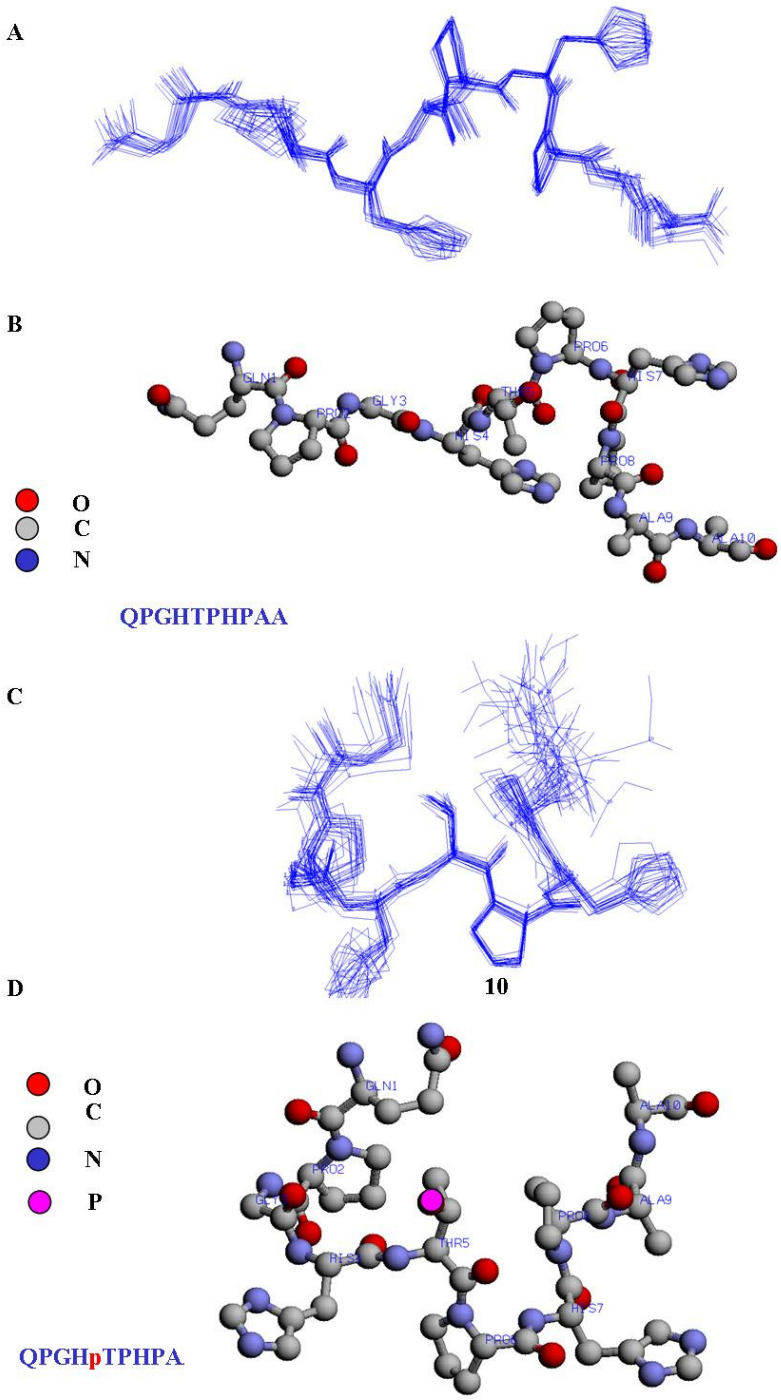

Fig.5.16 The solution structure of T56 and pT56

A) Superposition of 20 NMR-derived structures of T56. B) The ball the stick structure of T56. C) Superposition of 20 NMR-derived structures of pT56. D) The ball the stick structure of pT56. The peptide was dissolved in 20 mM phosphate buffer pH 6.5. The spectrum was recorded at 303 K and the data were analyzed with Topspin. The solution structures were calculated using CYANA.

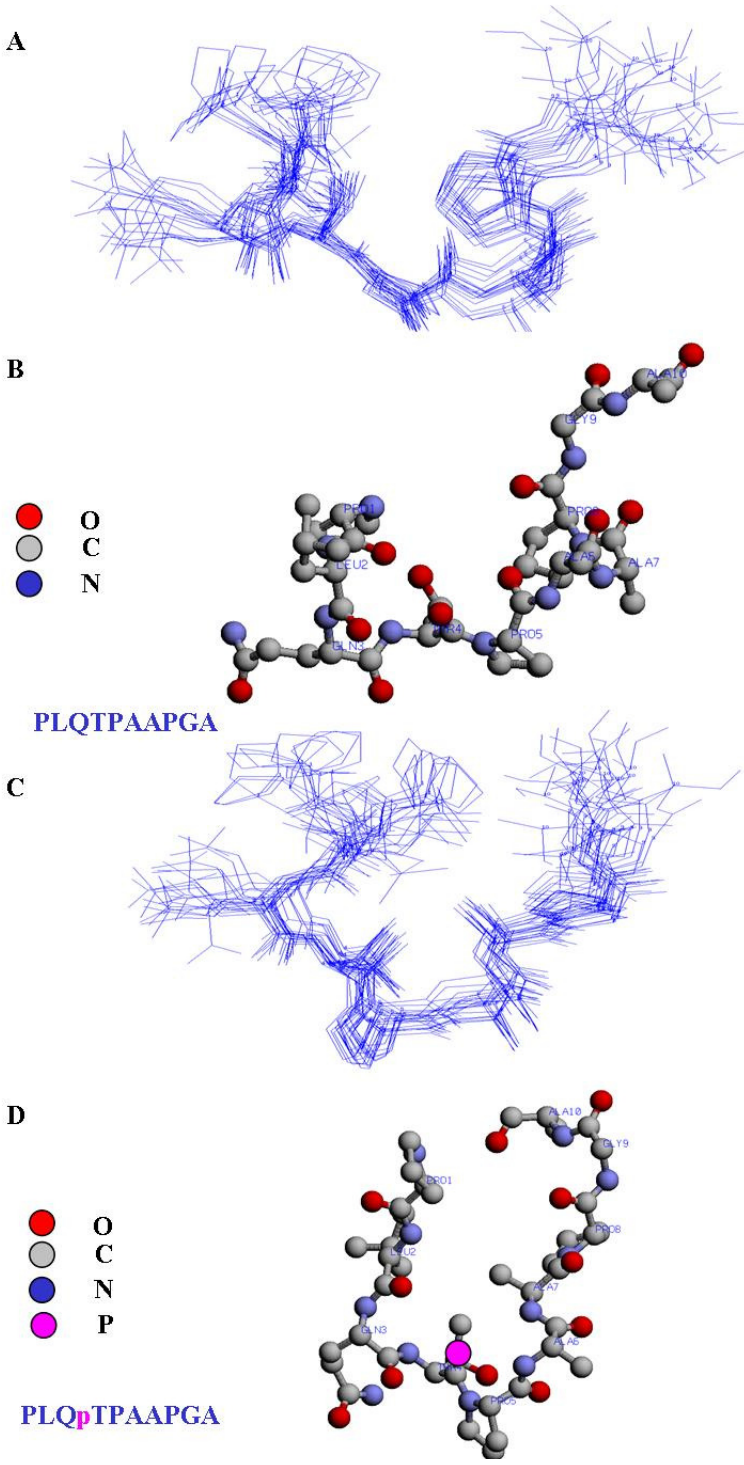

Fig.5.17 The solution structure of T74 and pT74

A) Superposition of 20 NMR-derived structures of T74. B) The ball the stick structure of T74. C) Superposition of 20 NMR-derived structures of pT74. D) The ball the stick structure of pT74. The peptide was dissolved in 20 mM phosphate buffer pH 6.5. The spectrum was recorded at 303 K and the data were analyzed with Topspin. The solution structures were calculated using CYANA.

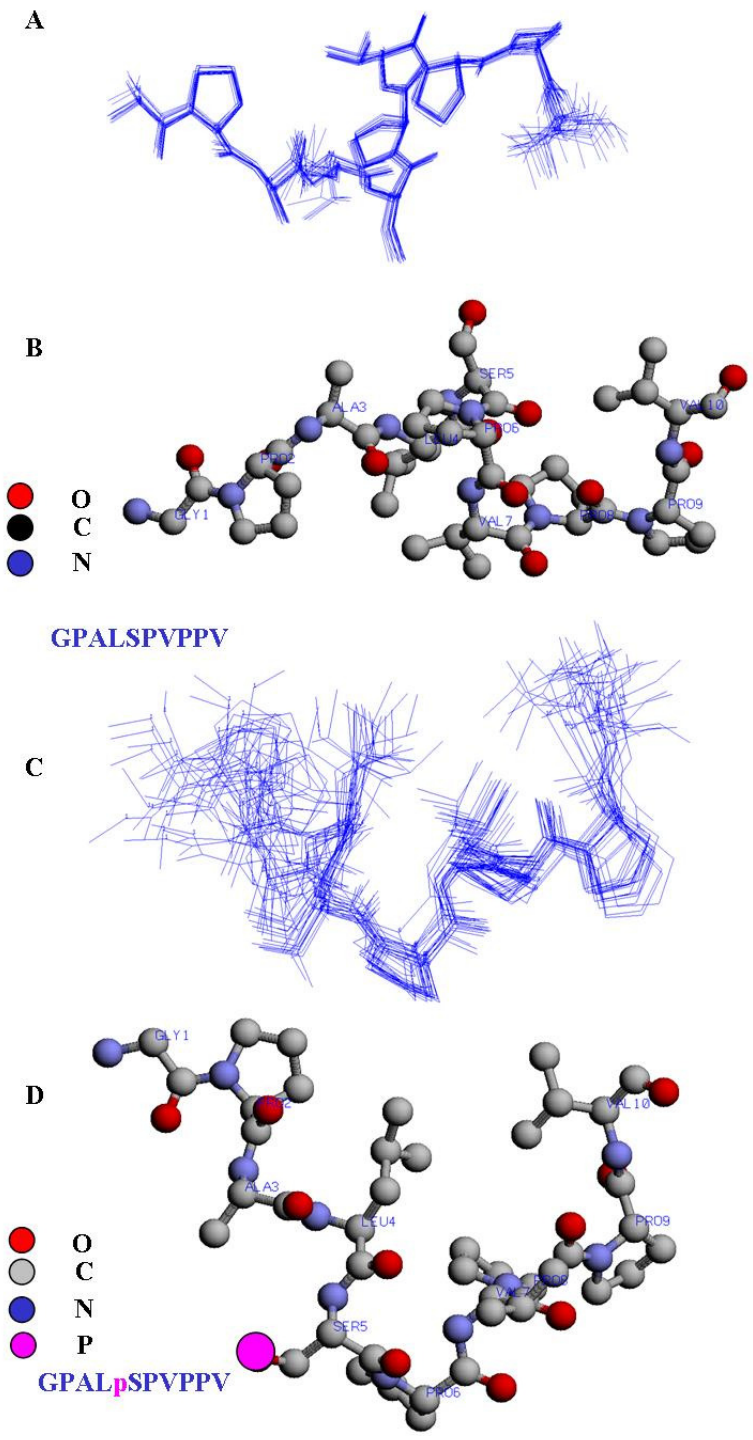

Fig.5.18 The solution structure of S87 and pS87

A) Superposition of 20 NMR-derived structures of S87. B) The ball the stick structure of S87. C) Superposition of 20 NMR-derived structures of pS87. D) The ball the stick structure of pS87. The peptide was dissolved in 20 mM phosphate buffer pH 6.5. The spectrum was recorded at 303 K and the data were analyzed with Topspin. The solution structures were calculated using CYANA.

5.6 Pin 1 shows molecular interaction with the phosphopeptides derived from the loop of Bcl-2

Pin1, which is a peptidylprolyl *cis-trans* isomerase, has been previously shown to interact with phosphorylated substrates including Bcl-2 (Ranganathan *et al.*, 1997, Pathan *et al.*, 2001). To probe the interaction between Pin 1 and Bcl-2 at molecular level, in this work, we employed a NMR spectroscopic method using the ^{15}N-labeled Pin 1 and the synthetic peptides and phosphopeptides derived from the loop of Bcl-2. The results showed that upon the addition of the non-phosphorylated peptide, no apparent chemical shift perturbations were detected in the 2D ^{1}H-^{15}N HSQC spectrum of the ^{15}N-labeled Pin 1. In contrast, upon the addition of the phosphopeptide, apparent spectral shifts were observed (Fig.5.19-5.26).

These results indicate that the phosphorylated peptide derived from the flexible loop of Bcl-2 binds to the molecular chaperone Pin1, but the non-phosphorylated peptide shows little interaction with Pin 1.

The binding constant K_D for each phosphorylated peptide was calculated as described in material and methods. The K_D result is shown in Table 5.4. NMR dissociation constant values are based on chemical shift perturbations of 4 residues. The K_D was calculated according to that described in material and methods.

Table 5.4 The dissociation constant values for different peptides

Peptides	KD(mM)
PT56	0.11± 0.02
PS70	0.18 ± 0.02
PT74	0.09 ± 0.03
PS87	0.14 ± 0.01

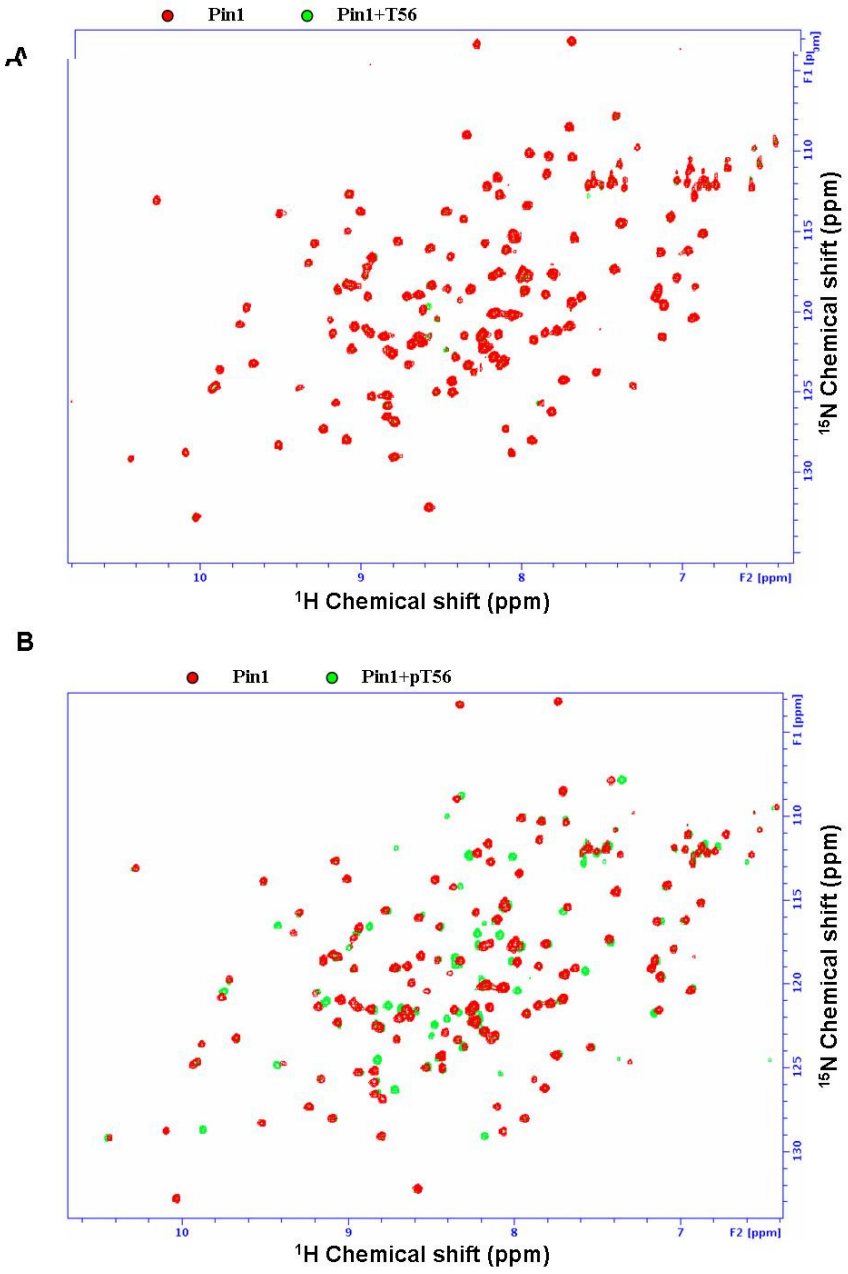

Fig.5.19 Pin 1 binds to the pT56 derived from the loop of Bcl-2

A) The interaction between Pin1 and T56. The 0.1 mM ^{15}N labeled Pin1 was recorded without and with 1 mM T56 using the 700 MHz equipped with cryoprobe. The HSQC spectra with or without p-T56 are shown in Green and Red, respectively. B) The interaction between Pin1 and p-T56. The 0.1 mM ^{15}N labeled Pin1 was recorded without or with 1 mM p-T56 peptide using the 700 MHz equipped with cryoprobe. The HSQC spectra with or without p-T56 are shown in green and red respectively.

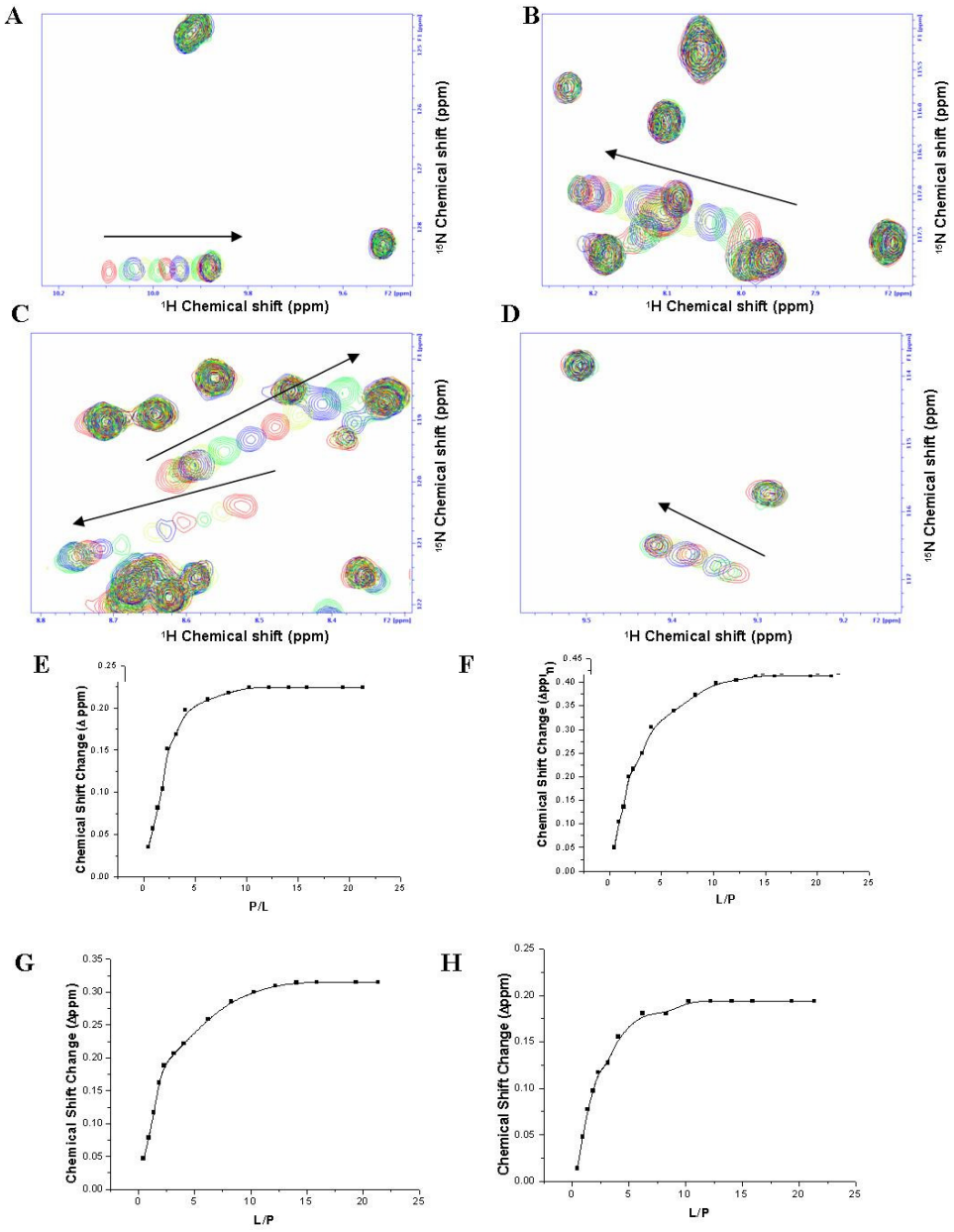

Fig.5.20 The spectra show the changes with increasing concentration of T56

A-D) Zoom in the chemical shift change after ligand was added. The arrows show the direction of chemical shift change with ligand. E-H) The relationship between chemical shift changes and the ratio of ligand to protein. The chemical shift change was calculated according to the equation in the material and methods. The figures were drawn using origin.

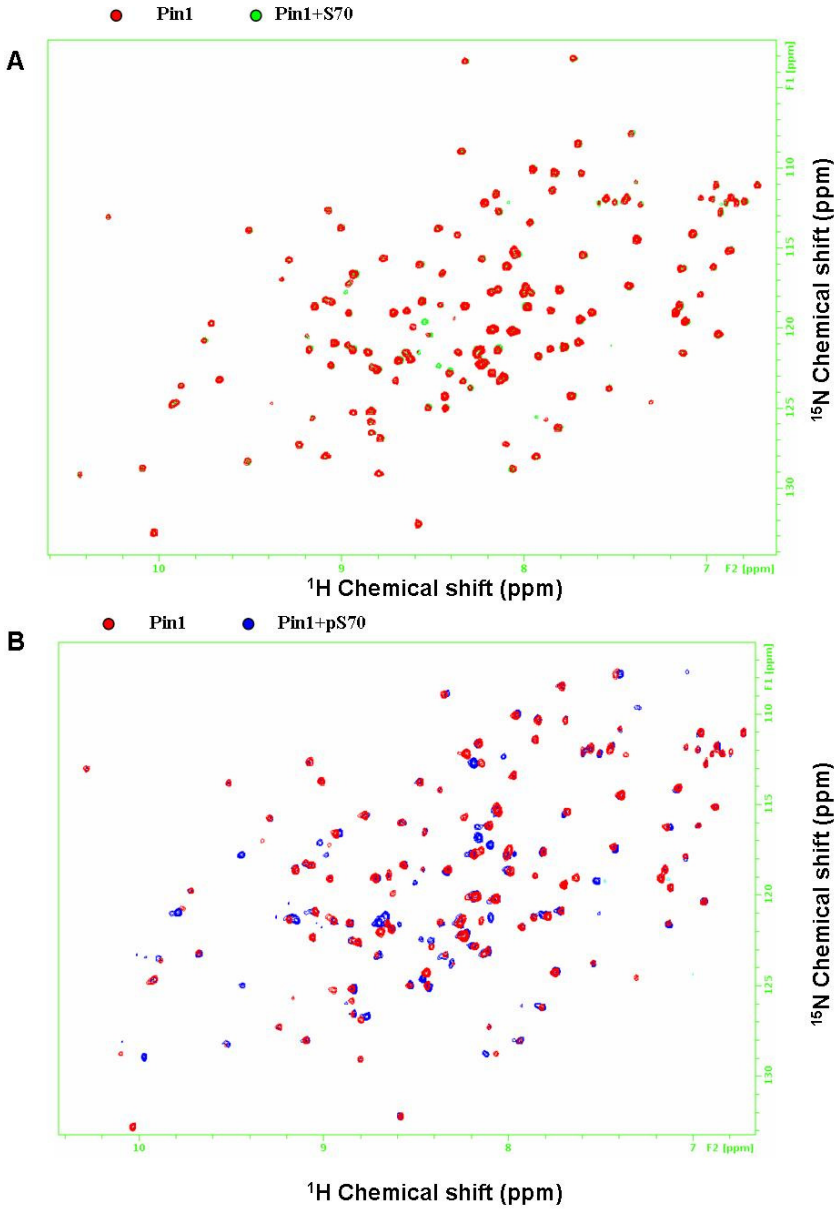

Fig.5.21 Pin 1 binds to the pS70 derived from the loop of Bcl-2

A) The interaction between Pin1 and S70. The 0.1 mM ^{15}N labeled Pin1 was recorded without and with 1 mM S70 using the 700 MHz equipped with cryoprobe. The HSQC spectra with or without p-S70 are shown in Green and Red, respectively. B) The interaction between Pin1 and p-S70. The 0.1 mM ^{15}N labeled Pin1 was recorded without or with 1 mM p-S70 peptide using the 700 MHz equipped with cryoprobe. The HSQC spectra with or without p-S70 are shown in green and red, respectively.

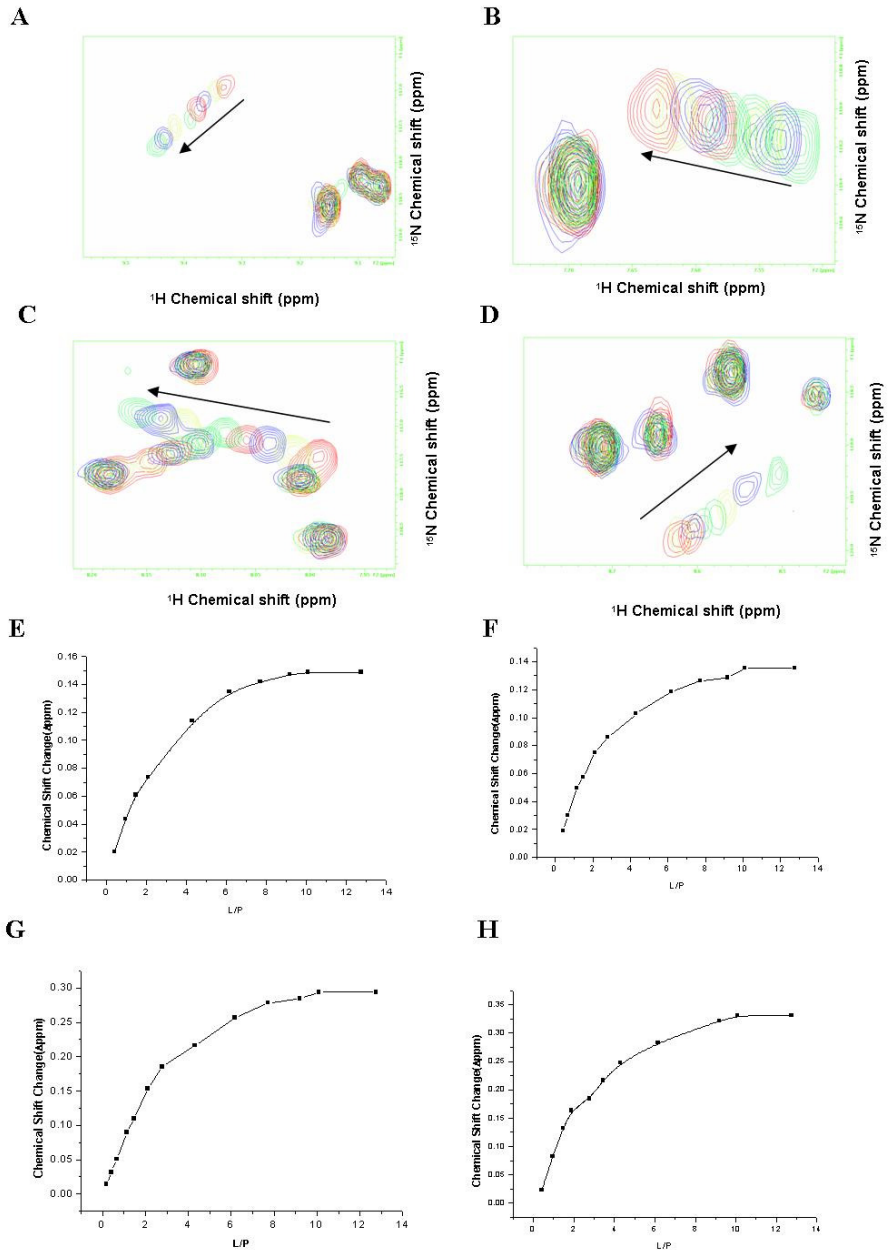

Fig.5.22 The spectrum show the changes with increasing concentration of pS70

A-D) Section of the chemical shift perturbed area after ligand was added. The arrows show the direction of chemical shift change with ligand. E-H) The relationship between chemical shift changes and the ratio of ligand to protein. The chemical shift change was calculated according to the equation in the material and methods. The figures were drawn using origin.

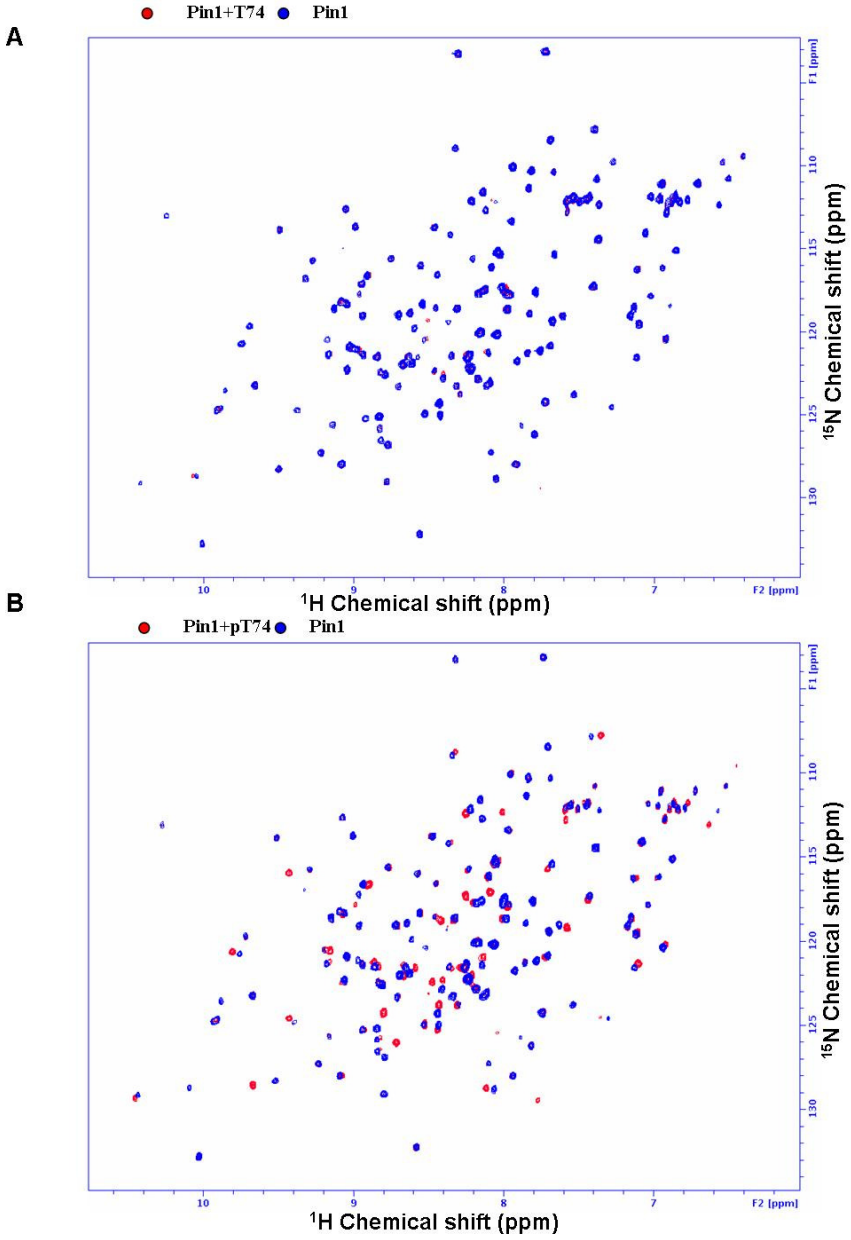

Fig.5.23 Pin 1 binds to the pT74 derived from the loop of Bcl-2

A) The interaction between Pin1 and T74. The 0.1 mM ^{15}N labeled Pin1 was recorded without and with 1 mM T74 using the 700 MHz equipped with cryoprobe. The HSQC spectra with or without p-T74 are shown in Green and Red, respectively. B) The interaction between Pin1 and p-T74. The 0.1 mM ^{15}N labeled Pin1 was recorded without or with 1 mM p-T74 peptide using the 700 MHz equipped with cryoprobe. The HSQC spectra with or without p-T74 are shown in green and red, respectively.

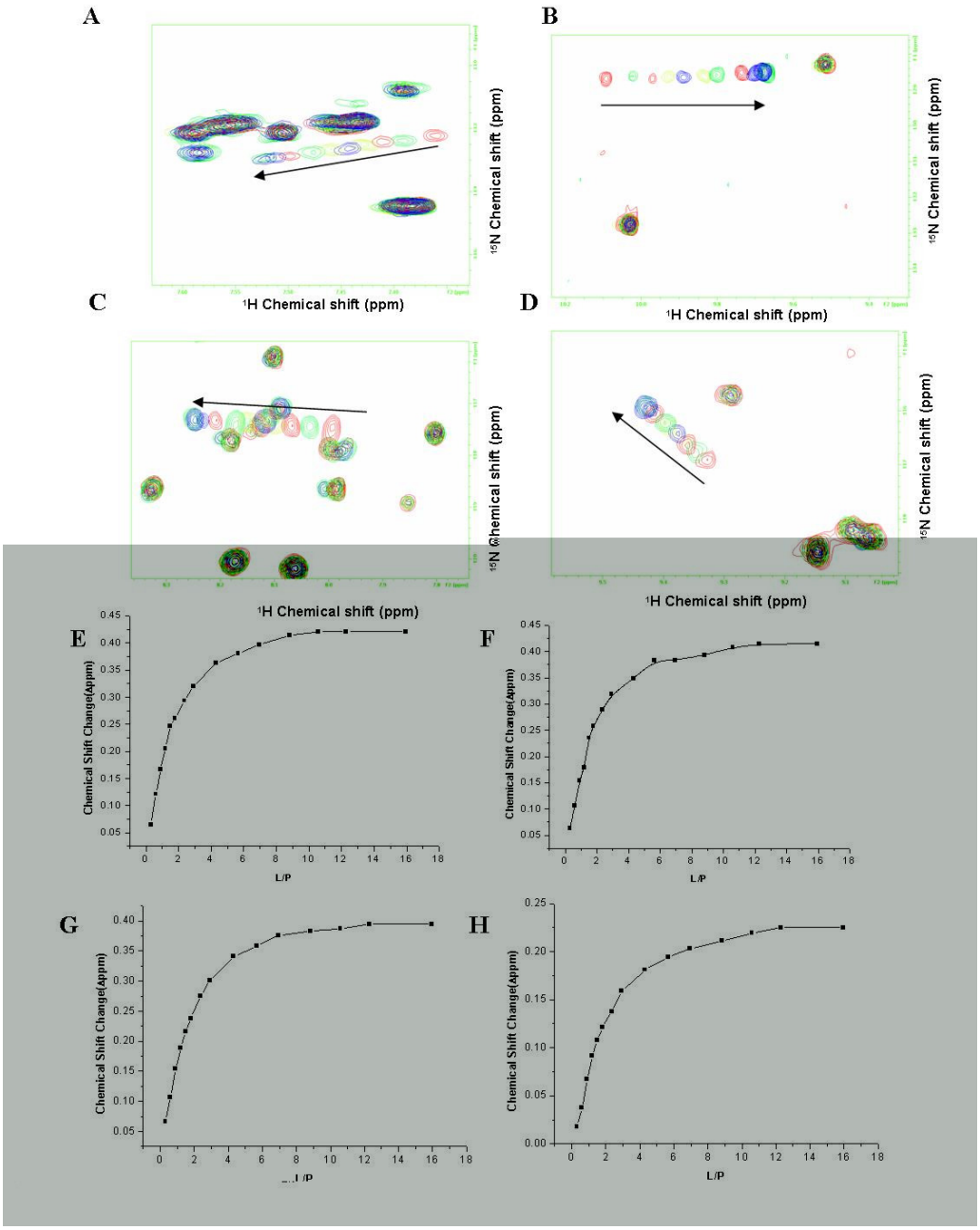

Fig.5.24 The spectrum show the changes with increasing concentration of pT74

A-D) Section of the chemical shift perturbed area after ligand was added. The arrows show the direction of chemical shift change with ligand. E-H) The relationship between chemical shift changes and the ratio of ligand to protein. The chemical shift change was calculated according to the equation in the material and methods. The figures were drawn using origin.

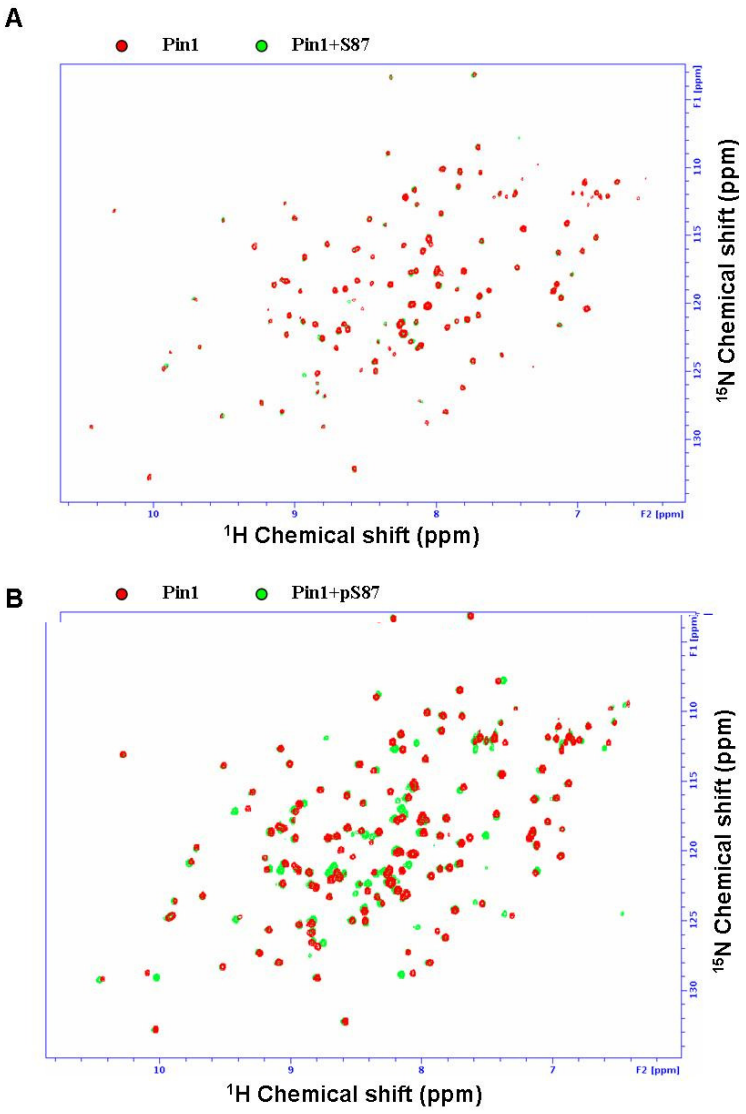

Fig.5.25 Pin 1 binds to the pS87 derived from the loop of Bcl-2

A) The interaction between Pin1 and S87. The 0.1 mM ^{15}N labeled Pin1 was recorded without and with 1 mM S87 using the 700 MHz equipped with cryoprobe. The HSQC spectra with or without p-S87 are shown in Green and Red, respectively. B) The interaction between Pin1 and p-S87. The 0.1 mM ^{15}N labeled Pin1 was recorded without or with 1 mM p-TS87 peptide using the 700 MHz equipped with cryoprobe. The HSQC spectra with or without p-S87 are shown in green and red, respectively.

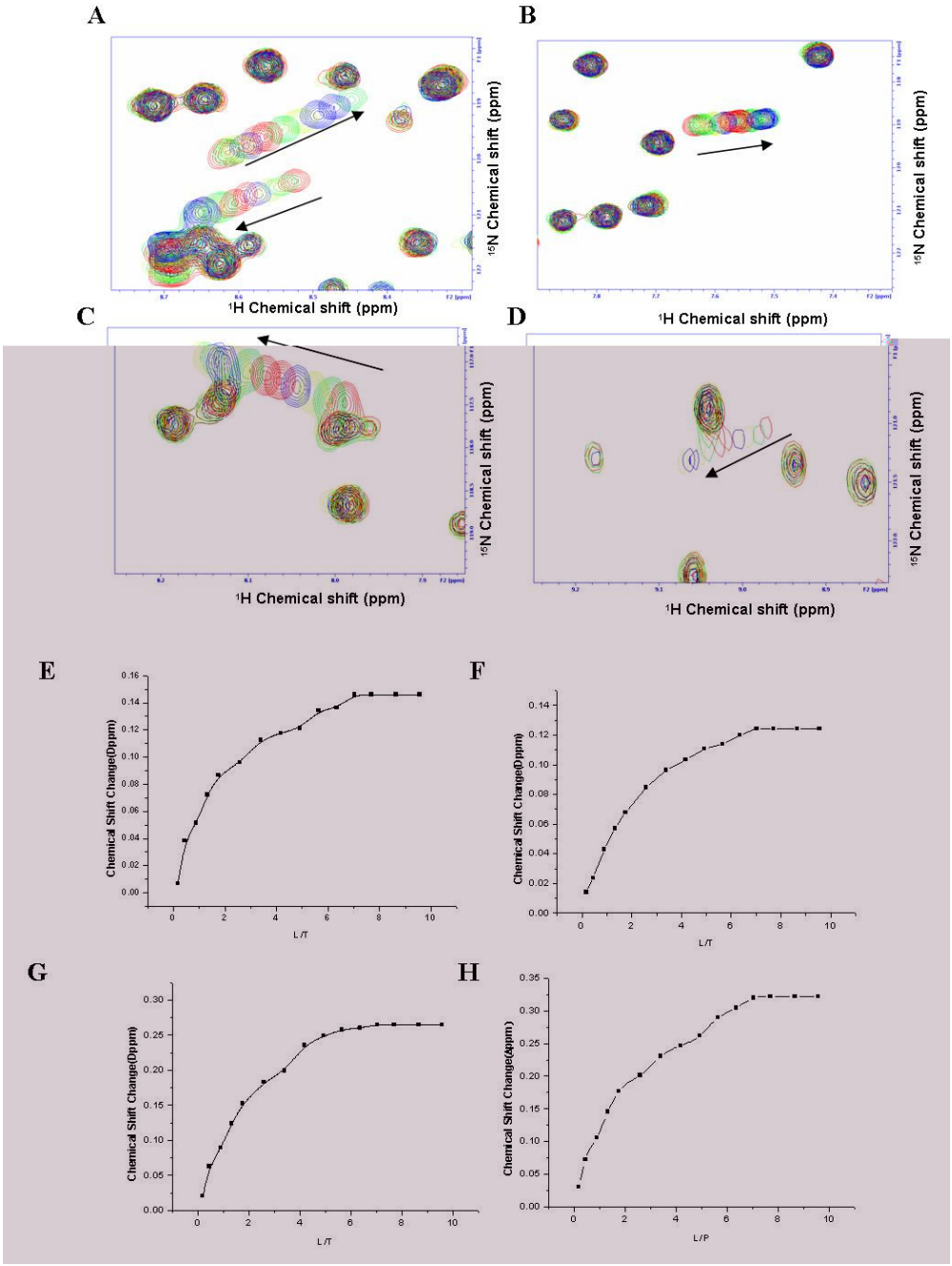

Fig.5.26 The spectra show the changes in Chemical shifts with increasing concentration of pS87

A-D) Section of the chemical shift perturbed area after ligand was added. The arrows show the direction of chemical shift change with increasing amony of ligand. E-H) the relationship between chemical shift changes and the ratio of ligand to protein measured. The chemical shift change was calculated according to the equation in the material and methods. The figures were drawn using origin.

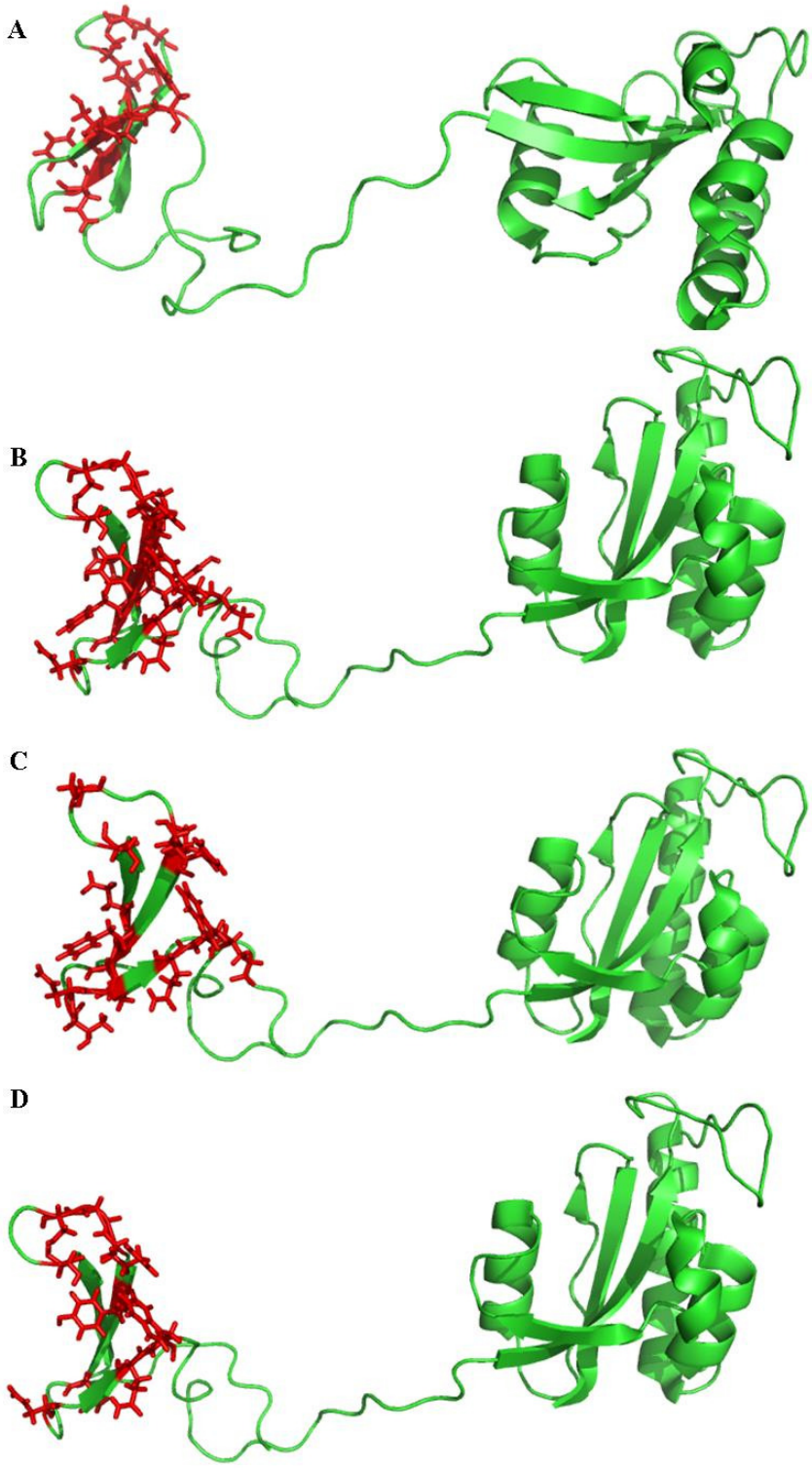

Fig.5.27 Comparison of the binding sites between Pin1 and phosphorylated peptides

The affected amino acids of Pin1 in the presence of peptides in WW domain are shown in the stick form. Most of them are located in the WW domain, which is consistant with previous observation. A, B, C, D show affected amino acids upon adding pT56, pS70, pT74 and S87, respectively.

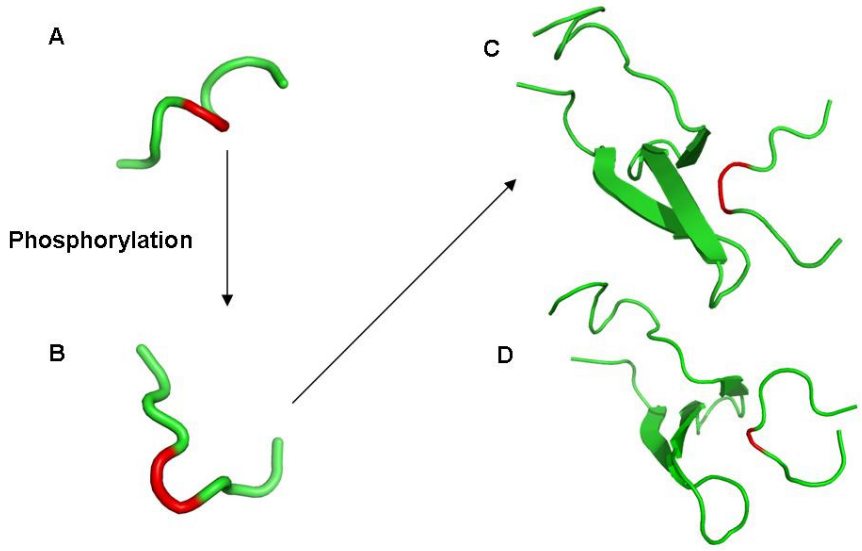

Fig.5.28 The prediction of the interaction between Pin1 and phosphorylated peptides from Bcl-2

A. S87 peptide. B. The pS87 peptide which contains the pSer-Pro motif undergoes a conformational change compared with S87. C. The docking result of the WW domain and pS87 peptide complex structure using Gold 3.0. D. The complex structure of Pin1 WW and peptide (PDB 1I8G). The pSer-Pro motif is shown in red.

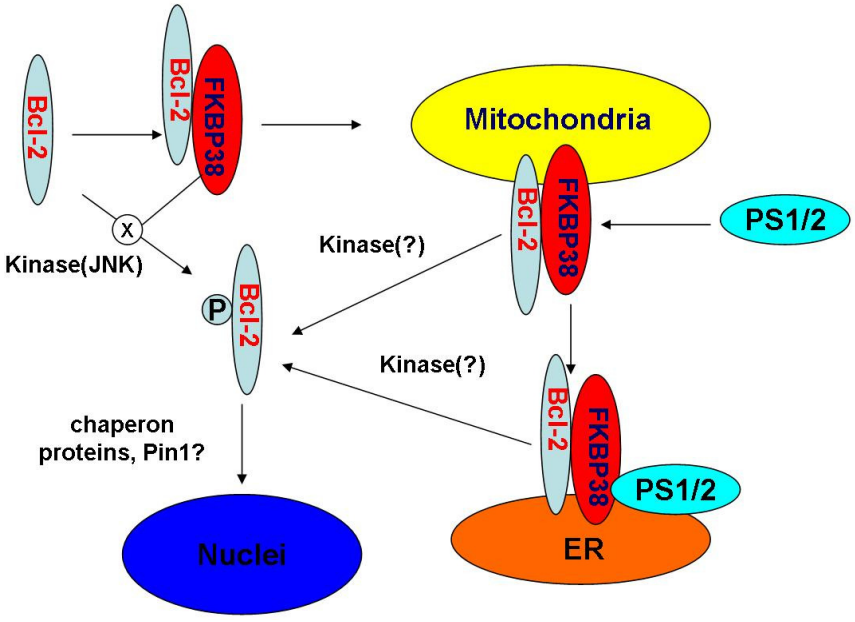

Fig.5.29 An alternative regulatory mechanism of Bcl-2

Possible regulation of Bcl-2 is that FKBP38 can help Bcl-2 localized at mitochondria or ER in the presence PS1/2. Pin1 may be possible to help p-Bcl-2 localized at nuclei or make Bcl-2 degraded by some unknown mechanisms.

5.7 Discussion

FKBP38 is a unique protein. It is different from typical FKBP family proteins; it contains a FKBP domain which is conserved among FKBP family proteins, but it appears to lack conserved residues for FK-506 binding and PPIase activity conserved in other FKBP family proteins (Galat, 2003, Shrine *et al.*, 2003, Van Duyne *et al.*, 1991). Recently, its co-localization with antiapoptotic proteins Bcl-2 and Bcl-xL and the inhibition of calcineurin activity in the absence of FK-506 have been reported (Shirane *et al.*, 2003).

Bcl-2 family proteins are frequently regulated by posttranslational modification that can control their activity and conformation. Bcl-2 has been shown to be phosphorylated on some specific residues within its unstructured loop under diverse stimuli (Chang *et al.*, 2001, Breitschopf *et al.*, 2000, Haldar *et al.*, 1998, Bassik *et al.*, 2004). It was reported that phosphorylation of Bcl-2 is associated with its inactivation and mutation of the phosphorylation sites was reported to enhance the antiapoptotic activity of Bcl-2 (Yamamoto *et al.*, 1999). The phosphorylated Bcl-2 was found to be localized at ER and inhibit its binding to proapoptotic proteins (Bassik *et al.*, 2004). Currently, biochemical function and specific molecular regulatory mechanism of FKBP38 with the antiapoptotic proteins are not well understood.

In this study, we were able to express and purify recombinant FKBP38 from bacteria for biochemical and structural studies in connection with Bcl-2 family proteins. From the co-expression (Fig.5.1, Fig.5.2), column binding, yeast two-hybrid, and phosphorylation studies, we demonstrated that the unstructured loop region of Bcl-2 was important for the binding between FKBP38 and Bcl-2. It was showed that the stress kinase JNK was efficiently able to phosphorylate the purified Bcl-2 *in vitro* and the phosphorylation of Bcl-2 was extensively inhibited in the presence of

FKBP38. On the other hand, to ask how JNK-mediated phosphorylation of Bcl-2 would affect its interaction with FKBP38, we performed GST pull-down experiments. Clearly, the data revealed that the phosphorylated Bcl-2 showed a considerable reduction in its binding with FKBP38 (Fig.5.15). Taken together, these results suggest that FKBP38 might modulate the phosphorylation in the unstructured loop of Bcl-2 and could prevent Bcl-2 from being phosphorylated. Besides, a kinase or kinases, including JNK, might regulate molecular interaction between Bcl-2 and FKBP38 through the phosphorylation.

To address the specificity of interaction, we carried out JNK-mediated phosphorylation of Bcl-xL, which is similar in function to Bcl-2. The data showed that Bcl-xL did not appear to be affected in the presence of FKBP38; rather our results showed an indication of a slight increase in the phosphorylation. This suggests that FKBP38 might show a difference in molecular interaction with the phosphorylation sites in the flexible loops of Bcl-2 family proteins. From our deletion mutant analyses, the sites containing or surrounding S70 and S87 in the flexible loop of Bcl-2 appear to be important for the physical interaction with FKBP38. The NMR titration with S87 peptide shows that there was the weak interaction between the FKBP38NTD and S87 (Fig.6.19). Additional studies need to be done to further characterize the regulation of FKBP38 on the phosporylation of Bcl-2 with respect to other sites.

Bcl-2 is an anti-apoptotic protein that plays very important roles in the regulation of apoptosis (Cory *et al.*, 2002, Vander Heiden *et al.*, 1999, Kroemer *et al.*, 1997, Schlesinger *et al.*, 1997). Three-dimensional structure of Bcl-2 reveals that it contains an elongated hydrophobic cleft through which the anti-apoptotic protein and its ligand interact to form heterodimers (Petros *et al.*, 2001, Muchmore *et al.*, 1996). The

residues T56, S70, T74, and S87 in the flexible loop of Bcl-2 have been shown to be phosphorylated in response to a variety of external stimuli (Bassik *et al.*, 2004). But the biological significance and molecular basis of the Bcl-2 phosphorylation at those sites still remain unclear. Several kinases including JNK and ERK2 have been shown to be associated with the phosphorylation of Bcl-2 in this work. To better understand the molecular basis of the Bcl-2 phosphorylation, we first studied the characteristics of the Bcl-2 phosphorylation by JNK and ERK2, which are repeatedly shown to be involved in the phosphorylation of Bcl-2 (Brichese *et al.*, 2004, Deng *et al.*, 2000). From our studies on the kinase specificity using the Bcl-2 mutants and the flexible loop-derived peptides, it is suspected that JNK and ERK2 appear to show substrate specificity with the four known phosphorylation sites. Our results indicate that S87 is the primary phosphorylation site for ERK2, but S70 and T74 appear to be poor substrates for both JNK and ERK2. The presence of a consensus substrate sequences is important for its recognition as a substrate by a specific protein kinase, since the specificity-determining characteristics of the phosphorylation site are contained in the flanking amino acids of the target phosphorylation site at Thr or Ser (Kennelly *et al.*, 1991). Previously, it has been shown that the substrate consensus sequence for ERK2 is PXaan(S/T)P, where Xaa is a neutral or basic amino acids and n = 1 or 2 (Gonzalez *et al.*, 1991). The analysis of the primary sequences of the known phosphorylation sites in Bcl-2 (Fig.5.6 A) reveals that the flanking sequence of the S87 appears to be conserved and consistent with the consensus sequence described previously. On the other hand, our studies on Bcl-2Δ(V35-D79), which contains only the S87 phosphorylation site, showed less efficient phosphorylation compared to the p-S87 peptide (Fig.5.5 B, lane 7 and Fig.5.6 B). We speculate that this could be attributed to the lack of a region in the loop domain of Bcl-2 which might be able to interact with

the common docking site of ERK2 and contribute to better substrate specificity for ERK2, as exemplified in the case of the bipartite recognition model of ERK2 and its substrate MKP3 (Zhang *et al.*, 2003).

The 3D structures of the peptides before and after phosphorylation were analyzed by NMR. First the proton chemical shifts were assigned according to the 2D TOCSY spectrum. The H^N chemical shift changed dramatically. The 3D structures show the difference after phosphorylation. The 3D structures of the peptides showed some change after phosphorylation. From the calculated result, it is clear that there is a conformational change upon phosphorylation. Pin1 interacted with the pSer/Thr-Pro motif (Wintjens *et al.*, 2001). In our study, we confirmed that the interaction between Pin1 and the loop region of Bcl-2 was phosphorylation-dependent. The conformational change upon phosphorylation provides the motif to interact with Pin1. Based upon the docking study (Fig.5.28), the Pin1-pS87 complex structure is similar to that of Pin1 and Cdc25 peptide (Wintjens *et al.*, 2001), which can explain Pin1 only interact with phosphorylated peptides from the loop region of Bcl-2. The effect of phosphorylation on the function of Bcl-2 is still unclear. Our finding suggested the phosphorylation on the loop region of Bcl-2 provided the structural switches which make Bcl-2 interact with different proteins and play a different role in regulation of apoptosis.

The association of PP2B (calcineurin) with Bcl-2 was described before (Shibasaki *et al.*, 1997). Here, we demonstrated that the phosphorylated T56 is the preferred site for PP2B, but the phosphorylated S70, T74, and S87 appear to be poor substrates for PP2B (Fig.5.8). These data indicate that the relevant protein kinases and protein phosphatases might exert different specificity with the target phosphorylation sites in the loop of Bcl-2. Previously, it has been shown that the phosphatases PP1 and PP2A

also interact with Bcl-2 and regulate the Bcl-2 phosphorylation (Shibasaki *et al.*, Brichese *et al.*, 2004, Deng *et al.*, 2000). To check their specificity, we used the synthetic phosphopeptides. From our results, it appears that the phosphatases PP1 and PP2A better recognize the phosphopeptides T56 and T74 as substrates, with T74 as the preferred one (Fig.5.10). The specificity pattern of PP2B with Bcl-2 protein and its mutants (Fig.5.8) appears to be similar to that of the peptides (Fig.5.9). This leads us to speculate that the similar specificity pattern could be translated to PP1 and PP2B. Previously, the potential anti-apoptotic function of pS70-containing Bcl-2 was described (Deng *et al.*, 2004). On the other hand, the inactivation of Bcl-2 activity by the phosphorylation was also described (Bassik *et al.*, 2004). In view of these findings, it is suspected that the different specificity of PP1, PP2A, and PP2B with the substrate sites in the Bcl-2 loop might provide a potential regulatory mechanism to control the activity of Bcl-2 by modulating the level of the phosphorylated and unphosphorylated Bcl-2.

Pin 1, which belongs to another class of peptidylprolyl *cis-trans* isomerase, and is different form the FKBP family, plays important roles in the regulation of phosphorylated proteins (Bayer *et al.*, 2003). It was shown that Pin 1 binds to the phosphorylated Bcl-2 (Pathan *et al.*, 2001). Its molecular basis for the interaction is currently not known. In this study, to determine molecular interaction we employed NMR methods. The results showed that upon the addition of the phosphopeptides derived from the loop of Bcl-2 to the ^{15}N-labeled Pin 1 apparent spectral changes were observed in the 2D ^{1}H-^{15}N HSQC of Pin 1(Fig.5.19-5.27), suggesting that Pin 1 binds to the phosphopeptides at molecular level. The interaction between Pin1 and Bcl-2 is phosphorylation dependent because Pin1 bind to the pSer/pThr-Pro motif through the WW domain and our NMR titration is consistant with the result. The 3D

structure of the peptide showed a conformational change after phosphorylation, which forms the binding motif for the molecular interaction with Pin1 (Fig.5.28). Since the fates of Bcl-2 and pBcl-2 appear to be different (Pathan *et al.*, 2001, Ciechanover *et al.*, 1994, haldar *et al.*, 1998, Reed, 1998), the molecular and structural basis for the molecular interaction between Pin 1 and pBcl-2 might contribute to our understanding of Pin 1 on the regulation of Bcl-2.

Proteins containing regions of denatured or random coil structure do not exhibit a long half-life due to cleavage by cellular protease (Ciechanover, 1994). We speculate that the loop of Bcl-2 is recognized and protected by certain proteins, and subsequently the molecular interactions would stabilize Bcl-2, and result in maintenance of the anti-apoptotic function of Bcl-2.

FKBP38 is a docking molecule which can help Bcl-2 to localize at the mitochondria (Shirane *et al.*, 2003). To check the effect on Bcl-2 after the depletion of FKBP38, we attempted to employ siRNA to suppress FKBP38 function. It was demonstrated that the knock-down of FKBP38 unexpectedly resulted in a reduction of anti-apoptotic protein Bcl-2 without much influence on the expression of pro-apoptotic protein Bax, while the similar anti-apoptotic protein Bcl-xL was slightly affected (Kang *et al*., 2005), suggesting that the ratio between pro-and anti-apoptotic proteins was changed, and consequently led to induction of apoptosis. The treatment of FKBP38 siRNA caused to reduce the level of Bcl-2 protein, but it didn't affect on Bcl-2 mRNA. This suggests that the down-regulation of Bcl-2 after suppression of FKBP38 takes place at protein level. Three-dimensional structural studies revealed that the anti-apoptotic proteins Bcl-2 and Bcl-xL contain an unusually long disordered loop (Petros *et al.*, 2001, Muchmore *et al.*, 1996). It was shown that the loop is regulated by kinases, in response to diverse external stimuli (Blagoskonny, 2001,

Breitschopf *et al.*, 2000), and also, proteosomes are involved in the posttranslational regulation of Bcl-2 (Wang *et al.*, 2005). Recently, we have shown that the disordered loop of Bcl-2 is involved in molecular interaction with FKBP38. Taken these data together, we speculate that Bcl-2 might be protected when complexed with FKBP38. But when Bcl-2 loses binding partner FKBP38, Bcl-2 might become unstable or be left unprotected from degradation, and eventually contributing to apoptotic cell death. There have been controversial reports about the function of FKBP38 in apoptosis; Shirane and Nakayama demonstrated the anti-apoptotic activity of FKBP38 by showing that FKBP38 inhibited Bcl-2 dependent apoptosis. On the other hand, Edlich *et al*. demonstrated the pro-apoptotic activity of FKBP by showing that the complex formation of FKBP38 with Ca^{2+}/calmodulin resulted in disruption of interaction with Bcl-2. Recently, it was shown that presenilins 1 and 2 (PS1/2), which have shown to be associated with familial Alzheimer's disease (FAD) and involved in apoptotic neuronal cell death, increased the susceptibility of cells to apoptosis by antagonizing anti-apoptotic function of FKBP38. Our results showed that the effect with the treatment of siRNA on FKBP38 was similar to that on Bcl-2 in inducing apoptosis (kang *et al*., 2005), so we speculate that FKBP38 exerts an anti-apoptotic activity by chaperoning the anti-apoptotic protein Bcl-2 to mitochondria or ER in the presence of PS1/2. Then the Pin1 may be useful for changing the conformation of p-Bcl-2 (Fig.5.29). It, however, cannot be excluded that the dual function (anti-apoptotic and pro-apoptotic) of FKBP38 could be due to differences in cells used in those studies. Different cells originated from different tissues may operate different apoptotic regulatory pathways. Further studies remain to be conducted for better understanding of function and role of FKBP38 in apoptosis and role of Pin1 in regulation of Bcl-2.

6 NMR study on the N-terminal domain of FKBP38

Nuclear Magnetic Resonance (NMR) is used to observe the precession movement of the magnetic moments of atomic nuclei in a magnetic field. The precession frequencies of the nuclei depend on their environment and on the structure and dynamics of the protein. In theory, it is possible to discriminate resonances of virtually all individual nuclei in a protein by using NMR because the peaks that are observed in an NMR spectrum are usually sufficiently narrow for a typical soluble protein (well structured protein with a molecular weight less than 30 kDa) and the frequencies are sufficiently dispersed due to the differences in the environment of the spins. Assignment of the thousands of resonance frequencies of the protein can be still a quite laborious task, but has been simplified by spectral labeling techniques (Sattler *et al.*, 1999). The information in NMR spectra is often produced by transferring magnetization from one nucleus to anther. Basically there are two mechanisms by which the information can be transferred: through bond and through space. The J-coupling magnetization can be transferred through bond, so that it can be used for determination of the molecular topology and the resonance frequencies of the nuclei, such as the 3D experiment for the protein backbone assignment. The nuclear Overhauser Effect (NOE) is a transfer of magnetization through space, and the information can be used to determine the distance between two nuclei. As all the nuclei resonance frequencies can be obtained in solution by NMR, NMR is a good tool for the structure determination of proteins which can not be easily crystallized and powerful tool to determine protein-protein or protein-ligand interaction (Simon *et al.*, 2004).

From the previous studies, FKBP38 was shown to be important protein in

regulating apoptosis by docking of Bcl-2/xL to the mitochondrial membrane (Shirne *et al.*, 2003). Other proteins PS1/2 also can interact with FKBP38 and affect its location between mitochondria and ER (Wang *et al.*, 2005). So three dimensional structure study of FKBP38 will provide insights about the molecular interaction between FKBP38 and other proteins. We purified FKBP38 without TM domain and tried the crystallization. But attempts to crystallize the FKBP38ΔTM failed. The N-terminal domain of FKBP38 (FKBP38NTD) exhibited good chemical shifts dispersion. Thus, in this study, the FKBP38NTD was uniformly labeled with ^{15}N and ^{13}C. A series of 3D experiments were performed as described in the methods to determine solution structure of FKBP38NTD (M1-D149).

6.1 Backbone ^{1}H, ^{13}C and ^{15}N resonance assignments of FKBP38NTD

The introduction of three- and four-dimensional NMR experiments and the availability of ^{13}C-, ^{15}N-labelled proteins allow researchers to assign the proton, nitrogen and carbon chemical shifts of proteins and protein complexes with molecular weights well above 30 kD and to determine their structures in solution (Lingel *et al.*, 2004, Sattler *et al.*, 1999). The resonance assignment of singly (^{15}N or ^{13}C) labeled proteins using 3D experiments is basically an extension of traditional strategy which exclusively relies on homonuclear ^{1}H NMR experiments. The dependence of the 3_J coupling constants used in COSY and TOCSY experiments on the conformation can also hinder the assignment process since cross peaks between spins that share a small coupling (i.e. the H^N and H^A protons in an α-helix) may be missing. The problems of limited resolution among the H^A resonances and the conformation dependence of the NOE and 3_J coupling constants are overcome in the assignment strategies for ^{13}C-, ^{15}N-labelled proteins since they employ coherence transfer via 1_J (and in part 2_J) couplings only, which are largely independent of conformation (Sattler *et al.*, 1999).

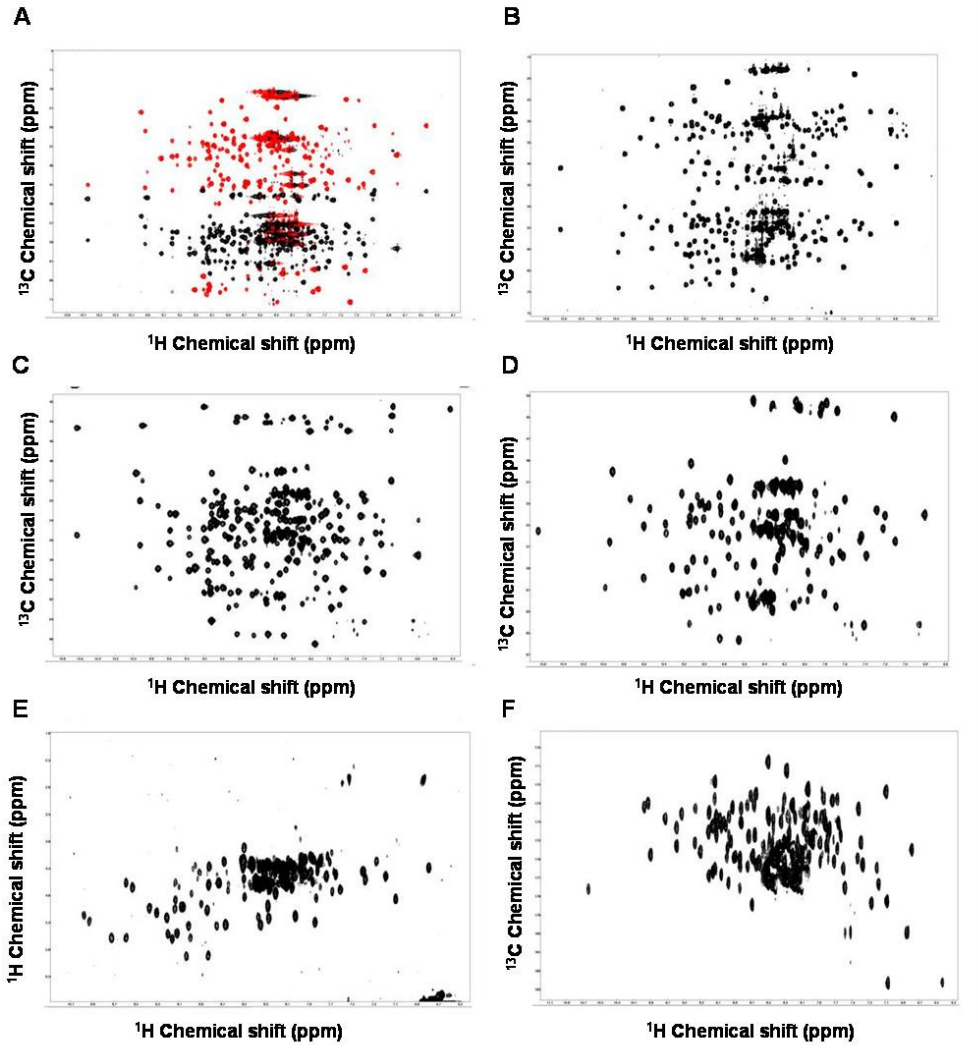

Fig.6.1 The 3D experiments shown in F1 and F3 dimensions

The experiment data were processed by nmrPipe and visualize by NMRView. The F1 (^{13}C or ^{1}H) and F3 (^{1}H) plane and full F2 dimension (^{15}N). A) HNCACB provides $C_{\alpha i}$, $C_{\alpha i-1}$, $C_{\beta i}$ and $C_{\beta i-1}$ information. B) CBCACONH provides $C_{\alpha i-1}$ and $C_{\beta i-1}$ information. C) HNCA provides $C_{\alpha i}$, $C_{\alpha i-1}$ information. D) HNCOCA provides C_{α} information. E) HNHA provides H^{A} information. F) HNCO provides C' (CO) information.

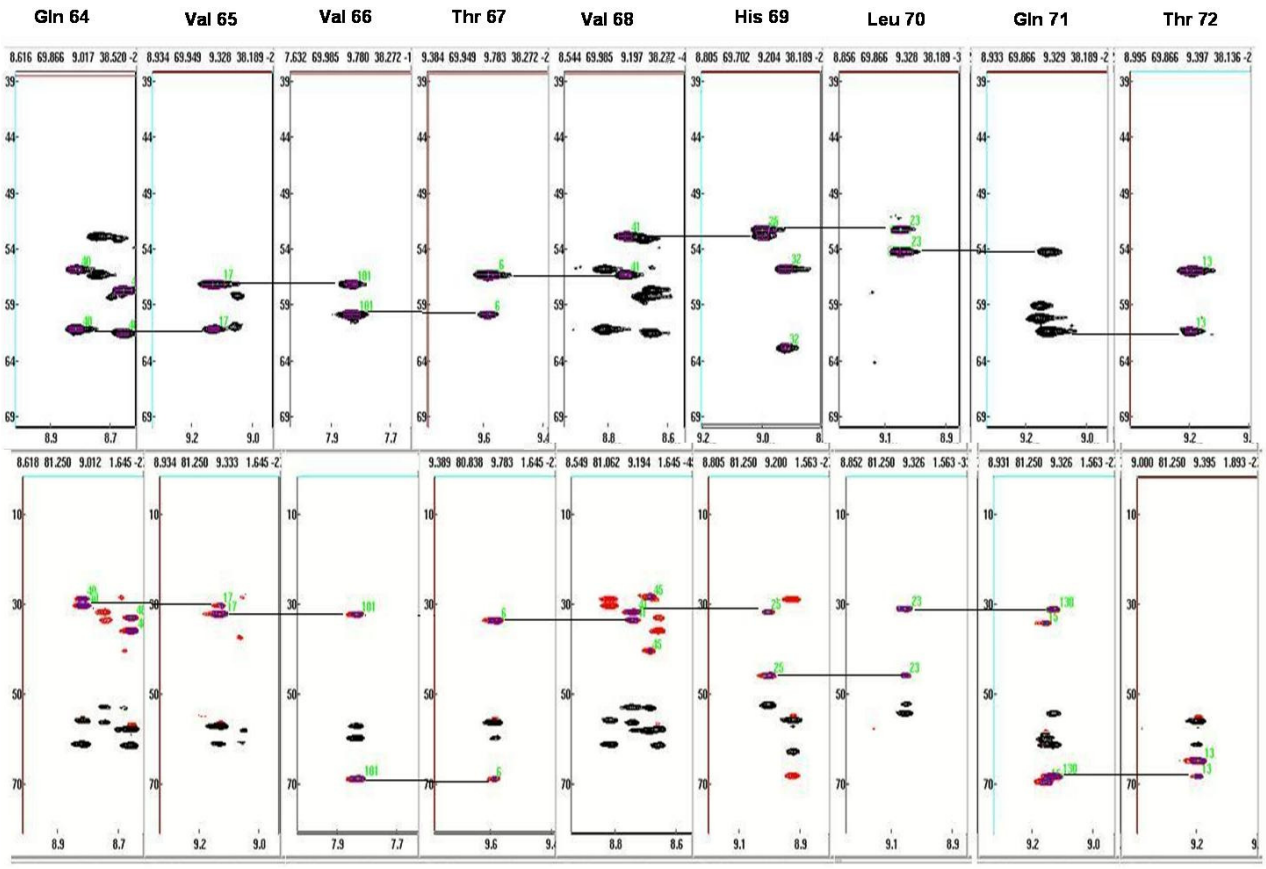

Fig.6.2 The backbone assignment of NTD of FKBP38

This figure shows the assigned fragment of NTD of FKBP38 from Gln 64 to Thr 72, which provides the procedure how other fragments are assigned. The upper strips are the connection of $C_{\alpha i}$ and $C_{\alpha i-1}$, the line gives the connection. The lower strips are the connection of $C_{\beta i}$ and $C_{\beta i-1}$. The red peaks are the $C_{\beta i}$ and $C_{\beta i-1}$, the black peaks are the $C_{\alpha i}$, $C_{\alpha i-1}$, which are same as the upper strips. All the strips are from HNCACB, HNCA, HNCOCA and CBCACONH, which are showed in the Fig.6.3.

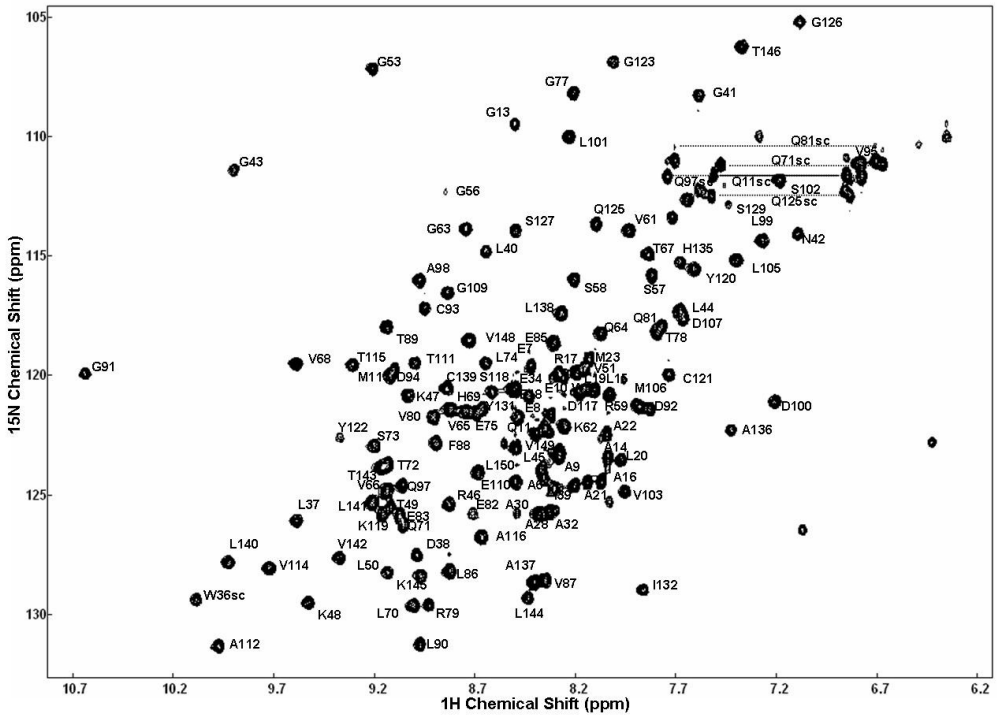

Fig.6.3 The assignment of the ^{15} N-HSQC spectrum

The assignment of the cross peaks in the ^{15}N-HSQC spectrum was shown with amino acid name and number. Also, the side chain assignment is labeled as sc.

A series of 3D experiments were performed and processed by nmrPipe and the backbone assignment was completed by NMRview (Fig.6.1, Fig.6.2, and Fig.A.3). Out of a total of 130 observable backbone ^{1}H-^{15}N correlations spanning residues 5-151 (which includes 17 prolines), 129 (99.2%) residues have been assigned. For carbon, 144 out of 147 13C$^{\alpha}$ (97.9%) and 133 out of 136 C$^{\beta}$ (97.8%, 11 glycines with no C$^{\beta}$) resonances have been assigned. The unassigned residues are M1, G2, Q3, P4, Pro54, Arg128, Pro133 and the C-terminal His$_6$-tag. Excluding the C-terminal His-tag residues, assignments of the side chain are about 90% completed. An analysis of its backbone chemical shifts using the program CSI (Wishart *et al.*, 1994) suggests that FKBP38NTD contains at least six-β-strands and two α-helices. We believe that the quality of the NMR data is sufficient for the structure determination of FKBP38NTD.

The assignment of FKBP38NTD (Fig.6.3) has been deposited in the BioMagResBank (accession number: 6923).

6.2 Sidechain assignment of FKBP38NTD

The resonance assignments of most of backbone nuclei were obtained by the triple resonance NMR spectroscopy. The assignment for the majority of side-chain ^{1}H and ^{13}C resonances was obtained from HCCCONH, CCCONH, CCCH-TOCSY and HCCH-TOCSY starting with knowledge of the backbone $^{1}H^{N}$, ^{15}N, $^{13}C^{\alpha}$, $^{13}C^{\beta}$, $^{13}C'$ and $^{1}H^{A}$. Fig.6.4 shows the two spectra in 2-dimensions. The aromatic ring proton resonances were assigned by using 2D-NOE data set. Also, the 2D-NOE can also provide some long distance NOE between the aromatic ring and the methyl group (Fig.6.5).

6.3 Protein secondary structure prediction based upon the backbone assignment

The chemical shift index (CSI) is a method for predicting protein secondary structures from the observed chemical shifts of the protein backbone and C^{β} atoms. In general, if a run of negative values is present in the consensus plot, a helix is predicted for this region of the protein. If a run of positive values is present, a beta strand is predicted. By using the NMRview software, the information of the secondary structure based upon the chemical shift values and CSI was obtained. FKBP38NTD contains a series of β-sheet and 3 regions of α-helical like structure as only 3 residues have the potential of forming α-helical structure. The secondary structure in the FKBP domain is similar to the published FKBP12, FKBP52, FKBP51 and X-ray structure of FKBP domain in protein data bank (Fig.6.6, Fig.6.7). The exact secondary structure should also be confirmed using the NOE data because each secondary structure has different NOE pattern (Wang *et al.*, 2002, Cornilescu *et al.*, 1999).

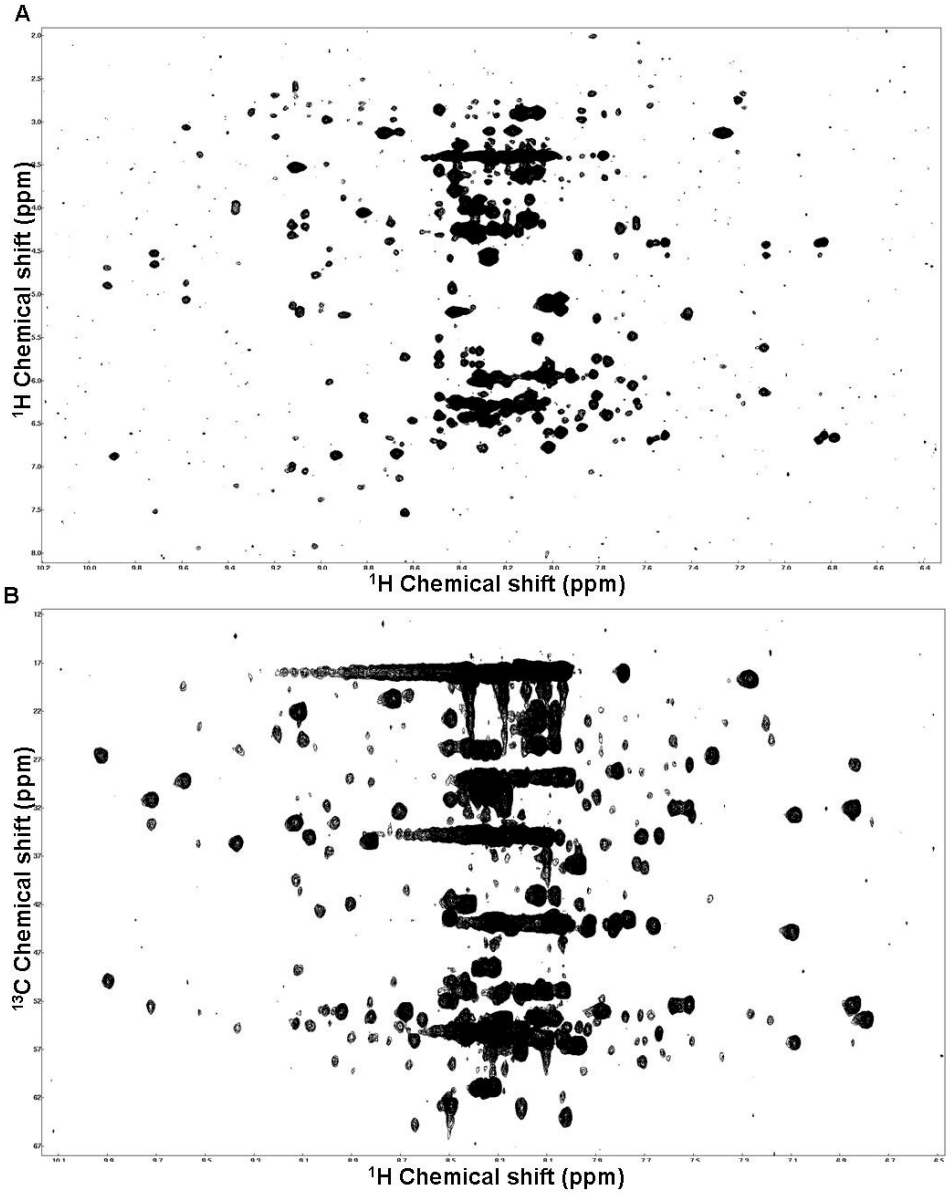

Fig.6.4 The results of side chain experiment

Uniformly $^{13}C/^{15}N$ labeled sample was used for data collection. Data was processed with nmrPipe and visualized by NMRview. The overlaid spectra were shown. A) HCCCONH. B) CCCONH.

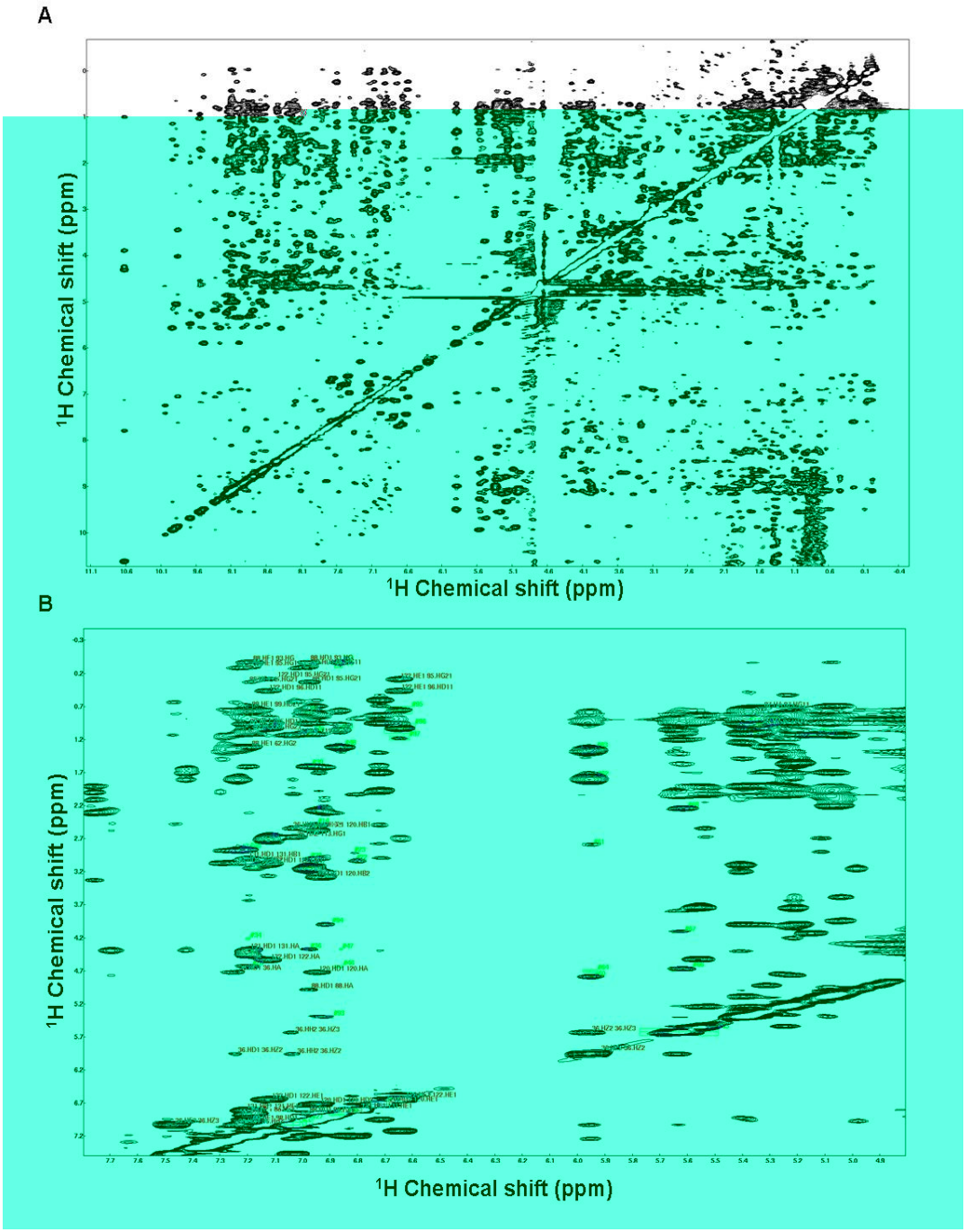

Fig.6.5 The 2D NOE result and the assignment of aromatic ring proton

A) 2D-NOE of FKBP38 NTD in H_2O was recorded with 100 ms mixing time. B) The 2D-NOE of FKBP38 NTD in D_2O was recorded with 100 ms mixing time. The aromatic ring protons were assigned based upon their NOEs with their own H^{α} and H^{β}.

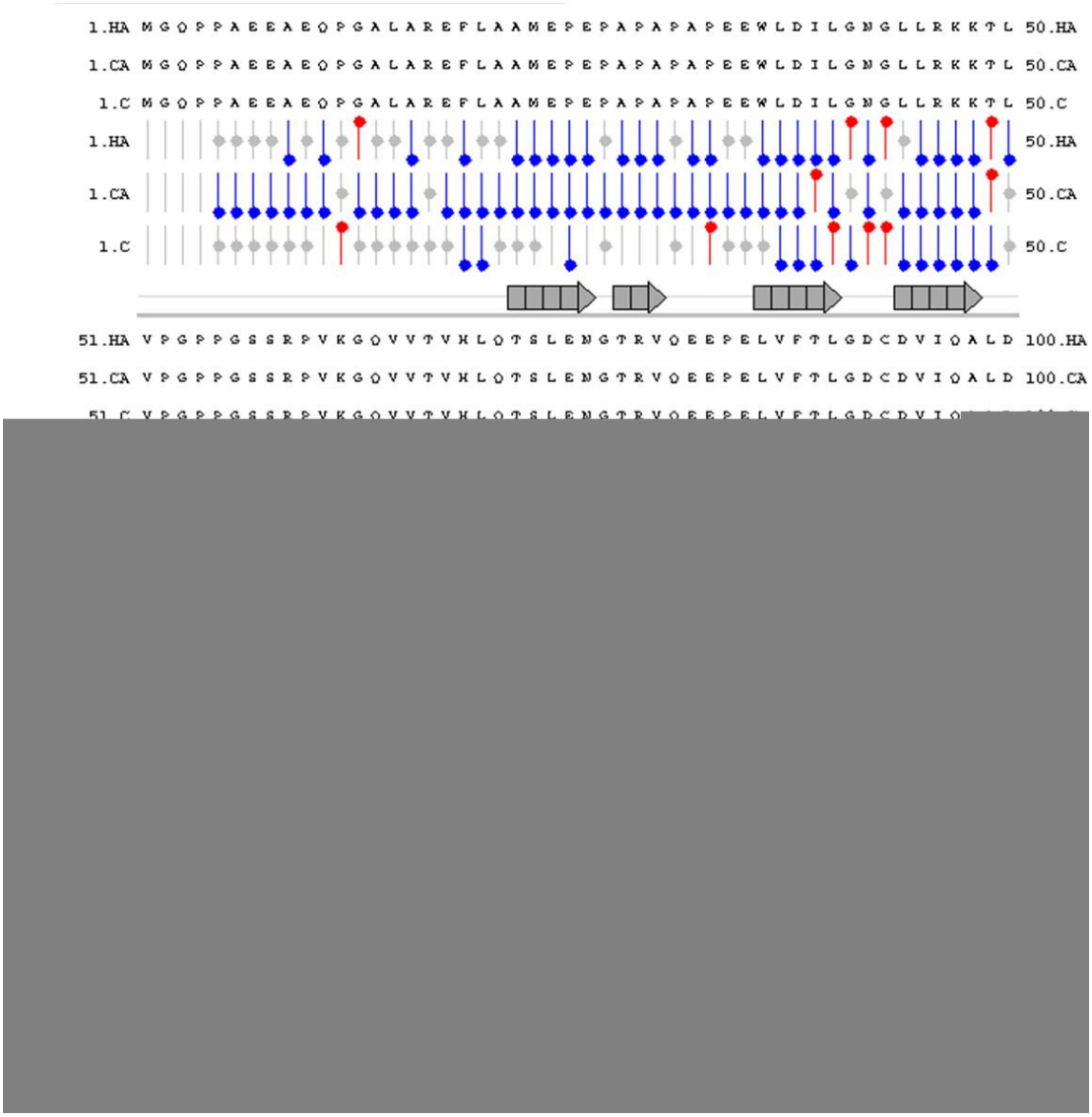

Fig.6.6 Protein secondary structure prediction based upon the backbone assignment

The secondary structure prediction was finished by using NMRview. Only HA, CA and C' were used for the prediction. The α-helix is also predicted based upon the NOE pattern.

6.4 Analysis of dihedral angles of FKBP38NTD

TALOS (Cornilescu *et al.*, 1999) is a database system for prediction of phi and psi backbone torsion angles using a combination of five kinds (HA, CA, CB, CO, N) of chemical shift assignments for a given protein sequence. The TALOS approach is an extension of the well-known observation that many kinds of secondary chemical shifts (i.e. differences between chemical shifts and their corresponding random coil values) are highly correlated with the aspects of protein secondary structure. The goal of TALOS is to use secondary shift and sequence information in order to make quantitative predictions for the protein backbone angles phi and psi, and to provide a measure of the uncertainties in these predictions. TALOS uses the secondary shifts of a given residue to predict phi and psi angles for that residue. TALOS also includes the information from the next and previous residues when making predictions for a given residue. So, in practice, TALOS uses data for three consecutive residues simultaneously (i.e. 15 total secondary shifts and 3 residue types) to make predictions for the central residue in a triplet (http://spin.niddk.nih.gov/NMRPipe/ talos/).

In practice, TALOS searches a database for the 10 best matches to a given triplet in the target protein. If these 10 matches indicate consistent values for phi and psi, then their averages and standard deviations are used as a prediction. However, if the 10 best matches have mutually inconsistent values of phi and psi, the matches are declared ambiguous, and no prediction is made for the central residue. In the TALOS approach, an initial classification of good vs ambiguous is performed automatically, and the classifications are then adjusted interactively through a graphical interface which is part of the TALOS system.

The TALOS database, while small, was constructed using the most well-defined parts of high resolution (2.2 Angstroms or better) X-ray crystal structures to define the

phi and psi angles. It currently includes data from 20 proteins, representing around 3,000 triplets.

The NTD chemical shifts were analyzed by Talos after backbone assignment. Fig. 6.8 shows the Talos analysis result using the rama.tcl command. The Good prediction was accepted and converted to the file format which can be read and analyzed by Aria (Table 6.1).

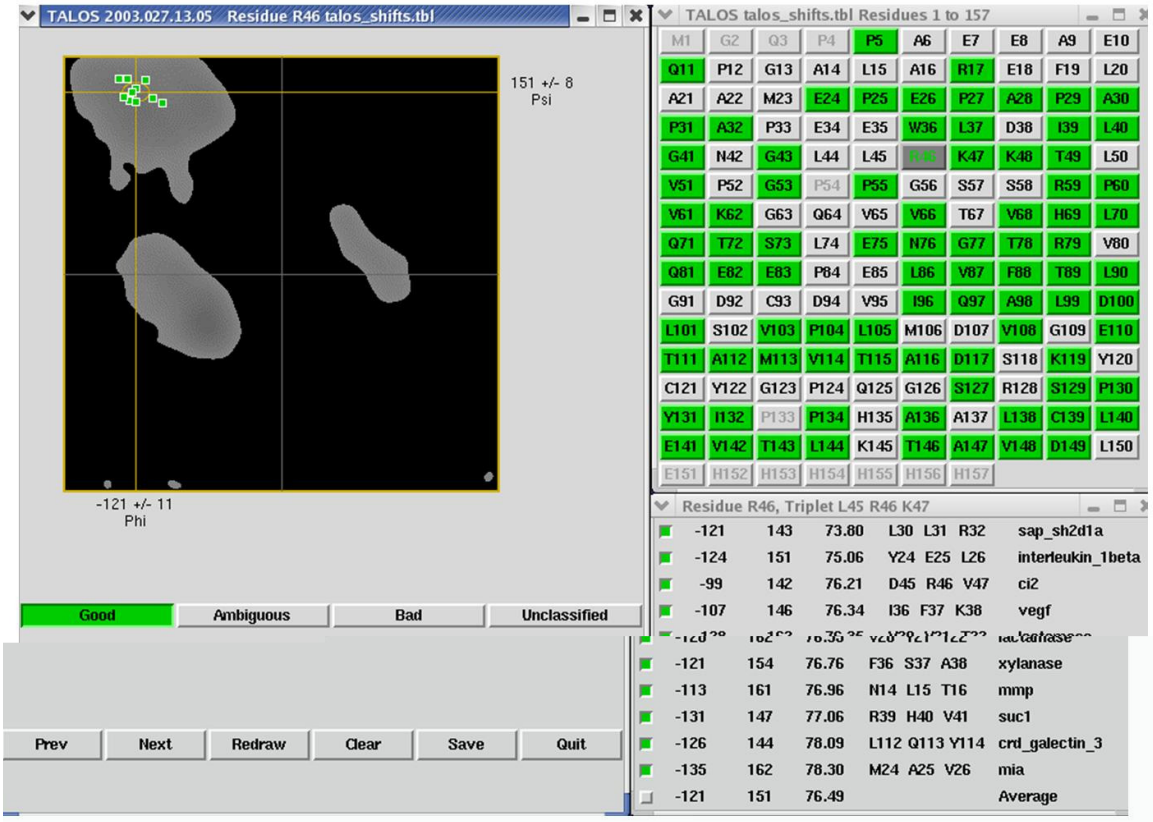

Fig.6.7 Talos analysis of the data

The backbone assignment was completed by using NMRview and the output file for talos analysis was automatically generated by NMRview. The output result was analyzed by using the talos.tcl-in command from talos, and the analyzed result was visualized by using the rama.tcl -in -auto, which is shown in figure. The 'Good' result was indicated in green color. The analyzed data can be converted to the format which can be read by cyana or aria by using the python scripts. The phi and psi angle generated by talos and processed by the python scripts was shown in Table 6.1.

Table 6.1 The PHI and PSI angles from the talos analysis

No	A.A	angle	value	error	No	A.A	angle	value	error	No	A.A	angle	value	error
11	GLN	PHI	-89.7	22.1	66	VAL	PSI	153	20.9	108	VAL	PHI	-61.8	11.8
11	GLN	PSI	131	31.9	67	THR	PHI	-	17.6	108	VAL	PSI	134.7	5.8
15	LEU	PHI	-96	18	67	THR	PSI	141.4	15.4	109	GLY	PHI	96	4
15	LEU	PSI	3	25	68	VAL	PHI	-	15.6	109	GLY	PSI	-14	7
16	ALA	PHI	-66.2	15.8	68	VAL	PSI	157	10.5	110	GLU	PHI	-80.1	18.6
16	ALA	PSI	-27.4	23.1	69	HIS	PHI	-125	7.7	110	GLU	PSI	135.6	12.6
17	ARG	PHI	-84.6	14.3	69	HIS	PSI	132.5	11.1	111	THR	PHI	-	9.9
17	ARG	PSI	-7.7	22.1	70	LEU	PHI	-	10.6	111	THR	PSI	128.7	6.5
24	GLU	PHI	-85	24.1	70	LEU	PSI	128.9	10	112	ALA	PHI	-	12.9
24	GLU	PSI	141.8	19.7	71	GLN	PHI	-	18.9	112	ALA	PSI	135.5	14
25	PRO	PHI	-62	8	71	GLN	PSI	124.3	7.3	113	MET	PHI	-	12.2
25	PRO	PSI	146	11	72	THR	PHI	-	9.6	113	MET	PSI	124.9	8.1
26	GLU	PHI	-86	14	72	THR	PSI	122.8	6.7	114	VAL	PHI	-	7.7
26	GLU	PSI	146	22	73	SER	PHI	-122	13.1	114	VAL	PSI	130.6	9.4
28	ALA	PHI	-93	23	73	SER	PSI	144.2	15.2	115	THR	PHI	-	18
28	ALA	PSI	136.8	31	74	LEU	PHI	-86	15	115	THR	PSI	126.5	8.7
29	PRO	PHI	-58.9	7.5	74	LEU	PSI	147	21	116	ALA	PHI	-	17.5
29	PRO	PSI	147	11.5	75	GLU	PHI	-62.9	3.6	116	ALA	PSI	146.1	14.6
30	ALA	PHI	-91	18	75	GLU	PSI	-23.8	10.1	117	ASP	PHI	-	31.7
30	ALA	PSI	138	26	76	ASN	PHI	-88	9	117	ASP	PSI	129.9	21.3
32	ALA	PHI	-94.8	22.5	76	ASN	PSI	5	9	118	SER	PHI	-59.8	6.8
32	ALA	PSI	135.2	32.6	77	GLY	PHI	87	8	118	SER	PSI	-31.5	9.3
37	LEU	PHI	-102	22	77	GLY	PSI	2	13	119	LYS	PHI	-65.6	5.9
37	LEU	PSI	128.8	14	78	THR	PHI	-78.9	14.8	119	LYS	PSI	-32.4	9.9
38	ASP	PHI	-95.2	18.4	78	THR	PSI	129.8	10.5	127	SER	PHI	-	22.9
38	ASP	PSI	122.7	34.8	79	ARG	PHI	-96	31	127	SER	PSI	144.1	15.2
39	ILE	PHI	-67	16	79	ARG	PSI	128	16	129	SER	PHI	-	29.1
39	ILE	PSI	-29	16	81	GLN	PHI	-	22.4	129	SER	PSI	154.8	14.6
40	LEU	PHI	-96	10	81	GLN	PSI	137.9	20.8	130	PRO	PHI	-70.2	14.2
40	LEU	PSI	4	9	82	GLU	PHI	-112	23.6	130	PRO	PSI	146.7	14.8
45	LEU	PHI	-	17.7	82	GLU	PSI	124.5	15.1	132	ILE	PHI	-	25.9
45	LEU	PSI	120.7	12.4	83	GLU	PHI	-118	23	132	ILE	PSI	129.4	18.4
46	ARG	PHI	-	10.4	83	GLU	PSI	128	17	134	PRO	PHI	-61	6
46	ARG	PSI	134.3	13.1	86	LEU	PHI	-101	11	134	PRO	PSI	148	11
47	LYS	PHI	-	14.8	86	LEU	PSI	113	12	135	HIS	PHI	59	5
47	LYS	PSI	132.9	9.7	87	VAL	PHI	-105	13.7	135	HIS	PSI	39	16
48	LYS	PHI	-	19.3	87	VAL	PSI	126.5	6.9	136	ALA	PHI	-92.5	27.2
48	LYS	PSI	119.8	11.6	88	PHE	PHI	-132	26.1	136	ALA	PSI	131.1	8.8
49	THR	PHI	-91.7	14.2	88	PHE	PSI	135.8	23	138	LEU	PHI	-	23.3
49	THR	PSI	125.6	14.2	89	THR	PHI	-	14.7	138	LEU	PSI	144.5	15.8
51	VAL	PHI	-	24.1	89	THR	PSI	121.8	14.9	139	CYS	PHI	-	12.6
51	VAL	PSI	145.8	14.6	96	ILE	PHI	-81.5	23.8	139	CYS	PSI	121.6	15.9
52	PRO	PHI	-62	7	96	ILE	PSI	153.3	24.7	140	LEU	PHI	-	12.2
52	PRO	PSI	149	11	97	GLN	PHI	-61.8	6.7	140	LEU	PSI	121.3	7.8
55	PRO	PHI	-66	16	97	GLN	PSI	-34.8	12.2	141	GLU	PHI	-	17.3
55	PRO	PSI	136	20	98	ALA	PHI	-62	5	141	GLU	PSI	123.6	10.2
58	SER	PHI	-	19.1	98	ALA	PSI	-28	6	142	VAL	PHI	-	9.2
58	SER	PSI	142.7	23.8	99	LEU	PHI	-85.8	13.1	142	VAL	PSI	122.2	10.1
61	VAL	PHI	-	19.9	99	LEU	PSI	-21.6	19.9	143	THR	PHI	-	14.3
61	VAL	PSI	151.6	20.6	100	ASP	PHI	-63	7.9	143	THR	PSI	121.8	9.3
63	GLY	PHI	95	6	100	ASP	PSI	-32.1	10.3	144	LEU	PHI	-105	19.8
63	GLY	PSI	-16	6	101	LEU	PHI	-76.6	14.2	144	LEU	PSI	114.6	10
64	GLN	PHI	-110	34	101	LEU	PSI	-19.5	14.2	146	THR	PHI	-	18.4
64	GLN	PSI	146	17	103	VAL	PHI	-58	12	146	THR	PSI	158.7	15.5
65	VAL	PHI	-92.3	18.2	103	VAL	PSI	-45	8	147	ALA	PHI	-	22.2
65	VAL	PSI	118.3	8.8	104	PRO	PHI	-68.7	9.2	147	ALA	PSI	147.2	15.2
66	VAL	PHI	-	20.8	104	PRO	PSI	-14	13.4	148	VAL	PHI	-	21.2

The talos analyzed result was processed by python scripts and the result table was obtained.

6.5 Hydrogen bond analysis using NMR

NMR can be used to monitor processes that depend on the protein characteristics. The measurement of the amide proton exchange rates is one of the processes. This kinetic process can tell to which degree the amide protons are protected from exchange with the solvent. Amide protons that are involved in regular secondary structural elements are generally longer lived than those that are present in unstructured parts of a protein.

From this information, the slow amide exchange rate can be used as an evidence for the presence of hydrogen bond. The hydrogen bond is a weak non-covalent interaction to stabilize the protein structure. Groups form hydrogen bonds with NH groups 3 residues along the chain forming a 3_{10} helix. They are called 3_{10} because there are 3 residues per turn and 10 atoms enclosed in a ring formed by each hydrogen bond. Like α-helices, β-sheets have the potential for amphiphilicity with one face polar and the other polar. However, unlike α-helices which are composed of residues from a continuous polypeptide segment (i.e., hydrogen bonds between CO of residue i and NH of residue i+4), beta-sheets are formed from strands with amino acids far away in the polypeptide sequence. In α-helix structure, we can easily see the hydrogen bond between CO_i and NH_{i+4}. While in β-sheet structure, it is difficult to see which HN and CO are in the hydrogen bond. For determination of the identity of the hydrogen bond, more explicit information is needed. NOE can be used for this purpose. In order to identify which amide group participates in the hydrogen bond, the ^{15}N labeled sample was exchanged with 100% D_2O and ^{15}N-HSQC was performed. Because the quick exchange between H^N and deuterium, only the signal from the amino acid whose H^N is involved in the hydrogen bond can be detected. The following figure shows the HSQC spectrum, and we confirmed the amino acids whose

amino protons are engaged in hydrogen bond with CO. Based upon the ^{15}N-HSQC-NOE result and secondary structure prediction, the numbers of hydrogen bonds were confirmed in Fig.6.9 A, which is consistent with the X-ray structure (PDB, 2AWG).

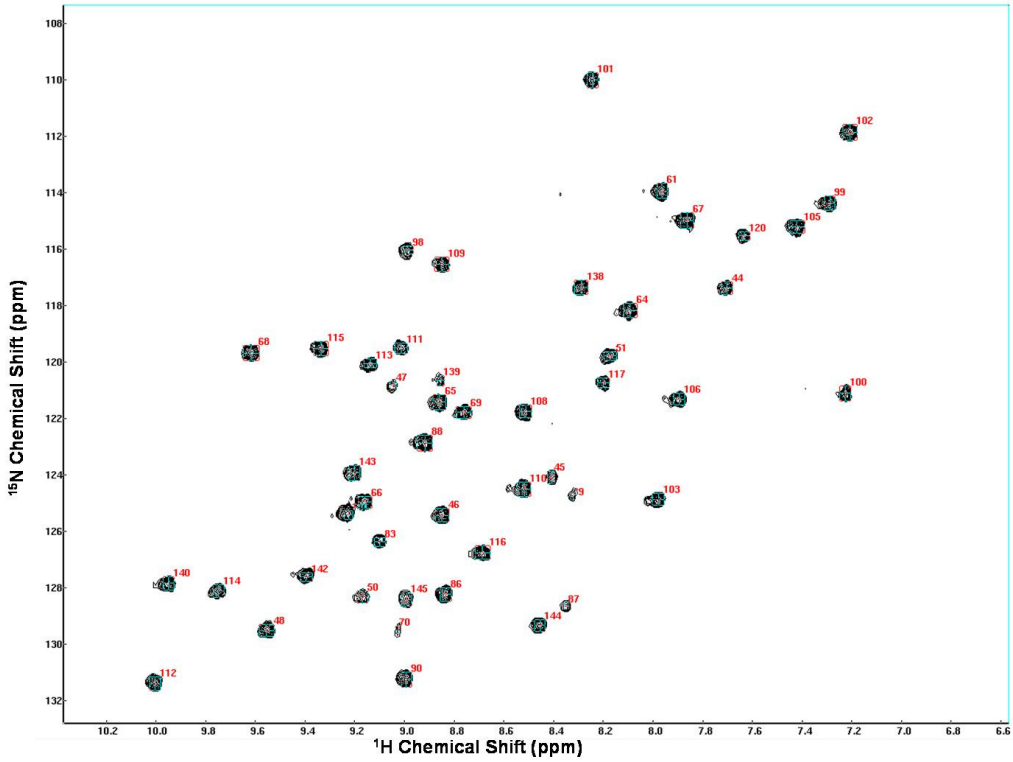

Fig.6.8 Hydrogen bond analysis of NTD of FKBP

The ^{15}N labeled sample was exchanged in 100% D_2O and the ^{15}N HSQC spectrum was recorded. If the amide proton is involved in the hydrogen bond formation, the signal can be detected. So the peaks in this figure are the amino acids that are involved in the hydrogen bond formation. Based upon the backbone assignment result, the peaks are easily identified.

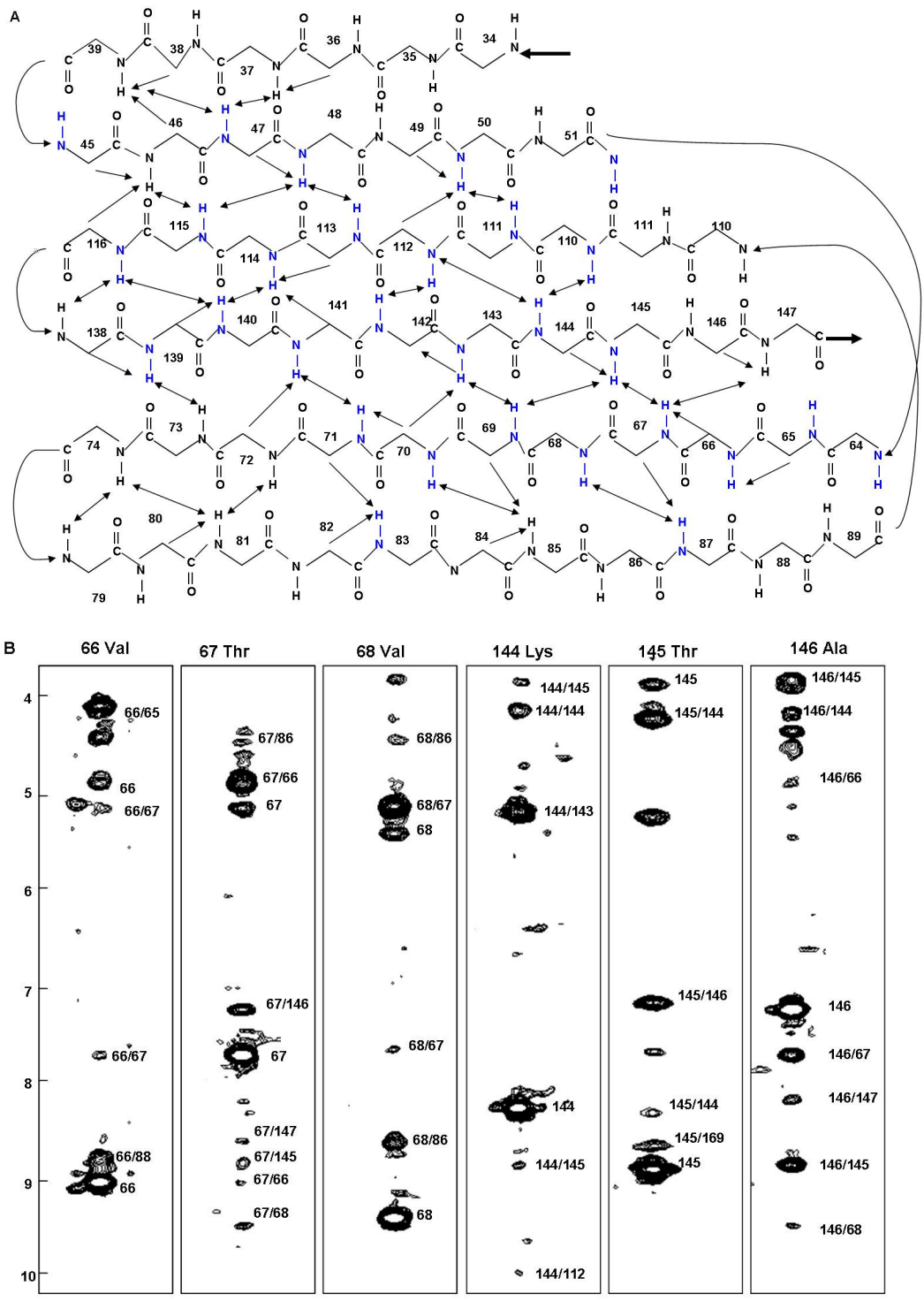

Fig.6.9 The hydrogen bond analysis based upon the H-D exchange and the 3D-^{15}N edited NOESY-HSQC experiment

A shows the NOE between H^N and H^A. The hydrogen bond detected between H and CO was shown in blue. Arrows show the NOE observed. B) NOE cross-peaks. The strips were from ^{15}N-HSQC-NOESY. The number indicates residues showing the NOE between two amino acids.

6.6 NOE analysis of FKBP38NTD

The most important source of structural information is the Nuclear Overhauser Effect (NOE). In a description, assuming a more or less rigid protein molecule that rapidly tumbles in solution, the initial buildup rate of the NOE between a pair of spins depends on the inverse sixth power of the distance between two spins: $I_{NOE} \propto 1/r^6$. The rapid decrease of the NOE intensity with increasing distances makes that a proton-proton NOE is in practice only observable for protons that are closer than 0.5 nm. If a sufficient number of atom-pair distances are known for a certain protein molecule, these distance can be used to build a three dimensional model. The reason is that information from NOEs between protons that are far apart on the primary sequence (also called long range NOE) strongly reduces the number of possible 3D conformations, these long range NOEs are very important for the determination of the global fold of the polypeptide chain. Several sets of NOE experiments were collected for FKBP38NTD.

The 2D-NOE in water or D_2O with different mixing time (80 ms, 100 ms, 150 ms) which are also important for assignment and structure calculation were collected shown in Fig.6.13. For the ^{13}C and ^{15}N double labeled sample in D_2O, the ^{15}N-HSQC-NOE and ^{15}N, ^{13}C simultaneous NOE were collected and some of the strips of ^{15}N-HSQC-NOE were shown in Fig.6.9 for the hydrogen bond determination. ^{13}C-HMQC-NOE and ^{13}C-HMQC-aromatic-NOE were collected and processed with nmrPipe which are shown in Fig.6.10 and Fig.6.11.

All these NOEs are very important for structure calculation. The peaks in the spectrum were picked and assigned in NMRView. The peaklist was analyzed by either ARIA or CYANA for structure calculation (Guntert, 2003 and 1997, Herrmann *et al.*, 2002).

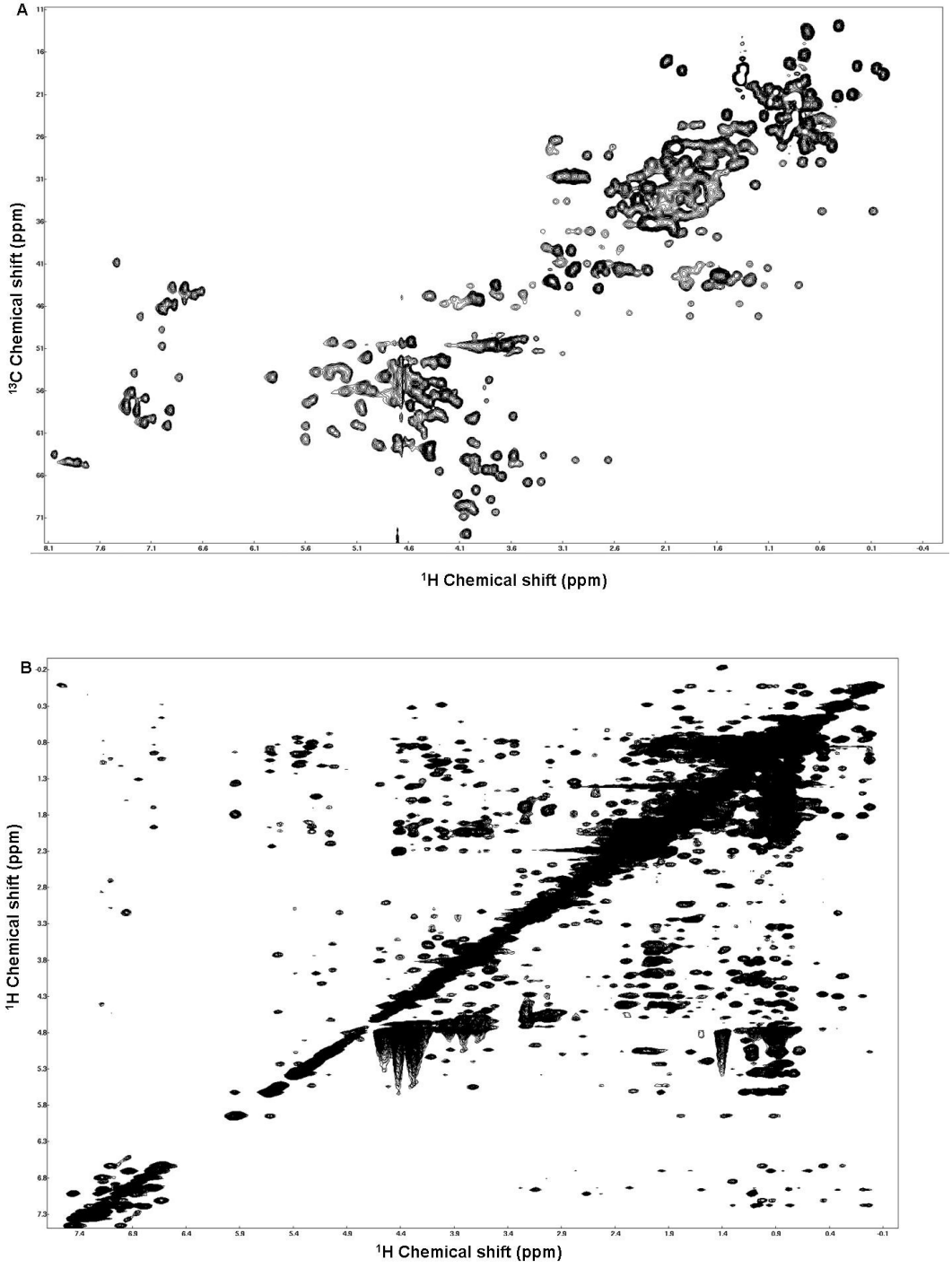

Fig.6.10 ^{13}C NOE of FKBP38NTD

A) ^{13}C-HSQC spectrum. The ^{13}C-HSQC was recorded using program provided by Dr. Sattler and Dr. Simon. The spectrum is same as the ^{13}C-^{1}H dimension of ^{13}C-HMQC-NOESY. B) The ^{1}H and ^{1}H dimension of ^{13}C-HMQC-NOESY.

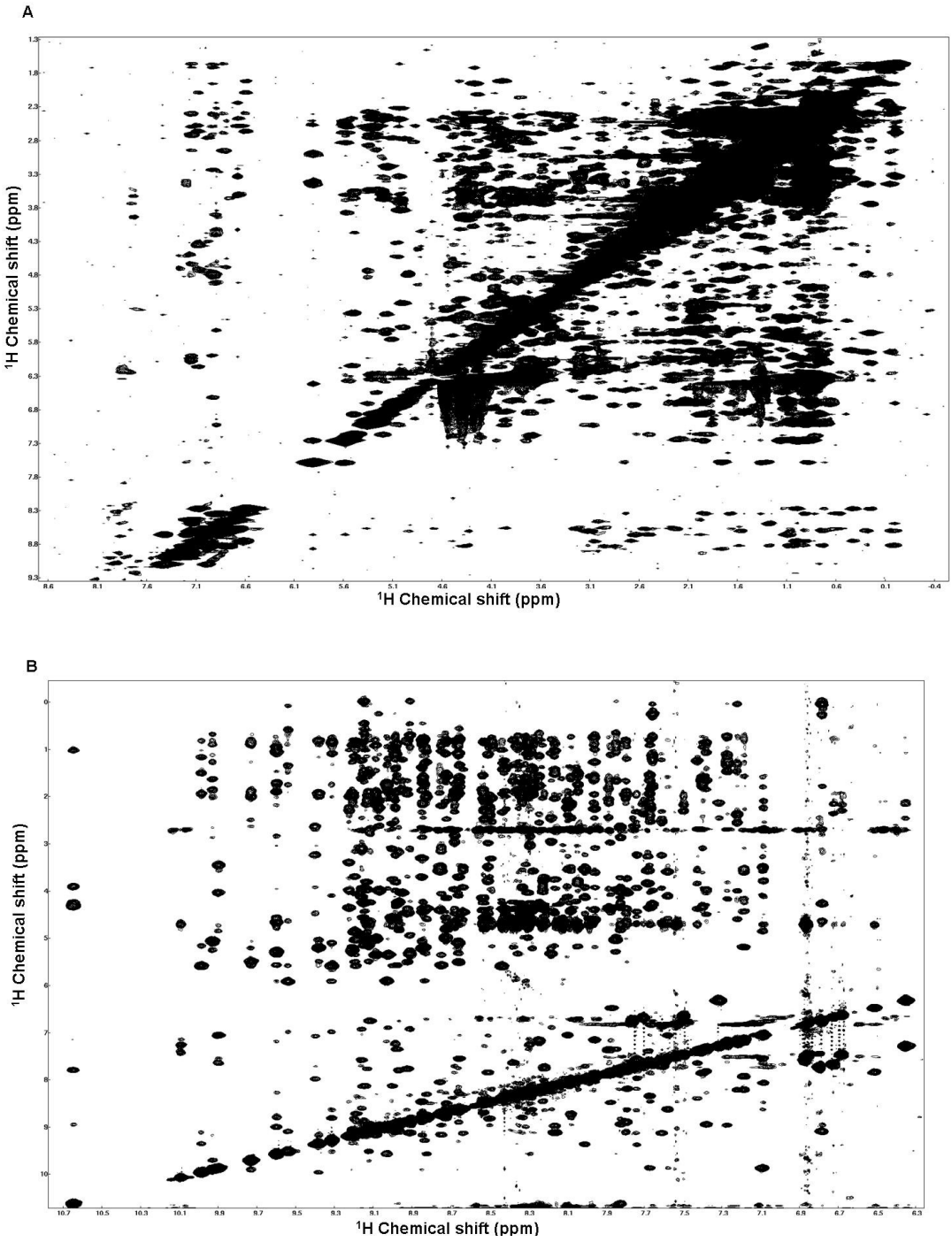

Fig.6.11 ^{13}C-HMQC-aromatic NOESY and ^{15}N-HSQC-NOESY

The ^{13}C and ^{15}N doublely uniformly labeled protein was used for ^{13}C-aromatic NOE (A) and ^{15}N-edited NOESY-HSQC (B). Data were processed by nmrPipe and visualized in NMRView. The overlaid spectra were shown.

6.7 RDC experiment

Dipolar coupling is the result of direct interaction of the magnetic dipoles through space. It is quite a strong interaction, but in general, if a protein molecule tumbles rapidly and isotropically in solution, the dipolar coupling interaction averages out to zero. However, if the protein molecules can be slightly oriented in a magnetic field, for example, using a liquid crystalline medium that orients itself with regard to the magnetic field, the interaction does not average out to zero, and the residual dipolar couplings (RDC) can be observed as a difference in the splitting of resonances, compared with the isotropic case. The observed coupling contains very useful information, because their size depends on the distance between the nuclei, as well as on the average orientation with regards to a common global reference frame. This reference frame is determined by the average orientation of the molecule in the magnetic field. In our study, the RDC will be used for the structure validation. The filamentous phage Pf1 was used as medium for the RDC measurement (Simon *et al.*, 2002).

Filamentous phage Pf1 is a 7,349-nucleotide DNA-phage in which the circular DNA is packaged with coat protein at a 1:1 (nucleotide:coat protein) ratio. The Pf1 phages form rods of ca 20,000 Å length and 60 Å diameter and spontaneously align by their intrinsic diamagnetic susceptibility in the magnetic field (Zweckstetter *et al.*, 2004). Pf1-Phages can be grown in *Pseudomonas aeruginosa* and are commercially available. Phages have a net negative surface charge and bimolecular are therefore mainly aligned via electrostatic interactions (Zweckstetter and Bax, 2001). The pH-values of the buffer recommended originally are 6.5-8.0 and NaCl-concentrations below 100 mM (Hansen *et al.*, 1998). The spectra in the presence and absence of phage were recorded and processed by nmrPipe and visualized by NMRview. The

RDC value of each amino acid is shown in Fig.6.12 and Fig.6.13.

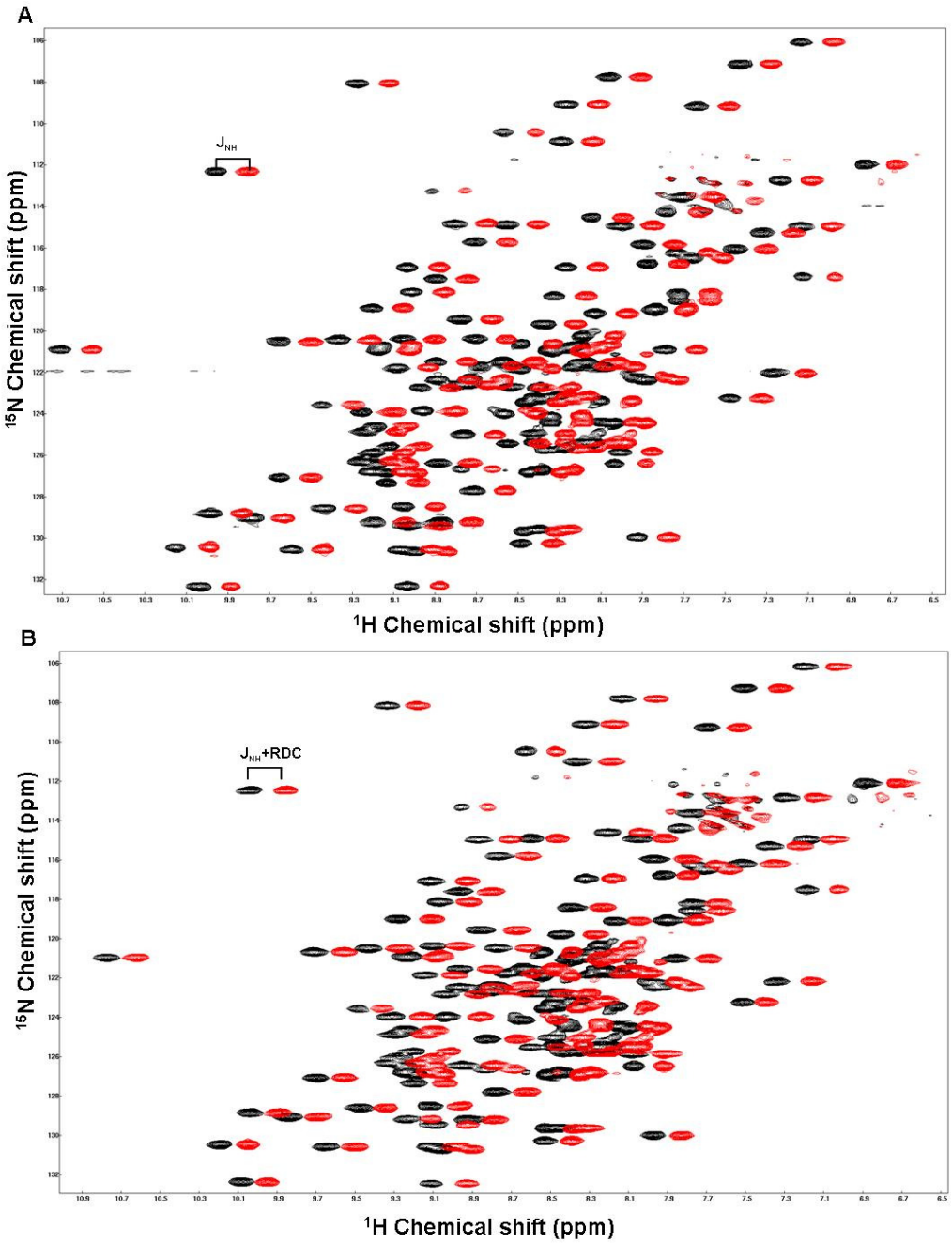

Fig.6.12 RDC analysis of FKBP38NTD

The ^{15}N-IPAP-HSQC experiments were performed using uniformly ^{15}N labeled sample. Pf1 phage was used as medium. A is spectrum without phage as reference so the splitting value is J_{HN} which is about 90 Hz. B is spectrum with the phage and the splitting of two peaks is equal to J_{HN} + RDC. By comparing the slitting value of each amino acid, RDC can be determined. All the experiments were run at 30 °C.

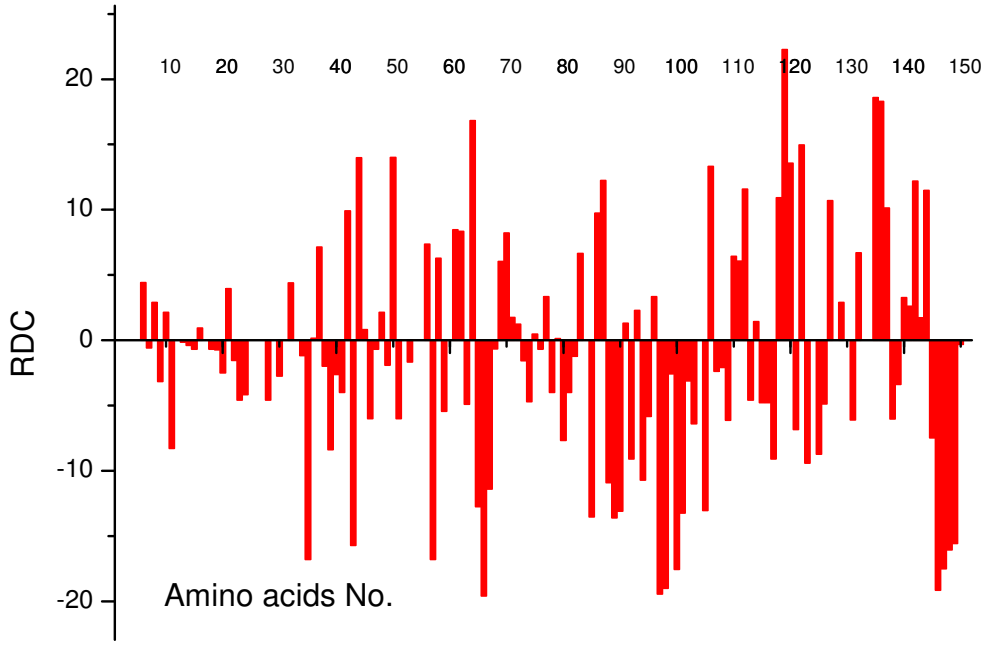

Fig.6.13 The RDC value of each amino acid

The RDC value was obtained by analyzing the data using NMRview. The value was input to Origin 6.0 and the figure was obtained.

6.8 solution structure of FKBPNTD

Protein structures were determined based on a total of more than 2000 nontrivial distance constraints. The ensemble of 10 low-energy structures calculated with the program CNS is shown in Fig.6.14. Excluding the flexible loop between β2 and β3 (residues 52-60), the five-N-terminal residues, and eight C-terminal residues containing Leu, Glu and a hexahistidine-tag, the root-mean-square deviation (RMSD) for the FKBPNTD was 1.52±0.15 Å for the backbone and 2.18±0.13 Å for all heavy atoms, indicating that the backbone conformation of FKBPNTD is defined. Analysis of the average-minimized structures with the program PROCHECK (Laskowski *et al.*,

1993) showed that 58.6% of residues of FKBPNTD lie in the most favored region of the Ramachandran plot and 30.5% in the allowed regions.

The N-terminal domain of FKBP38 consists of 5-stranded anti-parallel β-sheet wrapped around a central amphipathic α-helix. The central helix packs against the hydrophobic surface of the β-sheet and a short helix is located at the bottom of the hydrophobic cavity (Fig.6.14). NMR structure showed that the loops (residues 52-60) and (residues 122-137) are flexible. The residue Tyr-26, Phe-46, Val-55, I56, Trp-59, and Phe-99 in FKBP12 contribute to the formation of the hydrophobic pocket in FKBP12 and are important for the interaction with FK506 (Van Duyne *et al*., 1991). A sequence comparison revealed the substitutions of Try-26, Phe-46, Trp-59, Phe-99 in FKBP12 to Leu-70, Leu-86, Leu-99, L-140, which are corresponding residues in FKBP38. These residue differences are highlighted in Fig. 6.15. The ligand-binding surface of FKBP38 is similar to that of FKBP12. However, the hydrophobic packing and interactions in the region could be unfavorably influenced by the multiple substitutions of the aromatic residues in FKBP12 to Leu in FKBP38, probably due to the property of Leucine providing a smaller van der Waal surface than those aromatic residues. This difference in the ligand binding pocket was demonstrated by NMR-based binding studies showing that no apparent spectral changes were detected in ^{15}N-HSQC spectrum of the FKBPNTD while chemical shifts perturbations were observed in the ^{15}N-HSQC spectrum of FKBP12 upon the addition of FK-506 (Kang *et al*., 2005). FKBP38 and FKBP51 and FKBP52 contain extra N-terminal tails (Li *et al*., Sinars *et al*., 2003), which are not found in other FKBP family proteins. In X-ray structures of FKBP51 and 52, the information on the N-terminal regions (residues 1-32 in FKBP51; residues 1-20 in FKBP52) is missing (Li *et al*., Sinars *et al*., 2003). Clearly, our NMR data indicate that there are a number of inter-residue NOEs for this

N-terminal region of FKBP38, suggesting that the tail is not free but involved in molecular interactions with other residues. In fact, long-range NOE analysis reveals that the residues in the N-terminal tail (Leu20, Ala21, Ala22, and Met23) show specific NOE connections with Leu90, Gly91, and Asp92 in the loop β4/α1, and Gln97 in the helix α1. The flanking N-terminal tail runs across the top of the hydrophobic patch and is aligned close to the loop (residues 52-60) connecting β1 and β2, and the region containing residues 23-32 folds back and wraps around the top of the hydrophobic pocket.

The NMR structure is compared with previously published X-ray structure of FKBP12, the prototype in the FKBP family and the FK2 domain of FKBP51 (Fig.6.18). Overall FKBPNTD showed similar structural folds with the backbone RMSD between FKBPNTD (residue 3-149) and FKBP12 of 1.83 Å and FKBPNTD and the FK2 of FKBP51 of 1.6 Å (excluding flexible loops). Difference between FKBPNTD and FKBP12 was observed in the regions of helix 1, the loops connecting β2/β3, β4/α1 and α2/β6. The 40s loop, which comprises residues 40-44 in FKBP12 and forms a beta-bulge, critical for its function, is altered in FKBP38. In FKBP38 the corresponding strand forms a short beta-bulge with only two residues Pro-84 and Glu-85. Another difference was observed in 80s loop in FKBP38 introduced the insertion of Arg-128 and substitution of Ile-91 of FKBP12 to Try-131 in FKBP38. Recent X-ray structure reveals that the peptide backbone of this loop closes in on the active site by about 1.2 Å, moving the hydroxyl group of Tyr122 much closer to the putative proline binding site. Arg128 in the loop projects into and partially occludes the active site and the epsilon nitrogen of Arg127 connects to the carboxyl oxygen of Glu83 via hydrogen bonds with two water molecules (Sirano Dhe-paganon, personal communication).

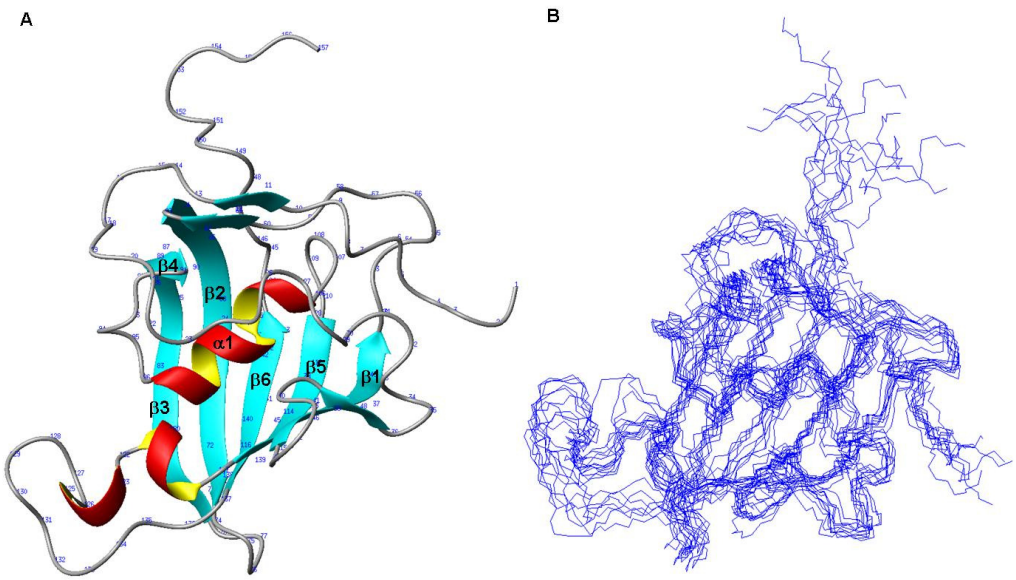

Fig.6.14 Solution structure of NTD of FKBP38 and comparison with other FKBP family proteins

A) The solution structure of FKBP38NTD. Ribbon diagram displays the secondary structure elements, which is shown in different color. B) The C^{α} traces of 10 selected structures visualized in Molmol.

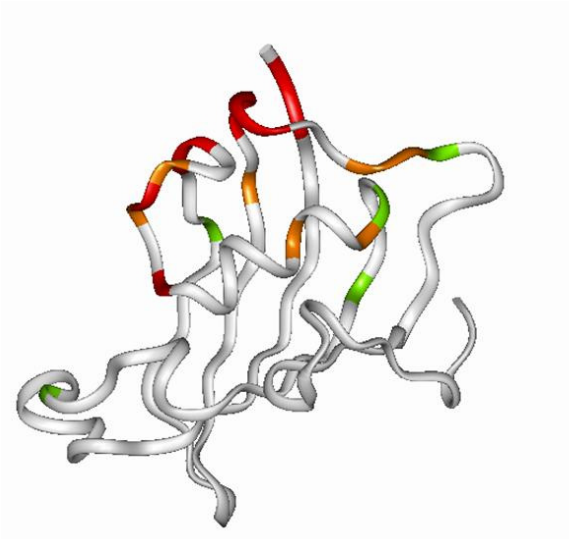

Fig.6.17 Ribbon representation of binding interface between FK-506 binding domain and the N-terminal tail of FKBP38

Amino acids perturbed upon removal of the N-terminal tail are shown in color.

Table 6.2 Summary of the top 10 FKBP38NTD NMR structures

Number of NOE derived distance restrains	2834
Intra-residual (i=j)	864
Sequential (|i-j|=1)	677
Medium-range(1<|i-j|<5)	397
Long-range (|i-j|>4)	896
Dihedral angle restraints	158
Hydrogen bond restrains	42
Total number of restraint violations >Å	124
Maximal restraint violations (Å) for top 10 structures	5.26
Total number of dihedral angle violations>5°	61
Maximal dihedral angel violation (°)	5
Ramachandran plot (%)	
Most favored regions	58.6%
Additionally allowed regions	30.5%
Generously allowed regions	8.7%
Disallowed regions	2.2%
Backbone atom RMSD (Å) for top 10 structures	
Secondary structure	0.42±0.05
All residues	1.86±0.15
Heavy atom RMSD (Å) for top 10 structures	
Secondary structure	0.87±0.09
All residues	2.39±0.13
Backbone atom RMSD (Å) for top 10 structures	
Residues 5-149	1.52±0.23
Residues 5-117	1.58±0.25
Residues 36-149	1.55±0.22
Heavy atom RMSD (Å) for top 10 structures	
Residues 5-149	2.18±0.28
Residues 5-117	2.24±0.30
Residues 36-149	1.79±0.21

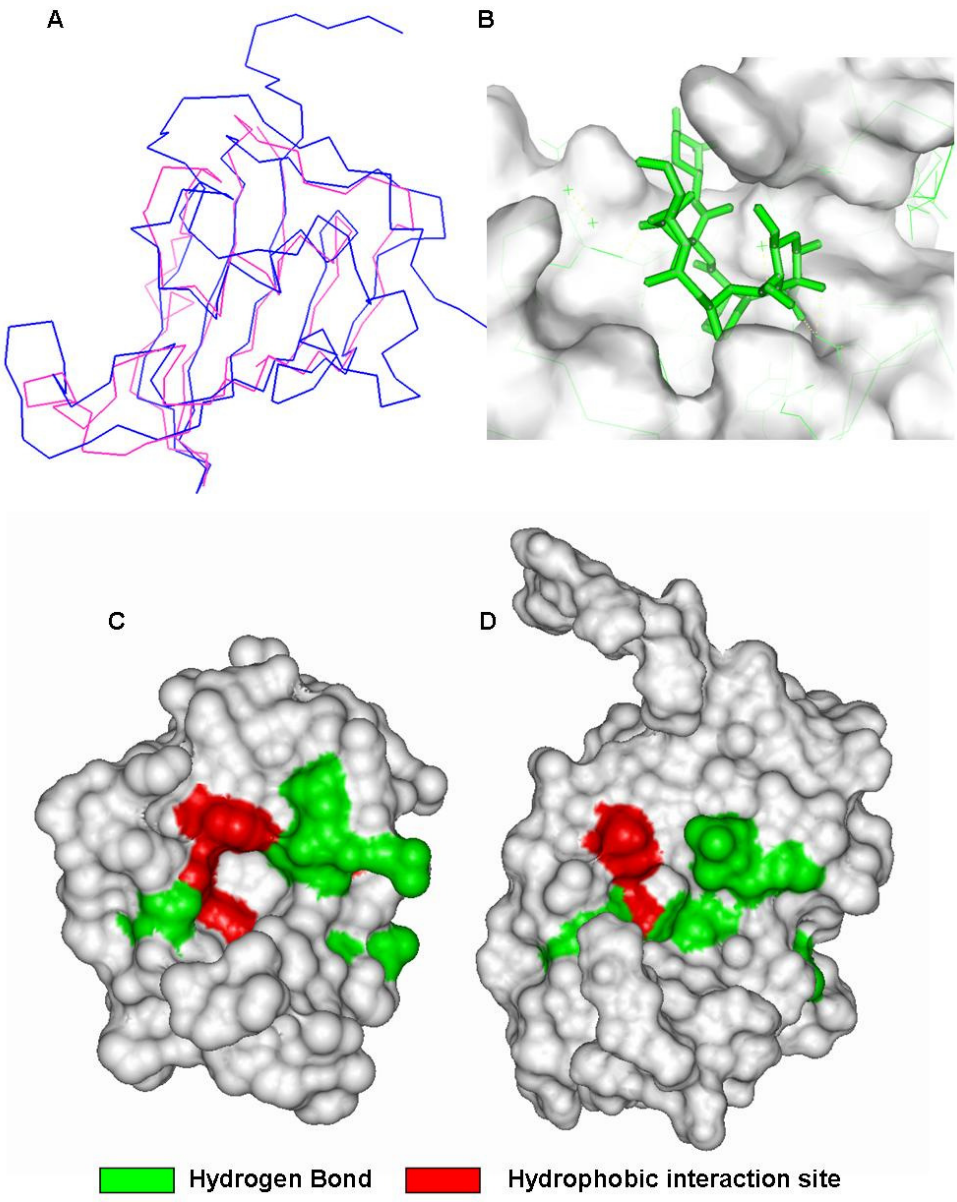

Fig.6.15 Comparison of the FK-506 binding site in FKBP38NTD and FKBP12

A) Comparison of FKBP38NTD with FKBP38. FKBP12 is shown in pink; FKBP38NTD is shown in blue. B) The comparison between FK506 binding site in FKBP12 and that in FKBP38NTD. Surface is the FKBPNTD binding surface. The FK506 and the FKBP12 are shown in green. C) The binding surface for FK-506. D) The binding surface in FKBP38NTD was compared with that of the FKBP12. The amino acids involved in hydrogen bond formation were shown in green. The amino acids which interact with FK-506 by hydrophobic interaction are shown in red.

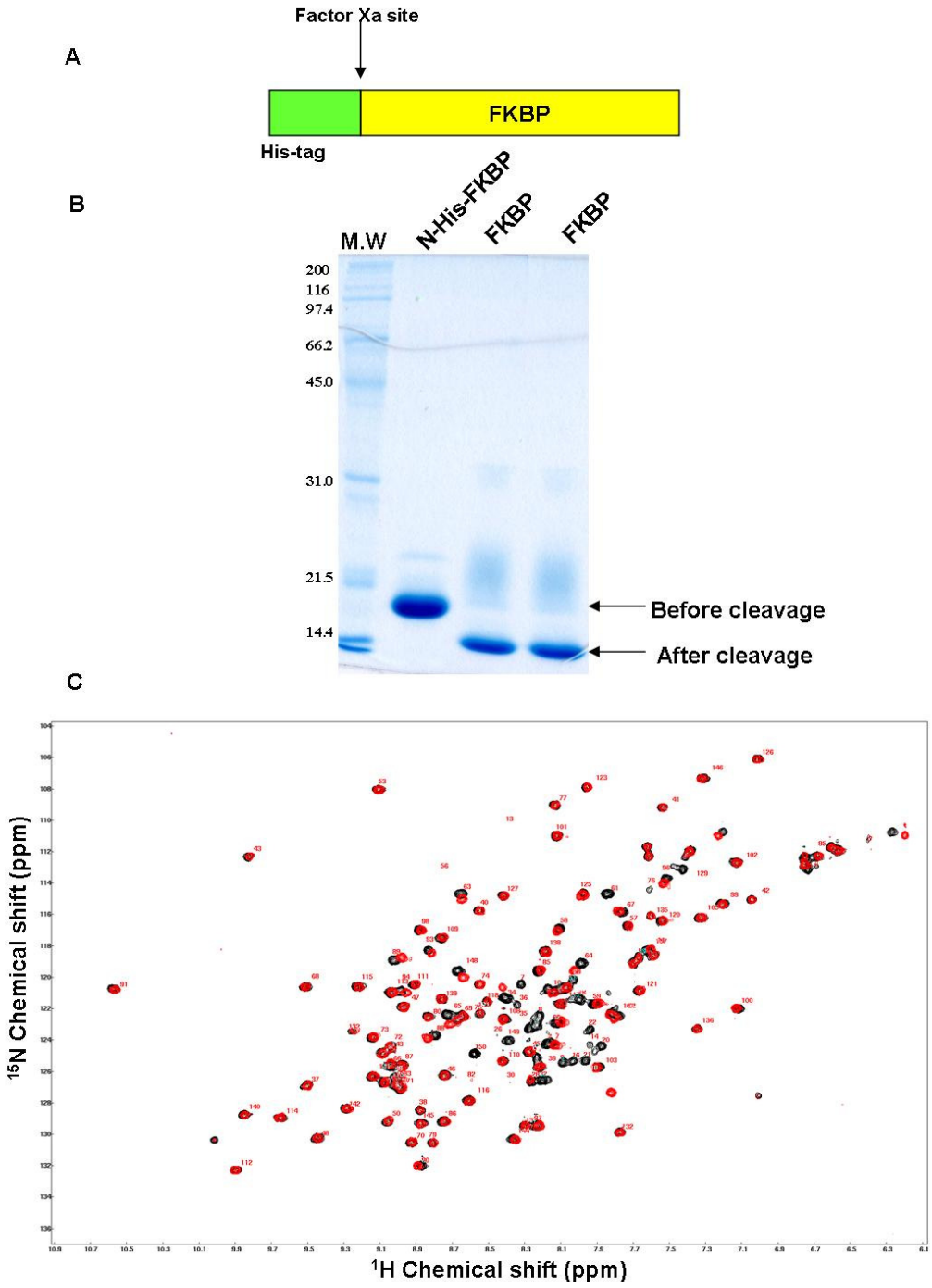

Fig.6.16 ^{15}N-HSQC spectra of FK-506 binding domain of FKBP38 and FKBPNTD

A) The diagram shows the construct of N-His fusion FKBP protein. B) The fusion protein was purified and analyzed by SDS-PAGE, the protein after factor Xa cleavage was also shown in the SDS-PAGE. C) ^{15}N HSQC spectrum of FKBP domain of FKBP38. The N-His fusion FKBP was digested with factor Xa. The factor Xa and cleaved His-tag were removed by resin and changed into the same buffer as that of FKBPNTD. The NMR spectrum was recorded under the same condition as that of FKBP38NTD.

6.9 Molecular regulation of FKBP38NTD

6.9.1 Molecular interaction between FKBP38NTD and Bcl-2

It was found that FKBP38 could interact with Bcl-2 and the FK-506 binding domain was important for the interaction. FKBP51 and 52, which are FKBP family members with multiple TPR-containing domains, contain tandem FK-506 binding domains (FK1 and FK2 domains, respectively). Only FK1 domains of them exhibit PPIase activities. It is particularly interesting to observe that the aromatic residues, which are important for the hydrophobic cavity in the active site, are conserved in the FK2 domains of FKBP51and FKBP52. The FK2 domains of FKBP51 and FKBP52 were shown to lack PPIase activity, but they were shown to be involved in associating with progesterone receptor (PR) and Hsp 90 (Sinars *et al*., 2003), respectively. It was suggested that FKBP38NTD, which contains FK-506 binding domain, had no molecular interaction with FK-506 (Kang *et al*., 2005). Rather it was shown that FKBP38 forming a complex with Ca^{2+}/calmodulin was able to interact with Bcl-2 reversibly and competitively and the binding of Ca^{2+}/calmodulin inhibited the enzyme activity of FKBP38, indicating the involvement of the active site of FKBP38 in the molecular interaction with Bcl-2 (Edlich *et al*., 2005). Recently, it was also reported that the interaction of presenilins 1 and 2 with FKBP38 promotes apoptosis by depleting the mitochondrial Bcl-2 (Wang *et al.*, 2005). In recent years, those accumulating data appear to suggest that FKBP38 may be important in protein-protein interaction and provide a critical role in modulating function of target proteins. The binding of FKBP38 to Bcl-2 was measured (Kang *et al.*, 2005). However, we were unable to probe the molecular interaction in our NMR binding assay using the same full-length Bcl-2 and FKBP38NTD, since the addition of the flexible loop-intact wild-type Bcl-2 caused the aggregation of proteins in NMR tubes. Bcl-2 contains a flexible

loop between the first and the second helix. It was demonstrated that the loop is important for the interaction with FKBP38 and within the loop the phosphorylation sites appear to be involved in the molecular interaction (Kang *et al*., 2005). Thus, to avoid the aggregation problem when titrating with the full length and also to examine the molecular interaction with Bcl-2, the S87 peptide, which contains the residues from Gly-83 to Val-92 in the flexible loop of Bcl-2, was used in our NMR-based binding study. In the presence of the peptide, chemical shifts perturbations in a 2D ^{1}H, ^{15}N-HSQC spectra were detected. The shift residues were Leu-50, Leu-70, Val-142, Val-80, Val-68, Asp-85, Cys-93, Gly-91, Thr-89, Val-61, Val-65, Asp- -57, Val-61, Thr-67, Val-68, Asp-94 and Gln-125 (Fig.6.19).

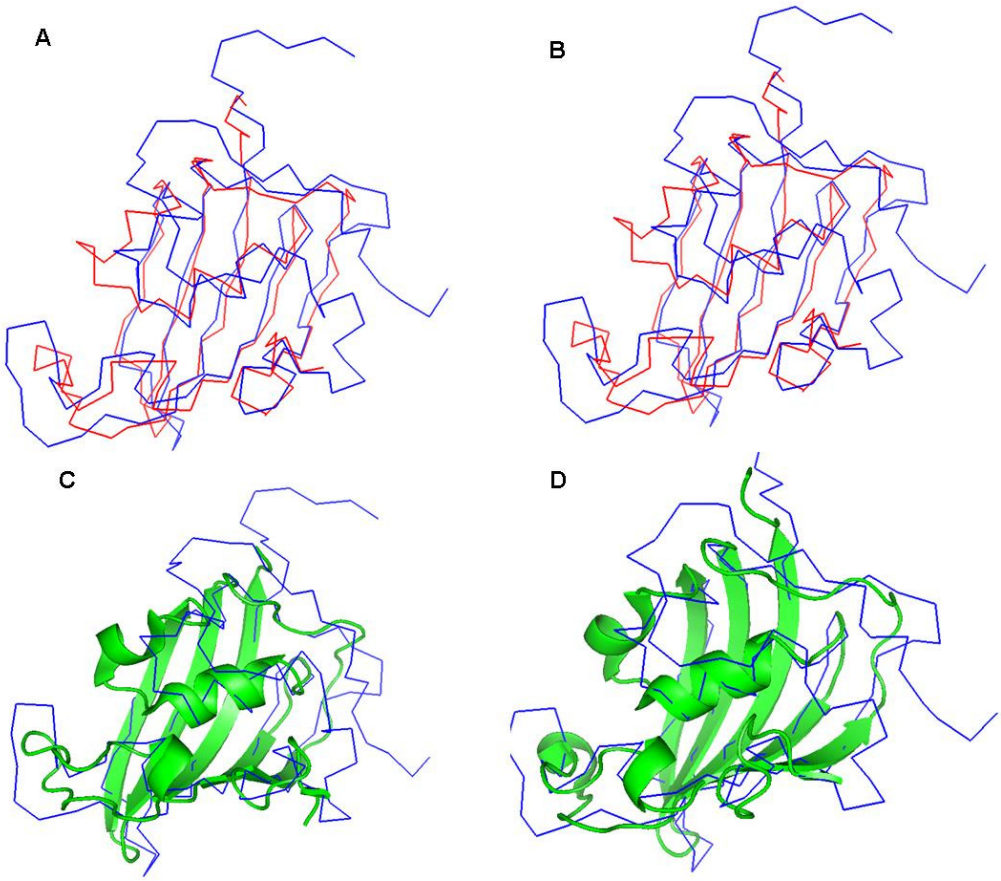

Fig.6.18 Comparision of FKBP38NTD with FKBP51-FK2 and FKBP52-FK2

A, C) Comparison of FKBP38NTD with FKBP51-FK2. FKBPNTD is shown in blue; FKBP51-FK2 is shown in red and green. B, D) Comparison of FKBP38NTD with FKBP52-FK2. FKBPNTD is shown

in blue; FKBP52-FK2 is shown in red and green.

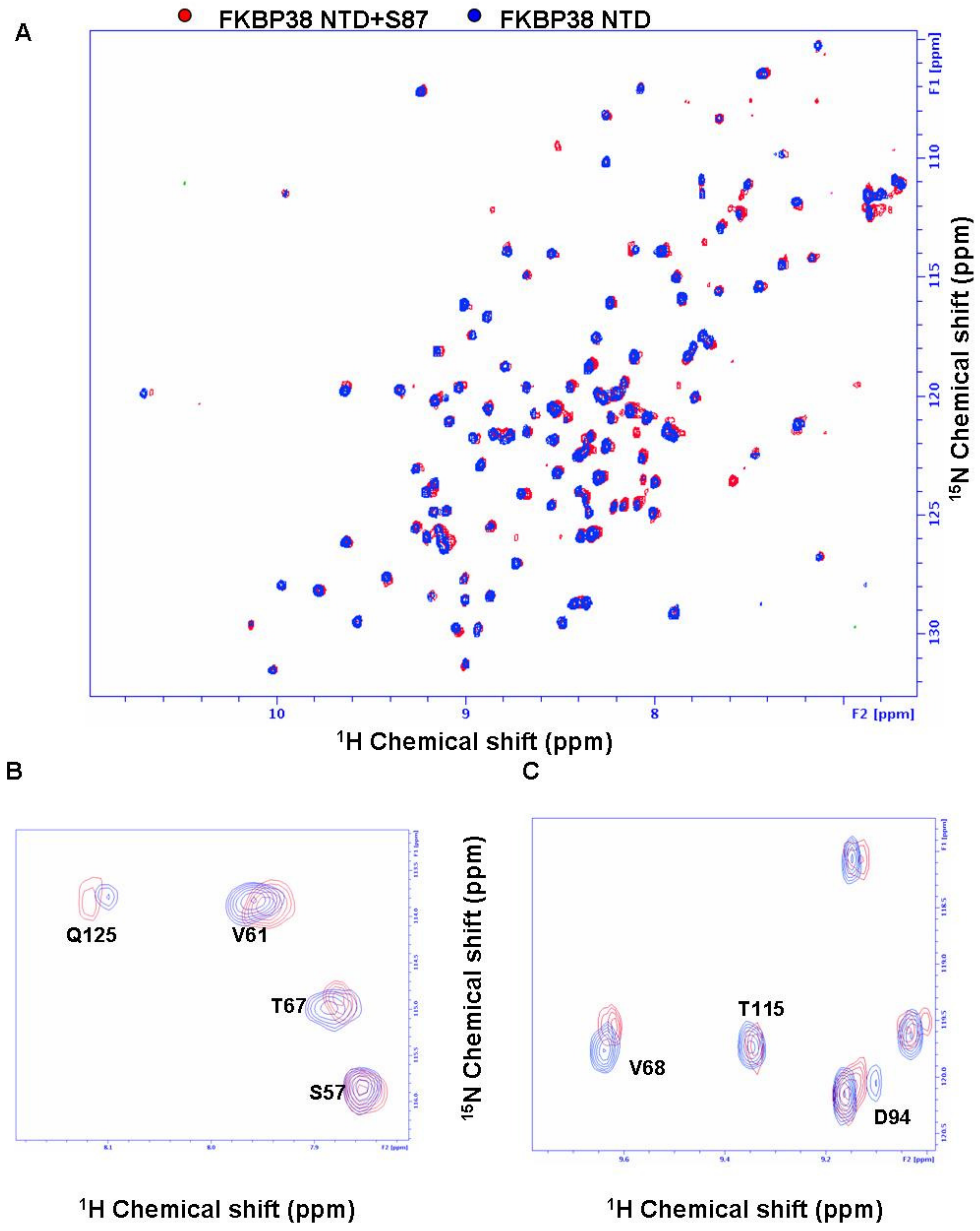

Fig.6.19 Titration of NTD with S87

A) Overlay of the spectra of NTD in the presence (red) and absence (blue) of S87. Dried S87 peptide was added into 0.1 mM NTD to a final concentration of 1.5 mM. The chemical shift change was shown in the figure. B) Section of a ^{15}N-HSQC spectrum of FKBP38NTD in the presence of 1.5 mM peptide. C) Overlay of spectra in the presence (red) and absence (blue) of the S87 (1.5 mM).

6.9.2 NTD of FKBP38 shows interaction with its calmodulin binding domain (CBD)

FKBP38 was reported to have a calmodulin dependent PPIase activity and FK-506 binding activity. In this study, to investigate the molecular mechanisms of FKBP38 with calmodulin, the FKBP-CBD (Fig.6.20), which contains the FKBP38NTD and the CBD domains of FKBP38, was constructed and the protein was uniformly ^{15}N labeled. The ^{15}N-HSQC spectrum was compared with that of the FKBP38NTD (Fig.6.22 A). The chemical shifts of some amino acids were changed, indicating the CBD domain of FKBP38 interacts with NTD. The amino acids which have chemical shift change are probably involved in the binding interface. Based upon the X-ray structures of FKBP51 and FKBP52 which contain the CBD domain, there is no indication of the interaction between CBD and the FKBP domains. The interaction we observed here between the CBD and the NTD might provide a novel mechanism in the regulation of FKBP38 by calmodulin.

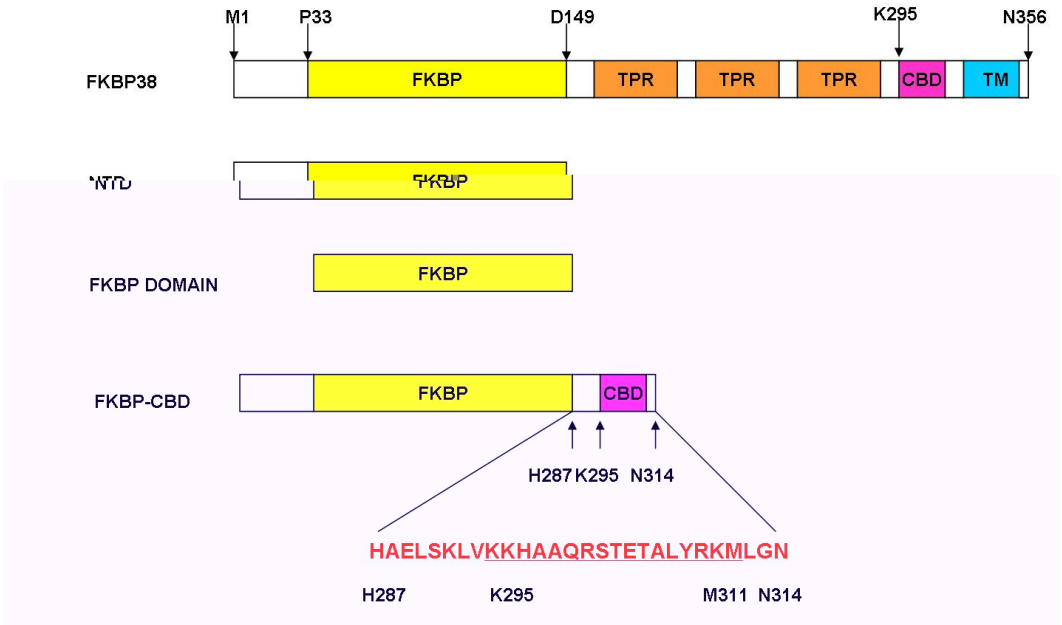

Fig.6.20 The diagram of the FKBP constructs in this chapter

6.9.3 NTD shows molecular interaction with the peptide from CBD

To further confirm the interaction between NTD and the CBD domain, the 17 mer peptide of the CBD domain was synthesized and the titration between FKBPNTD and the peptide was performed (Fig.6.21). Consistent with the FKBP-CBD, the chemical shifts changes of some amino acids were seen and shown in Fig.6.20 (B, C) and Fig.6.22. The results indicate that there is the interaction between FKBPNTD and CBD.

It was shown that the interaction between FKBP38 and calmodulin could change the conformation of FKBP38 (Edlich *et al*., 2005). Here, it was shown that the CBD is predicted to be important for the interaction between FKBP38 and calmodulin. Before we confirmed the interaction between CBD and calmodulin, the interaction between FKBP38NTD and calmodulin was checked. The results indicated that there is no interaction between FKBP38NTD and calmodulin (Fig.6.24). The ^{15}N uniformly labeled calmodulin was also titrated with FKBP38NTD, the same result was observed, confirming no molecular interaction between calmodulin and FKBP38NTD.

From the results obtained, it is clear that there is no interaction between the NTD and calmodulin, while the CBD of FKBP38 has interaction with the NTD. It was shown that FKBP38 and calmodulin can form complex (Edlich *et al*., 2005) and the CBD of FKBP38 is the predicted binding site for calmodulin (Shirane *et al.*, 2003, Edlich *et al*., 2005, Lam *et al*., 1995). Our NMR data confirmed the molecular interaction between FKBPNTD and its own calmodulin binding domain.

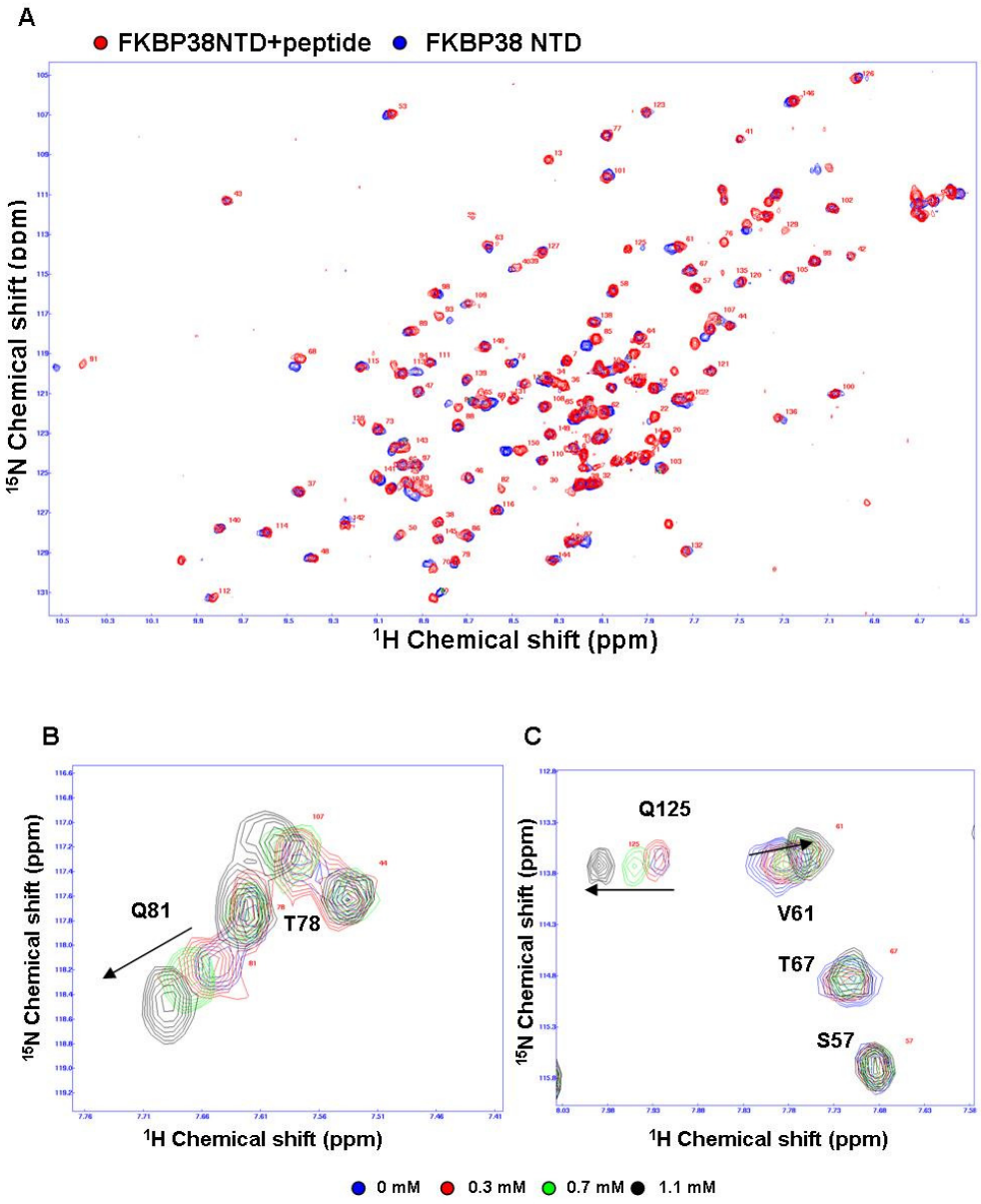

Fig.6.22 Titration of FKBPNTD with peptide from CBD of FKBP38

A) Overlay of the spectra of NTD (0.1 mM) in the presence (red) and absence of peptide. ^{15}N uniformly labeled NTD was titrated with peptide as described in the material and methods. Assigned amino acids were shown. B, C) The chemical shift changes with different concentration of peptide. The arrow indicates the direction of the peak change after peptide was added. The final peptide concentration was indicated in the figure. Affected amino acids were labeled with name and sequential number. All the spectra were recorded at 303 K.

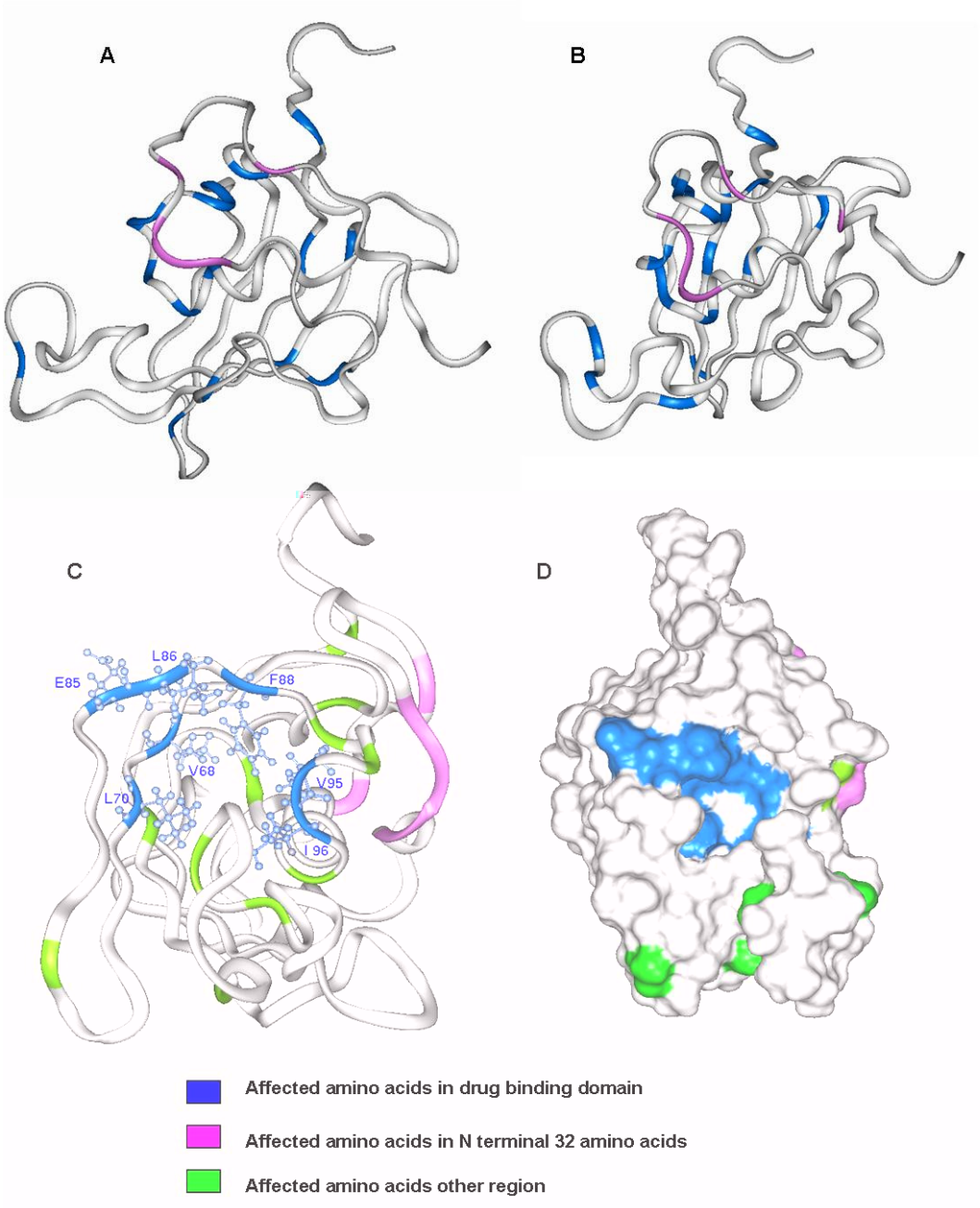

Fig.6.23 Comparision of the binding sites

A) The amino acids affected in the FKBP-CBD fusion. B) The amino acids affected in the FKBPNTD titration with CBD peptide. C) The amino acids affected in both A and B. The hydrophobic amino acids were shown in ball and stick format. D) The predicted binding surface in the FKBP38NTD. Blue color, the affected amino acids in the drug binding domain. Pink color, the affected amino acids in the N-terminal 32 amino acids. Green color, the affected amino acids in other parts.

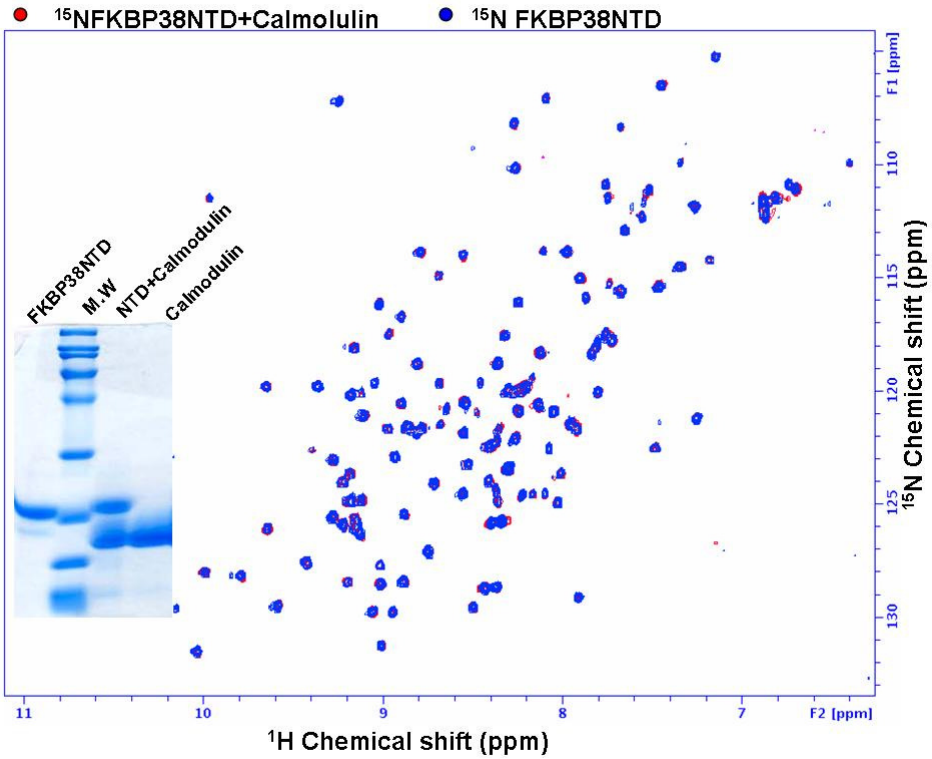

Fig.6.24 Interaction between NTD and calmodulin

The overlaid spectra with and without calmodulin were shown. NTD was uniformly labeled with ^{15}N and the calmodulin was added. More calmodulin was added into the ^{15}N labeled NTD which is shown in the SDS-PAGE.

6.9.4 CBD of FKBP38 interaction with calmodulin

The titration study between the peptide and calmodulin was performed to check if there is any interaction between CBD domain and calmodulin. It is very clear to see the interaction between calmodulin and the peptide in the presence or absence of Ca^{2+} (Fig.6.25), which confirmed that the calmodulin can interact with the CBD domain. Since no interaction between calmodulin and NTD was observed, this result suggests that the CBD of FKBP38 might be important in the biological function of FKBP38 through modulating molecular interaction with calmodulin which shows diverse activities in calcium-dependent signaling.

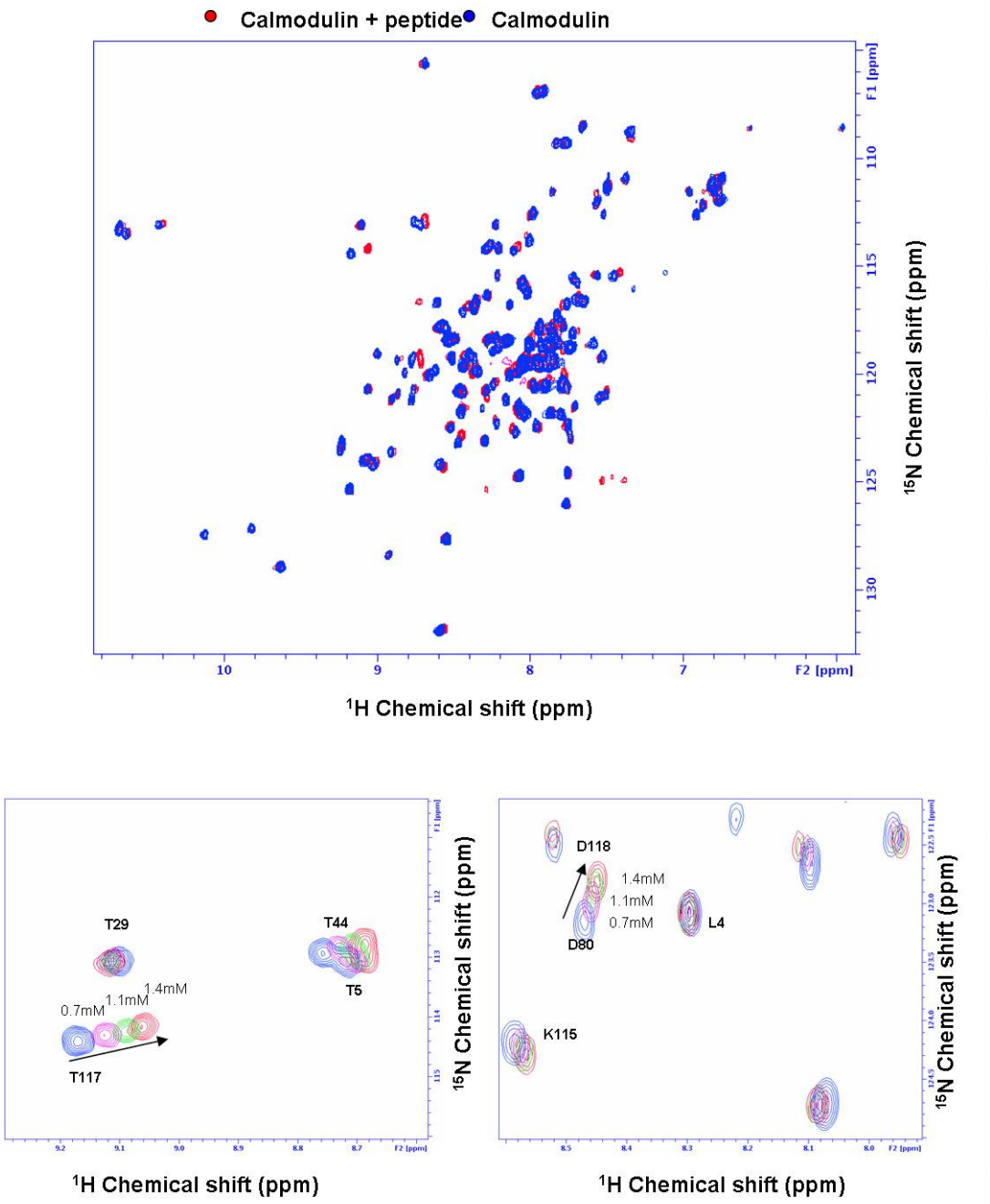

Fig.6.25 Titration of calmodulin with peptide from CBD of FKBP38

A) Overlay of calmodulin spectra in the presence (red) and absence of peptide (1.1 mM). ^{15}N uniformly labeled calmodulin (0.2 mM, 2 mM Ca^{2+}) was titrated with peptide as described in the material and methods. B, C) The chemical shift changes with different concentration of peptide.Some of the amino acids are shown (based upon assignment from BMRB547) with amino-acid abbreviation and sequencial number.

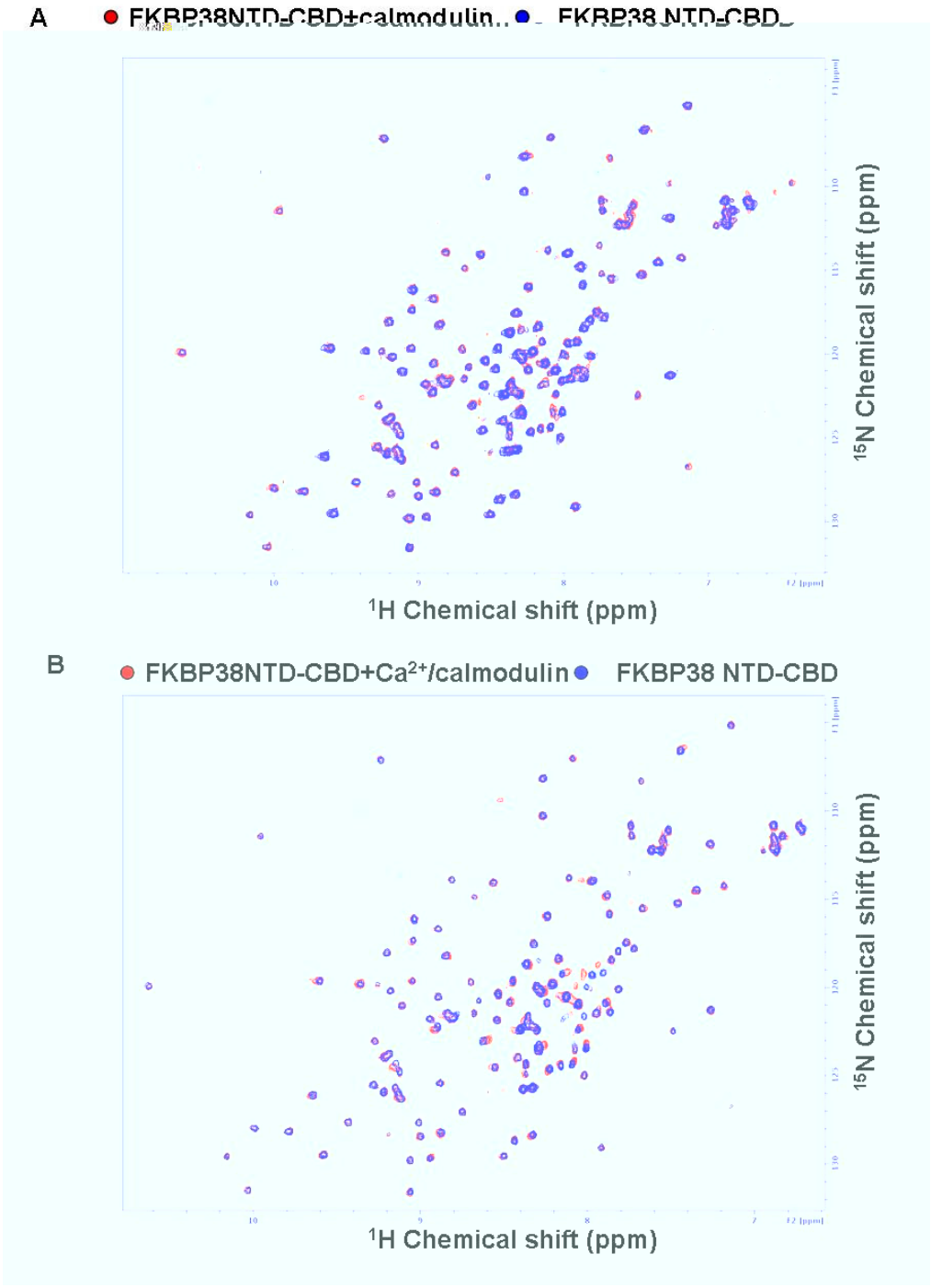

Fig.6.26 Titration of calmodulin with FKBP38NTD-CBD fusion protein

Overlay of NTD-CBD fusion protein (0.2mM) spectra in the presence (red) and absence of calmodulin (0.2 mM). ^{15}N uniformly labeled NTD-CBD (0.2 mM) was titrated with calmodulin in the absence (A) and presence of 0.4 mM Ca^{2+} (B) as described in the material and methods. All the spectra were recorded at 303K.

6.10 Discussion

In this chapter, we analyzed the solution structure of NTD of FKBP38 by NMR. Several experiments were done to finish the backbone assignment and side chain assignment of NTD and the data has been deposited at the BioMagResBank database under accession number BMRB-6923. In this study, we determined the structure of the N-terminal domain of FKBP38. Here we presented that overall the structural architecture of FKBPNTD is similar to that of typical FKBP family proteins. However, the hydrophobic groove in FKBP38NTD is different, probably due to substitutions of the conserved aromatic residues in the hydrophobic pocket. We also demonstrated that the N-terminal tail domain of FKBP38 appears to interact with its own calmodulin binding domain at the C-terminus, suggesting a potential regulatory role through the cross-talk. However, biological significance of this interaction remains to be further studied.

FKBP38 is an important protein that can help Bcl-2 localize at the mitochondria and ER. FKBP38 was shown to regulate apoptosis through interaction with Bcl-2. But exact function of FKBP38 is still not well understood. We first confirmed that the immuno-suppressive drug FK-506 did not interact with FKBP38 (Fig.4.12) and enhance inhibition effect on calcineurin (Fig.4.8), which is clearly evident that FKBP38 is different from other FKBP family proteins. Based upon the initial structure, we compared the potential FK-506 binding site in both FKBP12 (PDB ID 1KFJ) and the NTD of FKBP38. The result revealed the hydrophobic ligand binding-pockets are different in the two proteins (Fig.6.15), in the FKBP38 NTD, the β-strand which is consistent with the sequence alignment with FKBP12 and other FKBP proteins. Consequently, the side-chain of Glu83 in FKBP38NTD takes on a different orientation from the corresponding Ser39 side-chain in FKBP12, extending to the

putative binding site. The residue His87 near the entry pocket of FK-506 in FKBP12 is replaced by Arg127 could block the access to the ligand binding pocket. There is a loop from S118 to Ala135, which covers the proposed FK-506 binding pocket. FKBP38NTD has a shorter loop between β3 and β4 (Pro84-Glu85) than that in FKBP12, the loop is from Ser39 to Pro45. All these difference explained the reduction of hydrophobic surface and change of the hydrogen bond pattern and explained the reason why this domain has no FK-506 binding activity.

It was also found that FKBP38 interacted with PS1/2 and the interaction could make Bcl-2 localized at ER membrane (Wang *et al*., 2005). PS1/2 is a multi-trans-membrane protein and the loop domain outside the TM domain of PS1/2 is important for the interaction with FKBP38. We did titration study between NTD of FKBP38 and PS1, but no obvious chemical shifts perturbations were observed (unpublished data).

We also performed titration experiments between the NTD and peptide from the loop of Bcl-2, but the interaction seems to be weak. Even though the flexible loop region of Bcl-2 is important for the molecular interaction between FKBP38 and Bcl-2 (Fig.5.2), the interaction might require other domain such as TPR domain. So the effect of TPR domain on the interaction between FKBP38 and associating partners need to be further be studied.

FKBP38 also has a potential calmodulin binding domain CBD and can interact with calmodulin. By using NMR titration of peptide from the CBD domain of FKBP38 with calmodulin, it was confirmed that the CBD domain is important for the interaction between FKBP38 and calmodulin (Fig.6.25). The ^{15}N-HSQC spectrum of FKBP-CBD fusion protein showed the interaction between NTD and CBD (Fig.6.21). Interestingly, several hydrophobic amino acids are involved in the interactions (Fig.6.23). It was reported that the interaction between the FKBP38 and calmodulin

can cause the conformational change and the complex formation can make FKBP38 active and have the PPIase activity (Edich *et al*., 2005). From our results, calmodulin showed interaction with the FKBP38CBD (Fig.6.22), and the CBD also has interaction with the NTD domain (Fig.6.25), indicating that the regulation of demonstrated enzyme activity might be related to the interaction between CBD and NTD domains. The titration between NTD and calmodulin did not show any interaction between these two proteins, while the interaction between NTD-CBD fusion protein and calmodulin could be observed (Fig.6.26). All the data suggest that the interaction between CBD and its NTD plays the regulation role of Ca^{2+}/calmodulin on FKBP38. Calmodulin could affect the interaction between CBD and NTD by its interaction with CBD so as to change the characteristics of FKBP38.

There have been contradictory reports about the inhibitory effect of FKBP38 on calcineurin (Shirane *et al.*, 2003, Edich *et al*., 2005, Kang *et al*., 2005). Calmodulin is necessary for the activity of calcineurin, so it is possible that the inhibitory effect on calcineurin is also calmodulin-dependent. The interaction between CBD and calmodulin may make calmodulin unavailable for the phosphatase activity of calcineurin.

In summary, our NMR structure study on the NTD of FKBP38 provides the 3D information to explain the absence of the FK-506 binding activity. The titration experiment between the NTD and the peptides (proteins) shows that this domain is important for the protein-protein interactions. Also, the interaction between the NTD and CBD gives the insight of the regulation of the FKBP38 by calmodulin. The interaction between the calmodulin and FKBP38 through the CBD could also provide an explanation for the inhibitory effect of FKBP38 on calcineurin.

Conclusion

In this thesis, the cDNAs of Bcl-2, Bcl-xL, FKBP38, calmodulin, myristoyl-CoA: protein NMT, Pin1, KFBP12 were cloned, expressed, and purified for biochemical and biophysical studies. Protein kinases such as JNK and ERK2 and protein phosphatases were also purified from *E.coli* by using a newly established co-expression method.

Biochemical study on FKBP38 showed that the purified FKBP38 has the chaperone activity by preventing the citrate synthase aggregation and increases the solubility of Bcl-2 when they were co-expressed in *E.coli*. The NMR titration study on the NTD of FKBP38 confirmed that FKBP38 does not interact with FK506.

Bcl-2 contains a long loop and the loop was confirmed to be important for its interaction with FKBP38. We showed that protein kinases, JNK and ERK2, have different substrate specificities on the flexible loop of Bcl-2. Upon phosphorylation on the loop, protein phosphatases can use the phosphorylated form of Bcl-2 as substrate and prefer showed different dephosphorylation patterns. Pin1 shows the phosphorylation-dependent interaction with Bcl-2. In this study we demonstrated that the phosphorylation of the peptides derived from the loop caused a conformational change in the pSer/Thr-Pro motifs and allowed molecular interaction with Pin1.

Three-dimensional structure determination by solution state NMR revealed that the overall structural fold of the NTD is similar to that of the typical FKBP domain, but lacks the well-conserved residues that would enable it to behave as a canonical FKBP. It displayed a smaller ligand-binding that could provide a molecular basis of why this protein has no FK506 binding activity. Another interesting finding was that FKBP38NTD interacts with the putative calmodulin binding site of FKBP38. We speculate that the molecular interaction between Ca^{2+}/calmodulin and FKBP38 might provide a clue in understanding a potential molecular mechanism of how the catalytic activity of the chaperone FKBP38 is activated upon binding Ca^{2+}/calmodulin and subsequently modulates the function of the anti-apoptotic protein Bcl-2.

Author's publications

Published papers

1. Liang, Y., **Kang, C.B.**, Yoon, H.S. (2006) Molecular and structural characterization of the domain 2 of Hepatitis C virus non-structural protein 5A. ***Mol. Cells***., **22**: 13-20.
2. Ye, W., Nanga, R.P.R., **Kang, C.B.**, Song, J.H., Song, S. K., Yoon, H.S. (2006) Molecular characterization of the recombinant A-chain of a type II ribosome-inactivating protein (RIP) from *Viscum album coloratum* and its structural basis on ribosome-inactivating activity and sugar binding properties of the B-chain. ***J. Biochem***. ***Mol. Biol***., 39:560-570.
3. Xu, H., Tai, J., Ye, H., **Kang, C.B.**, and Yoon, H.S. (2006) The N-terminal domain of tumor suppressor p53 (p53NTD) is involved in the molecular interaction with the anti-apoptotic protein Bcl-xL. ***Biochem. Biophys. Res .Commun.***, **341**: 938-944.
4. **Kang, C.B.**, Feng, L., Chia, J., and Yoon, H.S. (2005) Molecular characterization of FK-506 binding protein 38 (FKBP38) and its potential regulatory role on the anti-apoptotic protein Bcl-2. ***Biochem. Biophys. Res. Commun.***, **337**: 30-38.
5. **Kang, C.B.**, Tai, J., Chia, J., and Yoon, H.S. (2005) The flexible loop of Bcl-2 is required for molecular interaction with immunosuppressant FK-506 binding protein 38 (FKBP38). ***FEBS Lett.***, **579**: 1469-1476.
6. **Kang, C.B.**, Ye, H., Vivekanandan, S., Simon, B., Sattler, M., and Yoon, H.S. (2006) Backbone ^{1}H, ^{13}C, and ^{15}N resonance assignments of the N-terminal domain of FKBP38 (FKBP38NTD). ***J. Biomol NMR.***, In Press

Conference papers

7. Ye W., Nanga R., **Kang C.B.**, Song J.H., Song S.K., Yoon H.S. Catalytic Activity And Sugar-Binding Property Of Type II Ribosome-inactivating Protein From Viscum Album Coloratum. 20th Symposium the Protein Society, San Diego, USA (August, 2006).
8. Xu X., Tai J., Ye H., **Kang C.B.**, Yoon, H.S. The Involvement Of The N-terminal Domain Of p53 In The Molecular Interaction With The Anti-apoptotic Protein Bcl-Xl. 20th Symposium the Protein Society, San Diego, USA (August, 2006).
9. **Kang, C.B.**, Tai, J., Chia, J., and Yoon, H.S. A molecular mechanism of immunosuppressant FK-506 binding protein 38 with anti-apoptotic protein Bcl-2. ***FASEB Journal***, **19**(4): A269-270, (April, 2005).
10. **Kang, C.B.**, Tai, J., and Yoon, H.S. Molecular interaction of immunosuppressant FK-506 binding protein 38 with anti-apoptotic protein Bcl-2. EMBL/Salk/EMBO Conference on Oncogenes & Growth Control, EMBL-Heidelberg, Germany (April, 2004).
11. **Kang C. B.**, Ye H., Chia J., Tai J., and Yoon H. S.. The flexible loop of Bcl-2 shows phosphorylation-dependent conformational change and interaction to Pin 1, the 2006 AOHUPO and Structural Biology conference, Singapore, accepted.
12. **Kang C. B.**, Chia J., and Yoon H. S.. The disordered loop of Bcl-2 exerts specific phosphorylation and dephosphorylation in vitro. The 2006 AOHUPO and Structural Biology conference, Singapore, accepted.
13. Yoon H. R., **Kang C. B.**, Chia J., and Yoon H.S.. Molecular Characterization of FK506 binding protein 35 from Plasmodium falciparum. The 2006 AOHUPO and Structural Biology conference, Singapore, accepted.

References

Abraham R T, Wiederrecht G. Immunopharmacology of rapamycin. *Annual Review immunology*, 1996, **14**: 483-510.

Adams J and Cory S. The Bcl-2 Protein Family: Arbiters of Cell Survival. *Science*, 1998, **281**: 1322-1328.

Adams, J.M. and Cory, S. Life-or-death decisions by theBcl-2 protein family. *Trends. Biochem. Sci.*, 2001, **26**: 61-66.

Adina B., Isabelle Camus. The involvement of mammalian and plant FK-506-binding proteins (FKBPs) in development. *Transgenic Research*, 2002, **11**: 321-335.

Alberici A, Moratto D, Benussi L, Gasparini L, Ghidoni R, Gatta LB, Finazzi D, Frisoni GB, Trabucchi M, Growdon JH, Nitsch RM, Binetti G. Presenilin 1 protein directly interacts with Bcl-2. J Biol Chem. 1999, 274(43):30764-9.

Ames JB, Ishima R, Tanaka T, Gordon JI, Stryer L, Ikura M. Molecular mechanics of calcium-myristoyl switches. *Nature*, 1997, **389**(6647): 198-202.

Andrain C, Creagh M, Martin S. J. Defying death: showing Bcl-2 the way home. *Nature cell Biology*, 2003, **5**: 9-11.

Antonsson B, Montessuit S, Lauper S, Eskes R, Martinou JC. Bax oligomerization is required for channel-forming activity in liposomes and to trigger cytochrome c release from mitochondria. *Biochem J.*, 2000, **345**: 271-278.

Asnaghi L, Calastretti A, Bevilacqua A, D'Agnano I, Gatti G, Canti G, Delia D, Capaccioli S, Nicolin A. Bcl-2 phosphorylation and apoptosis activated by damaged microtubules require mTOR and are regulated by Akt. *Oncogene*, 2004, **23**(34): 5781-5791.

Bachelor MA, Bowden GT. Ultraviolet A-induced modulation of Bcl-xL by p38 MAPK in human keratinocytes: post-transcriptional regulation through the 3'-untranslated region. *J Biol Chem.*, 2004, **279**(41): 42658-42668.

Bassik MC, Scorrano L, Oakes SA, Pozzan T, Korsmeyer SJ. Phosphorylation of BCL-2 regulates ER Ca(2+) homeostasis and apoptosis. *EMBO J.*, 2004, **23**: 1207-1216.

Basu A, Haldar S. Signal-induced site specific phosphorylation targets Bcl2 to the proteasome pathway. *J Oncol.*, 2002, **21**(3):597-601.

Basu, A. and Haldar, S. Identification of a novel Bcl-xL phosphorylation site regulating the sensitivity of taxol- or 2-methoxyestradiol-induced apoptosis. *FEBS Lett.*, 2003, **538**: 41-47.

Basu A, Das M, Qanungo S, Fan XJ, DuBois G, Haldar S.Proteasomal degradation of human peptidyl prolyl isomerase pin1-pointing phospho Bcl2 toward dephosphorylation.Neoplasia. 2002, 4(3):218-27.

Bayer E, Goettsch S, Mueller J W, Griewel B, Guiberman E, Mayr LM, Bayer P. Structural analysis of the mitotic regulator hPin1 in solution: insights into domain architecture and substrate binding. *J Biol Chem.*, 2003, **278**: 26183-26193.

Biose LH, Gonzalez-Garcia M, Postema C.E, Ding L, Nunex G. Bcl-x, a bcl-2 related gene that functions as a dominant regulator of apoptotic cell death. *Cell*, 1993, **77**: 597-608.

Biswas S.C and Greene L.A. Nerve Growth Factor (NGF) Down-regulates the Bcl-2 Homology 3 (BH3) Domain-only Protein Bim and Suppresses Its Proapoptotic Activity by Phosphorylation. *J. Biol. Chem.*, 2002, **277**(51): 49511-49516.

Blackledge M. Recent progress in the study of biomolecular structure and dynamics in solution from residual dipolar coupling. *Progress in Nuclear Magnetic Resonance Spectroscopy*, 2005, **46**: 23-61.

Blagoskonny M.V. Unwinding the loop of Bcl-2 phosphorylation. *Leukemia*, 2001, 15: 869-874.

Boise LH, Gonzalez-Garcia M, Postema CE, Ding L, Lindsten T, Turka LA, Mao X, Nunez G, Thompson CB. Bcl-x, a bcl-2-related gene that functions as a dominant regulator of apoptotic cell death. *Cell*, 1993, **74**(4): 597-608.

Borner c., Martinou I., mattmann C., Irmler M., shaerer E., martinou J.C. and Tschopp J. The protein Bcl-2 alpha does not require membrance attachment, but two conserved domains to suppress apoptosis, *J Cell Biol*., 1994, **126**: 1059-1068.

Bouillet P. and Strasser A. BH3-only proteins-evolutionarily conserved pro-apoptotic Bcl-2 family members essential for initiating programmed cell death. *J. Cell Sci.*, 2002, **115**: 1567-1574.

Boulton TG, Nye SH, Robbins DJ, Ip NY, Radziejewska E, Morgenbesser SD, DePinho RA, Panayotatos N, Cobb MH, Yancopoulos GD. ERKs: a family of protein-serine/threonine kinases that are activated and tyrosine phosphorylated in response to insulin and NGF. *Cell*, 1991, **65**(4): 663-675.

Breiman A., Camus I. The involvement of mammalian and plant FK-506 binding proteins in development. *Transgenic research*., 2002, **11**: 321-335.

Breitschopf K, Haendeler J, Malchow P, Zeiher AM, Dimmeler S. Posttranslational modification of Bcl-2 facilitates its proteasome dependent degradation: molecular characterization of the involved signaling pathway. *Mol. Cell. Biol.*, 2000, **20**: 1886-1896.

Brichese L, Cazettes G, Valette A. JNK is associated with Bcl-2 and PP1 in mitochondria: paclitaxel induces its activation and its association with the phosphorylated form of Bcl-2. *Cell Cycle*, 2004, **3**: 1312-1319.

Brunger, A.T., et al., Crystallography & NMR system: A new software suite for macromolecular structure determination. *Acta Crystallogr D Biol Crystallogr*, 1998, **54**: 905-21.

Campbell, A., Sudha, T.,Yuan, Z.M., Narula, J., Weichselbaum, R., Nalin, C. and Kufe, D. Translocation of SAPK/JNK to mitochondria and interaction with Bcl-x(L) in response to DNA damage. *J. Biol.Chem.*, 2000, **275**: 322-327.

Canagarajah BJ, Khokhlatchev A, Cobb MH, Goldsmith EJ. Activation mechanism of the MAP kinase ERK2 by dual phosphorylation. *Cell*, 1997, **90**(5): 859-869.

Chang, B.S., Minn, A.J., Muchmore, S.W., Fesik, S.W. and Thompson, C.B. Identification of a novel regulatory domain in Bcl-X(L) and Bcl-2. *EMBO J.*, 1997, **16**: 968-977.

Charbonneau J and Gauthier E. Protection of hybridoma cells against apoptosis by a loop domain deficient Bcl-xL protein. *Cytotechnology*., 2001, **37**: 41-47.

Chen Z, Gibson TB, Robinson F, Silvestro L, Pearson G, Xu B, Wright A, Vanderbilt C, Cobb MH. MAP kinases. *Chem Rev*., 2001, **101**(8): 2449-7246.

Ciechanover, A. The ubiquitin-proteasome proteolyticpathway. *Cell*, 1994, **79**: 13-21.

Clardy J. The chemistry of signal transduction (FK-506/ Rapamycin/cyclosporine A/cyclopilin). *Proc. Natl. Acad. Sci*. 1995, **92**: 56-61.

Cobb MH, Goldsmith EJ. How MAP kinases are regulated. *J Biol Chem.*, 1995, **270**(25): 14843-14846.

Constanzo M R. New immunosuppressive drugs in heart transplantation. *Current Controlled Trials in Cardiovascular Medicine*, 2001, **2**(1): 45-53.

Cornilescu G., Delaglio F. and Bax A.: Protein backbone angle restraints from searching a database for chemical shift and sequence homology. *J. Biomol. NMR*, 1999, **13**: 289-302.

Cory A.H., T.C. Owen, J.A. Barltrop, J.G. Cory. Use of an aqueous soluble tetrazolium/formazan assay for cell growth assays in culture. *Cancer Commun.*, 1991, **3**: 207-212.

Cory S., Adams J.M. The Bcl-2 family: regulators of the cellular life-or-death switch. *Nat. Rev.*, 2002, **2**: 647-656.

Crow M.T., Mani K., Nam Y.J., Kitsis R.N. The mitochondrial death pathway and cardiac myocyte apoptosis. *Circ. Res.*, 2004, **95**: 957-970

Cuconati A., White E. Viral homologs of BCL-2: role of apoptosis in the regulation of virus infection. *Genes Dev*., 2002, **16**(19): 2465-2478.

Delaglio, F., et al., NMRPipe: a multidimensional spectral processing system based on UNIX pipes. *J Biomol NMR*, 1995, **6**(3): 277-93.

Davies TH, Sanchez ER. FKBP52. *J Biochem Cell Biol.*, 2005, **37**(1): 42-47.

DeLano, W.L. The PyMOL Molecular Graphics System (2002) on World Wide Web http://www.pymol.org

Deng X, Gao F, Flagg T, May WS Jr. Mono- and multisite phosphorylation enhances Bcl2's antiapoptotic function and inhibition of cell cycle entry functions. *Proc. Natl. Acad. Sci. USA*, 2004, **101**: 153-158.

Deng X, Xiao L, Lang W, Gao F, Ruvolo P, May WS Jr. Novel role for JNK as a stress-activated Bcl2 kinase. *J Biol Chem*., 2001, **276**(26): 23681-23688.

Deng Z., Ruvolo P., Carr B., May W.S.J. Survival function of ERK1/2 as IL-3 activated, staurosporine resistant Bcl2 kinases. *Proc. Natl. Acad. Sci. USA*, 2000, **97**: 1578-1583.

Denisov AY, Madiraju MS, Chen G, Khadir A, Beauparlant P, Attardo G, Shore GC, Gehring K. Solution structure of human BCL-w: modulation of ligand binding by the C-terminal helix. *J Biol Chem*., 2003, **278**(23): 21124-21128.

Desagher S, Osen-Sand A, Nichols A, Eskes R, Montessuit S, Lauper S, Maundrell K, Antonsson B, Martinou JC. Bid-induced conformational change of Bax is responsible for mitochondrial cytochrome c release during apoptosis. *J Cell Biol*., 1999, **144**(5): 891-901.

Deutscher M P. Guide to protein Purification, methods in Enzymology, **182**, Harcourt Brace jovanocich, Publishers, San Diego, 1990.

Dimmeler S, Breitschopf K, Haendeler J, Zeiher AM. Dephosphorylation targets Bcl-2 for ubiquitin-dependent degradation: a link between the apoptosome and the proteasome pathway. *J Exp Med*., 1999, **189**(11): 1815-1822.

Du L, Lyle CS, Chambers TC. Characterization of vinblastine-induced Bcl-xL and Bcl-2 phosphor ylation: evidence for a novel protein kinase and a coordinated phosphorylation/dephosphorylation cycle associated with apoptosis induction. *Oncogene*, 2005, **24**(1): 107-117.

Dziembowski A, Seraphin B. Recent developments in the analysis of protein complexes. *FEBS Lett.*, 2004, **556**(1-3): 1-6.

Dzivenu OK, Park HH, Wu H. General co-expression vectors for the overexpression of heterodimeric protein complexes in *Escherichia coli. Protein Expr Purif.*, 2004, **38**(1): 1-8.

Edlich F, Weiwad M, Erdmann F, Fanghanel J, Jarczowski F, Rahfeld JU, Fischer G. Bcl-2 regulator FKBP38 is activated by Ca^{2+}/calmodulin. *EMBO J.*, 2005, **24**(14): 2688-2699.

Fantin VR, Leder P. F16, a mitochondriotoxic compound, triggers apoptosis or necrosis depending on the genetic background of the target carcinoma cell. *Cancer Res*., 2004, **64**(1): 329-336.

Feng H, Xiang H, Mao YW, Wang J, Liu JP, Huang XQ, Liu Y, Liu SJ, Luo C, Zhang XJ, Liu Y, Li DW. Human Bcl-2 activates ERK signaling pathway to regulate activating protein-1, lens epithelium-derived growth factor and downstream genes. *Oncogene*, 2004, **23**(44):7310-7321.

Ferri KF, Kroemer G. Organelle-specific initiation of cell death pathways. *Nat Cell Biol.*, 2001, **3**(11): E255-263.

Fesik S.W. Insights into programmed cell death through structural biology. *Cell*, 2000, **102**: 273-282.

Fischer g., Tradler T., Zarnt T. The mode of action of peptidyl prolyl cis/trans isomerase in vivo: binding vs catalysis. *FEBS Lett*., 1998, **426**: 17-20.

Fischer, G. Chemical aspects of peptide bond isomerization. *Chem. Soc. Revs.*, 2000, 119-127.

Fong S, Mounkes L, Liu Y, Maibaum M, Alonzo E, Desprez PY, Thor AD, Kashani-Sabet M, Debs RJ. Functional identification of distinct sets of antitumor activities mediated by the FKBP gene family. *Proc Natl Acad Sci U S A*, 2003 Nov 25, **100**(24): 14253-14258.

Fruman DA, Burakoff SJ, Bierer BE. Immunophilins in protein folding and immunosuppression. *FASEB Journal*., 1994, **8**: 391-400.

Furukawa Y, Iwase S, Kikuchi J, Terui Y, Nakamura M, Yamada H, Kano Y, Matsuda M. Phosphorylation of Bcl-2 protein by CDC2 kinase during G2/M phases and its role in cell cycle regulation. *J Biol Chem*., 2000, **275**(28): 21661-21667.

Furutani M, Ideno A, Iida T, Maruyama T. FK-506 binding protein from a thermophilic archaeon, methanococcus thermolithotrophicus, has chaperone-like activity in vitro. *Biochemistry*, 2000, **39**(10): 2822.

Gabriel Cornilescu, Frank Delaglio, and Ad Bax.Protein backbone angle restraints from searching a database for chemical shift and sequence homology. *J. Biomol. NMR*, 1999, **13**: 289-302.

Galat A. Sequence diversification of the FK-506-binding proteins in several different genomes. *Eur. J. Biochem.*, 2000, **267**: 4945-4959.

Galat, A. Peptidylprolyl cis/trans isomerases (immunophilins):biological diversity-targets-functions. *Curr. Top. Med.Chem.*, 2003, **3**:1315-1347.

Garcia-Echeverria C, Kofron JL, Kuzmic P, Rich DH. A continuous spectrophotometric direct assay for peptidyl prolyl cis-trans isomerases. *Biochem Biophys Res Commun.*, 1993, **191**(1): 70-75.

Germain M, Shore GC. Cellular distribution of Bcl-2 family proteins. *Sci STKE*., 2003, **173**: pe10.

Gibson L, Holmgreen SP, Huang DC, Bernard O, Copeland NG, Jenkins NA, Sutherland GR, Baker E, Adams JM, Cory S. Bcl-w, a novel member of the bcl-2 family, promotes cell survival. *Oncogene*, 1996, **13**(4): 665-675.

Gonzalez FA, Raden DL, Davis RJ. Identification of substrate recognition determinants for human ERK1 and ERK2 protein kinases. *J. Biol. Chem.*, 1991, **266**: 22159-22163.

Gonzalez-Garcia M, Garcia I, Ding L, O'Shea S, Boise LH, Thompson CB, Nunez G. Bcl-x is expressed in embryonic and postnatal neural tissues and functions to prevent neuronal cell death. *Proc Natl Acad Sci U S A*., 1995, **92**(10): 4304-4308.

Gonzalez-Garcia M, Perez-Ballestero R, Ding L, Duan L, Boise LH, Thompson CB, Nunez G. Bcl-xL is the major bcl-x mRNA form expressed during murine development and its product localizes to mitochondria. *Development*, 1994, **120**(10): 3033-3042.

Gotow T, Shibata M, Kanamori S, Tokuno O, Ohsawa Y, Sato N, Isahara K, Yayoi Y, Watanabe T, Leterrier JF, Linden M, Kominami E, Uchiyama Y. Selective localization of Bcl-2 to the inner mitochondrial and smooth endoplasmic reticulum membranes in mammalian cells. *Cell Death Differ*., 2000, **7**(7): 666-674.

Griffith J.P. , J.L. Kim, E.E. Kim, M.D. Sintchak, J.A. Thomson, M.J. Fitzgibbon, M.A. Fleming, P.R. Caron, K. Hsiao, M.A. Navia. X-ray structure of calcineurin inhibited by the immunophilin-immunosuppressant FKBP12-FK-506 complex. *Cell*, 1995, **82**: 507-522.

Güntert, P., Mumenthaler, C. and Wüthrich, K. Torsion angle dynamics for NMR structure calculation with the new program DYANA. *J. Mol. Biol.*, 1997, **273**: 283-298.

Güntert, P. Automated NMR protein structure calculation. *Prog. NMR Spectrosc.*, 2003, **43**: 105-125.

Guntert, P., Automated NMR structure calculation with CYANA. *Methods Mol Biol*, 2004, **278**: 353-78

Haldar, S., Basu, A. and Croce, C.M. Serine-70 is one of the critical sites for drug-induced Bcl-2 phosphorylation in cancer cells. *Cancer Res.*, 1998, **58**: 1609-1615.

Handrick R, Rudner J, Muller I, Eibl H, Belka C, Jendrossek V. Bcl-2 mediated inhibition of erucylphosphocholine-induced apoptosis depends on its subcellular localisation. *Biochem Pharmacol.*, 2005, **70**(6): 837-850.

Hansen, M. R., L. Mueller, et al. Tunable alignment of acromolecules by filamentous phage yields dipolar coupling interactions. *Nature Structural Biology*, 1998, **5**(12): 1065-1074.

Harborth J., S. M. Elbashir, K. Bechert, T. Tuschl, K. Weber. Identification of Essential Genes in Cultured Mammalian Cells Using Small Interfering RNAs. *J. Cell Science*, 2001, **114**: 4557-4565.

Harding MW, Galat A, Uehling DE, Schreiber SL. A receptor for the immunosuppressant FK-506 is a cis-trans peptidyl-prolyl isomerase. *Nature*, 1989, **341**(6244): 758-760.

Harris, C. A., and Johnson, E. M., Jr. BH3-only Bcl-2 Family Members Are Coordinately Regulated by the JNK Pathway and Require Bax to Induce Apoptosis in Neurons. *J. Biol. Chem.*, 2001, **276**: 37754-37760.

Herrmann, T., Güntert, P. and Wüthrich, K. Protein NMR structure determination with automated NOE assignment using the new software CANDID and the torsion angle dynamics algorithm DYANA. *J. Mol. Biol.*, 2002, **319**: 209-227.

Hengartner M. O. The biochemistry of apoptosis. *Nature*, 2000, **407**(12): 770-776.

Hinds MG, Lackmann M, Skea GL, Harrison PJ, Huang DC, Day CL. The structure of Bcl-w reveals a role for the C-terminal residues in modulating biological activity. *EMBO J.*, 2003, **22**(7): 1497-1507.

Huang ST, Cidlowski JA. Phosphorylation status modulates Bcl-2 function during glucocorticoid-induced apoptosis in T lymphocytes. *FASEB J.*, 2002, **16**(8): 825-832.

Ideno A, Furutani M, Iwabuchi T, Iida T, Iba Y, Kurosawa Y, Sakuraba H, Ohshima T, Kawarabayashi Y, Maruyama T. Expression of foreign proteins in *Escherichia coli* by fusing with an archaeal FK-506 binding protein. *Appl Microbiol Biotechnol.*, 2004, **64**(1): 99-105.

Ideno A, Yoshida T, Iida T, Furutani M, Maruyama T. FK-506-binding protein of the hyperthermophilic archaeum, Thermococcus sp. KS-1, a cold-shock-inducible peptidyl-prolyl cis-trans isomerase with activities to trap and refold denatured proteins. *Biochem J.*, 2001, **357**(Pt 2): 465-471.

Jacobs DM, Saxena K, Vogtherr M, Bernado P, Pons M, Fiebig KM. Peptide binding induces large scale changes in inter-domain mobility in human Pin1. *J Biol Chem.*, 2003, **278**(28): 26174-26182.

Janowski B, Wollner S, Schutkowski M, Fischer G. A protease-free assay for peptidyl prolyl cis/trans isomerases using standard peptide substrates. *Anal Biochem.*, 1997, **252**(2): 299-307.

Jin L, Harrison SC. Crystal structure of human calcineurin complexed with cyclosporin A and human cyclophilin. *Proc Natl Acad Sci U S A*, 2002, **99**(21): 13522-13526.

Johnson B.A., Blevins, B., NMRView: A computer program for the visualization and analysis of NMR data. *J. Biomol. NMR*, 1994, **4**: 603-614.

Kang CB, Tai J, Chia J, Yoon HS. The flexible loop of Bcl-2 is required for molecular interaction with immunosuppressant FK-506 binding protein 38 (FKBP38). *FEBS Lett.*, 2005, **579**(6): 1469-1476.

Kang, CB, Feng, L, Chia, J, and Yoon, HS. Molecular characterization of FK-506 binding protein 38 (FKBP38) and its potential regulatory role on the anti-apoptotic protein Bcl-2. Biochem. Biophys. Res. Commun. 2005, 337: 30-38.

Kasibhatla S and Tseng B. Why target apoptosis in cancer treatment. *Molecular Cancer Therapeutics*, 2003, **2**: 573-580.

Kaufmann T, Schinzel A, Borner C. Bcl-w(edding) with mitochondria. *Trends Cell Biol.*, 2004, **14**(1): 8-12.

Kelekar A, Thompson CB. Bcl-2-family proteins: the role of the BH3 domain in apoptosis. *Trends Cell Biol.*, 1998, **8**(8): 324-330.

Kennelly PJ, Krebs EG. Consensus sequences as substrate specificity determinants for protein kinases and protein phosphatases. *J. Biol. Chem.*, 1991, **266**: 15555-15558.

Khaled AR, Kim K, Hofmeister R, Muegge K, Durum SK. Withdrawal of IL-7 induces Bax transloca tion from cytosol to mitochondria through a rise in intracellular pH. *Proc Natl Acad Sci U S A*, 1999, **96**(25): 14476-14481.

Kharbanda S, Pandey P, Schofield L, Israels S, Roncinske R, Yoshida K, Bharti A, Yuan ZM, Saxena S, Weichselbaum R, Nalin C, Kufe D. Role for Bcl-xL as an inhibitor of cytosolic cytochrome C accumulation in DNA damage-induced apoptosis. *Proc Natl Acad Sci U S A*, 1997, **94**(13): 6939-6942.

Kharbanda S, Saxena S, Yoshida K, Pandey P, Kaneki M, Wang Q, Cheng K, Chen YN, Campbell A, Sudha T, Yuan ZM, Narula J, Weichselbaum R, Nalin C, Kufe D. Translocation of SAPK/JNK to mitochondria and interaction with Bcl-x(L) in response to DNA damage. *J Biol Chem.*, 2000, **275**(1): 322-327.

Khoklatchev A., Xu S., English J., Wu P., Schaefer E. and Cobb M.H. Reconstitution of mitogen-activated protein kinase phosphorylation cascades in bacteria. *J. Biol. Chem.*, 1997, **272**: 11057-11062.

Kim S, Cullis DN, Feig LA, Baleja JD. Solution structure of the Reps1 EH domain and characterization of its binding to NPF target sequences. *Biochemistry*, 2001, **40**: 6776-6785.

Klettner A, Baumgrass R, Zhang Y, Fischer G, Burger E, Herdegen T, Mielke K. The neuroprotective actions of FK-506 binding protein ligands: neuronal survival is triggered by de novo RNA synthesis, but is independent of inhibition of JNK and calcineurin. *Brain Res Mol Brain Res.*, 2001, **97**(1): 21-31.

Kluck RM, Bossy-Wetzel E, Green DR, Newmeyer DD. The Release of Cytochrome c from Mito chondria: A Primary Site for Bcl-2 Regulation of Apoptosis. *Science*, 1997, **275**: 1132-1137.

Kofron JL, Kuzmic P, Kishore V, Colon-Bonilla E, Rich DH. Determination of kinetic constants for peptidyl prolyl cis-trans isomerases by an improved spectrophotometric assay. *Biochemistry*, 1991,

30(25): 6127-6134.

Kojima, H., Endo, K., Moriyama, H., Tanaka, Y., Alnemri, E.S.,Slapak, C.A., Teicher, B., Kufe, D. and Datta, R. Abrogation of mitochondrial ytochrome c release and caspase-3 activation in acquired multidrug resistance. *J. Biol. Chem.*, 1998, **273**: 16647-16650.

Komatsu K, Miyashita T, Hang H, Hopkins KM. Human homologue of *S. pombe* Rad9 interacts with BCL-2/Bcl-xL and promotes apoptosis. *Nature cell biology*, 2000, **2**: 1-6.

Koradi, R., Billeter, M., and Wüthrich, K. MOLMOL: a program for display and analysis of macromolecular structures. J Mol Graphics,1996, **14**, 51-55.

Krajewski S, Krajewska M, Reed JC. Immunohistochemical analysis of in vivo patterns of Bak expression, a proapoptotic member of the Bcl-2 protein family. *Cancer Res*., 1996, **56**(12): 2849-2855.

Kroemer,G. The proto-oncogene Bcl-2 and its role in regulating apoptosis. *Nat. Med.*, 1997, **3**: 614-620.

Kumar R, Adams B, Musiyenko A, Shulyayeva O, Barik S. The FK-506-binding protein of the malaria parasite, Plasmodium falciparum, is a FK-506-sensitive chaperone with FK-506-independent calcineurin -inhibitory activity. *Mol Biochem Parasitol.*, 2005, **141**(2): 163-173.

Kuboniwa H, Tjandra N, Grzesiek S, Ren H, Klee CB, Bax A.Solution structure of calcium-free calmodulin. Nat Struct Biol. 1995(9):768-76.

Lam E, Martin M, Wiederrecht G. Isolation of a cDNA ecoding a novel human FK-506 binding protein homlog containing leucine zipper and tetratricopeptide repeat motisf. *Gene*, 1995, **160**: 297-302.

Lam E, Martin MM, Timerman AP, Sabers C, Fleischer S, Lukas T, Abraham RT, O'Keefe SJ, O'Neill EA, Wiederrecht GJ. A novel FK-506 binding protein can mediate the immunosuppressive effects of FK-506 and is associated with the cardiac ryanodine receptor. *J Biol Chem*., 1995, **270**(44): 26511-26522.

Laskowski R A, MacArthur M W, Moss D S & Thornton J M. PROCHECK: a program to check the stereochemical quality of protein structures. *J. Appl. Cryst.*, 1993,**26**, 283-291.

Li H, Zhu H, Xu CJ, Yuan J. Cleavage of BID by caspase 8 mediates the mitochondrial damage in the Fas pathway of apoptosis. *Cell*, 1998, **94**(4): 491-501.

Li P, Ding Y, Wu B, Shu C, Shen B, Rao Z. Structure of the N-terminal domain of human FKBP52. Acta Crystallogr D Biol Crystallogr. 2003 Jan;59:16-22.

Liang H, Fesik SW. Three-dimentional structures of proteins involved in programmed cell death. *J Mol Bio*., 1997, **272**:291-302.

Lindenboim L, Yuan J, Stein R. Bcl-xS and Bax induce different apoptotic pathways in PC12 cells. *Oncogene*, 2000, **19**(14): 1783-1793.

Lindsten T, Ross AJ, King A, Zong WX, Rathmell JC, Shiels HA, Ulrich E, Waymire KG, Mahar P, Frauwirth K, Chen Y, Wei M, Eng VM, Adelman DM, Simon MC, Ma A, Golden JA, Evan G, Korsmeyer SJ, MacGregor GR, Thompson CB. The combined functions of proapoptotic Bcl-2 family members bak and bax are essential for normal development of multiple tissues. *Mol Cell*., 2000, **6**(6): 1389-1399.

Linge, J.P., S.I. O'Donoghue, and M. Nilges, Automated assignment of ambiguous nuclear overhauser effects with ARIA. *Methods Enzymol*, 2001, **339**: 71-90.

Lingel A., Simon B., Izaurralde E., and Sattler M. NMR Assignment of the Drosophila Argonaute2 PAZ Domain. *J. Biomol. NMR*, 2004, **29**: 421-422.

Liu J, Durrant D, Yang HS, He Y, Whitby FG, Myszka DG, Lee RM. The interaction between tBid and

cardiolipin or monolysocardiolipin. *Biochem Biophys Res Commun.*, 2005, **330**(3): 865-870.

Lu KP, Liou YC, Zhou XZ. Pinning down proline-directed phosphorylation signaling. *Trends Cell Biol.*, 2002, **12**(4): 164-172.

Lu KP. Pinning down cell signaling, cancer and Alzheimer's disease. *Trends Biochem Sci.*, 2004, **29**(4): 200-209.

MacFarlane M., Williams A.C. Apoptosis and disease: a life or death decision. *EMBO reports*, 2004, **5**(7): 674-678.

Mai H, May WS, Gao F, Jin Z, Deng X. A functional role for nicotine in Bcl2 phosphorylation and suppression of apoptosis. *J Biol Chem.*, 2003, **278**(3): 1886-1891.

Main ER, Fulton KF, Jackson SE. Folding pathway of FKBP12 and characterisation of the transition state. *J Mol Biol.*, 1999, **291**(2): 429-444.

Manon S, Chaudhuri B, Guerin M. Release of cytochrome c and decrease of cytochrome c oxidase in Bax-expressing yeast cells, and prevention of these effects by coexpression of Bcl-xL. *FEBS Lett.*, 1997, **415**(1): 29-32.

Mansour SJ, Matten WT, Hermann AS, Candia JM, Rong S, Fukasawa K, Vande Woude GF, Ahn NG. Transformation of mammalian cells by constitutively active MAP kinase kinase. *Science*, 1994, **265** (5174): 966-970.

Marc G. and Gordon C., Shore. Cellular distribution of bcl-2 family proteins. *Science's stke*, 2003, **173**: 1-3.

Martinou, J.C. and Green, D.R. Breaking the mitochondrialbarrier. *Nat. Rev. Mol. Cell Biol.*, 2001, **2**: 63-67.

McFerrin MB, Snell EH. The development and application of method to quantify the quality of cryoprotectant solutions using standard area-dector X-ray images. *Journal of Applied Crystallography*, 2000, **35**: 538-545.

Mollinedo F, Gajate C. Microtubules, microtubule-interfering agents and apoptosis. *Apoptosis*, 2003, **8**(5): 413-450.

Monaghan P., Bel A. A *Plasmodium falciparum* FK-506-binding protein (FKBP) with peptidyl-prolyl cis-trans isomerase and chaperone activities. *Mol. Biochem. Parasitol.*, 2005, **139**: 185-195.

Mondragon A., Griffith E.C., Sun L., Xiong F., Armstrong C.and Liu J.O. Overexpression and purification of human calcineurin α from *Escherichia coli* and assessment of catalytic functions of residues surrounding the binuclear metal center. *Biochemistry*, 1997, **36**: 4934-4942.

Montessuit S., Mazzei G, Magnenat E., Antonsson b., Expression and purification of full length human Bax α. *Protein Expression and purification*, 1999, **15**: 202-206.

MosmannT. Rapid colorimetric assay for cellular growth and survival: application to proliferation and cytotoxicity assays. *J. Immunol. Methods*, 1983, **65**: 55-63.

Muchmore SW, Sattler M, Liang H, et al. X-ray and NMR structure of human Bcl-xL an inhibitor of programmed cell death. *Nature*, 1996, **381**: 335-341.

Muchmore SW, Sattler M, Liang H, Meadows RP, Harlan JE, Yoon HS, Nettesheim D, Chang BS, Thompson CB, Wong SL, Ng SL, Fesik SW. X-ray and NMR structure of human Bcl-xL, an inhibitor of programmed cell death. *Nature*, 1996, **381**: 335-341.

Murphy KM, Streips UN, Lock RB. Bax membrane insertion during Fas(CD95)-induced apoptosis precedes cytochrome c release and is inhibited by Bcl-2. *Oncogene*, 1999, **18**(44): 5991-5999.

Nielsen JV, Mitchelmore C, Pedersen KM, Kjaerulff KM, Finsen B, Jensen NA. Fkbp8: novel isoforms, genomic organization, and characterization of a forebrain promoter in transgenic mice. *Genomics*, 2004, **83**(1): 181-192.

Nilges, M. A calculation strategy for the structure determination of symmetric dimers by ^{1}H. *Proteins*, 1993, **17**: 297-309.

Nilges, M. Calculation of protein structures with ambiguous distance restraints. Automated assignment of ambiguous NOE crosspeaks and disulphide connectivities. *J. Mol. Biol.*, 1995, **245**: 645-660.

Nilges, M., Macias M. J., O'Donoghue, S. I. and Oschkinat H. Automated NOESY interpretation with ambiguous distance restraints: the refined NMR solution structure of the pleckstrin homology domain from -spectrin. *J. Mol. Biol.*, 1997, **269**: 408-422.

O'Connor, L., Strasser, A., O'Reilly, L. A., Hausmann, G., Adams, J. M., Cory, S., and Huang, D. C. Bim: a novel member of the Bcl-2 family that promotes apoptosis. *EMBO J.*, 1998, **17**: 384-395.

Ojala PM, Yamamoto K, Castanos-Velez E, Biberfeld P *et al*. The apoptotic v-cyclin-CDK6 complex phosporylateds and inactivates Bcl-2. *Nature cell biology*, 2000, **2**: 819-824.

Oltvai ZN, Milliman CL, Korsmeyer SJ. Bcl-2 heterodimerizes in vivo with a conserved homolog, Bax, that accelerates programmed cell death. *Cell*, 1993, **74**(4): 609-619.

O'Reilly LA, Print C, Hausmann G, Moriishi K, Cory S, Huang DC, Strasser A. Tissue expression and subcellular localization of the pro-survival molecule Bcl-w.*Cell Death Differ*. 2001, **8**(5): 486-494.

Osawa M, Tokumitsu H, Swindells MB, Kurihara H, Orita M, Shibanuma T, Furuya T, Ikura M.A novel target recognition revealed by calmodulin in complex with Ca2+-calmodulin-dependent kinase kinase. Nat Struct Biol. 19996(9):819-24.

Ou WB, Luo W, Park YD, Zhou HM. Chaperone-like activity of peptidyl-prolyl cis-trans isomerase during creatine kinase refolding. *Protein Sci.*, 2001, **10**(11): 2346-2353.

Palmer AM, Greengrass PM and Cavalla D. The Role of Mitochondria in Apoptosis. *Drug News Perspect*, 2000, **13**(6): 378-386.

Park ST, Aldape RA, Futer O, DeCenzo MT, Livingston DJ. PPIase catalysis by human FK-506-binding protein proceeds through a conformational twist mechanism. *J Biol Chem*., 1992, **267**(5): 3316-3324.

Pathan N, Aime-Sempe C, Kitada S, Basu A, Haldar S, Reed JC. Microtubule targeting drugs induce Bcl-2 phosphorylation and association with pin1. *Neoplasia*, 2001, **3**: 550-559.

Pedersen KM, Finsen B, Celis JE, Jensen NA. muFKBP38: a novel murine immunophilin homolog differentially expressed in Schwannoma cells and central nervous system neurons in vivo. *Electrophoresis*, 1999, **20**(2): 249-255.

Petros AM, Medek A, Nettesheim DG, Kim DH, Yoon HS, Swift K, Matayoshi ED, Oltersdorf T, Fesik SW. Solution structure of the antiapoptotic protein Bcl-2. *Proc. Natl. Acad. Sci. USA*, 2001, **98**: 3012-3017.

Petros AM, Olejniczak ET, Fesik SW. Structural biology of the Bcl-2 family of proteins. *Biochim Biophys Acta.*, 2004, **1644**(2-3): 83-94.

Print CG, Loveland KL, Gibson L, Meehan T, Stylianou A, Wreford N, de Kretser D, Metcalf D, Kontgen F, Adams JM, Cory S. Apoptosis regulator bcl-w is essential for spermatogenesis but appears otherwise redundant. Proc Natl Acad Sci U S A. 1998,**95**(21):12424-31.

Putcha, G. V., Moulder, K. L., Golden, J. P., Bouillet, P., Adams, J. A., Strasser, A., and Johnson, E. M.

Induction of BIM, a proapoptotic BH3-only BCL-2 family member, is critical for neuronal apoptosis**.** *Neuron*, 2001, **29**: 615-628.

Ranganathan R, Lu KP, Hunter T, Noel JP. Structural and functional analysis of the mitotic rotamase Pin1 suggests substrate recognition is phosphorylation dependent. *Cell*, 1997, **89**: 875-886.

Reed J, Double identity for proteins of the Bcl-2 family. *Nature cell biology*, 1997, **387**: 773-777.

Reed J.C. Bcl-2 family proteins. *Ongogene*, 1998, **17**: 3225-3236.

Reimer U, Mokdad NE, Schutkowski M, Fisher G. intramolecular assistance of cis/tris isomerization of the histidine-proline moiety. *Biochemistry*, 1997, **36**: 13802-13808.

Riedl SJ, Shi Y. Molecular mechanisms of caspase regulation during apoptosis. *Nat Rev Mol Cell Biol*., 2004, **5**(11): 897-907.

Rodi DJ, Janes RW, Sanganee HJ, Holton RA, Wallace BA, Makowski L. Screening of a library of phage-displayed peptides identifies human bcl-2 as a taxol-binding protein. *J. Mol. Biol.*, 1999, **285**: 197-203.

Rosenquist M. 14-3-3 proteins in apoptosis. *Braz J Med Biol Res*., 2003, **36**(4): 403-408.

Rosner M, Hofer K, Kubista M, Hengstschlager M. Cell size regulation by the human TSC tumor suppressor proteins depends on PI3K and FKBP38. *Oncogene*, 2003, **22**(31): 4786-4798.

Ruvolo P.P., X. Deng, W.S. May. Phosphorylation of Bcl2 and regulation of apoptosis. *Leukemia*, 2001, **15**: 515-522.

Elbashir S. M., Harborth J., Lendeckel W., Yalcin A., Weber K., Tuschl T.. Duplexes of 21-nucleotide RNAs Mediate RNA Interference in Cultured Mammalian Cells. *Nature*, 2001, **411**: 494-498.

Sambrook J., Russell D W. Molecular Cloning: A Laboratory Manual, Cold Spring Harbor Laboratory Press.

Sinars CR, Eheuny-Flynn F, Rimerman RA. Scammell TG *et al,* Structure of the large FK506 binding protein FKBP51, an Hsp 90-binding protein and component of steroid receptor complex. *Proc. Natl. Acad. Sci. USA*, 2003, **100**(3): 868-873.

Satchell P. G., Gutmann J. L. & Witherspoon D. E. Apoptosis: an introduction for the endodontist. *International Endodontic Journal*, 2003, **36**: 237-245.

Sattler M, Liang H, Nettesheim D, Meadows R.P, Harlan *et al.* Structure of Bcl-xL peptide complex: recognition between regulators of apoptosis. *Science*, 1997, **275**(14): 983-986.

Schendel SL, Azimov R, Pawlowski K, Godzik A, Kagan BL, Reed JC. Ion channel activity of the BH3 only Bcl-2 family member, BID. *J Biol Chem.*, 1999, **274**(31): 21932-21936.

Schimmer A.D., hedley D.W., Penn L.Z., Minden M.D. Receptor and mitochondrial mediated apoptosis in acute leukemia: a translational view. *Blood*, 2001, **98**: 3541-3553.

Schlesinger PH, Gross A, Yin XM, Yamamoto K, Saito M, Waksman G, Korsmeyer SJ. Comparison of the ion channel characteristics of proapoptotic BAX and antiapoptotic BCL-2. *Proc. Natl. Acad. Sci. USA*, 1997, **94**: 11357-11362.

Shibasaki F, Kondo E, Akagi T, McKeon F. Suppression of signalling through transcription factor NF-AT by interactions between calcineurin and Bcl-2. *Nature*, 1997, **386**(6626): 728-731.

Shinjyo, T., Kuribara, R., Inukai, T., Hosoi, H., Kinoshita, T., Miyajima, A., Houghton, P. J., Look, A. T., Ozawa, K., and Inaba, T. Downregulation of Bim, a Proapoptotic Relative of Bcl-2, Is a Pivotal Step in Cytokine-Initiated Survival Signaling in Murine Hematopoietic Progenitors. *Mol. Cell. Biol.*, 2001,

21: 854-864.

Shiraiwa N, Inohara N, Okada S, Yuzaki M, Shoji S, Ohta S. An additional form of rat Bcl-x, Bcl-xbeta, generated by an unspliced RNA, promotes apoptosis in promyeloid cells. *J Biol Chem.*, 1996, **271**(22): 13258-13265.

Shirane M, Nakayama K, Inherent calcineurin inhibitor FKBP38 targets Bcl-2 to mitochondria and inhibit apoptosis. *Nature cell Biology*, 2003, **5**: 28-37.

Sich C, Improta S, Cowley DJ, Guenet C, Merly JP, Teufel M, Saudek V. Solution structure of a neurotrophic ligand bound to FKBP12 and its effects on protein dynamics. *Eur J Biochem.*, 2000, **267**(17): 5342-5355.

Siekerka J.J., Hung S.H.Y., Poe M., Lin S.C. and Singal N.H. A cytosolic binding protein for the immunosuppressant FK-506 has peptidyl-prolyl isomerase activity but is distinct from cyclophilin. *Nature*, 1989, 341: 755-757.

Simon B. and Sattler M. Speeding up biomolecular NMR spectroscopy. *Angew. Chem. Int. Ed. Engl.*, 2004, **43**: 782-786.

Simon B. and Sattler M. De Novo Structure Determination from Residual Dipolar Couplings by NMR Spectroscopy. *Angew. Chem. Int. Ed.*, 2002, **41**: 437-440.

Simizu S, Tamura Y, Osada H. Dephosphorylation of Bcl-2 by protein phosphatase 2A results in apoptosis resistance. *Cancer Sci.*, 2004, **95**(3): 266-270.

Sinars CR, Cheung-Flynn J, Rimerman RA, Scammell JG, Smith DF, Clardy J. Structure of the large FK-506-binding protein FKBP51, an Hsp90-binding protein and a component of steroid receptor complexes. *Proc Natl Acad Sci U S A*, 2003, **100**(3): 868-873.

Smet C, Duckert JF, Wieruszeski JM, Landrieu I, Buee L, Lippens G, Deprez B. Control of protein-protein interactions: structure-based discovery of low molecular weight inhibitors of the interactions between Pin1 WW domain and phosphopeptides. *J Med Chem.*, 2005, **48**: 4815-4823.

Sorenson CM. Bcl-2 family members and disease. *Biochim Biophys Acta*., 2004, **1644**(2-3): 169-177.

Stanislaw M., Stepkowski. Molecular targets for existing and novel immunosuppressive drugs. *Expert Reviews in Molecular Medicine*, Cambridge University Press, 2000, **2**: 1-23.

Stein RL. Mechanism of enzymatic and nonenzymatic prolyl cis-trans isomerization. *Adv Protein Chem*., 1993, **44**:1-24.

Sugiura R, Sio SO, Shuntoh H, Kuno T. Molecular genetic analysis of the calcineurin signaling pathways. *Cellular Molecular Life Science*, 2001, **58**: 278-288.

Suzuki M., Youle RJ, Tjandra N. Structure of Bax: coregulation of dimer formation and intra cellular localization. *Cell*., 2000, **103**(4): 645-654.

Suzuki R., Nagata K., Yumoto F., Kawakami M., Nemoto N., Furutani M., Adachi K., Maruyama T., and Tanokura M. Three-dimensional solution structure of an archaeal FKBP with a dual function of peptidyl prolyl cis-trans isomerase and chaperone-like activities. *J Mol Biol*., 2003, **328**(5): 1149-1160.

Tamura Y, Simizu S, Osada H. The phosphorylation status and anti-apoptotic activity of Bcl-2 are regulated by ERK and protein phosphatase 2A on the mitochondria. *FEBS Lett*., 2004, **569**(1-3): 249-255.

Timerman AP, Wiederrecht G, Marcy A, Fleischer S. Characterization of an exchange reaction between soluble FKBP-12 and the FKBP.ryanodine receptor complex. Modulation by FKBP mutants deficient in peptidyl-prolyl isomerase activity. *J Biol Chem.*, 1995, **270**(6): 2451-2459.

Tsujimot Y., Croce CM. Analysis of the structure, transcripts, and protein products of bcl-2, the gene involved in himan follicular lymphoma. *Proc. Natl. Acad.Sci. USA*, 1986, **83**: 5214-5218.

Van Duyne GD, Standaert RF, Karplus PA, Schreiber SL, Clardy J. Atomic structure of FKBP-FK-506, an immunophilin-immunosuppressant complex. *Science*, 1991, **252**(5007): 839-842.

Vander Heiden MG, Thompson CB. Bcl-2 proteins: regulators of apoptosis or of mitochondrial homeostasis. *Nat Cell Biol.*, 1999, **1**(8): E209-216.

Vaux DL, Strasser A. The molecular biology of apoptosis. *Proc Natl Acad Sci U S A*, 1996, **93**(6): 2239-2244.

Vekrellis K, McCarthy MJ, Watson A, Whitfield J, Rubin LL, Ham J. Bax promotes neuronal cell death and is downregulated during the development of the nervous system. *Development*, 1997, **124**(6): 1239-1249.

Vekrellis K, McCarthy MJ, Watson A, Whitfield J, Rubin LL, Ham J. Characterization of an exchange reaction between soluble FKBP12 and the FKBP ryanodine receptor complex. *J. Biological. Biochemistry*, 1992, **270**(6): 2451-2459.

Wada T, Penninger JM. Mitogen-activated protein kinases in apoptosis regulation. *Oncogene*, 2004, **23**(16): 2838-2849.

Wang B PGilmore A.P., and Streuli CH. Bim Is an Apoptosis Sensor That Responds to Loss of Survival Signals Delivered by Epidermal Growth Factor but Not Those Provided by Integrins. *J. Biol. Chem.*, 2004, **279**(40): 41280-41285.

Wang HG, Pathan N, Ethell IM, Krajewski S, Yamaguchi Y, Shibasaki F, McKeon F, Bobo T, Franke TF, Reed JC. Ca^{2+}-induced apoptosis through calcineurin dephosphorylation of BAD. *Science*, 1999, **284**(5412): 339-343.

Wang HQ, Nakaya Y, Du Z, Yamane T, Shirane M, Kudo T, Takeda M, Takebayashi K, Noda Y, Nakayama KI, Nishimura M. Interaction of presenilins with FKBP38 promotes apoptosis by reducing mitochondrial Bcl-2. *Hum Mol Genet.*, 2005, **14**(13): 1889-1902.

Wang K, Yin XM, Chao DT, Milliman CL, Korsmeyer SJ. BID: a novel BH3 domain-only death agonist. *Genes Dev*., 1996, **10**(22):2859-69.

Wang[b] S, Wang Z, Boise L, Dent P, Grant S. Loss of the bcl-2 phosphorylation loop domain increases resistance of human leukemia cells (U937) to paclitaxel-mediated mitochondrial dysfunction and apoptosis. *Biochem Biophys Res Commun.*, 1999, **259**(1): 67-72.

Wang Y. and Jardetzky O. Probability-based protein secondary structure identification using combined NMR chemical-shift data. *Protein Sciences*, 2002, **11**: 852-861.

Weiwad M., F. Edlich, F. Erdmann, F. Jarczowski, S. Kilka, M. Dorn, A. Pechstein, G. Fischer. A reassessment of the inhibitory capacity of human FKBP38 on calcineurin. *FEBS Lett.*, 2005, **579**: 1591-1596.

Wintjens R., Wieruszeski JM, Drobecq H., Rousselot-Pailley P., Buee L., Lippens G., Landrieu I. 1H NMR study on the binding of Pin1 Trp-Trp domain with phosphothreonine peptides. *J Biol Chem.*, 2001, **276**(27): 25150-25156.

Wishart, D.S. and Sykes, B.D. The 13C Chemical-Shift Index: A simple method for the identification of protein secondary structure using ^{13}C chemical shift data. *J. Biomol. NMR.*, 1994, **4**: 171-180.

Wishart, D.S., Sykes, B.D., and Richards, F.M. Relationship between Nuclear Magnetic Resonance Chemical Shift and Protein Secondary Structure. *J. Mol. Biol.*, 1991, **222**: 311-333.

Wolter KG, Hsu YT, Smith CL, Nechushtan A, Xi XG, Youle RJ. Movement of Bax from the cytosol to

mitochondria during apoptosis. *J Cell Biol.*, 1997, **139**(5): 1281-1292.

Wu B, Li P, Liu Y, Lou Z, Ding Y, Shu C, Ye S, Bartlam M, Shen B, Rao Z. 3D structure of human FK-506-binding protein 52: implications for the assembly of the glucocorticoid receptor/Hsp90/ immunophilin heterocomplex. *Proc Natl Acad Sci U S A*, 2004, **101**(22): 8348-8353.

Yamamoto, K., Ichijo, H. and Korsmeyer, S.J. BCL-2 is phosphorylated and inactivated by an ASK1/Jun N-terminal protein kinase pathway normally activated at G(2)/M. *Mol. Cell Biol.*, 1999, **19**: 8469-8478.

Yang E, Zha J, Jockel J, Boise LH, Thompson CB, Korsmeyer SJ. Bad, a heterodimeric partner for Bcl-xL and Bcl-2, displaces Bax and promotes cell death. *Cell*, 1995, **80**(2): 285-291.

Yang J, Liu X, Bhalla B, Kim CN, Ibrado AM *et al.* Prevention of Apoptosis by Bcl-2: Release of Cytochrome c from Mitochondria Blocked. *Science*, 1997, **275**: 1129-1133.

Yasukawa T, Kanei-Ishii C, Maekawa T, Fujimoto J, Yamamoto T, Ishii S. Increase of solubility of foreign proteins in Escherichia coli by coproduction of the bacterial thioredoxin. *J Biol Chem.*, 1995, **270**(43): 25328-25331.

Yin M, Ochs RS. Mechanism for the paradoxical inhibition and stimulation of calcineurin by the immunosuppresive drug tacrolimus (FK-506). *Arch Biochem Biophys*, 2003, **419**(2): 207-213.

Yokote H, Terada T, Matsumoto H, Kakishita K, Kinoshita Y, Nakao N, Nakai K, Itakura T. Dephosphorylation-induced decrease of anti-apoptotic function of Bcl-2 in neuronally differentiated P19 cells following ischemic insults. *Brain Res.*, 2000, **857**(1-2): 78-86.

Yu C, Minemoto Y, Zhang J, Liu J, Tang F, Bui TN, Xiang J, Lin A. JNK suppresses apoptosis via phosphorylation of the proapoptotic Bcl-2 family protein BAD. *Mol Cell.*, 2004, **13**(3): 329-340.

Yu H, Kong H, Chung D. Cloning and characterization of Giardia intestinalis cyclophilin. *The Korean Journal of Parasitology*, 2002, **40**(3): 131-138.

Zha H, Christine AS, Takaaki S and John C.R. Pro-apoptotic protein Bax Heterodimerizes with Bcl-2 and Homodimerizes with Bax via a Novel Domain(BH3) distinct from BH1 and BH2. *Journal of Biological Chemistry*, 1996, **271**(13): 7440-7444.

Zha J, Harada H, Yang E, Jockel J, Korsmeyer SJ. Serine phosphorylation of death agonist BAD in response to survival factor results in binding to 14-3-3 not BCL-X(L). *Cell*, 1996, **87**(4): 619-628.

Zhang J, Zhou B, Zheng CF, Zhang ZY. A Bipartite Mechanism for ERK2 Recognition by Its Cognate Regulators and Substrates. *J. Biol. Chem.*, 2003, **278**: 29901-29912.

Zhang K.Z., Westberg J.A., Holtaa E and Andersson L.C. Bcl-2 regulates neural differentiation. *Proc Natl Acad Sci USA*, 1996, **93**: 4504-4508.

Zhang M, Tanaka T, Ikura M. Calcium-induced conformational transition revealed by the solution structure of apo calmodulin. Nat Struct Biol. 1995,2(9):758-67.

Zornig M, Hueber AO, Baum W, Evan G. Apoptosis regulators and their role in tumorigenesis. *Biochimica et Biophysica Acta*, 2001, **1551**: F1-F37.

Zweckstetter, M. and A. Bax. Characterization of molecular alignment in aqueous suspensions of Pf1 bacteriophage. *Journal of Biomolecular Nmr*, 2001, **20**(4): 365-377.

Zweckstetter M. and Bax A. Prediction of sterically induced alignment in a dilute liquid crystalline phase: aid to protein structure determination by NMR. *J. Am. Chem. Soc.*, 2000, **122**: 3791-3792.

Zweckstetter M., Hummer G., Bax A. Prediction of charge-induced molecular alignment of biomolecules dissolved in dilute liquid-crystalline phases. *Biophys J.*, 2004, **86**(6): 3444-3460.

Appendix 1

A FKBP38NTD

Analysis	Entire Protein
Length	157 aa
Molecular Weight	16891.22 m.w.
1 microgram =	59.202 pMoles
Molar Extinction coefficient	9890
1 A[280] corr. to	1.71 mg/ml
A[280] of 1 mg/ml	0.59 AU
Isoelectric Point	4.92
Charge at pH 7	-11.53

B Bcl-2

Analysis	Entire Protein
Length	225 aa
Molecular Weight	25448.91 m.w.
1 microgram =	39.294 pMoles
Molar Extinction coefficient	44620
1 A[280] corr. to	0.57 mg/ml
A[280] of 1 mg/ml	1.75 AU
Isoelectric Point	6.87
Charge at pH 7	-0.57

C Bcl-xL Δ (M45-A84) ΔTM

Analysis	Entire Protein
Length	177 aa
Molecular Weight	20359.02 m.w.
1 microgram =	49.118 pMoles
Molar Extinction coefficient	36250
1 A[280] corr. to	0.56 mg/ml
A[280] of 1 mg/ml	1.78 AU
Isoelectric Point	5.04
Charge at pH 7	-11.50

D Bcl-xL ΔTM

Analysis	Entire Protein
Length	241 aa
Molecular Weight	27126.43 m.w.
1 microgram =	36.864 pMoles
Molar Extinction coefficient	47630
1 A[280] corr. to	0.57 mg/ml
A[280] of 1 mg/ml	1.76 AU
Isoelectric Point	5.25
Charge at pH 7	-11.32

E Calmodulin

Analysis	Entire Protein
Length	158 aa
Molecular Weight	18012.79 m.w.
1 microgram =	55.516 pMoles
Molar Extinction coefficient	2560
1 A[280] corr. to	7.04 mg/ml
A[280] of 1 mg/ml	0.14 AU
Isoelectric Point	4.35
Charge at pH 7	-24.56

F FKBP38

Analysis	Entire Protein
Length	364 aa
Molecular Weight	39558.20 m.w.
1 microgram =	25.279 pMoles
Molar Extinction coefficient	33840
1 A[280] corr. to	1.17 mg/ml
A[280] of 1 mg/ml	0.86 AU
Isoelectric Point	7.32
Charge at pH 7	0.88

Fig.A.1 The information of the proteins used in this thesis

The proteins used in this thesis were analyzed by Vector NTI.

Appendix 2

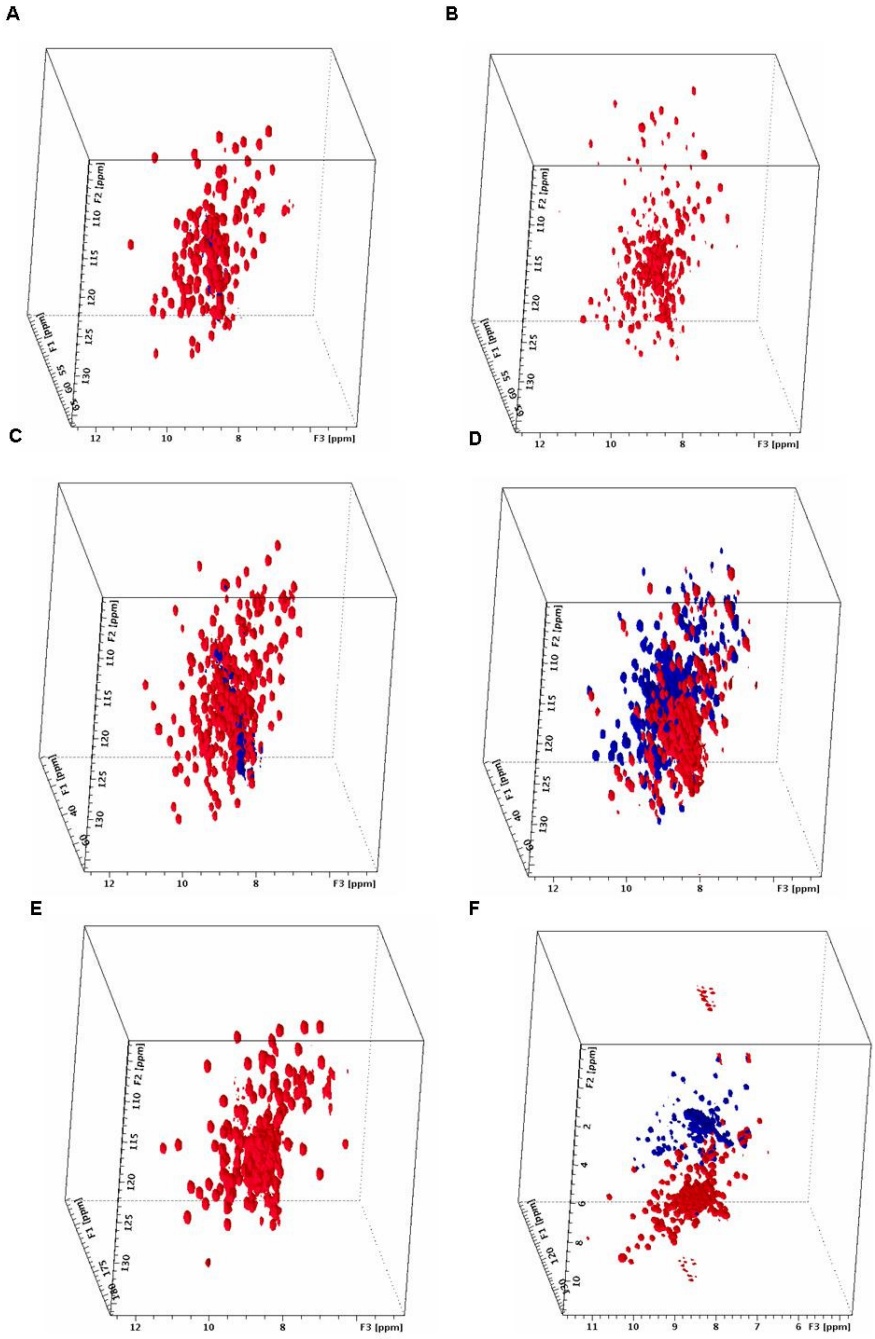

Fig.A.2 The experimental results of backbone assignment showed in three dimension

The ^{13}C and ^{15}N labeled sample was in the phosphate buffer as introduced in the material and methods part. The HNCOCA (A), HNCA(B), CBCACONH(C) and HNCACB (D) data were collected, which can provide the information of $C_{\alpha i}$, $C_{\alpha i-1}$, $C_{\beta i}$ and $C_{\beta i-1}$, all this information will connect with H^N-N cross peak in the ^{15}N HSQC spectrum. E. HNCO experiment. F. HNHA experiment. F1, ^{13}C dimension; F2, ^{15}N dimension; F3, proton dimension. The data was processed by topsin 1.3 from Bruker.

Appendix 3

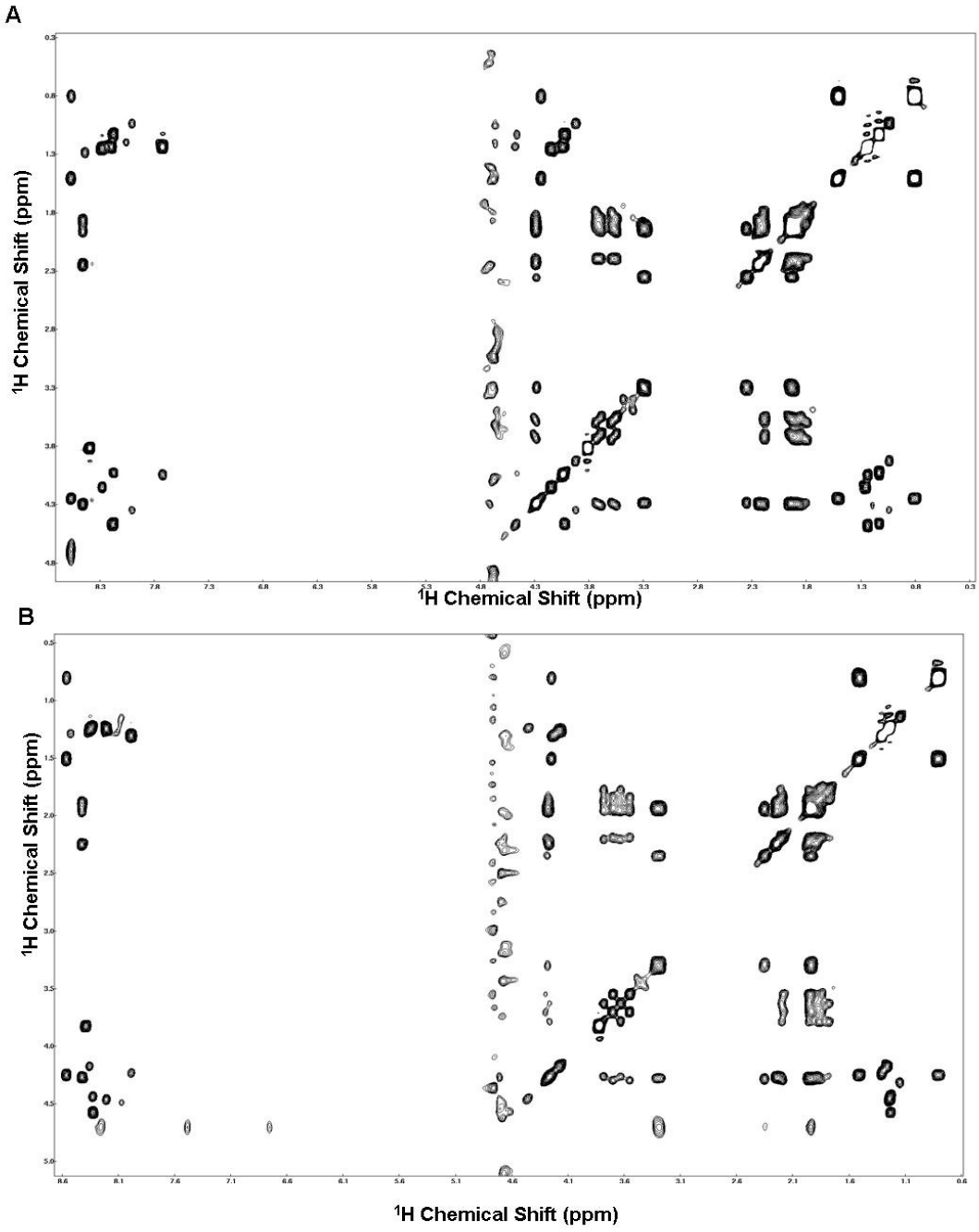

Fig.A.3 Tocsy of T74 and pT74

The Tocsy scpectra of T74 (A) and pT74 (B) were recorded as described in material and methods and visualized in NMRview. The assignment result was list in Table 5.2.

Appendix 4

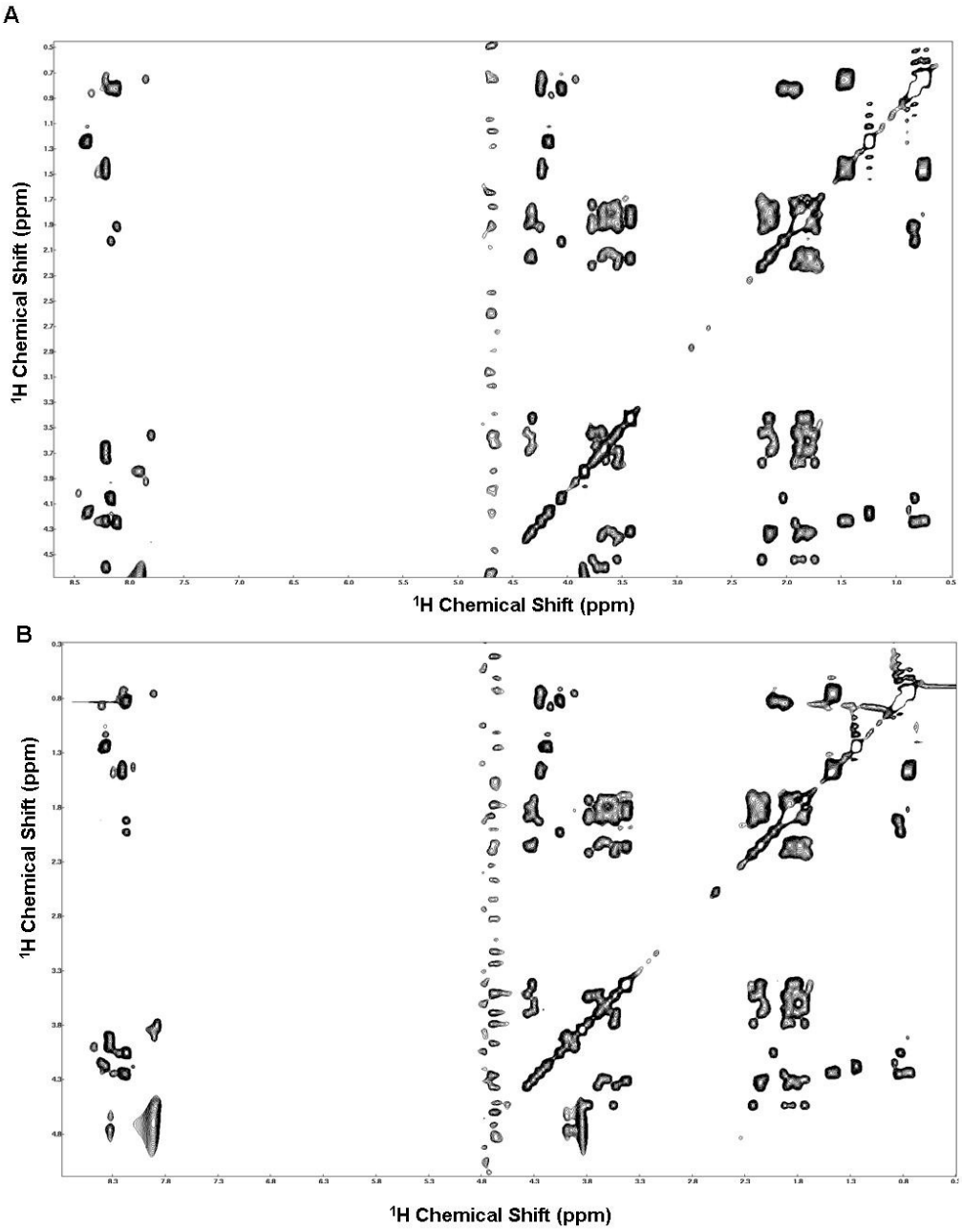

Fig.A.4 Tocsy of S87 and pS87

The Tocsy scpectra of pS87 and S87 were recorded as descripted in materials and methods and visualized in NMRview. The assignment result was list in Table 5.3.

Appendix 5

Table A.1 The assignment of FKBP38NTD

No.Amino acid	Chemical Shift	No.Amino acid	Chemical Shift	No.Amino acid	Chemical Shift	No.Amino acid	Chemical Shift	No.Amino acid	Chemical Shift	No.Amino acid	Chemical Shift
5.CA	61.7	10.CA	55.219	15.CA	53.921	19.HB1	3.045	24.HG2	3.846	29.HD1	3.327
5.HA	4.422	10.HA	4.259	15.HA	4.321	19.C	174.996	24.HG1	3.659	30.N	125.77
5.CB	30.698	10.CB	29.094	15.CB	41.069	20.N	123.512	25.CA	61.476	30.HN	8.488
5.HB2	2.319	10.HB2	2.012	15.HB2	1.647	20.HN	7.966	25.HA	4.724	30.CA	49.368
5.HB1	2.319	10.HB1	1.899	15.HB1	1.561	20.CA	53.923	25.CB	32.919	30.HA	4.529
5.CG	26.171	10.CG	34.77	15.CG	25.519	20.HA	4.288	25.HB2	2.367	30.CB	16.642
5.HG2	2.04	10.HG2	2.272	15.HG	1.572	20.CB	41.131	25.HB1	2.367	30.HB1	1.383
5.HG1	1.945	10.HG1	2.272	15.CD1	22.975	20.HB2	1.572	25.HG2	2.047	31.CA	61.567
5.CD	48.483	10.C	175.928	15.HD11	0.923	20.HB1	1.648	25.HG1	1.915	31.HA	4.405
5.HD2	3.817	11.N	122.226	15.CD2	21.754	20.CG	25.316	25.HD2	2.053	31.CB	30.693
5.HD1	3.646	11.HN	8.343	15.HD21	0.872	20.HG	1.577	25.HD1	1.915	31.HB2	2.281
5.C	176.073	11.CA	52.286	15.C	176.597	20.CD1	23.271	25.C	175.258	31.HB1	2.281
6.N	124.309	11.HA	4.64	16.N	124.5	20.HD11	0.919	26.N	122.848	31.HG2	1.901
6.HN	8.355	11.CB	27.61	16.HN	8.13	20.CD2	22.109	26.HN	8.552	31.HG1	1.901
6.CA	51.401	11.HB2	2.108	16.CA	51.371	20.HD21	0.869	26.CA	53.556	31.CD	48.65
6.HA	4.289	11.HB1	1.948	16.HA	4.303	20.C	176.248	26.HA	4.48	31.HD2	3.815
6.CB	17.961	11.CG	32.033	16.CB	17.692	21.N	124.486	26.CB	28.384	31.HD1	3.656
6.HB1	1.398	11.HG2	2.392	16.HB1	1.417	21.HN	8.07	26.HB2	1.953	31.C	175.686
6.C	177.317	11.HG1	2.392	16.C	177.358	21.CA	51.343	26.HB1	1.865	32.N	125.77
7.N	119.527	11.CD	180.187	17.N	119.96	21.HA	4.225	26.CG	54.931	32.HN	8.324
7.HN	8.417	11.NE2	111.494	17.HN	8.19	21.CB	17.835	26.HG2	2.207	32.CA	49.003
7.CA	55.429	11.HE21	6.83	17.CA	55.514	21.HB1	1.39	26.HG1	2.198	32.HA	4.593
7.HA	4.267	11.HE22	7.52	17.HA	4.229	21.C	176.714	27.CA	61.48	32.CB	16.827
7.CB	28.983	12.CA	62.37	17.CB	29.424	22.N	122.449	27.HA	4.404	32.HB1	1.388
7.HB2	2.059	12.HA	4.428	17.HB2	1.796	22.HN	8.037	27.CB	30.711	33.CA	62.032
7.HB1	1.94	12.CB	30.687	17.HB1	1.623	22.CA	51.111	27.HB2	2.282	33.HA	4.433
7.CG	34.984	12.HB2	2.311	17.CG	25.838	22.HA	4.303	27.HB1	2.282	33.CB	30.719
7.HG2	2.272	12.HB1	2.03	17.HG2	1.402	22.CB	17.893	27.CG	48.656	33.HB2	2.313
7.HG1	2.222	12.CG	26.33	17.HG1	1.402	22.HB1	1.39	27.HG2	2.021	33.HB1	2.313
7.C	175.986	12.HG2	1.908	17.CD	41.983	22.C	176.859	27.HG1	2.021	33.HG2	2.031
8.N	121.652	12.HG1	1.946	17.HD2	3.203	23.N	119.395	27.CD	26.077	33.HG1	1.929
8.HN	8.317	12.CD	50.148	17.HD1	3.203	23.HN	8.127	27.HD2	3.798	33.HD2	3.803
8.CA	55.333	12.HD2	3.807	17.C	175.987	23.CA	54.015	27.HD1	3.632	33.HD1	3.694
8.HA	4.275	12.HD1	3.694	18.N	120.89	23.HA	4.459	27.C	175.704	33.C	176.51
8.CB	29.081	12.C	177.179	18.HN	8.429	23.CB	31.878	28.N	125.902	34.N	120.56
8.HB2	2.094	13.N	109.434	18.CA	55.306	23.HB2	2.08	28.HN	8.376	34.HN	8.505
8.HB1	1.922	13.HN	8.498	18.HA	4.206	23.HB1	2.08	28.CA	49.093	34.CA	55.181
8.CG	34.78	13.CA	44.111	18.CB	29.15	23.CG	30.302	28.HA	4.609	34.HA	4.275
8.HG2	2.258	13.HA2	3.9	18.HB2	1.925	23.HG2	2.594	28.CB	16.857	34.CB	28.923
8.HG1	2.258	13.HA1	3.9	18.HB1	1.885	23.HG1	2.531	28.HB1	1.364	34.HB2	1.943
8.C	175.52	13.C	173.541	18.CG	34.984	23.CE	20.744	29.CA	61.267	34.HB1	1.943
9.N	124.574	14.N	123.401	18.HG2	2.173	23.HE1	1.994	29.HA	4.531	34.CG	34.882
9.HN	8.199	14.HN	8.033	18.HG1	2.103	23.C	175.287	29.CB	32.894	34.HG2	2.236
9.CA	51.223	14.CA	51.6	18.C	175.724	24.N	123.379	29.HB2	2.474	34.HG1	2.236
9.HA	4.303	14.HA	4.287	19.N	120.62	24.HN	8.274	29.HB1	2.474	34.C	175.87
9.CB	18.175	14.CB	17.993	19.HN	8.108	24.CA	53.059	29.CG	30.386	35.N	121.706

Assignment of FKBP38NTD (CONT)

No.Amino acid	Chemical Shift	No.Amino acid	Chemical Shift	No.Amino acid	Chemical Shift	No.Amino acid	Chemical Shift	No.Amino acid	Chemical Shift	No.Amino acid	Chemical Shift
35.HB2	2.06	40.HN	8.638	45.HA	5.227	48.HG2	1.458	53.N	107.176	60.CG	26.657
35.HB1	2.06	40.CA	52.566	45.CB	42.182	48.HG1	1.458	53.HN	9.207	60.CD	50.506
35.CG	35.061	40.HA	4.593	45.HB2	1.273	48.CD	22.873	53.CA	42.504	60.C	173.715
35.HG2	2.228	40.CB	40.635	45.HB1	1.273	48.HD2	1.458	53.HA2	3.384	61.N	113.932
35.HG1	2.283	40.HB2	1.604	45.CG	26.234	48.HD1	0.135	53.HA1	4.013	61.HN	7.928
35.C	175.986	40.HB1	1.604	45.HG	1.273	48.CE	40.581	55.CA	62.605	61.CA	57.938
36.N	120.078	40.CG	25.404	45.CD1	25.591	48.HE2	2.407	55.HA	4.427	61.HA	4.408
36.HN	8.254	40.HG	1.342	45.HD11	0.784	48.HE1	2.407	55.CB	30.069	61.CB	33.641
36.CA	55.652	40.CD1	24.892	45.CD2	23.817	48.C	174.646	55.HB2	2.308	61.HB	1.98
36.HA	4.717	40.HD11	0.811	45.HD21	0.507	49.N	125.504	55.HB1	2.276	61.CG2	19.51
36.CB	29.592	40.CD2	21.041	45.C	174.006	49.HN	9.112	55.HG2	2.022	61.HG21	0.927
36.HB2	3.074	40.HD21	0.797	46.N	125.371	49.CA	64.135	55.HG1	1.905	61.CG1	19.51
36.HB1	2.961	40.C	177.529	46.HN	8.82	49.HA	3.964	55.HD2	3.813	61.HG11	0.772
36.HD1	7.246	41.N	108.238	46.CA	53.185	49.CB	67.608	55.HD1	3.67	61.C	174.56
36.NE1	129.387	41.HN	7.581	46.HA	5.915	49.HB	4.046	55.C	177.558	62.N	122.138
36.HE1	10.084	41.CA	44.948	46.CB	33.787	49.HG21	1.886	56.N	112.355	62.HN	8.248
36.HZ2	5.96	41.HA2	4.126	46.HB2	1.814	49.C	172.667	56.HN	8.835	62.CA	57.883
36.HH2	7.036	41.HA1	3.593	46.HB1	1.76	50.N	128.264	56.CA	44.02	62.HA	3.607
36.HZ3	6.101	41.C	172.376	46.CG	25.519	50.HN	9.134	56.HA2	4.171	62.CB	31.177
36.HE3	7.477	42.N	114.058	46.HG2	1.347	50.CA	54.91	56.HA1	3.743	62.HB2	1.742
36.C	175.287	42.HN	7.088	46.HG1	1.347	50.HA	4.464	56.C	174.123	62.HB1	1.7
37.N	126.035	42.CA	49.97	46.CD	42.718	50.CB	41.423	57.N	115.805	62.CG	23.484
37.HN	9.583	42.HA	4.883	46.HD2	2.782	50.HB2	1.572	57.HN	7.814	62.HG2	1.314
37.CA	53.316	42.CB	37.657	46.HD1	2.782	50.HB1	1.572	57.CA	57.205	62.HG1	1.333
37.HA	4.577	42.HB2	2.769	46.C	174.036	50.CG	28.7	57.HA	4.351	62.CD	27.554
37.CB	42.418	42.HB1	3.298	47.N	120.855	50.HG	1.413	57.CB	63.081	62.HD2	1.513
37.HB2	1.493	42.C	175.753	47.HN	9.022	50.CD1	25.505	57.HB2	4.034	62.HD1	1.513
37.HB1	1.493	43.N	111.442	47.CA	53.369	50.HD11	0.835	57.HB1	3.976	62.CE	27.147
37.CG	37.461	43.HN	9.894	47.HA	5.948	50.HD21	0.751	57.C	173.104	62.HE2	3.721
37.HG	1.493	43.CA	44.395	47.CB	35.787	50.C	176.539	58.N	115.941	62.HE1	3.721
37.CD1	26.245	43.HA2	4.059	47.HB2	1.801	51.N	119.748	58.HN	8.202	62.C	176.364
37.HD11	0.97	43.HA1	3.485	47.HB1	1.762	51.HN	8.15	58.CA	56.146	63.N	113.816
37.CD2	24.253	43.C	174.036	47.CG	23.585	51.CA	58.064	58.HA	4.771	63.HN	8.739
37.HD21	0.97	44.N	117.509	47.HG2	1.377	51.HA	4.466	58.CB	64.114	63.CA	43.535
37.C	175.316	44.HN	7.661	47.HG1	1.481	51.CB	34.948	58.HB2	3.912	63.HA2	3.545
38.N	127.496	44.CA	54.823	47.CD	28.063	51.HB	1.981	58.HB1	3.823	63.HA1	4.4
38.HN	8.98	44.HA	4.378	47.HD2	1.446	51.HG21	0.927	58.C	172.26	63.C	174.327
38.CA	51.582	44.CB	42.372	47.HD1	1.358	51.HG11	0.773	59.N	120.855	64.N	118.199
38.HA	4.767	44.HB2	1.639	47.CE	40.072	52.CA	61.247	59.HN	8.019	64.HN	8.059
38.CB	38.476	44.HB1	1.639	47.HE2	2.775	52.HA	4.415	59.CA	52.553	64.CA	55.839
38.HB2	1.908	44.CG	34.78	47.HE1	2.575	52.CB	31.026	59.HA	5.174	64.HA	4.464
38.HB1	1.908	44.HG	1.639	47.C	173.541	52.HB2	2.284	59.CB	28.966	64.CB	28.866
38.C	175.462	44.CD1	25.57	48.N	129.488	52.HB1	2.284	59.HB2	1.768	64.HB2	2.154
39.N	124.707	44.HD11	0.921	48.HN	9.524	52.CG	21.278	59.HB1	1.768	64.HB1	2.154
39.HN	8.299	44.CD2	26.724	48.CA	53.318	52.HG2	2.012	59.HG2	1.544	64.CG	35.493
39.CA	65.621	44.HD21	0.872	48.HA	4.674	52.HG1	1.9	59.HG1	1.544	64.HG2	2.461

Assignment of FKBP38NTD (CONT)

No.Amino acid	Chemical Shift	No.Amino acid	Chemical Shift	No.Amino acid	Chemical Shift	No.Amino acid	Chemical Shift	No.Amino acid	Chemical Shift	No.Amino acid	Chemical Shift
65.CA	61.148	70.CA	52.277	74.HB1	1.925	79.HG2	1.697	84.HA	4.3	88.HA	4.985
65.HA	4.265	70.HA	5.367	74.CG	25.926	79.HG1	1.697	84.CB	31.424	88.CB	39.463
65.CB	30.268	70.CB	45.887	74.HG	1.738	79.CD	26.028	84.HB2	2.315	88.HB2	3.134
65.HB	2.327	70.HB2	1.508	74.CD1	23.585	79.HD2	3.243	84.HB1	2.241	88.HB1	3.134
65.CG2	20.156	70.HB1	1.508	74.HD11	0.972	79.HD1	3.243	84.CG	25.7	88.HD1	6.983
65.HG21	0.871	70.CG	45.677	74.CD2	21.143	79.C	175.899	84.HG2	2.02	88.HE1	7.198
65.CG1	20.156	70.HG	1.508	74.HD21	0.843	80.N	121.768	84.HG1	1.922	88.HZ	6.869
65.HG11	0.871	70.CD1	25.824	74.C	178.431	80.HN	8.906	84.CD	50.16	88.C	171.823
65.C	176.51	70.HD11	0.936	75.N	121.52	80.CA	61.403	84.HD2	3.812	89.N	117.934
66.N	124.84	70.CD2	24.094	75.HN	8.682	80.HA	4.368	84.HD1	3.689	89.HN	9.13
66.HN	9.13	70.HD21	0.803	75.CA	58.259	80.CB	32.364	84.C	175.142	89.CA	60.853
66.CA	57.127	70.C	174.21	75.HA	3.964	80.HB	2.02	85.N	118.598	89.HA	4.561
66.HA	5.06	71.N	126.168	75.CB	28.367	80.HG21	0.89	85.HN	8.304	89.CB	67.014
66.CB	32.199	71.HN	9.049	75.HB2	2.035	80.HG11	0.805	85.CA	53.756	89.HB	4.147
66.HB	1.629	71.CA	54.238	75.HB1	2.035	80.C	174.822	85.HA	4.416	89.CG2	20.736
66.CG2	20.796	71.HA	5.036	75.CG	34.882	81.N	118.195	85.CB	29.669	89.HG21	0.953
66.HG21	0.668	71.CB	31.099	75.HG2	2.235	81.HN	7.792	85.HB2	2.053	89.C	174.676
66.CG1	20.796	71.HB2	2.236	75.HG1	2.235	81.CA	54.865	85.HB1	2.053	90.N	131.215
66.HG11	0.668	71.HB1	2.201	75.C	176.073	81.HA	4.658	85.CG	35.289	90.HN	8.964
66.C	172.726	71.CG	33.378	76.N	113.418	81.CB	30.627	85.HG2	2.053	90.CA	55.484
67.N	114.879	71.HG2	2.313	76.HN	7.712	81.HB2	2.195	85.HG1	2.053	90.HA	4.364
67.HN	7.832	71.HG1	2.313	76.CA	51.373	81.HB1	2.114	85.C	173.279	90.CB	40.968
67.CA	59.857	71.CD	178.677	76.HA	4.561	81.CG	32.338	86.N	128.293	90.HB2	1.934
67.HA	5.303	71.NE2	111.2	76.CB	35.984	81.HG2	2.387	86.HN	8.814	90.HB1	1.934
67.CB	68.855	71.HE21	7.478	76.HB2	2.888	81.HG1	2.387	86.CA	53.89	90.HG	1.609
67.HB	3.983	71.HE22	6.67	76.HB1	2.888	81.NE2	111.085	86.HA	4.609	90.CD1	23.891
67.CG2	19.413	71.C	174.181	76.C	175.753	81.HE21	6.348	86.CB	41.315	90.HD11	1.044
67.HG21	1.064	72.N	123.777	77.N	108.105	81.HE22	6.704	86.HB2	1.59	90.CD2	25.214
67.C	174.298	72.HN	9.128	77.HN	8.207	81.C	172.58	86.HB1	1.59	90.HD21	0.746
68.N	119.527	72.CA	61.34	77.CA	43.641	82.N	125.785	86.CG	26.181	90.C	177.587
68.HN	9.584	72.HA	4.911	77.HA2	3.755	82.HN	8.709	86.HG	1.274	91.N	119.907
68.CA	56.315	72.CB	68.226	77.HA1	4.4	82.CA	54.605	86.CD1	25.159	91.HN	10.63
68.HA	5.611	72.HB	4.4	77.C	174.385	82.HA	5.054	86.HD11	0.938	91.CA	44.637
68.CB	33.519	72.CG2	22.364	78.N	117.954	82.CB	30.586	86.CD2	25.621	91.HA2	3.933
68.HB	2.217	72.HG21	1.166	78.HN	7.768	82.HB2	2.085	86.HD21	0.778	91.HA1	4.271
68.CG2	20.125	72.C	173.482	78.CA	62.827	82.HB1	2.085	86.C	173.977	91.C	173.657
68.HG21	1.085	73.N	122.981	78.HA	4.051	82.CG	34.984	87.N	128.559	92.N	121.432
68.CG1	19.209	73.HN	9.194	78.CB	68.132	82.HG2	2.206	87.HN	8.344	92.HN	7.825
68.HG11	0.951	73.CA	55.936	78.HB	3.272	82.HG1	2.206	87.CA	59.378	92.CA	53.103
68.C	173.104	73.HA	5.544	78.CG2	19.727	82.C	173.861	87.HA	5.335	92.HA	4.867
69.N	121.52	73.CB	64.829	78.HG21	1.237	83.N	125.878	87.CB	32.446	92.CB	39.703
69.HN	8.741	73.HB2	3.727	78.C	173.32	83.HN	9.071	87.HB	1.825	92.HB2	2.73
69.CA	52.845	73.HB1	3.727	79.N	129.621	83.CA	51.111	87.CG2	19.413	92.HB1	2.53
69.HA	5.363	73.C	172.522	79.HN	8.921	83.HA	5.012	87.HG21	0.996	92.CG	0
69.CB	31.733	74.N	119.527	79.CA	55.755	83.CB	30.716	87.CG1	19.413	92.C	175.054
69.HB2	3.118	74.HN	8.64	79.HA	4.48	83.HB2	1.922	87.HG11	0.731	93.N	117.137

Assignment of FKBP38NTD (CONT)

No.Amino acid	Chemical Shift	No.Amino acid	Chemical Shift	No.Amino acid	Chemical Shift	No.Amino acid	Chemical Shift	No.Amino acid	Chemical Shift	No.Amino acid	Chemical Shift
93.HB2	3.21	98.N	115.941	102.C	174.676	107.CB	40.657	113.CB	33.972	119.N	125.813
93.HB1	3.21	98.HN	8.969	103.N	124.84	107.HB2	2.271	113.HB2	2.022	119.HN	9.156
93.HG	0.039	98.CA	53.527	103.HN	7.946	107.HB1	2.271	113.HB1	1.985	119.CA	57.808
93.C	174.006	98.HA	3.835	103.CA	66.475	107.C	177.063	113.CG	31.422	119.HA	3.97
94.N	119.926	98.CB	19.047	103.HA	3.972	108.N	121.785	113.HG2	2.544	119.CB	30.366
94.HN	9.089	98.HB1	1.128	103.CB	28.851	108.HN	8.476	113.HG1	2.677	119.HB2	1.633
94.CA	53.989	98.C	178.344	103.HB	2.282	108.CA	65.49	113.C	173.808	119.HB1	1.633
94.HA	4.665	99.N	114.348	103.CG2	0	108.HA	3.32	114.N	128.027	119.CG	22.771
94.CB	40.667	99.HN	7.262	103.HG21	1.294	108.CB	29.406	114.HN	9.715	119.HG2	0.915
94.HB2	2.715	99.CA	55.23	103.HG11	1.012	108.HB	2.057	114.CA	58.816	119.HG1	0.618
94.HB1	2.464	99.HA	4.179	104.CA	64.255	108.HG21	0.935	114.HA	5.601	119.CD	27.758
94.C	175.491	99.CB	41.781	104.HA	4.425	108.HG11	0.832	114.CB	34.091	119.HD2	1.382
95.N	111.027	99.HB2	1.494	104.CB	29.522	108.C	176.364	114.HB	2.024	119.HD1	1.382
95.HN	6.782	99.HB1	1.497	104.HB2	2.314	109.N	116.473	114.CG2	19.616	119.CE	22.262
95.CA	57.486	99.CG	25.621	104.HB1	2.282	109.HN	8.828	114.HG21	0.915	119.HE2	2.774
95.HA	4.288	99.HG	1.347	104.HG2	2.019	109.CA	43.576	114.CG1	18.395	119.HE1	2.774
95.CB	33.13	99.CD1	23.382	104.HG1	1.948	109.HA2	4.405	114.HG11	0.857	119.C	176.51
95.HB	1.816	99.HD11	0.74	104.HD2	3.815	109.HA1	3.713	114.C	175.608	120.N	115.543
95.CG2	19.922	99.CD2	22.364	104.HD1	3.693	109.C	173.599	115.N	119.527	120.HN	7.601
95.HG21	0.338	99.HD21	0.773	104.C	175.113	110.N	124.445	115.HN	9.302	120.CA	56.011
95.CG1	16.563	99.C	176.452	105.N	115.145	110.HN	8.492	115.CA	59.089	120.HA	4.724
95.HG11	0.106	100.N	121.121	105.HN	7.39	110.CA	54.333	115.HA	5.133	120.CB	37.771
95.C	174.734	100.HN	7.202	105.CA	51.955	110.HA	4.645	115.CB	68.329	120.HB2	3.289
96.N	112.621	100.CA	56.382	105.HA	4.368	110.CB	31.935	115.HB	4.122	120.HB1	2.576
96.HN	7.637	100.HA	4.612	105.CB	39.711	110.HB2	2.008	115.CG2	20.227	120.HD1	6.953
96.CA	60.901	100.CB	40.772	105.HB2	1.778	110.HB1	2.008	115.HG21	1.134	120.HE1	6.717
96.HA	4.26	100.HB2	2.412	105.HB1	1.693	110.CG	36.779	115.C	173.046	120.HD2	6.721
96.CB	37.3	100.HB1	2.412	105.CG	26.13	110.HG2	2.788	116.N	126.832	120.C	172.842
96.HB	2.258	100.C	177.238	105.HG	1.632	110.HG1	2.718	116.HN	8.659	121.N	119.926
96.HG12	1.756	101.N	109.965	105.CD1	24.705	110.C	175.899	116.CA	48.888	121.HN	7.726
96.HG11	1.4	101.HN	8.229	105.HD11	0.979	111.N	119.527	116.HA	5.355	121.CA	55.709
96.CD1	27.872	101.CA	54.043	105.CD2	21.855	111.HN	8.985	116.CB	23.983	121.HA	4.461
96.HD11	0.489	101.HA	4.264	105.HD21	0.858	111.CA	60.767	116.HB1	1.113	121.CB	25.991
96.CG2	16.919	101.CB	42.234	105.C	175.142	111.HA	5.595	116.C	173.744	121.HB2	3.249
96.HG21	0.857	101.HB2	1.784	106.N	121.387	111.CB	69.033	117.N	120.723	121.HB1	2.85
96.C	176.83	101.HB1	1.784	106.HN	7.873	111.HB	4.071	117.HN	8.173	121.C	173.279
97.N	124.574	101.CG	20.939	106.CA	53.499	111.CG2	20.329	117.CA	53.992	122.N	122.582
97.HN	9.05	101.HG	1.784	106.HA	4.396	111.HG21	1.182	117.HA	4.472	122.HN	9.362
97.CA	58.201	101.CD1	25.01	106.CB	34.011	111.C	173.191	117.CB	45.531	122.CA	57.421
97.HA	3.997	101.HD11	0.836	106.HB2	2.186	112.N	131.348	117.HB2	2.489	122.HA	4.538
97.CB	28.184	101.CD2	25.01	106.HB1	2.186	112.HN	9.969	117.HB1	2.489	122.CB	35.893
97.HB2	2.484	101.HD21	0.664	106.CG	30.864	112.CA	49.224	117.C	176.19	122.HB2	3.178
97.HB1	2.484	101.C	177.354	106.HG2	2.48	112.HA	5.187	118.N	120.723	122.HB1	3.09
97.CG	33.661	102.N	111.824	106.HG1	2.48	112.CB	22.113	118.HN	8.609	122.HD1	7.131
97.HG2	2.644	102.HN	7.176	106.HE1	2.072	112.HB1	1.526	118.CA	61.218	122.HE1	6.65
97.HG1	2.644	102.CA	59.308	106.C	172.784	112.C	173.083	118.HA	3.961	122.C	175.899

Assignment of FKBP38NTD (CONT)

No.Amino acid	Chemical Shift	No.Amino acid	Chemical Shift	No.Amino acid	Chemical Shift	No.Amino acid	Chemical Shift	No.Amino acid	Chemical Shift	No.Amino acid	Chemical Shift
123.HA1	4.157	128.HD2	3.248	135.HB2	3.264	140.CD2	24.196	145.CA	57.763	150.N	124.043
124.CA	62.428	128.HD1	3.248	135.HB1	3.195	140.HD21	0.693	145.HA	4.324	150.HN	8.675
124.HA	4.549	128.C	175.957	135.C	173.279	140.C	174.53	145.CB	31.647	150.CA	54.911
124.CB	31.206	129.N	112.887	136.N	122.316	141.N	125.371	145.HB2	1.666	150.HA	4.185
124.HB2	2.32	129.HN	7.434	136.HN	7.415	141.HN	9.203	145.HB1	1.571	150.CB	41.461
124.HB1	2.32	129.CA	53.556	136.CA	51.179	141.CA	54.818	145.CG	23.493		
124.CG	26.329	129.HA	4.496	136.HA	4.38	141.HA	5.227	145.HG2	1.405		
124.HG2	2.027	129.CB	62.487	136.CB	18.714	141.CB	30.025	145.HG1	1.405		
124.HG1	1.897	129.HB2	3.763	136.HB1	1.262	141.HB2	2.072	145.CD	27.656		
124.CD	50.783	129.HB1	3.606	136.C	175.52	141.HB1	2.072	145.HD2	1.405		
124.HD2	3.806	130.CA	61.507	137.N	128.691	141.CG	35.9	145.HD1	1.405		
124.HD1	3.806	130.HA	4.734	137.HN	8.398	141.HG2	2.199	145.CE	22.93		
124.C	175.811	130.CB	33.055	137.CA	50.967	141.HG1	1.955	145.HE2	2.994		
125.N	113.684	130.HB2	2.367	137.HA	4.637	141.C	175.142	145.HE1	2.994		
125.HN	8.089	130.HB1	3.367	137.CB	17.844	142.N	127.629	145.C	176.277		
125.CA	56.448	130.CG	23.404	137.HB1	1.45	142.HN	9.368	146.N	106.246		
125.HA	4.146	130.HG2	2.054	137.C	176.801	142.CA	59.024	146.HN	7.367		
125.CB	27.784	130.HG1	1.912	138.N	117.402	142.HA	5.051	146.CA	58.979		
125.HB2	2.164	130.CD	48.749	138.HN	8.266	142.CB	34.142	146.HA	4.514		
125.HB1	2.157	130.HD2	3.848	138.CA	52.147	142.HB	2.111	146.CB	71.579		
125.CG	32.03	130.HD1	3.663	138.HA	5.238	142.CG2	19.947	146.HB	4.073		
125.HG2	2.548	130.C	174.705	138.CB	44.348	142.HG21	0.844	146.CG2	20.743		
125.HG1	2.427	131.N	121.387	138.HB2	1.921	142.CG1	19.579	146.HG21	1.105		
125.CD	179.961	131.HN	8.655	138.HB1	1.921	142.HG11	0.844	146.C	171.212		
125.NE2	112.27	131.CA	57.7	138.CG	22.262	142.C	174.181	147.N	123.111		
125.HE21	7.508	131.HA	4.403	138.HG	1.921	143.N	123.777	147.HN	8.277		
125.HE22	6.832	131.CB	35.914	138.CD1	24.196	143.HN	9.154	147.CA	50.691		
125.C	178.257	131.HB2	2.996	138.HD11	1.017	143.CA	60.191	147.HA	5.02		
126.N	105.184	131.HB1	2.997	138.CD2	24.807	143.HA	5.603	147.CB	20.819		
126.HN	7.078	131.HD1	7.21	138.HD21	0.851	143.CB	69.509	147.HB1	1.129		
126.CA	43.432	131.HE1	6.809	138.C	175.928	143.HB	4.072	147.C	174.743		
126.HA2	3.783	131.C	173.686	139.N	120.59	143.CG2	19.413	148.N	118.465		
126.HA1	3.476	132.N	128.957	139.HN	8.83	143.HG21	1.035	148.HN	8.723		
126.C	170.787	132.HN	7.856	139.CA	56.503	143.C	173.861	148.CA	58.499		
127.N	113.949	132.CA	55.946	139.HA	5.088	144.N	129.356	148.HA	4.582		
127.HN	8.492	132.HA	4.107	139.CB	26.979	144.HN	8.427	148.CB	34.345		
127.CA	54.94	132.CB	40.155	139.HB2	2.881	144.CA	53.251	148.HB	2.119		
127.HA	4.506	132.HB	1.136	139.HB1	2.696	144.HA	4.652	148.CG2	19.702		
127.CB	63.05	132.HG12	1.136	139.HG	0	144.CB	39.7	148.HG21	0.876		
127.HB2	3.136	132.HG11	1.136	139.C	172.988	144.HB2	1.37	148.CG1	19.148		
127.HB1	3.058	132.HD11	0.922	140.N	127.895	144.HB1	1.37	148.HG11	0.842		
128.CA	56.323	132.HG21	0.922	140.HN	9.919	144.CG	22.771	148.C	173.803		
128.HA	4.425	134.CA	62.523	140.CA	51.986	144.HG	1.37	149.N	122.981		
128.CB	29.698	134.CB	31.791	140.HA	5.283	144.CD1	26.028	149.HN	8.49		
128.HB2	1.956	134.C	175.404	140.CB	41.681	144.HD11	0.811	149.CA	52.986		
128.HB1	1.823	135.N	115.277	140.HB2	1.646	144.CD2	26.028	149.HA	4.844		

Appendix 6

Table A.2 The primers used in the study

Items	Remarks	Sequence
HYD36	Forward primer for deletion from D28 to M83 of Bcl-xL	GCA GCA GTA AAG CAA GCG CTG AGG
HYD37	Reverse primer for deletion from D28 to M83 of Bcl-xL	ACAAAACTGACTCCAGCTGTATCC
HYD38	Reverse primer for deletion form D34 to P90 of Bcl-2	ATC TCC CGC ATC CCA CTC GTA GCC
HYD39	Forward primer for deletion from D34 to P90 of Bcl-2	CCTGTGGTCCACCTGGCCCTGCGC
HYD40	Reverse primer for Bcl-xL with termination codon –SalI	GCGAAGCTGTCGACTTATCATTTCCGACTGAAGAGTGAGCCCAG
HYD41	Reverse primer for Bcl-2 from the end with termination codon –SalI	GCGAAGCTGTCGACTTATCACTTGTGGCTCAGATAGGCACCCAG
HYD43	FORWARD PRIMER FOR FKBP-38 WITH Bam HI	CACTCAGGATCCGAATGGGACAACCCCCGGCGGAGGAGGCT
HYD48	forward primer for FKBP38 starting from M58 –Nde I	CACTCAGCATATGGGACAACCTCCGGCGGAGGAGGCT
HYD49	reverse primer for FKBP38 ending N370 – Xho I WITH TERMINATION CODON	GCGAAGCTCGAGTCACTAGTTGCCCAGCATTTTCCGGTACAA
HYD50	reverse primer for FKBP38 ending N370 – Xho I	GCGAAGCTCGAGGTTGCCCAGCATTTTCCGGTACAA
HYD51	Reverse primer for deletion from D28 to M83 of Bcl-xL	ACTAAACTGACTCCAGCTGTATCC
HYD75	Bcl-2 without TM for pAS2-1	GCGAAGCTGTCGACCTATCACCGCATGCTGGGGCCGTACAGTTC
HYD76	Bcl-2 from P44 REVERSE	GGGGGCGGCCCCCGGGGGCGCGGC
HYD77	Bcl-2 from G54	CCCGGGCTGGGAGGAGAAGAT
HYD78	Bcl-2 loop deletion	GCC GCC GCG GGG CCT GCG CTC AGC
HYD79	Bcl-2 loop deletion	TCGCCGCTGCAGACCCCGGCTGCC
HYD80	HS SOD2	CACTCAGCATATGttgagccgggcagtgtgc
HYD81	HS SOD2	GCGTGATCTCGAGttacttttgcaagccatgt
HYD82	Bcl-2 loop deletion from P64 forward primer	CCGGTCGCCAGGACCTCGCCGCTG
HYD89	forward primer for L and D mutation in the BH3 pocket of Bcl-2	AGCcgccaggccggcAGCgacttctcccgccgctac
HYD90	reverse primer for the LD mutation in the BH3 pocket of Bcl-2 (there are some over lap so PCR can be performed to do mutation)	GCTGCCGGCCTGGCGGCT GGTCAGGTGGACCACAGGTGGCACCGG
HYD91	461(p) OF FKBP38	TGGGCTCCTGCTGCCTTGGGG
HYD92	879 DELETION OF FKBP38	ATCCCCATCCTGAGGGCAGCCCT
HYD139	forward primer for deletion from D28 to M83 of Bcl-xL with additional 6A	GCAGCAGCAGCAGCAGCAatggcagcagtaaagcaa
HYD140	forward primer for Bcl-xL loop deletion from D28 to D61	AGCCCCGCGGTGAATGGAGCCACT
HYD143	V80 to F80 Mutant of FKBP38 (Forward Primer)	GAGAATGGCACACGGTTTCAGGAGGAGCCGG
HYD144	V80 to F80 Mutant of FKBP38 (Reverse Primer)	CCGGCTCCTCCTGAAACCGTGTGCCATTCTC
HYD147	FKBP38 Full Length for pEGFP-C2 Forward Primer (XhoI)	CACTCAGCTCGAGCggacaacccccggcggaggaggct
HYD148	FKBP38 Full Length for pEGFP-C2 Reverse Primer (BamHI)	GCGAAGGGATCCTCAGTTCCTGGCAGCGATGACCACAGA
HYD149	FKBP38 ?TM for pEGFP-C2 Reverse Primer (BamHI)	GCGAAGGGATCCTCACTAGTTGCCCAGCATTTTCCGGTACAA
HYD150	forward primer for Bcl-xL loop deletion from D28 to E41	aatcggagatggagaccccc
HYD151	Reverse loop deletion from S48 to	gggggtctccatctccgattc
HYD152	forward primer for FKBP38 containing N-sequencing. Longer version	CAC TCA G CATatggcgtcttgggctgagccctct
HYD172	forward primer to amplify Pin1 homolog sequence	CAC TCA G CATatgGtcctggccgccaactccta
HYD173	reverse primer to amplify Pin1 homolog sequence(XhoI)	GCG AAG CTCGAGCacagagagtgccacaccccc
HYD176	Forward primer to amplify Erk2	CAC TCA G CAT atggcggcggcggcggcgcg
HYD177	Reverse primer to amplify Erk2	GCG AAG CTCGAGttaagatctgtatcctggctg
HYD178	Reverse primer for FKBP38, end at D205 FKBP domain	GCG AAG CTCGAGgtccacagccgtcttcagggt
HYD179	Reverse primer for FKBP38, end at L209 FKBP domain	GCG AAG CTCGAGcaggtcaggcccgtccacagc
HYD180	Forward primer for Bcl-2 mutation. ACG changed into GCA (T56) Bcl-2, use with HYD77	cacGCAccccatccagccgcatcccgg
HYD181	Reverse primer for S70-A70, used with next primer	ggtcctggcgaccgggtcccg
HYD182	Forward primer for S70-A70, tcg to GCA	GCAccgctgcagaccccggctGCC
HYD183	Reverse primer for Bcl-2 mutation S80-A80	gagcgcaggccccgcggcggc
HYD184	Forward primer for Bcl-2 mutation agc changed into GCA	GCAccggtgccacctgtggtcCAC

HYD185	Reverse primer for FKBP38ΔTM stop at A394	GCGAAGCTCTCGAGCTATCAcgccccaaacagccacttcca
HYD186	Forward primer for FKBP38 start from M1	CACTCAGCATatggcatcgtgtgctgaaccc
HYD187	Forward primer for FKBP38 start at R103	CACTCAGCATATG aggaagaagacgctggtccca
HYD188	Reverse primer for FKBP38 stop at A394	GCG AAG CTCGAGcgccccaaacagccacttcca
HYD189	Forward primer for FKBP38 start from L21	CACTCAGCATATG ctcgaggacttcgaggtactg
HYD190	FKBP38 START FROM G98	CACTCAGCATATG gggaacgggctgttgaggaag
HYD191	pEGFP-C2 1266-1287 sequencing forward primer	catggtcctgctggagttcgt
HYD192	pEGFP-C2 sequencing REVERSE primer	tgtggtatggctgattatgatcag
HYD195	Overlap with 180 reverse PRIMER	tgcggctggatggggtgcgtgcccgggctgggaggagaagat
HYD196	Overlap with hyd 182 , reverse primer	agccggggtctgcagcggtgcggtcctggcgaccgg
HYD197	Overlap with HYD184	gtggaccacaggtggcaccggtgcgagcgcaggccccgcggc
HYD198	Bcl-2 for bicistronic system Hind III reverse	GCGAAGCTaagcttcattaCCGCATGCTGGGGCCGTACAGTTC
HYD199	FKBP38 forward hind III	CACTCAGaagcttGGACAACCCCCGGCGGAGGAGGCT
HYD235	Forward Primer for Bcl-2 Mutant T56A	GCCCGGGCACGCACCCCATCCAGCC
HYD236	Reverse Primer for Bcl-2 Mutant T56A	GGCTGGATGGGGTGCGTGCCCGGGC
HYD237	Forward Primer for Bcl-2 Mutant S70A	GTCGCCAGGACCGCCCCGCTGCAGACC
HYD238	Reverse Primer for Bcl-2 Mutant S70A	GGTCTGCAGCGGGGCGGTCCTGGCGAC
HYD239	Forward Primer for Bcl-2 Mutant S87A	GGGGCCTGCGCTCGCACCGGTGCCACCTG
HYD240	Reverse Primer for Bcl-2 Mutant S87A	CAGGTGGCACCGGTGCGAGCGCAGGCCCC
HYD295	FKBP38 forward primer with TEV site	CACTCAGCATATG GAGAATCTTTATTTTCAGGGC GGACAACCTCCGGCGGAGGAGGCT
HYD296	FKBP38 with Hind III site for amplication	CACTCAG Aagctt gga cgc agc ctt cag cca tcg
HYD297	fkbp38 revese to N370 with Hind III site for expression of full length of fkbp 45. With termination condon for pET 24 a	GCGAAGAAGCTTTCACTAGTTGCCCAGCATTTTCCGGTACAA
HYD298	fkbp38 revese to N370 with Bam HI site for expression of full length of fkbp 45. With termination condon for pET 16 b	GCGAAGGGATCCTCACTAGTTGCCCAGCATTTTCCGGTACAA
HYD299	xbaI site for pCDNA. general use, using pET29 as template	CACTCAG TCT AGA AGC CGG ATC TCA GTG GTG GTG
HYD300	Forward primer for Calmodulin cloning	Ctgacga catAtggctgaccagctgactgag
HYD301	Reverse primer for Calmodulin cloning	Ctgacga CTCGAGctttgcagtcatcatctgtac
HYD302	reverse primer for signal peptide, containing Nde I site	CACTCAG CAT ATG aga gag gac gca ccc gag gga
HYD330	Forward primer for Bcl-xL, S62/A	GGCACCTGGCAGACGCACCCGCGGTGAATGG
HYD331	Reverse primer for bclxl S62/A	CCATTCACCGCGGGTGCGTCTGCCAGGTGCC
HYD332	Forward primer for MEK 1 with Nde I site	t gct agc CATatgcccaagaagaagccgacg
HYD333	Reverse primer for MEK1 with Xho I site	CGAAGCT CTC GAG ttagacgccagcagcatgggt
HYD334	Forward primer for ERK2 containing Sac I site	CAC TCA G GAG CTC G atggcggcggcggcggcgcg
HYD335	Reverse Primer for the ERK2 containg Sal I site for pET DUET	GCG AAG GTCGACttaagatctgtatcctggctg
HYD376	Reverse Primer for FKBP38 E201	GCGAAG CTC GAG gtcaggcccgtccacagccgt
HYD377	Forward primer from E22 for FKBP38 nde I	GaGtAGtCAT ATG gaggacttcgaggtactggat
HYD378	forward primer for BAD with Nde I	GaGtAGtCAT atgttccagatcccagagt
HYD379	reverse primer for BAD with stop condon Xho I	GCGAAG CTC GAGTCActgggaggggcggagctt
HYD400	forward primer for loop of bcl-2, NdeI	CATCTCACAT atg gccgcgcccccgggggccg
HYD401	Reverse primer for loop of Bcl-2 Xho I	GCGAAGCTCTCGAGtggcaccgggctgagcgcagg
HYD449	Forward primerPS1 Nde I site	CAC TCA CAT ATGcatcgctctacacctgagtca
HYD450	Reverse primer for PS1 Xho I site	CAC TCA CTC GAGgatataaaattgatggaatgc